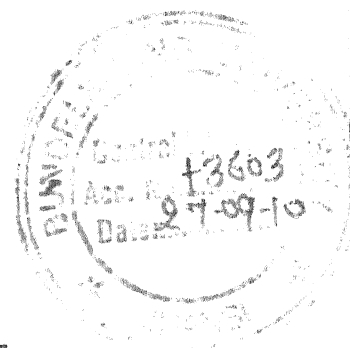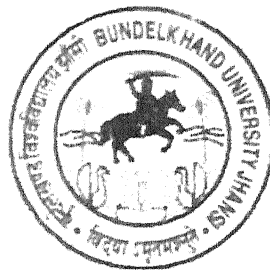# PETROLOGICAL STUDIES OF ROCKS OF BUNDELKHAN CRATON AROUND MAHOBA AREA, UTTAR PRADESH, CENTRAL INDIA

Yamini Singh

THESIS

SUBMITTED FOR THE DEGREE OF

Doctor of Philosophy

In

Geology

OF THE

BUNDELKHAND UNIVERSITY
JHANSI -284128 (U.P.)
INDIA

DEPARTMENT OF GEOLOGY
INSTITUTE OF EARTH SCIENCES
BUNDELKHAND UNIVERSITY, JHANSI

Certificate

This is to certify that **Ms. Yamini Singh**, has worked under my supervision on the present work entitled, **"Petrological studies of rocks of Bundelkhand craton around Mahoba area, Uttar Pradesh, Central India"** in the Department of Geology, Institute of Earth Science, Bundelkhand University, Jhansi. She completed the research work for the full period as prescribed under caluse of the Ph.D. ordinance and the thesis embodies the result of her investigation conduced conducted during the period she worked as a Ph.D. research scholar.

Supervisor

9.1.2009

(S.P. Singh)
Professor of Geology
& Dean Science

Acknowledgement

I express my sincere gratitude to **Prof. S.P. Singh** Department of Geology, Institute of Earth Science and Dean Faculty of Science ; who has been a source of inspiration throughout this work. I am grateful to him for suggesting the problems. Supervision, encountrament and constant guidance.

Gratitude has no means of expression and I am at a loss of words when I express the feeling of regard and heartfull thanks for respected **Dr. G.S. Tiwari** G.S.I. Lucknow whose sense of precision, deep knowledge long experience and invaluable suggestions has always helped me.

I extend my sincere thanks to **Dr. M.M.Singh** Reader Department of Earth Science, who gave his time during research works.

Thanks are also extended to Director of GSF **G.S. Srivastava** and Mr. Himraj scientist of GSI Bhopal Mr Shrivastava provide the Idea study of thin section of petrological rocks. I express my sincere gratitude to my all the departmental teachers **Dr. Ramchandra, Dr. B.C. Joshi, Dr. S.C. Bhatt, Dr. V.K. Singh, Dr. Ratnakar and Dr. M.M. Singh.**

I am also thankful to **Dr. Santosh Kumar** he give me the training of DSTR sponsored Training program which is very useful in my research work.

I wish to express my heartful thanks to my friends **Mr. Arun Nihal Singh, Mr. Akhelas Kumar Srivastava Mr. Shiv Kumar Singh, Mr. Ashik, Mr. Manjor Kumar Gupta** and all department member, for their constant help various ways to a accomplish this research work successfully

I would be failing to my duty if I do not acknowledge my father **Mr. R.B. Singh** and Madam **Pushpa Singh,** for their continuous inspiration during the research work. I this opportunity to thank all those who helped and guided me to completed this research work, finally I am highly indebted to my parents for their love, affection and constant inspiration at every moment of my life.

Thankful to **Mr. Sumit Kumar** (Sumi Computer) for careful and neatly typing the manuscript.

yaminisingh

Contents

List of Figures

S. No.		Title

List of Plates

S. No.	Title
1	**Field of photographs**
	(a) Gneisses – 1, 2, 3, , 5, 6, 7
	(b) Granite gneisses – 7a
	(c) Granite – 2, 5c, 7, 8, 9, 10, 11, 12
	(d) Shear – 3, 15, 6, 7, 8, 9, 10
	(e) Fold – 1, 3, 4a, 4b, 5, 8
	(f) Fault – 12a
	(g) Joint – 12a
	(h) Gneisses enclaves – 2, 5a
2	**Micro photographs**
	Gneisses – 1, 2, 3, 4, 5, 6, 7, 8, 10c, 11
	Amphibolite – 9a, 10b, 17a
	Schist – 13a, 13b, 13c
	Granite – 14b, 14c, 16
	Solerite dyke – 17b, 17c, 18
3	**Fluid photographs**
	Gneisses – 4.12, 4.18, 4.19, 4.20, 4.21, 4.22
	Primary inclusion – 4.30, 4.37, 4.44
	Secondary inclusion – 4.38, 4.39, 4.52
	Daughter inclusion – 4.43
	Pink granite – 4,12, 4.13, 4.14, 4.15, 4.16
	Primary inclusion – 4.12, 4.24
	Secondary inclusion- 4.57, 4.58
	Daughter inclusion- 4.57, 4.58

List of Tables

The knowledge on the assembly, evolution and dispersal of landmasses is one of the fundamental aspect for understanding the continental dynamism and evolutionary history of the earth. The information related to different geological processes, operated within individual continental block in a particular geological time span also provide valuable signatures to know the cyclic phenomena of supercontinents. The sufficient imprints of geological, geochemical and geochronological and tectonometamorphic events are preserved in the various super continental cycles. These data would be useful in furnishing the evolutionary models of cratonic blocks as well as the correlation of their characters. Apart from this, these evidences may be effectively used for bridging the gaps between cratonic blocks and the super continents.

Precambrian shields of the world would have been the nerve centre for the global research and are meticulously studies by several workers to decipher the early history of the earth. The formation of the supracrustal rocks or first landmass, is infact an irreversible process in the geological history of earth, which led the processes of initiation of stabilization, continental growth and micro-continent and supra-continental development. The peninsular India is known as one of the prominent Precambrian shield of the world, and is exposed in the south of the Son Narmada lineament. Rogers et. al., 1986 divided the peninsular shield into five distinct crustal areas viz. Bhandara, Singhbhum, Aravalli, Eastern Ghats and Dharwar granulite terrain. Later on they divided the Indian shield into several cratons (Radhakrishna 1989) viz. Eastern Dharwar, Western Dharwar, Bastar, Singhbhum and Bundelkhand-Aravallie. Each craton was perhaps characterized by a central part known as nucleus which is consisting of extensive outcrop of granite-gneisses and granitoids and is separated by a mobile belt. The core parts of these cratons are commonly associated with a sequence of metamorphosed rocks of green schist and amphibolite facies. These metamorphic sequences are mainly represented by common features such as the presence of ultramafic and mafic volcanism with wide occurrences of banded

magnetite quartz (BMQ) and chert formation. The granite appears as great batholithic massifs in all the cratonic blocks in Indian shield viz. closepet granite in the Dharwar, Singhbhum granite in the eastern region, the Bastar granite and Dongargarh granite in the Central India, the Untala, Berach and Gingla granite in Rajasthan and Bundelkhand granitoids in Bundelkhand craton. The granitoids were found as acidic intrusive in respective cratons. The relationship of widely exposed older granitoids with the 'Schistose' formation (metasedimentary and metavolcanic rocks) is a matter of petrological and geochemical interest for exploring the earlier crustal history of earth from these cratons.

The Bundelkhand massif occurs in the northern part of the Indian peninsular shield lies between the 24° 11' to 24° 27' latitude and 78° 10' to 81° 34' longitude which covers the area about 3600 sq. km. and is the 10% of central India. The entire massif is dominated by batholiths of acidic magmatism. The schists and banded iron formation from Baraitha basin of the southern part of massif was first reported by Medlicott in 1859. Subsequently, Mallet (1869) reported granite gneisses in the massif. Later on, Mathur (1954), Saxena (1961), Prakash et al., (1975), Mishra and Sharma (1974), Mishra (1975), Basu (1986), Sarkar et al., (1996), Shukla and Pati (1999), Prasad et al., (1999), Mondal et al., (2002), Malviya et al., (2006), Singh et al., (2007) and several workers have recognized various type of schist and gneisses as lensoidal bodies within the granitic massif. Singh and Dwedi (in press) have deduced the metamorphic history of high grade gneisses and suggested clock wise path for the crustal evolution of oldest gneisses of Bundelkhand craton.

The Bouger anomaly map of India (NGRI, Hyderabad, GPH/5, 1975) shows steep gravity gradient near the southern contact of the Bundelkhand granite massif with Bijawar and Vindhyan. It envisaged that there might be a sympathetic development of rifting along the Son-Narmada lineament. The northern part of Bundelkhand craton is covered by the Ganga-Yamuna alluvium that exhibits a very gentle gravity gradient. Sharma (2000) suggested that E-W trend of gneisses foliation in the Bundelkhand massif may continues westward and possibly joins with the Berach granite of Rajasthan before truncated by the NE-SW Aravalli and Delhi trend. The recent researches (Singh 2007, Basu 2007) suggest that Bundelkhand massifs is

fringed by Bijawar/Gwalior group of late Paleo-Proterozoic in two sectors and by the Vindhyan Supergroup of Meso to Neo Proterozoic period almost all around and has no continuity with BGC rocks of Aravalli.

The signature of several stages of crustal growth for the Archean of Bundelkhand is well preserved. Tonalite-Trondhjemite-Granodiorite (TTG) gneisses, forming one of the oldest rocks in the massif have been reported from several localities (Mondal et al 2008) but extensive occurrences are mainly in the central part of the massif. The rocks have been studied from different locations and have provided signature of Archean crustal evolution. The high- grade (BnGC) and low grade metamorphic (BMM) rocks trending in NW-SE and WNW-ESE respectively suggests two distinct phases of metamorphism in Bundelkhand (Singh *et al.,* 2005). The field relations indicate an older age for the high grade metamorphic (BnGC) in comparison to the low grade BMM. The most extensively widespread occurrences of Bundelkhand Granitoids have been found intrusive relationship with both BnGC and BMM.

The NE-SW trending series of short and long shear zones occupied by quartz reef are unique in the Bundelkhand craton and are represented by NE-SW trending quartz reefs that may be related to the result of drags of Son Narmada sinisterly mega fault and rebound of the resultant collision of the Bundelkhand carton with the Aravalli craton. The NW-SE trending swarms of the mafic dykes possibly related to opening of the Bijawar basin mark the end of the magmatism in Bundelkhand. Coeval marks of crustal evolution in the Bundelkhand and Aravalli areas point to their close connection during the Precambrian crustal evolution. The griddle like combined Bijawar-Vindhyan basin around the granitic massif also points to their possible inherent linkage. The crustal evolution and magmatic activities in Bundelkhand in the light of recent researches are poorly known whereas the significant researches have been carried out on these objectives in Singhbhum, Bastar, Rajasthan and Dharwar cratons. Many geologists worked out the geochemistry and tectonothermal activity in these cratons. Mondal *et al.,* (1998) and Sharma (2000) first time discussed a geodynamic evolution model for the Bundelkhand craton with limited geochemical and geochronological data of granites, gneisses and other associated rocks. Attempts

have also been made to unravel the tectonic evolution of the Bundelkhand craton on the basis of structural data of quartz reef, granitoids and associated rocks in the shear zones (Roday *et al.,* 1995, Prasad *et al.,* 1999). The recent researches (Sarkar *et al.,* 1996, Basu 2001, Mondal *et al.,* 2002, Rao *et al.,* 2005) about evolution of Bundelkhand craton were based primarily on the acid magmatic evolution and geochronological data (Sarkar *et al.,* 1996, Mondal *et al.,* 1998, 2002) of the Tonalite-Trondjemite-Granodiorite (TTG), gneisses, granitoids and the mafic dykes only.

The junction between the early Proterozoic magmatic terrains of Bundelkhand and the northern part of peninsular shield is marked by central Indian tectonic zone (CITZ)). This view was firstly proposed by Yadekar *et al.,* (1990) and suggested that the two ancient cratonic blocks represented by Bundelkhand protocontinent and Deccan protocontinent were separated by a narrow intra cratonic discontinuity basin, which can be marked by the central Indian shear zone (CIS). The current view of research is also growing the consensus on Son Narmada lineament that represents an ancient suture for the collision of Northern and Southern Indian shield (Archarya 2003). The lineament witness the repeated rejuvenation in geological past and continue to do so even today (Jokhan Ram *et al.,* 1996, Acharya 2003). Thus Northern part of Indian shield may be considered as separate blocks that may include Bundelkhand, Aravalli and the Himalyas which were delineated amalgamated and welded by different mobile belts in the extra peninsula (Sharma 2000).

Bundelkhand craton is separated by three major faults viz. NW-SE trending Yamuna fault in the north, the NE-SW trending Great Boundary Fault in the west and ENE-WSW trending Son Narmada fault in the south. Besides these major dislocation boundaries of the Bundelkhand massif, the craton represents the several intra cratonic faults viz. Shivpuri Kalpi fault, Sawai Madhopur- Damoh fault and Nogaon Panna faults that may be related to different tectonic activity. These faults are also visible on the satellite imagery. The southern margin of craton is overlain by sedimentary of Vindhyan and they are also delineated by various NE-SW trending dextral faults viz. Ratlam-Basoda Narsingarh fault, Damoh fault, Kota fault and Shivpuri fault. The detailed geomorphological and Landsat imagery studies points three important lineaments viz. Kalpi-Shivpuri shear zone (KSS), Mohar Mauranipur Mahoba shear

(MMS) and Sonrai Shahgarh shear zone in the massif part of Bundelkhand craton. The extension of these shear zones were not found to continue in the Vindhyan sediments/ Bijawar and therefore, they are the Pre Vindhyan/Pre-Bijawar architects and must be part of Archean paleoproterozoic tectonics. The present study area is the eastern part of this zone where gneisses and granitoids have some distinct pattern.

1.1 LOCATION AND APPROACH OF THE JHANSI :

The study area belong to the northern part of the Bundelkhand lies between 78° 25'E to 79° 10' E longitudes and 25° 10' N to 25° 20' N latitudes in Mahoba district. The detail geological and structural mapping were carried on enlarge toposheet No. 54O/15 of survey of India. The Mahoba town can be easily approached as it is situated on the branch line of Jhansi - Allahabad railway line. Mahoba can also be arrived by the Jhansi Banda-Calcutta national highway road and is about 40 km east to Jhansi.

1.2 CLIMATE AND VEGETATION :

The Bundelkhand region exhibits a particular type of climate and is characterized by excessive heat during the summer months and chilled cold during the winter month. Thus the Bundelkhand falls under arid climate. The temperature rises upto the 50° C in May and June. The hot winds, locally known as "loo" is common in this period. The rainfall distribution pattern is irregular. Most of the rainfall is caused by the mansoon, falling from June to October in the region. The annual precipitation in Bundelkhand varies from 90cm to 100cm. The maximum rain occurs in the July to August months.

Northwestern area of the Bundelkhand region receive nearly 90cm while in southern area receives 120cm. There is scant winter rainfall in this region. April to November is the driest month of the year. The mean monthly temperature has been recorded as 45.7° C while the peak maximum temperature of 50° C in the May to June. The lowest temperature of 3° C recorded at the month of January. The soil of the region is generally found shallow to medium depth attaining a thickness ranging from a few cms to as much as 15 cms. The thickness of soil section is variable and

contains mixture of residual and transported soil. The Bundelkhand region different types of soils are present, reddish soils, grayish black soil and yellowish black soil locally known as rakar, parwa, mar and kabar soil respectively but the reddish rakar soil is characteristic of this region.

1.3 FLORA AND FAUNA :

The flora of the Bundelkhand region belongs to climatic condition of this region. The flora of the region is tendu, mango, timber, neem, macca, barged, palash, babool, peepal etc. The wood of the semal and mango tree are used for matchsticks, tendu for the pipe making, gum is also extracted from babool tree and the khair for preparing for katha, neem leaves are used for preparing medicine and sope industries. The therapeutic plant such as raljia, sprintine and usaka are used in blood pressure, hypertension and lung problems. The wheate, pulses, rice, groundnut are the main crop of this region. The wheat is grown in the October to March month. The Rice is grown in rainy season.

The fauna of the Bundelkhand are present as lion, elephant, bear, cheetal, neelgai, leopard, jackal, fox, rabbit, goat, monkey etc and also birds like crow, vulture, neelkhanth, eagle, koyal, parrot, peacock, duck etc.

1.4 AIM AND SCOPE OF THE WORK :

Detail account of geological work, field work, and laboratory work have been carried out under present studies as follows.

(i) A detailed geological mapping on the enlarged toposheet (No. 540/15) has been carried out and the emphasis is given to the older rock sequences found as lensiodal of biotite gneisses and tonalitic gneisses (TTG) etc with in the granitoids .

(ii) A detailed structural mapping at the contact of tonalitic gneisses has also been done and lineament study along with drainage system map prepared.

(iii) Based on the available radiometric data and the regional works on structural and geological data, a tectonothemal events and has been proposed for Bundelkhand and study area.

(iv)   On the basis of satellite imaginary, the lineament and structural features of the Bundelkhand area were examined with ground truth data obtained during three years.

(v)   The thin sections of different rocks of petrological interest were prepared and their textural relationship and petrography of rocks with reference to crystallization, deformation and time relationship were carried out to describe the tectonic crystallization history of the rocks.

(vi)   The fluid inclusion study for granite, gneisses, quartz reef were carried out to find out nature and composition of fluid during the evolution and continental growth. Its application is also used to deduced the tectonic history of the area and genesis of rocks.

(vii)   On the basis of textural study the metamorphic reaction involved in the formation of different mineral parageneses were discussed through graphical presentation and a chemogrpahic relationship in the different system of ACF, AKF, and AFM diagrams have been deduced in the CFMASH, KFMASH, NCKFMASH systems.

vii.   On the basis of petrographical works and their field relationship the 29 rock samples of petrological interest were submitted for chemical analyses. The chemical analysis data portrayed in different models and varian diagram for major and trace elements suggest the petrogenesis, tectonic environment and crustal evolution of rocks developed during the different events around the Mahoba area in the Mid Archean time.

viii.   Geochemistry of the gneisses and granite were used to evaluate the nature composition and possible tectonic environment responsible for the continental crust in Archean period. On the basis of generated geochemical data, and available field evidences as well as in laboratory works, an attempt were made to describe the petrogenic evolutionary and tectonic phases of the Bundelkhand cratonic rocks.

Chapter-2

GEOLOGICAL SETTING

2.1 INTRODUCTION :

The Bundelkhand massif, primarily a granite -gneissic type complex, situated in the northern part of the Indian shield out crops as semicircular shape (Fig-2.1). The massif out crop covers an area of about 36,000 Km^2 that lies between $24^{\circ}15'N$- 26^0 $15'N$ latitude and $78^{\circ}10'$ E-$81^{\circ}34'$ E longitudes. The terrain of Bundelkhand is more or less plateau type topography, flat top hillock and gentle slope. The Son- Narmada lineament (SNNF and SNSF) trending nearly in the E-W, passes from 24° N latitude in the south of Bundelkhand complex, has been considred to be the oldest active zone in the central part of Indian peninsula that separates the southern Indian shields from Bundelkhand craton (Mondal *et al* 2006, Basu 2007 and Singh *et al* 2007).Yamuna fault trending in the NW-SE delineats the gangetic and Himalayan folded belt from Bundelkhand craton in the north (Fig-2.1). The NE-SW trending Great Boundry Fault lies in the western part of the massif delineats the Rajasthan craton.

2.2 REGIONAL GEOLOGY :

The Bundelkhand block is separated from Ganga alluvium in the north, and to the south by the Baster/ Bhandara block.The junction of these two blocks has been marked as a major tectonic zone (Fig-2.1) which is called as central India shear zone (CIS). The blocks are bounded by Mahakosal Group of rocks that further extends to the Aravalli super group in the west. The junction of these mobile belts with Bundelkhand craton is known as Great boundary fault in west (Agrawal et al, 1995, Basu 2001, Mondal et al, 2002).

The gravity gradient determined by gerphysical method in the Bundelkhand craton points several steep structure discontinuities (Verma and Banerjee 1992, Jain *et al* 1995). The cross section along the Gwalior –Malanjkhand, shows remarkable correlation with surface geology (Agrawal *et al* 1995). The topography relief indicates full isostatic compensation with respect to geophysical data. Bouger gravity anomaly

over the Bijawar basin is considerably high. The gravity gradient of Bijawar basin is defined slightly offset of the basin towards the northern margin. The gravity below the Mahakoshal belt is remarkable high though a little off-set to the south. This may be due to the Mahakoshal sympathetic development to rifting (Roy *et al* 2002) along the Son-Narmada lineament (SNL). The geophysical signatures present in the crust suggest that both Bundelkhand and Malanjkhand granite terrain occur across the son Narmada lineament consists the low gravity field (Verma and Banerjee 1992) with the remarks of high gravity in the NW part of Bundelkhand (Basu 1986). This is possibly due to large masses of basic rock or high grade metamorphic beneath the granitoids.

The Bundelkhand massif comprises mainly of granitoids of different episodes, low to high- grade metamorphic of pelitic, psammatic, mafic and ultramafic rocks, quartz reef and mafic dykes and swarms.The metamorphic rocks are usually present as lensoidal bodies within the granitoids. Basu (1986) reviewed the geology of the Bundelkhand massif comprehensively, based on his own research and work of his contemporaries in the Geological Survey of India (GIS) and the brought out that massif consisted largely of relics and occur as dismembered lensoidal bodies with in the vast mass of intrusive granitoids. Sarkar et al (1984, 1996) carried out a detailed account on the geochronological and petrology of granitoids of Babina area of the west central part of the massif and obtained an isochron age of 3500 + 99Ma for the gneisses (TTG) of Baghora and described it as the oldest crustal component in Bundelkhand craton which is geochronologically and geochemically equivalent to TTG rocks reported from the other part of the Indian shield.They suugested that these older crustal rock are further invaded by (i) grey granodiorite (2500Ma), (ii) pink leucogranite (2350Ma) and (iii) fine –grained leucogranite (2270Ma). Sharma and Rahman (1995) described the geochemistry of granitoids and early Archaean to Palaeoproterozoic crustal growth of the Bundelkhand massif, and pointed out that of the evolutionary history of early Archaean Bundelkhand massif is supported by the occurrences of amphibolites, quartzites, banded iron formation, schist and calc – silicate rock in which tonalite –trondhjhemitic gneisses were emplaced at 3200Ma (Mondal et. al. 1998, 2002). Prasad *et al.,* (1999) found out that the metavolcanic and matasedimantary sequences from central part have been suffered five phases of

deformation in the massif. Mondal and Zainuddin (1997) and Mondal *et al.,* (1998, 2002) carried out geochemistry and geochronology of granite and gneisses of the Bundelkhand massif and suggested that the emplacement of the Bundelkhand granitoids is related to volcanic arc tectonic environment at the Palaeoproterozoic, with a very short time span. Mondal *et al.,* (1998) and Sharma (2000) discussed a geodynamic evolution model for the Bundelkhand craton with limited geochemical and geochronological data of granite, gneisses and other associated rocks. Attemped have also been made to unravel the tectonic evolution of the Bundelkhand craton on the basis of structural data of quartz reef, granitoids and associated rocks in shear zone (Roday *et al.,* 1995; Prasad *et al.,* 1999). The recent researches (Sarkar *et al.,* 1996 Basu 2001; Mondal *et al.,* 2002 and Rao *et al.,* 2005) about evolution of Bundelkhand craton is based Primarily on the acid magmatic evolution and geochronological data (Sarkar *et al.,* 1996; Mondal *et al.,* 1998; 2002) of theTonalite-Trondhghemite-Granodiorite (TTG), gneisses, granitoids and the mafic dykes only.

The Bundelkhand massif is formed by multiple phases of mafic and felsic magmatism during the Archean and Paleoproterozoic period. These major phases of Paleoproterozoic felsic megmatism in Bundelkhand massif, viz hornblende granitoids, biotite granitoids, leucogranitoids can be recorded in order of decreasing age (Mondal and Zainudin, (1996).

The high-grade and low- grade metamorphics events have been proposed as Bundelkhand gneissic complex (BnGC) and Bundelkhand metasedimentary and metavolcanics (BMM) group respectively for the first time (See details in Table 2.1,2.2 and 2.3). From detailed field and lab studies, the rocks of Bundelkhand massif were divided into different groups and a geochronostratigraphy and tectonothermal events were marked for the Bundelkhand craton was first time (Singh *et al.,* 2007). They suggested two phases of metamorphism and alteast four phases of deformation in Bundelkhand massif before the emplacement of Paleoproterozoic Bundelkhand granitoids. They also noted an angular unconformity between these two events at several places. The BnGC rocks comprises gneisses, TTG migmatite, granite gnessis, granite sillimanite gneisses, cordierite gneisses, amphibolites, hornblende biotite gneisses and migmatite –quartzite etc.The BnGC rocks have been found as lensoidal

body of E-W to NW-SE linear trend at the low land area. The structural study reveals that the BnGC rocks have been experienced six phesses of deformation and the two phases of metamorphism while BMM rock has four phases deformation with low grade metamorphism.

Table-2.1 : Stratigraphy of Bundelkhand Craton

(After S.P. Singh *et.al* 2007)

Vindhyan Supergroup (1400-700 Ma)	Lower Vindhyan limestones and dolomites, quartzite Kaimure sandstone, Rewa sandstone and shales, Bhander carbonates.
Bijawar/Gwalior (1800-1600Ma)	Sandstones, quartzites, micacious quartzite, meta basics, ferruginous shale and sansdstones, BHJ, limestones and dolomites
Mafic emplacement (2000-1800Ma)	Dolerites,gabroo, lamprites, quartz vens and reefs, granites
Late phase granitic emplacement (2300-2000Ma)	Quartz reef, Granitoids, Pegmatites, diaspore and pyrophyllites
Bundelkhand Granitoids (BG) (2600-2500 Ma)	Leucogranite, biotite granite, hornblende granite, hornblende-biotite granite
Bundelkhand metasedimentaries and metavolcanics (BMM) (3300-2600 Ma)	BMQ, rhyolite, andesite, rhyodacite, quartzite, micaceous quartzite, chlorite schist, talc schist, pyroxenite, gabbro, peridotite, calc-schist
Bundelkhand Gneissic Complex (>3300 Ma)	Granite-gneisses, calc silicate, gneisses, quartzites, garnitiferous gneiss, sillimanite-cordierite gneiss, amphibolite, TTG.

2.3 BUNDELKHAND GNESSIC COMPLEX (> 3300MA) :

TTG rock is one of the important crustal components of Archean craton throughout the world (Martin 1984). The small relics and some times as patches of migmatites and older metamophites have been noted from the several locations of the Bundelkhand massif (Basu 1986, Singh et al 2007). They were merely been described as gneisses, mafics, ultramafics, metasedimentry and metavolcanics and are usually occur as relict component within the granite (Jhingran 1958, Basu 1986, Saxena 1961, Pati 1996, and Sharma 1982). Prakash *et al.*, (1975) reported the migmatites and gneisses from various places of southern part of the Bundelkhand massif. Jhigran (1958) described about the presence of granulites in the Bundelkhand massif without giving any specific location. Das (1959-60) also described granulite rocks from 1.6 km north of Pandara, near Mauranipur. The wide occurrence of gneisses and migmaites and other high- grade metamorphics associated with TTG have been reported by Sarkar et. al., (1995) from the Babina area where pink granitoids occur as intrusive in the TTG around Baghora village. Sarkar et al, (1997) designated them as Boghora trondhjhemitic gneisses (BTG). Prasad *et. al.* (1999) reported the migmatitic gneisses at north of Simara and Dhaurra from the Tikamgarh district of Madhya Pradesh (Prasad *et. al.* 1999). Mondal *et. al.* (2002) described the five giant lensoidal gneissic bodies from the different parts of the massif. Mondal *et. al* (2002) obtained disconchordant dates for the age of TTG from different places of Bundelkhand region. On the basis of the field evidences, these rocks were proposed to be the oldest crustal component in Bundelkhand craton (Prakash *et al* 1975, Sharma 1982). The gneisses and migmatites exposed at Baghora were investigated in detailed and for the first time they were disignated as TTG and were compared with the TTG, reported at other part of Indian shield (Sarkar *et al* 1996).

In general, Bundelkhand gneisses are well foliated with steep northerly dip 50°N and with the WNW-ESE strike and show evidences of polyphase deformations.The occurrances of granite- gneisses are another common type rock found in many part of Bundelkhand massif. These rocks are mostly found around

Mehroni subdivision of Lalitpur district in south eastern part and some times around Kabrai in north eastern part of craton. The calc- silicates and amphibolites are also noted together with quartzites and quarzofeldspathic gneisses at Saprar river section (Singh and Dwedi 2008). They usually are banded type gray to light gray in colour. The bands of amphibolites and high -grade metamorphites were also found together.

TTG (tonalite- trondhjemitic granodiorites) rocks were identified for first time from Bundelkhand massif by Sarkar *et. al* (1996) from the Baghora area Jhansi District and subsequently it was encountered at many places of Mahoba and Lodha-pahar in Kabrai area (Sharma *et. al* 1998). The two different names were proposed mainly on the basis of location viz. Boghora trondhjemitic gneisses and Lodha-pahar trondhjemitic gneisses respectively. The high- grade rocks are charecterised by syn to late kinematics and N-S compression. The geological mapping of these rocks in the central part reveals a large synclinal structure that was developed in the middle to early Archean time (Singh 2005, Singh *et al.,* 2007).

Sharma and Rahman (1996) reported the occurances of large number of relicts of the trondhjemitic gneisses from Kabrai and Rampura area on Mahoba Charkhari road. Rampura gneisses are highly deformed tightly folded closely associated with amphibolites. Near Rampura village along the Mahoba- Charkhari road these deformed gneisses have been intruded by the undeformed hornblende granite plutons. The TTG gneisses of Lodha-pahar of Kabrai area are grey to pink in colour and medium to fine grained where trondhjemitic gneisses is found to be intrusive into highly deformed basic rocks (Sharma and Rahman 1995). Singh et al (2007) described that Bundelkhand gneisses are prominently exposed in a linear belt of about 500m to 2500m width along 200km long. Mahoba-Mauranipur-Babina- Mohar shear zone. A detailed mapping, textural and metamorphic history of these meatmorphics were carried out and this has been suggested that Bundelkhand gneissic complexe should be considered as the oldest signature of metamorphism in the Bundekhand craton as well as in the entire North Indian Shield. Singh *et al* (2007) and Singh and Dwedi (In Press) suggested 670 to 720 0 C for the metamorphism of these rocks.

2.4 BUNDELKHAND METASEDIMENTARIES AND METAVOLCANICS (BMM) (3300-2600 MA) :

2.4.1 Metamorphics of mafics and ultramafics :

The occurrences of ultramafic rocks were reported mainly from Madaura, Girar, Baraitha areas by the earlier workers (Hacket 1870, Basu 1986, Roday et al 1998). Recently, Malviya et al (2006) described the relics of ultramafic rocks from Baragaon and Saprar river section of the Kuraicha area (Mauranipur) and similar rocks were noted from Kabrai in the Mahoba (Sharma and Rahman 1996). The older metamorphic enclaves of mafic and ultramafic and metavolcano sedimentary are observed as lensoidal from at many places.

Medlicott (1859) recorded amphibolite and greenstone rocks in association with the Bundelkhand crystalline at Baraitha and Girar. Jhingran (1958) mentions numerous enclaves of hornblende chlorite schist and amphibolites. Prakash *et al.,* (1975) find out chlorite/ biotite schist and metabasalts associated with biotite gneisses around Madaura. Misra and Sharma (1974) suggested the high grade metasedimentary as Kuraicha formation and proposed them to be the oldest crustal rocks in the region. They also pointed out that low grade metamorphic of the pelites, semipelites and volcanogenic metasediments and meta-arkose rocks should be considered as Palar formation. They merely considered hornblende schist and quartz amphibolite schist as the main constituent of Kuraicha formation and basic dykes transformed into talc schist in the Kuraicha area.

The metabasic and metaultrabasic enclaves generally occurs as small sized isolated bodies within the gneisses which are mostly massive and foliated, but are devoided of major structure. They are supposed to receive metamorphism up to / green schist/ lowere amphibolite facies. Basu (1986) identified three major out crops of metaultrabaic and metabasic rocks from southern part of Bundelkhand massif. Metaultrabasic rocks are represented by large bodies of talc tremolite schist, which occurs around Balwantgarh and tremolite actinolites schist to the southeast of Kakarwaha.The recent studies suggest that the ultra-mafic exposed at the Kakarawaha and Khudgaon areas has the separate identitity and has been designed as Epidiorites (metabasic) are the most widespread among basic rocks, occurs in small patches and

as corroded nodules with in granitic rocks. They can be seen on Haidarpur - Kakarwaha track. Srivastava (1970-71) reported small body of epidiorite from the northwest of Baghora. Mani and Bhattacharya (1969-70) describe a large body of basic ultra basic rock to north and northeast of Baraitha village westerly continuation of the rock can be seen at Girar (Basu 1986). The recent studies (Singh *et al* 2008) suggest that ultra mafics of Madawara area are different than ultra mafics found in the Central zone.

2.4.2 Metasedimentaries :

Medlicott (1859) reported metasedimentary enclaves are the" ribboned iron oxide and quartz schist" from Baratha and Girar area. Jhingran (1958) mentioned quartzites, quartz magnetite rock, slate, and sandstone and limestone enclave from the Bundelkhand granite. Prakash *et. al.* (1975) reported the 300 m thick sedimentary unconformable overlying the Rajaula formation near Berwar village in the southern most part of the massif that consist of a basal lenticular quartz conglomerate, fuschsite-quartzite, gray to green chlorite shale and banded magnetite hematite quartzites.

Mishra and Sharma (1974) put the iron formation refer to above at the top of Kuraicha formation. They describe red beds followed upwards by glauconitic quartzites to the north and northwest of Mauranipur railway station and note that lateral lithologic variation from hematite beds to siderite argillites and glauconitic quartz. Prasad *et al.,* (1999) identified three suits of volcanics from sedimentaries at the contact of gneisses at Dhaura. The volcano- sedimentary and gneissic rocks occurs in the form of ditached lensoidal out crop where pink and biotite granite is found to be intrusive to its north and south. The xenolithic lenses of amphibolites, schist and BIF from pink granite are common at the contact of granitoids. Mishra and Sharma (1974) and Basu (1986) have reported xenoliths and remnants of metasediments from pink granite at several places.

2.4.2.1 Banded iron formation :

The iron formation consists mainly of banded quartz- magnetite rock, banded magnetite amphibolite rock and banded amphibolite. The banded –quartz- magnetite rocks of Girar, Braitha and Chanrro are hard and compact, while those at Babina,

Paponi, Gora, Balyara and Mauranipur are slightly fissile. These rocks are well banded with alternating bands of magnetite and quartz. At places these band shows wavy boundaries, generally symmetrical in nature which indicates that these iron formation have suffered low grade metamorphism. Some times penecontemporaneous deformational structure are found in the BIF. The rocks usually have E-W strike trend and occurs in the tightly folded synclinal structures with axial planes dipping on the 65^0 to the north. Actinolites, cummingtonite, grunerite, garnet, hornblende, clinochlore and spinel are the common silicates and oxides noted in the iron formation (Singh *et al* 2007). The peridotite, pyroxenite and gabbro are closely associated with ultrabasic rocks and banded iron formation.

BIF has been reported at many places of Bundelkhand massif. e.g. (i) At Baraitha and Girar by Medlicott (1859), (ii) Wilson (1986-69) recorded the BIF in Babina and Papaoni, (iii) Das (1959-60) recorded a few small bodies near Gora and Balyara, (iv) at Kamla-sagar dam (Mishra and Sharma, 1974); (v) Basu (1970-71) describe three more bodies to the west and northwest of Mauranipur railway station, (vi) At Chanrro by Goyal and Jain (1972-73).

2.4.2.2 Quartzites :

The conspicuous hillocks of fuchsite- bearing quartzites of the Girar Baraitha area were reported by Prakash *et al* (1975) and also by Basu (1986). Jhingran (1958) mentions small pockets of pinkish grey and grayish white quartzite as inclusions in granites at several places but does not specify any locality. Das (1959-60) recorded biotite quartzite inclusion with in medium to coarse grained pink granite west of Kuryankhirk east of Gailwara, about 0.8 km west of Laron, and to the northwest of Pandra. Saxena (1961) mentioned a number of bands of quartzites around the Kabrai area; these commonly strike 100^0-280^0 and 50^0-230^0 degree. Mukherjee (1973-74) recorded a lenses of fine grained and saccharoidal quartzite at Rajpur and Jaswantpur, trending NE-SW. Goyal and Jain (1972-73) records schistos and fine grained quartzite about 2.5 km east of Patha in the river Jamini. Sharma (1982) described NE trending massive quartz veins and quartzites without specify any location. Mukherjee and Senthiappen (1973-74) recorded the quartzite at Garhmau and Palar Gaurari area in the east of Jhansi town.

2.4.3 Metavolcanics :

Sharma (1982) reported a sequence of volcanics at Jhakhaura, Bansi, Mathra, Paron areas in the southern part of Bundelkhannd, which are charactersied by highly fine grained, compact and bedded nature. Mondal *et al.,* (1988) reported rhyolite in Charkhari Mahoba and Bansi on the Jhansi Lalitpur road. Mishra and Sharma (1974) recorded a keratophyre like dyke at the base of the Matatila dam on the Betwa River. The mafic volcanic rocks have outcrops of variable size and these rocks are interbedded with metasedimentary rocks and BIF.

Recent studies reveal that the Bundelkhand massif granitic complex comprises the lensoidal bodies of high grade metamorphic rocks and at places low grade metasedimentaries and metavolvanics. Prakash *et. al.* (1975) described Maharani Group into two formations. (1) lower Rajula formation and (2) upper Berwar formation. The Rajula was reported comprise amphobolites and megmatitic gneisses while the Berwar formation consists with the range of volcanics and sedimentary association.

2.4.4 Phyllite and schist :

Pascoe (1950) describe the talcose schist, hornblende schist, chlorite schist, quartz-schist and argillaceous schist in the area around Mahroni in the southwestern part of Lalitpur. Jhingran (1958) mentions quartz schist and feldspathic schist in the Sadhi nadi about 12 km WNW of Bastgawan. Basu (1986) records various schistose rocks including chlorite, hornblende-mica, talc-quartz and feldspathic schist in a narrow region between the granite at Madla (Tikamgarh). Saxena (1961) described biotitic muscovite schist interbedded with flaggy micaceous quartzites and garnetiferous muscovite schist at Kabrai area. He also describes greenish white quartzite and muscovite schist at the same place.

Mishra and Sharma (1974) mentioned phyllite and low grade schist in association with quartzites at Palar formation. Basu (1970-71) located some stringers of schistose rocks with sillimanite occurring south of the Jhansi (4 km milestone from

Jhansi on Mauranipur road). Goyal and Jain also find a band of sillimanite schist east of the 7.6km milestone from Jhansi on the Jhansi Orcha road. Jhingran (1958) described inclusions of slaty rocks in Bundelkhand granites at NE of Nadgaon. Mishra and Sharma (1974) included black shales but they did not specify any locality.

2.5 ACID MAGMATISM AND BUNDELKHAND GRANITOIDS :

The Bundelkhand granite shows a wide variety of plutonic and hyperbassal rocks. On the basis of mineral compositions, texture, colour and location the granite of Bundelkahand massif has been classified into different categories viz. Jhansi granite, Matatila granite, Garhmau granite, pink granite, porphyritic granite, hornblende granite, foliated biotite, gray granite etc. Jhingran (1958) recognized ten types of granite in Bundelkhand region. Saxena (1961) considered that the granite of the massif is result of transformation of quartzites and other metasedimantary. Prakash *et al.,* (1975) considered the granite north of Lalitpur to have originated as a result of regional granitisation of metasedimentary and metabasic. Basu (1970-71) recognized three main type of granite in Bundelkhand massif. (1) Porphyritic coarse grained granite, (2) porphyritic medium grained granite, (3) non porphyritic to sparsely porphyritic medium to fine grained leucogranite.

Mishra and Sharma (1974) worked out the anatectic evolution of these rocks. Sharma (1982) divided of the granite on the basis of the locations (1) Garhmau granite and (2) Matatila granite and further classification into three phases. The Bundelkhand granite rocks have been also classified on the basis of texture, structure and location. Due to similarity and overlapping characters these classification could not be satisfactorily functional for the purpose of geological study. Recently, five phases of Bundelkhand granites has been proposed by Rahman and Zainuddin (1993), Mondal and Zainuddin (1996), Modal *et al.,* (2002). Their classification is mainly based on geochemical characters and colour index and mineralogy beside the texture and structure of rock. The earlies phase was (1) Hornblende granite. (2) Porphyritic biotite granite, (3) Foliated biotite granite, (4) Coarse grain leucogranite, (5) Fine grained leucogranite

2.5.1 Hornblende granite :

Porphyritic coarse grained granite is mainly exposed around Jhansi, extending upto 14 km milestone on Jhansi Lalitpur road, on the south across the Jhansi Kanpur road and the east and Konchhabhawar region of Jhansi district end upto the quartz reef north of the Jhansi railway station and Betwa river Jhararghat up to 6 km south of Talbehat, west of bar and at many of other places. The rock is comanly pinkish red on fresh surface and become deeper red when contain the weathering. Weathering also result in zoned structutre in many grains of feldspar phenocrysts which might to be indicative of zoning in the crystal. The feldspar phenocrysts are tabular and large in size. The size ranging from 7.2cm x 2.4cm, 7cmx2.5cm etc, the average being of older of 2.5cm1cm. High degree of packing of feldspar reported in Pawa. Pegmatoids textures are also present at the margins of some of the granitised basic enclaves. Some amount of porphyritic granite are noted in Kabrai area also.

Orbicular rocks have been reported from several localities of the peninsular shield in recent years (Srikantia 1994, Srinivasan 1995, Prakash 1996). Pati (1996); first time reported multi obicular rock from a quarry face of a foliated grey granitoid to the south of Rauli Kalyanpur of Banda. The size of the orbiculers ranges between 3.4cmx3.3cm to 6.5cmx4.5cm and their shapes vary from sub-spherical to ellipsoidal. It occurs in linear outcrop with 1.5m width since major part of the area is covered with alluvium. The orbicular granite has been reported from the Pichore area (Srivastava et al 2004) for the first time in the western part of massif.

2.5.2 Biotite granite :

The rock is grayish white in colour. They are spadaricaly exposed at many places of massif but occur as dominant phase in the northeastern part of Mahoba. Texturally, it is characterized porphyritic coarse grained biotite granite. The biotite granitoids hillocks mostly present to the south of Kabrai to the northwest of Ganj, 2 km SSW of at Bilbai, at Tikamgarh and many other places. To the northeast of Karchra- Kalan a contact with the porphyritic coarse grained biotite granitoids has sharp contact with the gneisses. At few places like Agori, the quartz grains are larger than the feldspar phenocrysts. In biotite granite the microcline is dominant phase as phenocrysts. The hornblende may exist with this rock.

2.5.3 Foliated biotite granite :

The foliated biotite granite is commonly dark pink to light pink in colour and exhibit local foliation, and also show coarse grained porphyritic texture. The phenocrysts of feldspar are prismatic and are highly packed.

2.5.4 Coarse grained leucogranite :

The granite vary from "granodiorite" to "synogranite", on the modal quartz alkali feldspar, plagioclase (QAP) diagram. The porphyritic biotite granite, coarse grained leuco granite and fine grained leucogranite, all lies in the "monzogranite" and "synogranite" field. The granite porphyry was first recorded by Basu (1970-71) at south of Jhansi on Jhansi Lalitpur road and south of Ghurari nala. A prominent zone can be seen from Khajraha Buzurg and also seen to the south east of Manpur -Tal. The rock is of light fawn colour with tiny phenocrysts of white feldspar. The granite porphyry dykes with coarse grained feldspar phenocrysts are noticed at various parts of the massif. To the south of Talbehat, leucogranites are discontinuous parallel bodies' upto 20m wide and 50m to 200m long. The porphyry type granites are recorded at Jhansi Lalitpur road between 53km to 58km milestone from Jhansi. Mukherjee (1970-71) recorded synite porphyry (synogranitoids) at Birdha and southern bank of Dukwan reservoir.

A medium to coarse grained nonporphyritic lucogranite body occurred on the western flank of Chhikara village (Basu 1970-71). It is a massive rock with a pegmatite structure. It is intruded by the Kabrai leucogranite. Small viens and patches of synitic and metasynetic rocks are commonly seen in the Jhansi granite and to a lesser extent in the Kabrai granite. Some lenses of synitic rocks are recorded at Jhararghat on the Betwa River. The synogranite bodies exhibit a blocky habit. These are reddish pink to chocklaty coloured rocks. A light grey variety is commonly seen only in the coarse grained Jhansi granite. Such nearly bodies occurs to the NE of Barora near 34.6km stone on Jhansi Lalitpur road, 3.6km south of Jhararghat, 0.6km north of Matatila railway station and along the west bank of the Jamini river to the east of Birdha.

2.5.5 Medium grained leucogranite :

Large composite bodies are also found in the west of Nathikhera in the Kuraicha hill forming the east abuntment of the Kamla -Sagar dam, on the Jamini dam right canal, Jhansi town, Pawa area and scores of the other places. A number of prominent bodies are seen in Kabrai. The bodies at Kabrai range upto 80m in width and 900 m in length. It is grayish white pink rock with moderate proportion of dispersed ferromagnesian constituents.

2.5.6 Fine grained leucogranite :

The fine grained leucogranite has been encountered (Basu 1970-71) on the southern flank of a hill to the west of Ratauli. Among all five type of granitoids, the fine grained leucogranite is supposed to be the youngest phase. These are conspicuoiusly devoid of hornblende and they have low content of ferromagnesium minerals. Basu (1970-71) reported the occurrence of fine grained leucogranite in west of Nathikhera in a trainding NNW-SSE direction upto the Dukawan reservoir on the Betwa for about 9 km. it is a moderately dark body with dominant fawn ,fine grained ground mass and aparse small sized phenocrysts of cream colour feldspar.

Mukherjee (1971-72) maps another 1.6km extension of the body to south. A similar body is noted across the Jhansi Mauranipur road at the Ghugwa rest house 23 km from Jhansi.

2.6 POST BUNDELKHAND GRANITOIDS ROCKS :

2.6.1 Quartz reefs :

NE-SW trending parallel ridges of quartz are the characteristic feature of Bundelkhand massif. The quartz vein which form abrupt wall like ridges rising about 100 to 175m above the surrounding country. The reefs give out small offshoots; in someplaces several reefs collapse into one reef. The cataclastic and the granulated nature of the cherty reef rock suggest that long narrow zones along reefs would represent the intense mylonitization. There are eleven major quartz reefs in Bundelkhand. They are spaced at 12.5 km to 19 km apart, the average width of 50m to 60m and length of 35 km to 40 km (Fig 2.5). The longest body of quartz reef passes

through Nivari and is traceable almost continuously for 100 km in length. The majority of the quartz reefs occur in the area bounded by Jhansi on the NW, Chhatarpur on the SE, Supa to the NE and Tikamgarh to the SW. Quartz is the sole mineral constituent in most of the reefs. Locally the reefs exhibit disseminated grains of pyrite, specular hematite and rarely also chalcopyrite. The reefs show a dominantly grayish white colour. Pinkish white and milky white colours are also common. Dark grey, rosy and black patches are observed through very rarely. The emplacement of NE-SW trending giant quartz reef along brittle ductile shear zone and their associated polymettalic sulphide and pyrophyllite-diaspore mineralization, marked the end stage. This suggests hydrothermal fluid activity even after the crystallization of the granite plutons. Thus, it is evident from the above that the reefs do not represent any sedimentary phase this is purely epigenetic manifestations and product of shearing and mylonitization.

It is also observed that the wall rock of the reef is showing signatures of crushing, and some places highlighting the sinistral displacement of the BIF ridge at several places for example south of Babina BIF has been displaces 3kms along the reef (Singh *et al* 2007). Roday *et. al.* (1995) developed a kinematic model to describe the geometry of the quartz reef and mafic dykes of the Bundelkhand massif. According to him, the mafic dyke and quartz reef were emplaced along the fractures developed due to change in the maximum compressive tress from an initial NE-SW trend to a final NW-SE trend, but the dominant EW trending shear zone are not continued, but at many places they were either terminated into another shear zone or discontinued by brittle fractures or quartz veins.

2.6.2 Mafic dykes and swarms :

A NW-SE trending mafic dyke, more frequent near the eastern and southwestern margins is also a characteristic feature of the Bundelkhand massif (Fig 2.5). A vast majority of the dykes NW-SE is found to be cutting across the NE-SW trending quartz reef. Some of the maffic dyke also have ENE-WSW trending are also observed in the Bundelkhand massif. Most of these dykes are discontiniuous and follow an echelon fractures. The maximum width recorded is 45m near Kakarwaha in

the southwestern part of the massif. They are usually dark grayish green in colour, in generally dykes are of doleritic in nature. Most of the dyke trend in NW-SE direction and a few dykes including great dyke of Mahoba strike in NE-SW direction.

Three generations of mafic dyke have been encountered in the massif. A coarse grained variety is present across the medium grained which in turn include transverse bodies and lenticles, a very fine grained aphanitic dolerite. The medium grained variety is more wide spread and is described here as Mahoba dolerite after Mahoba where a 11km long ENE-WSW trending medium grained dolerite (Basu1970-71, Basu *et al* 1972-73 (Cf. Basu 1986). The coarse variety has a gabbroic look and designated as a kakarwaha dolerite (Basu 1969-70). The sporadically occurring fine grained variety, which resembles the Malwa plateau basalts lying immediately to the south west of the Bundelkhand massif, is designated as the Chhikahra dolerite.

2.6.3 Bijawar group :

Rifting of the Bundelkhand granitoid massif along its NE-SW margin results the development of Bijawar basin. Bijawar group of rocks occurs on the southern fringe of the Bundelkhand massif. The Bijawar basin has been found to overlying the basement of Bundelkhnd granite and unconformily overlained by Vindhyans. Exposoures of these rocks are mainly in two sectors. The eastern one lies mainly in the Chattarpur and Sagar districts of Madhya Pradesh and Lalitpur district of Uttar Pradesh The Bijawar group comprises a succession of a basal conglomerate and quartzite that were overlained by hornstone breccia, limestone, phyllitec shales, red jaspar and basaltic traps.

2.6.4 Vindhyan supergroup :

Vindhyan are occupying a large extent of the country a stretch more than 1,03,600 sq.km areas from Sasaram and Rohtas in western Bihar to Chitorgarh in Rajasthan with the exception of a central tract in Bundelkhand, while a large area of Vindhyan is covered by Deccan trap. The outcrop has its maximum breath in the country between Agra and Neemuch. The Vindhyan supergroup forms a vast

semicircle patterns and is delineated from Son Narmada fault in south. The Yamuna-Ganga alluvium in the north conceals both the Bundelkhand massif and the Vindhyan. The lower Vindhyan best exposed in north of the Narmada valley, particularly in Malwa and Bundelkhand in central India. The lower division (Semri group) is well exposed in the Son valley but its presence has been also noted at Chitrakoot and Shahgarh and adjoining area of Bundelkhand massif. The upper Vindhyan (Kaimur, Rewa, Bhander) best exposed in north of Narmada and East Indian railway from Katni to, Allahabad, Satna, Manikpur area. The basal conglomerates, limestone porcellanite, shale, gluconite, sandstone, fawn sandstone, quartzites etc are the main rock type of Vindhyan supergroup. Alternate layers of sandstone shales, limestone and quartzite are the characteristic feature of Vindhyan supergroup. The carbonate facies are dominating in Semri and Bhander group (Fig-2.1).

2.6.5 Deccan trap :

Deccan traps encompass today an area of about 500,000sq.km. They have covering a large part of Kutch, Surshtra, Gujarat, Deccan, central India, Madhya Pradesh, Hyderabad region etc. The Deccan trap extending northwards covers a substantial part of Vindhyan syncline. The western extention of the traps is observed in Saurashtra. The extensive lava flows which gives rise flat topped mountains and plateaue with step like terraces are believed that they have erupted subaerially through the fissures in the earh crust. Several dyke system and fissures zones trending parallel to the ENE-WSW son Narmada Godawari lineament, NS Konkan lineament and NNE-SSW Cambay graben lineament are known to occur in thick pile of lava flow. The lower unit exposed in the eastern aand southern part of the Deccan country is composed of uniform horizontal thoditic flows representing the quiet type of eruption. The upper unit exposed in the northern part of the Deccan plateau is characterized by an explosive activity; fissure dykes in the trap of large size, massive irregular intrusions and ash beds are observed at a number of places in the neighbourhood of the trap area around its boundary.The Deccan traps are found directly on the granite rocks near Biratha but mostly lies on the Sandstone of Vindhyan.

2.7 REGIONAL STRUCTURES :

Bundelkhand massif lies in the northern part of the Indian shield. The massif part of Bundelkhand is characterized by several regional structures like quartz reefs, mafic dykes, lineaments and mesoscopic structures likes fold, faults, joints shear zones, schistocity, foliation. The different rocks were developed along certain structural trend. These structures are well preserved at several places in Bundelkhand massif. The early formed lithounit have also experienced several generation of deformations. These deformational signatures can be analysed on the different domains and can be correlated with the regional scale strcuctures for the evolution of craton. Bundelkhand granite massif may preserve the records of strcuctures of Bijawar group/Gwalior Group and Vindhyan supergroup. The effects of deformational evolution of Son Narmada tectonics and Yamuna faults on the Bundelkhand massif can not be ruled out (Fig-2.1). This is also evidenced by the satellite imagery dat presented in the Fig.-2.2 and 2.3.

2.7.1 Structure in migmatite, gneiss and amphibolite (BnGC) :

Basu (1986) described that the gneisses exhibit a general WNW-ESE strike with moderate to steep dips (35^0 to 65^0) in many parts of the complex. The stromatic gneisses also exhibit well developed banding represented by melanosome and leucosome of variable thickness at many places. The leucosome are mostly of quartz feldspar with minor biotite. The melanosome are granodioritic to dioritic with biotite and minor amount of amphiboles. Bhattachrya (1986), Singh (2005) and Bhatt et al (2008) point out various type of folds and shears from the gneisses of Bundelkhand.

Prasad *et al* (1999) described the six phases of deformational structures from the gneisses of Dhaura. Similarly five phases of deformation were recorded from the migmatite gneisses and amphibolites of Mauranipur (Sharma 1982). On the basis of deformation and style of folding in gneisses Singh et al (2007) opined that atleast three phases of deformation were developed before the development of BMM rocks. They also identified the sheath fold cross folds and shear folds from the gneissic rocks of the Central part of Massif that may be correlated with Mohar- Babiba-Mauranipur shear zone. The F1 folds in the BnGC rocks are tight isoclinal, with acute hinge

trending E-W. F2 folds are open to tight upright fold coaxial to F1 trending E-W. The F3 fold are steeply plunging subverticle and vertical folds, F4 folds upright to steeply inclined fold trending between north and north east and F5 fold are up right fold trending between west and northwest. They also suggested that the isoclinal to tight reclined and open folds (F1, F2, F3) are those fold which developed during first, second and third phase of deformations and confined only in BnGC fourth phase of deformation is sinistral shear zone and developed in formed in NE-SW direction while in the last phase of deformation dextral shear zone were developed in NW-SE direction and displaced earlier structure.

2.7.2 Structure in metavolcanic and metasedimentary rocks (BMM)

The Bundelkhand metavolcanic and metasedimentary (BMM) rocks are found in a form a narrow linear belt. These rocks lie over the BnGC and an anguler relationship with BnGC has been established (Singh *et al.,* 2007). These rocks are present along the Babina- Mauranipur Mohar shear zone (Fig.-2.4). The BMM rocks are usually trending in the E-W direction with dip to the north but at several places and in many parts of complex schistosity shows orientation of strike NW-SE and NE-SW that may be due to the subsequent deformation in the massif. The schistosity planes are also developed in the metabasalt calc-schist, matapelites and BIF. Prasad *et al.,* (1999). Suggested three phases of deformation in the volcanic and sedimentary rocks of Bundelkhand from Prithivipur area. The first phase (F1) of deformation result formation of tight to isoclinal WNW-ESW to EW axial plane and steep NW plunging fold axes (75^0). The second phase (D2) of deformation is characterized by tight reclined F2 folds that may co-axial and co-planer with the F1 first phase of the folds. The third phase of deformation developed tight to open F3 fold with axial surface at high angle to those F1 and F2 folds. The axial surface of the third phase fold trends NW-SE to NE-SW and the fold axes plunged 25^0-60^0N. During the second and third phase of deformation the F1 schistosity in metabasalts was folded.

The three phases of folding in the volcanic and sedimentary rocks are comparable to those recorded in the gneisses of BnGC (table-2.5). The highly compact and bedded nature of metavolcanics is best seen around the village Mathra;

where the vescular features are also preserved. The Basu (1986), Singh *et al.,* (2007) postulated that BIF were formed in the small basin. The BIF is tightly folded synclinal structure with axial planes dipping on the average 65^0 to the north. They have also noticed the slump and other penocontemporaneous deformation structure. Similar slump structure and penicontemporanious structure were reported by other worker (Prasad *et al.,* 1999 and Sharma 1998).

The supracrustal sequence consisting metabasic and metaultrabasic, banded iron formation, iron formation, fuchite quartzite is folded in the E-W due to north – south compressive force. In the southern part of massif the E-W trending fold axes subsequently changed to into tight to isoclinal folds overturned to the south (Prakash et al 1975, Roday et al, 1995). They suggested that F1 folds in these rocks are generally variable oriented coplanar folds and F2 fold structures lie at high angle to early structures and are either sinusoidal fold. They appeas to have formed after most of the granitoids were emplaced as the shear zone. Tight similar isoclinal folds are found in the banded iron formation of Bundelkhand complex. Generally folds axis of open and tight folds are parallel to the strike of the iron bodies, i.e. E-W and axial planes dips to towards the north direction.

2.7.3 Structure in granites and other rocks :

The two principal varieties of foliation in the granitoids have been marked mainly on the basis of the orientation of tabular grains of feldspars. Joints are developed to various extent in all granite rocks of the massif. In the granites, three sets of joints are developed, two steeply dipping NE-SW and NW-SE trending and the third horizontal. Fractures are also developed in these granitic rocks. Basu (1986) mentioned that foliation in granite do not posses a regional control but are possibly the result of local stress. But Singh *et al.,* (2007) pointout regional trend of foliation in granitic i.e. WNW-ESE. Prakash et al (1975) described that most of the ductile shear zone in the granitoids were developed towards the end phase of late kinematics diapairs and this is generally about in contiguity with supra crustal rocks, or in proximity with adjoining daipairs. Two set of shear zone are recognized in granite

rocks (Basu 1986, 2001; Sharma, 1988 and Roday et al, 1998). Both set of shear zones are generally steeply dipping or vertical. The E-W trending sinistral shear zones are more unbiquitous than their NW-SE trending dextral counter parts. Shear zones are generally located at the boundary of supracrustal rocks; sometimes they are also located at the boundaries of individual diapairs. Both the set have steep to subvertical dips.

The granitoids of Bundelkhand massif is transversed by two prominent sets of lineaments one having the general NE-SW trend while second set of lineament are characterized by NW-SE direction. NE-SW trending lineament were probably reactivated and occupied by quartz reefs, having slightly sigmoidal geometry, characteristic of the tensile veins, generated by a brittle-ductile in the homogenuous simple shear. The lineaments patterns of the Bundelkhand massif based on landsat imageries reveals that there are three principal set of lineaments in the massif (Basu 1986) viz. NE-SW, ENE-WSW and NW-SE. The south western part of the massif has more density of lineaments than any other part. At many places lineaments intersects to each other but some places it occurs as cunvilinear or parallel to each other. The low density of lineaments fabrics in the massif is characterized by absence of intense tectonism. The lineament fabrics of Bundelkhand craton based on imagery data and field data is depicted in Fig.-2.5 (Singh et al 2006).They suggest three major trend of lineaments viz.NNW-SSE, NE-SW and NNE-SSW for the Bundelkhand granitoids.

In the granites, three set of joints are commonly developed in which two are trending NE-SW and NW-SE with steep dips and the third one horizontal (Basu 1986). Most of the joints are open but the gaps rarely exceed 10cm in width and the length is not exceeded from 50m. Some places these joints are filled up the pegmatite veins.Fractures are also commonly developed in these granitic rocks. The massif granite rocks are extremely fractured at places ond other dyke have fallowed particular set of fracture. Granite rocks show ENE-WSW trending fracture, pegmatites vein and quartz reefs both are followed by NE-SW trending fractures and dolerites have almost exclusively followed NW-SE trending fractures.

2.8 REGIONAL STRATIGRAPHY :

The first physical feature and geology of Bundelkhand was perhaps published by Franklin (1825, 1828) that was followed by Adam (1832, 1842) and Jaquemant (1832). Medilicott (1859) described the occurances of iron ore formation, basic dykes and quartz reefs from the Baraitha for the first time. Mallet (1869) reported extensive gneisses and prominent quartz veins the massif. Fermor (1909) refered the Bundelkhand as a post Dharwarian age. Pascoe (1950) described geology of Bundelkhand and adjoining areas that comprises rocks of different episods gneisses, migmatites, metabasic schist and volcano sedimentary where the quartz reefs and dykes are developed in NE-SW and NW-SE. The regional stratigraphy work carried out by different workers at time to time are complied and are described in Table-2.2.

Jhingran (1958) mentioned that relicts of metasediments in the granites are equivalent to Dharwar group of rocks. They have also mentioned that granite, quartz reef and basic dykes respectively are of younger episodes. Saxena (1961) also described that stratigraphy of Bundelkhand massif. Prakash et al (1975) also proposed stratigraphy of the Bundelkhand and classified the straigraphic sequences of Bundelkhand massif into four formations viz. (1) Rajaula formations: consist of metamorphosed volcano sedimentary rock which, unconformably overlained by Berwar formation. (2) Berwar formation: consisting of ferroginious metasediments and mafic and ultramafic rocks (3) Bundelkhand granite formation: consist of variety (ten types) of granites including migmatites and (4) Madaura formation: the Madaura formation consists of dolerite dykes, quartz veins, pegmatite, gabrro, pillow lava etc.

Mishra and Sharma (1974) proposed a four fold classification of Bundelkhand massif (1) Kuraicha formation: consist the rocks of megmatites, gneisses, schist and also the quartzite rock. The Kuraicha formation is unconformable overlain by the Palar formation. (2) Palar formation: consist of phyllits, schist, shales diaspore, ferrogenuous quartzite etc. (3) Intrusive of Bundelkhand granitoids and (4) mafic dykes and swarms. Prasad et al., (1999) also proposed a lithostratigraphic succession of Bundelkhand massif. According to them banded iron formation as the oldest rock unit of Bundelkhand massif. They have marked a gap of deposition in the Pre-Bundelkhand granite and the Bundelkhand igneous complex rocks. Basu (2002 and

2007) put the gneisses as oldest followed by various phases of granites of different episodes. According to Basu (1986) lithostratigraphy the quartz reefs and dolerite dykes are youngest, lithounits of the Bundelkhand massif complex.

Sharma (1982) described the lithostratigraphy of the Bundelkhand complex. They considered that Kuraicha is the oldest formation in Bundelkhand massif which comprises magmatites, gneisses, amphibolites, chlorites and biotite schists, quartzite etc. it is unconformmably overlained by the Bundelkhand group. The Bundelkhand group has been divided into six formations which have been containing different lithology. They are (1) Palar formation (2) Paron meta-acidic volcanics (3) Garmau granite (4) Matatila granite (5) Mahoba doletite dyke (6) Madaura ultrabasic rocks.

Sharma et al (1998) proposed the straitigraphy of Bundelkhand in perview of the tectonic events. They proposed the straitigraphy sequence of Bundelkhand massif on following order (1) Mahroni formation of Archean is conformably overlained by Bundelkhand complex (2) Bijawar and Gwalior group (2400-2300 Ma), (3) Vindhyan supergroup (1500-550 Ma) which is unconformably overlain by (4) Malwa (Deccan) traps of Cretaceous –Eocene age.

Recently Singh et al (2007) reviewed the stratigraphy of Bundelkhand craton on the basis of recent developments in geochronological, petrological and structure works and they proposed six Groups for the stratigraphy of Precambrian of Bundelkhand craton. The two new terms viz.Bundelkhand gneissic complex (BnGC) and Bundelkhand metasedimentary and metavolcanics (BMM) were proposed for the rocks that crystallized metamorphased and deformed before the Bundelkhand granitoids intrusives. The anguler relationships and distict change in grade of metamorphism and deformation between these rock units (BnGC and BMM) were also encountered by them. Thus the status of Group for the pre- Bundelkhand rocks was first time suggested by these workers (Table-2.3).

2.9 GEOCHRONOLOGY AND GEOCHRONOSTRATIGRAPHY :

The Bundelkhand massif, semicircular outcrops represents one of the oldest nuclei of the northern part of Indian shield. The Bundelkhand massif separated from

the north by the Son -Narmada lineaments, from Aravalli rocks by the Great Boundary Faults in the west and from the Himalaya by Yamuna Fault in the north (Singh *et al* 2007). The proximity of the Bundelkhand massif to the Son Narmada lineaments which may be an ancient micro plate suture deserves special attaintion with regards to its evolution. The Bundelkhand massif comprises multiphases of the tectonic and magmatic activity that have been taken place around this lineament. The evidence of these tectonic activities can be also available in the older crustal material of Bundelkhand massif in the form of reset date or disconchorded ages. The satpura orogeny (1600 ma) has been considered as the strongest and perhaps last orogenic phase of Precambrian in the central Indian craton so far (Pandy *et al* 1995).

The review of the geocronologycal data in Bundelkhand massif and central part of Indian peninsula suggest that perhaps Bundelkhand and Bastar craton were the two oldest Archean nucleous in the north and south of SONAT respectively. Various geologists worked on Bundelkhand massif and several attempts have been made by different workers times to times. The published geochronologycal data of different workers has beeen compiled and represent in table 2.4.

The oldest age 3500±99 Ma and 3297±9Ma have been obtained from the banded gneisses of tonalite trondhjemitic affinity of Baghora and Mahoba area of Bundelkhand by Sarkar et al (1996) and Mondal et al (2002) respectively. This age is comparable to the other tonalitic-trondhjemitic gneisses reported from the other part of Indian shield viz. (Beckinsole *et al* 1980, Moorbath et al 1986, Dhoundial et al 1987, Sarkar and Gupta 1990, Sarkar *et al* 1986). Three major phases of palaeoproterozoic acidic magmatism in Bundelkhand viz. hornblende granitoids, biotite granitoids and leucogranitoids has been recognized in order of decreasing age (Mondal and Zainuiddin 1996). Age of Bundelkhand granitic activity is also supported by the Rb-Sr whole rock isochron age of 2569 ± 106 Ma (Crowford 1970) from the Jhansi, Khajarao granitoids of Bundelkhand and also radiometric date of Pb\Pb age of 2518±6Ma (Mondal *et al.,* 2002), 2492 Ma (Mondal *et al* 2002). Sarkar et al 1984, 89, 90, 95) also divided the granite into three distinct intrusive phases. (1) gray granodiorites and granites (2400Ma) or Biotite granitoids (2521±-6Ma) (2) pink

leucogranite (Ca.2350Ma) and (3) fine grained leucogranite (ca.2270Ma) or hornblende granitoids (2516±9Ma), leucogranite (2429±10Ma). The radioactive age data of different gneisses from various location of Bundelkhand massif yield more than 300Ma. The zircon age of Kuraicha gneisses (3297±8Ma) and Mahoba gneisses (3270±-3Ma), TTG of Lodhapahar (3300Ma) are reported more than 3200 Ma (Mondal *et al* 2002). The Sm\Nb method also provides similar geochronological data for these gneisses. The available radiometric data represent the oldest event of the granitic magmatism in the region took place at 3297 Ma as indicated by the TTG gneisses cofolded with amphibolites and meta sediments from Mahoba (Mondal *et al.*, 2002). Therefore 3297Ma age as the minimum crytalization age of the metamorphites can be proposed on the basis of age of TTG that is associated with high grade rocks of BnGC.

The age of gneisses Viz. 2700Ma for Babina gneisses and 2500 Ma for Karera gneisses, 2500 Ma for Panchwara gneisses may be considered as disconchordant age and may be correlated with the subsequents thermal events in the craton. The data obtaoined by radiamatic age dating indicates presence of multiple phase of thermal activity occurred with in the massif after the M1 metamorphism

The other discordant data age viz. 2700Ma of Babina gneisses may be related to the M2 metamorphism. The 2500Ma (Karera, Panchwara gneisses disconchordat of gneisses may be emplacement of undeformed granitoids). The composition of younger gneisses from Karera and Panchwara 2500Ma may be different from the older Kuraicha and Mahoba gneisses (3270±3Ma) (Mondal *et al.*, 2002). The younger gneisses dates of Karera and Panchwara 2500Ma may be disconcordanrt age which is either cooling or recrytalization age formed during reactivation of shears or may be related with large scale granitic magmatism in this region (Singh *et al.*, 2007).

The age of different granitoids of Bundelkhand (hornblende granitoids:2516±4Ma, biotite granitoids: 2521Ma, and leucogranitoids 2492±10Ma) have been also obtained recently by different methods (Mondal et al 2002) which suggest that Bundelkhand granitoids activities was for the short duration and active at

the paleoproterozoic time. The radiomatic age dating Rb\Sr methods points out that long time of acid magmatism occurred in Bundelkhand massif in the early Proterozoic time (Sarkar *et al.,*, 1990). Three major type of felsic magmatism in Bundelkhand massif correlated with Bundelkhand continental growth and late stage pegmatitic and hydrothermal process in the evolution of the Bundelkhand batholiths. The batholitic granitic complex also comprises post orogenic granite rock (Sarkar et al 1984, 1990, 96) belonging to three distinct thermal imprint events viz. (1) gray granodiorites and granite (ca 2400Ma), (2) pink leucogranite (ca.2350Ma) and (3) fine grained (aplitic leucogranite(ca 2270 Ma). Thus these dates may be related to development of quartz reef and late phase acid magmatism in the massif. The mafic dykes, which generally truncate the quartz reef, represent a younger thermal perturbation in the lithosphere. The mafic magmatism took place during the time interval between the terminal phase of hydrothermal activity associated with the Bundelkhand magmatism and initiation of the Gwalior and Bijawar marginal basins (Rao et al, 2005). Crawford and Compston (1970) reported a Rb-Sr isochron age of 1830± 200 Ma for the mafic volcanic rock associated with the Gwalior group sedimentary rock. Pandey *et al* (1995) reported Rb-Sr isochron age 1691±180Ma for the Kurrat volcanic rocks. Sarkar et al, 1990 reported K-Ar isochron age of Kalinjar fort and Alipura is 1799Ma, 1523Ma for Dargawan sill of Bijawar basin. The clustering of these geochronolical data around 1800Ma points that last thermal activity perhaps took place due to the change over from the compressional to extensional regime caused by the domal upwarping result in rapid uplift of the region. The plume related mesoproterozoic basic magmatism in the Bundelkhand craton caused intrusion of the mafic dykes swarms into the granitoids batholiths extrusive (Mondal *et al.,* 2008).

Thus the basis of the geological signatures present in the rocks, imageries interpretation and geochronological data and their relation with different metamorphic, magmatic and sedimentation along with deformation history, the tectothermal and geochronololithostratigraphy of Bundelkhand has been proposed (Table-2.6) for the evolution of Bundelkhand craton.

2.10 GEOLOGY OF THE AREA :

The study area around Mahoba and Kabrai covers about 640 sq. km of the central part of northen block of Bundelkhand massif. The Mahoba is about 150Km east to away from Jhansi district. The study area forms a part of the topographical sheet 54O\15, 63C\3 of survey of India and consist mainly the different variety of granites. The high grade metamorphic represented by TTG, biotite gneisses and amphibolites, schist, quartzites of BnGC are also exposed at many places (Fig.-2.6). The mafic and ultramafic and mylonites are also observed. The study area has been mapped for detailed study of petrogenesis of different rocks and their structureal relationship (Fig.-2.6). The field investigations could be completed during several field sessions covering with a period of about two years. The geological map of the study area is prepared after detailed field work on the enlarged toposheet of SOI and some lab work. The setallite data were also used to find out the accuracy of the mapping (Fig.-2.6)

2.10.1 Topography and Drainage :

The entire study area is characterized by more or less plateau type of topography where NE-SW trending quartz reef and NW-SE trending great Mahoba dyke are exposed (Fig 2.8). Quartz reef are generally raising about 100m above the surrounding plain while the great Mahoba dyke are raising about 150 m above the surrounding plain. Both the ridges are symmetrical contain the gentle slope, and characterized by the dextral as well as sinistral displacement signatures (Fig 2.6). The gneissic rocks are found to occur at the low level topography. Geomorphologically, the study area has been divided two parts (Fig.-2.7 & 2.8).

(1) contains hillocks as well as ridges

(2) plains with large valleys

The river and streams always follow the slope of the terrain and serve as drainage channels. Regional drainage system of the study area is dendritic to subdendritic pattern (Fig.-2.7). Small water bodies like ponds viz. Bijanagar sagar dam, Kirat sagar dam, Thana-sagar kalian sagar are the main sources of water in the

study area. The small tals also present in my study area. Drainage pattern in the study has followed the NW –SE trending weak shear zone of the study area. Bhairon nadi is the major perennial stream in the study area, which flow from north to south in the study area. The area is marked by the presence of drainage having its orientation in NS, ESE-WNW, NNW-SSE ansd NE-SW.

2.10.2 Lineaments :

Three prominent lineaments (Fig 2.8) have been observed in study area (1) NE-SW (2) E-W (3) NW-SE. The oldest linear feature is the E-W trending lineament which is displaced by the NE-SW trending lineament that mainly corresponds to quartz reefs. The NW SE lineament is represented by the most prominent mafic dyke swarns in the massifs (Fig.-2.8). It is suggested that the NE-SW trending lineaments along which the great mafic dyke were embedded is the youngest lineament in the study area. This youngest NW-SE trending lineament has been also cut across by the NE-SW trending quartz reef.

2.10.3 Rock types :

2.10.3.1 Migmatites, gneisses, amphibolites and TTG :

Good exposures of gneisses have been observed at Nathurpura, NE of Sahphari and Lodha pahar (Fig-2.6). Small out crops of BnGC were also found at Mahoba railway station, Shutwai and Damaura villages. The gneisses of the study area is characterized by leucogranite to melanocritic, medium to coarse grained and well developed gneisses texture (plate-1 A, 1B, 1C). The bands of leucosomes and melanosomes are present in gneisses rock. But some places the band of leucosome and melanosomes are variable in thickness (plate-2A). The partial melting characters are also observed in the gneisses (plate-2B). The gneisses are highly deformed medium to coarse grained and grey to pink colour. Feldspar, quartz, biotite, magnetite, sericite, sillimanite, apatite, zircon, opaque and epidotes are the dominant mineral constituents of this rock unit. The strike direction of TTG is generally NW-SE and having N 60^0 E strike direction. Xenoliths of gneisses have been found in the granite at many places, particularly at northwest of Shapahar and leucogranite contain

xenoliths of gneisses at Patch phara village (plate 2C). Xenolith also observed in the Fatehpur bazaria village. At Lodha pahar patches of gneisses with in the amphibolite is found. The lensoidal bodies of magmatite gneisses as enclaves were also observed at Prem Nagar of Mahoba. At Fatehpur Bararia village the banded gneisses are change into the grey granite due to partial melting and recrystalization during the advance stage of metamorphism and deformation (plate-4A). In the study area highly deformed and streaky gneisses, banded gneisses are exposed at many places (plate-2C). The patches of gneisses with in amphibolite have been found at the Lodha pahar (east of Kabrai). The medium to coarse grained, light to dark gray intensively foliated and also mylonitised gray granite gneiss is exposed near Jhankhera ridge. At the Dahra village, sheared gneisses and granite gneisses are exposed. In the SW of Lodha pahar high grade gneisses are exposed and also containing pegmatite vein along the S-C fabric (plate-1C). At Dahara area, streaky gneisses are also observed (plate-5B). They are grey in colour, medium grained hard and compact.

In nature, the gneisses of study area contain well developed structural features. At Mahoba to Charkharo road the waxing and winning pattern of gneissic bands are also observed. Dominant minerals of these gneisses are biotite and quartz minerals. The gray granite has been found to be intrusive in the gneisses of Mahoba area (Plate-2B)

2.10.3.2 Amphibolites and hornblende-biotite-gneisses

In the study area amphibolites of BnGC are observed at many places. The best outcrop of the amphibolites occurred at the Lodh pahar hilloks. The amphibolites are hard and compact massive fine to medium grained and dark coloured rock. Megascopically they contain hornblemde, biotite, plagioclase, quartz and chlorite minerals. At Lodhapahar the amphibolites are usually observed in the form of lenticular patches in gneisses. They have also undergone different deformational events. At the Sahapahar the pink granite rocks contains the enclaves of amphibolites. Amphibolites bearing gneisses rocks are also observed along the Mahoba -charkhari road at Nathupura village. The sillimanite bearing gneisses are present along amphibolite (Plate-5A) at Nathupura village.

2.10.3.3 Metamorphosed mafics and ultramafics :

Mafics and ultramafics schist are medium to gine grained bluish grey to grayish green in colour. The mafics and ultramafics are generally observed at highly weathered form. Chlorite, talc and amphiboles are main constituent minerals found in such rocks. The foliation planes are generally in ENE-WSE steeply dipping north westerly ($>70^0$). At the fatehpur Bazaria coarse grained grey granite contains the flaks of maffics.

2.10.3.4 Medium to fine grained (± horneblende ± biotite) pink granite :

Hornblende granite at Pawa Rajapur and Banlatola is pink in colour, highly packed rarely deformed, medium grained hard and compact. Some times coarse crystals of feldspar are also observed as porphyritic texture. The granite rocks also contain the xenoliths of gneisses rocks. The major mineral constituents of the granite of Banlatala are biotite, orthoclase, quartz and magnetite (plate-9C)

2.10.3.5 Coarse grained pink granite

Coarse to medium grained pink granite rock is exposed at Mahoba railway station, Panchapahra village, Gukhar Pahar and Churbura, northern part of Shahpahar, Karahra Kalan and Bagrauri area (Plate-12C). Coarse grained pink granites are also exposed south west of Bijanagar sagar (Panchi Vihar) and Ratauli road of Bijanagar Sagar dam. In the Paswara, grey granite is dominant over the pink granite. The rock type is characterized by dark pink in colour, coarse to medium grained texture, hard and compact. It mainly composed of orthoclase, quartz and hornblende minerals. At some places pink granite also having the pegmatite veins at Pach Pahara village and small and medium size enclaves of older metamorphic rocks found near Chandu village. N 70^0 epidote vein is also present in the Karahra kalan pink granite and also mafic microgranular enclaves are present in Karahra kalan. Quartz vein trending NNE-SSW is noticed 2km from Dharamshala right side of Mahoba to Charkhari road. The pink granite also contains lensoidal xenolith of gneisses. Near the Bijaynagar sagar dam on the Ratauli road, the highly sheared pink granite are exposed (plate 10A, 10B, and 10C).

2.10.3.6 Porphyritic grey granite :

The leucocratic to mesocratic, massive medium to coarse grained batholithic body of the grey granite is well exposed at Nathupura (plate-2B) but the small bodies of grey granite is exposed in the near the Churbura village and Gukhar pahar and also reported in the left side of Jhansi Mahoba road between the Pachapahara and Chandu villages. At places the grey granite is characterized by large phenocrysts of quartz and feldspar minerals. The sharp contact of the grey granitic and gneisses are observed at Nathupura village (plate-5A). The thermal shearing signatures were available in the graniteic rock in Nathupura village (plate-2B). At some places small patches of TTG are observed as enclaves with in grey granite, west of Mahoba railway station.

2.10.3.7 Porphyritic biotite -granite

The biotite granite is exposed in Raipura Kalan village, right side of Jhansi Mahoba road, Utiyan village; biotite granite is data pink in colour, medium to coarse grained rock. The biotite granite is characterized by quartz, orthoclase and biotite minerals. Hornblende minerals are reported in occasioannly. At Raipura Kalan area the biotite granite contain pegmatitite veins (plate-12C) enclaves of undigested grey granite are found in the biotite granite many places.

2.10.3.8 Granite-gneisses

Granite-gneisses are well exposed at the Balbai village which is charcterised by quartz, orthoclase and biotite minerals. Granite gneisses of Balbai village are medium to coarse grained hard and compact rock mass (Plate-7A).

2.10.3.9 Quartz reef

Quartz reefs are exposed at Mallipura, Imeliya and Malingang areas. They show different types of colour like as grayish white, milky white, pinkish white and are hard and compact. Quartz reef in mainly constituent of reef minerals but feldspar, epidote, chlorite minerals. The quartz reef has general trend of NE-SW direction. But at some placees it shows NNW-SSE and EW trending.

2.10.3.10 Dolerite dyke

In the study area dolerite dykes are located at the Bijanagar -Sagar dam, Churbura and Dmaura, Kachhin Kapura villages which are characterized by fine to medium grained, black to dark grey in color hard and compact rock. The general trend of these dykes is E-W and NW-SE direction. The major mineral constituents of the dolerites are pyroxene, plagioclase and feldspar minerals.

2.11 STRUCTURES :

In the study area several macro and meso scale structure were observed. These structure are disscused on the following paragraphs.

2.11.1 TTG, gneisses and migmatites :

Gneisses and magmatite rocks are well foliated with steep northerly dips and with WNW-ESE strike. Different kind of complex structure have been observed in gneisses (Plate-1A). Tight to isoclinal fold (F1, F2) with axial plane NW-SE is observed from the biotite gneisses (plate-1A, 2B, 3C). In Nathupura village shear folds are observed in the gneisses. The high grade rocks exposed in the SW of Lodha Pahar containing pegmatite veins along the S-C fabrics (plate-4B). The open and tight folds are observed at many places in gneisses (plate-5A). The presence of shear fold, well developed S-C fabrics the rotation of forphyroblastic fabric structure in the gneisses indicate that gneisses were subjected to the shearing as well as thrusting in the Archean period. The gneisses rocks of the study area contain the E-W shear zone with predominant dextral shear sense. Several late phase granite and pegmatite which were intrusive into the gneisses were deformed to form E-W trending S-C mylonites with dextral shear sense (plate-4B). The structural study indicates that the high grade metamorphic gneisses have reveived at least three phases of deformations after the metamorphism. Most of the gneisses of the Mahoba area subjected to poly deformation and metamorphism.

The field study suggest that E-W trending brittle and ductile shear zone and related structures is developed due to comprising force acting N-S direction and

deformation across the gneissosity was active after the crystallization of the high grade metamorphic rocks. The presence of mylonitic structures in gneisses rock indicates that rock has been suffer brutile and ductile deformation. The fifth phase deformation structure are related to numerous sigmoidal tensile fissures generated as a result of an E-W sinistral brittle ductile simple shear but the secrection of quartz veins with in the reefs occurred under an approximately EW horizontal extension. Sinistral faults trending NNW-SSE to NW-SE are comman with some dextral fault as well.

2.11.2 Amphibolites and schist rocks :

Highly deformed and altered peridotites and mafic schistose rocks are the host into which the trondhjemitic gneisses intruded in the study area. Amphibolites are occurred in lenticular patches interbedded with schist (Plate-6A, 7C). The schist and quartzites have been found to be shear bands in granite.

2.11.3 Granitoids :

Well developed S-C fabric is observed at many places of granitoids rocks. They observed at Ratauli road (plate-10C) SC fabric and well developed oriented crystals of quartz and feldspar (plate VIII). E-W trending dextral shear zone have been observed at Bijanagar sagar area and Churbura village. The E-W trending shear zone is also visible at the Jhankara ridge. Northern part of the Bijanagar sagar is highly mylonitized zone. Thin to thick shear zone trending is EW and NE-SW was observed at many places.

2.11.4 Quartz reef :

NE-SW trending quartz reefs are well exposed at the Imiliya village and the Mallipura village in my study area. The emplacement of the quartz reef along NE-SW direction is related to major tectonic activity. NE-SW trending quartz reef iindicate that they were emplaced after deformation received by the metamorphism and granitoids in the study area. The two generations of quartz veins are exposed in quartz reef. The first generation of quartz veins is NE-SW direction but the generation of quartz vein is intersected by the NNE-SSW trending quartz veins.

2.11.5 Dolerite dyke :

The dolerite dyke is emplaced into the Bijanagar -sagar, Thana village, Mallipura, Paswara village. These NW-SE trending dolerite dykes are displaced the NE-SW trending quartz reefs. The dolerite dyke is fine to medium grained and black to gray in colour. In the study area medium grained 11km long dyke is well exposed which is known as great Mahoba dykes, these dykes are trending ENE-WSW prominent ridge form.

2.12 MYLONITE AND SHEAR ZONE STRUCTURES :

Mylonite can be defined as the strongly deformed rocks (due to mechanical forces applied in a definite direction) in which strain are localized in a narrow planar zone. Under conditions of high stress and moderately high temperature, wall rocks along a fault contact can be converted into cataclastic and mylonitic rocks.

The zones where the mylonitization occur are called as mylonite zone\ shear zone. Grain size reduction in the mylonite rock is mainly due to the dynamic recrystalization of original grains. The grain size reduction and the recrystalization is commonly observed in the form of foliation in the shear zone. Shear zone can be easily recognized on the basis of displacement occurs in the present rocks mass. Mylonitic foliation developed in zones of intence non coaxial laminar flow, concentration on a particular class of microstructures which we term part S-C mylonites. Where the S surface related to the accumulation of finite strain and C-surface related to localised high shear strains. In study area numerous thick to narrow shear zone of different type have been identified at several location. These shear zones are a few cm. wide to 100m long. Well developed mylonitic S-C fabric structures are available in E-W trending shear in (plate-5C). The mylonites at places vitreous appearances where commonly sinistral and rarely dextral displacement of pre existing element upto a meter have been observed. In my study area well developed SC fabric have been observed in granitoids at many places. The development of Sc tectonics in a deformed granitoids due to the accumulation of finite strains first lcd to the development of a foliation (s-surface) and later deformation lead to the formation

of cross cutting shear bands and displacement discontinue which defines the c-surface. The SC surface are clearly discernible on the mesoscopic scale and narrow shear zone of high strain. In the study area shear bands of the granite exhibits the pink and grey lamination. On the basis of chemical composition of the granite earlier worker recognized that granite rock have been sedimentary origin. In the investigated area mainly three type of shear zone have been recognized. The EW trending shear zone is very thick and exposed throughout in many places in the area under investigation. The highly deformed and mylonitized gneisses are exposed along this shear zone. In coarse grained gneisses the porphyroblasts of quartz feldspar are observed big in size and the tails of these porphyroblasts are much rotated and less recrystalized. The stretching mylonitic lineation (1cm), aligned sub parallel to main foliation is also a characterstic feature of these rocks. The anticipant lines of shear seem to have occupied by the quartz veins. A NE-SW trending shear zone are mainly visible granite gneisses and quartz reef.

2.12.1 E-W shear zone :

E-W trending shear zone are marked in gneisses, granite rocks. The well developed shearing features are observed in the form of S-C fabric. The scene of shearing is marked by rotated porphyroblast of feldspar crystal in the gneisses and granite (plate-5C and 6C).

The E-W trending shear zone have been sinistraly displaces have been seen in Bijanagar -Sagar dam, Ratauli road where the sc fabrics are clearly demarked the rotation and displacement structure. The schistocity is well observed in the bands.

2.12.2 NE-SW shear zone :

Shear zone trending NE-SW direction and dipping towards NW direction are highly exposed at Jhankhera ridge. The highly deformed and mylonitized gneisses are along this shear zone. At some places of Bijanagar- Sagar – Ratauli road the EW trending shear zone is cut across by the NE-SW trending shear (plate X). The NE-SW trending shear zone is mainly confined along the quartz reef on the basis of the field

study quartz reefs are product of shearing and mylonization. Most of the NE-SW trending shear is sinistral in nature. On the basis of field study shear zone are formed by the brittle and ductile condition. The NE-SW trending shear zones are characterized by the highly altered minerals and the hydrous minerals are dominant at the end stage of hydrothermal fluid activity. On the basis of structural study point indicate that the EW trending shearing is the oldest deformational phase of the area. The EW trending shears are cut across by the NE-SW trending shear zone.

Table: 2.2 Stratigraphic Succession of the Bundelkhand craton

Pascoe, 1950	Prakash et. al. 1975	Sharma, 1982	Basu, 1986 & 2001	Present Study
Vindhyan System	Vindhyan Supergroup	Vindhyans	Vindhyan Supergroup	Vindhyan Supergroup
Bijawar Series	Bijawar and Gwalior Group	Bijawars	Bijawar, and Gwalior Group	Bijawar and Gwalior Groups
	Madura Formation : (Pre-to-post-Bijawar age) :	**Bundelkhand Group**	Madaura basic, ultrabasic coarse intrusives	Madaura Ultrabasics
	a : dolerite dykes, granite member, quartz vein pegmatite, graphic granite, b : Gabbro member : coarse to medium grained gabbro, pillow lava, ultrabasic member; milky dense sheared veins quartz.	**Madura ultrabasic :** Pyroxenites, gabbro, serpentine, metabasic.	Dolerites	Mafic Dyke swarms
Peridotites, pyroxenites (partially altered to serpentinites and talc-actionlite dolerite-trap dykes)		**Mahoba Dolerite :** Dolerite dyke, keratophyres, lamprophyres, carbonatite.	Quartz reefs (mega veins along shear zones)	Quartz Reef
	Bundelkhand granite Formation:		Esmeraldite	
	Dull pink, dense fine grained to porphyritic granite : coarsely crystalline pink un-foliated granites and migmatities.	**Matatila Granite :** Pink granite, coarse to fine, massive.	Porphyry dykes	
		Garhmau granite : Grey, coarse to fine, massive, porphyroblastic gneisses.	Aplite	**Bundelkhand Granitoids:**
		Paron meta-acid volcanics : Porphyroblastic, compact, sheet like granitic rocks.	Pegmatite	Fine grained leucogranite
	---- Unconformity -----		Leucocratic granites	Coarse grained leucogranite
			Migmatites, & syenites	Foliated biotite granite
			Medium porphyritic granite	Biotite granite
	Berwar Formation :	**Palar Formation :** Quartzite, phyllite, spotted phyllite, black shale, limestone, ferruginous quartzite with trace of chalcopyrite, galena, malachite, secondary.	Coarse porphyritic granite	Hornblende granite
	Iron-formation, carbonate rock, grey green slates, Fuchsite quartzsite and conglomerate.		Hornblende granite	
			Coarse biotite granite	
	---- Unconformity ----	---- Unconformity ----	Intrusive gneisses.	**Bundelkhand Metasedimentaries and Metavolcanics :**
			--- Unconformity ----	Metavolcanics
	Rajaula Formation :	**Kuraicha Formation :**	**Pre Bundelkhand Rocks:**	Banded Magnetite Quartzite, micaceous quartzites, commingtonite-grunerite-garnet-magnetite schist, talc-chlorite schist, actinolite-tremolitte-talc schist, hornblende-chlorite-epidote schist, garnet-chlorite-actinolite schist
Bundelkhand Granite Complex with quartz reef, and with inclusions of Mahroni schist.	Sedimentation- volcanism (amphibolites, biotite-feldspar foliated gneisses.)	Magmatites, gneisses, para-, ortho- and augen gneisses, amphibolite, chlorite and biotite schists, quartzites, meta-arkose, garnet-biotite gneisses.	Madla Fm: phyllite, schist, micaceous quartzite, banded amphibolite.	**Bundelkhand Gneissic Complex:**
			Older supracrustals: Banded iron-formation, streaky gneisses, marble, calc-silicate, sillimanite schists, metamorphosed mafics and ultramafics, amphibolites.	Biotite-gneiss, hornblende-biotite gneisses, sillimanite gneisses, amphibolite, garnet-sillimanite gneisses. Tonalite-trondhjemite granodiorite, granite-gneisses and migmatites.

Deformation and Mesoscopic Structures

Litho unit	Sharma 1982	Basu, 1986 & 2001	Roday, et al., 1995	Prasad et al., 1999	Present Study
Basic Dykes	NW-SE trending mafic dykes swarm displaced.	Swarms of NW-SE dolerite dykes along en-echelon fractures cutting across NE-SW trending quartz reefs, mainly along southern border zones.			Dolerite dyke swarms evidence of extensional tectonic and mark last phase of thermal activity, unaffected by deformation. General trend NW-SE and across the NE-SW trending quartz reefs.
Quartz Reefs	NE-SW trending reef, secondary quartz veins observed.	NE-SW trending quartz reefs along intermittent shear zones, displaced granites, BMQ & porphyry; closely spaced in west than in east, southern boder zone free from veins; Sigmoidal schistose bodies due to E-W couple; E-W shears.	Cataclastic & mylonitic nature, & sigmoidal quartz veins brittle-ductile shear displaced sinistrally the BIF.		Quartz reef in NE-SW trend, product of brittle ductilte deformation. Sigmoidal quartz veins developed within the main body of reef in late stage deformation. Displaced low and high-grade metamorphic rocks sinistrally. At places quartz reef displaced sinistrally by NW-SE trending faults. (D_6 Deformation).
Bundelkhand Granitoids	Two phases of deformation (D_4&D_5). Upright to steeply inclined folds (F_4) trending between W& NW.	Biotites in thin streaks; long axes of feldspar in preferred foliation and lineation; shearing at the borders of intrusive granites; joints common; gneissose structure streaky; local late stage migmatitisation aided by deformation; floating ductile shear bands dismembered.	Two-phases of deformed shear zones. Both steeply or vertical dip. E-W sinistral shearing and NE-SW dextral shearing, brittle ductile nature. Minor sinistral and dextral strike ship faults observed.	E-W trending dextral shear zones (DS) observed where subhorozontal stretching lineation were also developed	The hornblende granitoids and biotite granite emplaced along E-W trending fracture zones. E-W trending dextral and sinistral shear zones. S-C and S-C^l fabrics developed in granite and felsic volcanics. E-W trending dextral & sinistral shear zones indicates brittle ductile nature. Rare augen structure, sheath fold and subhorizontal lineation occurred in D_3 and D_4 deformation. Shear zones are ductile to brittle ductile in nature. Three phases of simple shear deformation recorded from granites.
Bundelkhand Metasedimentaries and Metavolcanics (Palar/Berwar Formation, BMQ, Quartzites, Meta-volcanics.)	Two phases of deformation (D_4&D_5). Upright to steeply inclined folds (F_5) trending between W and NW. Alternate bands of magnetite and quartz observed.	Bedding by alternate magnetite – quartz layers; trending E-W with steep dip (65^0) due north; tight similar fold, axes parallel to the strike of the body, plunging west; joints common; BMQ bands more continuous along southern border, disemembered and more folded to the north	Folds generally tight to isoclinal, overturned to the south or north, F_2 folds are variably oriented co-planner with F_1 fold. F_2 fold structures are sinusoidal folds or single or conjugate rock bands.	E-W trending sinistral shear zones (D_4), S-C mylonite, ultramylonite developed. E-W trending dextral shearzone (D_5) observed. Tight to isoclinal & reclined F_1 folds tight to open (F_3) and tight to reclined (F_2) folds observed.	E-W trending dextral shear (D_4) zones, sub-horizontal stretching lineations mylonites and ultra mylonites. Intense schistosity at the contact between meta-sedimentary and meta-volcanics indicate sinistral shearing. Four phases of deformation recorded. Development of S_1 and S_2 schistosity in the meta-sedimentaries and meta-volcanics. Tight to open folds, axial surface trend NW-SE to NE-SW, folds axes plunging towards north. N 80 E trending (BIF) beds steeply dip towards north.
Bundelkhand Gneissic Complex (Rajaula/Kuraicha Formation: Migmatites, Mehroni schists, Gneisses, Amphibolites etc.)	Five phases of deformation (D_1, D_2, D_3, D_4 and D_5). F_1 folds–tight isoclinal, hinge trending E-W. F_2 folds open to tight upright, coaxial to F_1, hinge trending E-W. F_3 folds sub-vertical and steeply plunging. F_4 folds upright steeply plunging. F_5 folds – upright.	Banded gneiss absent; mafic minerals as lenticles, strike trend NE-SW dip north westerly and WNW-ESE strike steep dip south westerly forming synform; metabasic enclaves restitic but without ghost structure.	F_1 fold observed initially developed in diorite to tonalitic rocks and developed sinistral shear zones.	Steep, E-W trending shear zones gave sinistral sense (D_4) and dextral (D_5) sense, D_1, D_2, D_3 as folds. NW-SE to EW trending axial surface (D_1 & D_2) and NW-SE to NE-SW (D_3) axial trend. Folds (F_1, F_2, F_3) are isoclinal to tight reclined and open types.	Tight to isoclinal fold (F_1), axial plane NW-SE to E-W trend and plunging towards NW. F_2 folds – tight to reclined, co-axial and co-planer with F_1. Tight to open fold (F_3), axial plane trending NW-SE to NE-SW plunging towards north. Sheath and quartz ribbons observed in the shear zone of gneisses. Six phases of deformation recorded

Table 2.4
Radiometric dating of rocks of Bundelkhand

S. No.	Location & Rock Type	Method	Age in M.a.	Reference
1.	Majhgawn Kimberlite plug		1140±20	Crawford & Compston, 1970 and Mathur, 1960
2.	Vindhyan Sedimentary Rocks		~1600	Rasmussen et al., Roy et al., 1990
3.	Alipura Mafic Dyke	K-Ar	1523	Sarkar et. al., 1990
4.	Kurat Volcanic rocks	Rb-Sr	1691±180	Pandey et. al.,1995
5.	Dargawan Mafic rocks as Sill (Bijawar Basin)	Rb-Sr	1789±71	Sarkar et. al., 1997
6.	Kalinjar Fort Mafic dyke	K-Ar	1799	Sarkar et. al., 1990
7.	Mafic volcanics (associated with Gwalior Sedimentary Rocks)	Rb-Sr	1830±200	Crawford & Compston, 1970
8.	Quartz Reef		2000	Sharma & Rahman
9.	Bdera Gneissic migmatite	Rb-Sr	2130±102	Sarkar et. al., 1984
10.	Coarse grain granites, granite porphyry and Aplite (Babina Talbehat)	Rb-Sr	2246±78	Sarkar et. al., 1984
11.	Grey granodiorite near Jhansi	Rb-Sr	2359±53	Sarkar et. al., 1984
12.	Granodiorite near Jhansi	Rb-Sr	2402±70	Sarkar et. al., 1990-1996
13.	Bansi Rhyolite	Pb^{207}/Pb^{206}	2517±7	Mondal et. al; 2002
14.	Lalitpur Biotite Granitoid	Pb^{207}/Pb^{206}	2521±6	Mondal et. al; 1998.
15.	Bansi Rhyolite	Pb^{207}/Pb^{206}	2521±7	Mondal et. al; 1998.
16.	Granites	Rb-Sr	2560±106	Crawford, 1970
17.	Karera Gneisses	Pb^{207}/Pb^{206}	2563±6	Mondal et. al; 2002
18.	Pillow lava (nearBijawar)		2600	Crawford & Compston, 1970
19.	Bansi Rhyolite	Pb^{207}/Pb^{206}	2517±7	Mondal et. al; 2002
20.	Lalitpur Biotite Granitoid	Pb^{207}/Pb^{206}	2521±6	Mondal et. al; 1998.
21.	Bansi Rhyolite	Pb^{207}/Pb^{206}	2521±7	Mondal et. al; 1998.
22	Granites	Rb-Sr	2560±106	Crawford, 1970
23	Karera Gneisses	Pb^{207}/Pb^{206}	2563±6	Mondal et. al; 2002
24	Pillow lava (nearBijawar)		2600	Crawford & Compston, 1970
25	Migmatitic Gneisses	Pb^{207}/Pb^{206}	2696±3	Sharma et. al; 1998
26	Babina Gneisses	Pb^{207}/Pb^{206}	2697±3	Mondal et. al; 1998.
27	Panchwara Gneisses	Pb^{207}/Pb^{206}	3189±5	Mondal et. al; 1998.
28	Lodhaphar gneisses	Sm-Nd	3200	Sharma & Rahman
29	Mahoba Amphibolites	Pb^{207}/Pb^{206}	3249±5	Mondal et. al; 2002
30	Mahoba Gneisses	Pb^{207}/Pb^{206}	3270±3	Mondal et. al; 2002
31	Kuraicha Gneisses	Pb^{207}/Pb^{206}	3297±8	Mondal et. al; 2002
32	Lodhaphar gneisses	Sm-Nd	3300	Sharma & Rahman 1995,1996
33	Baghora Gneisses(TTG)	Rb-Sr	3503±99	Srkar et. al; 1996

Table-2.5

	Litho Unit	Deformation	Tectonics, metamorphism and magmatism
POST BUNDELKHAND GRANITOID (2300_1600MA)	**Basic Dykes**	D_6 (2000 Ma to 1800 Ma)	General trend of dyke is NW-SE, displaced sinistrally the quartz reefs trending NE-SW. Alteration along the shear zones, crystllised the minerals chlorite, muscovite, seriate, epidote, pyrite, pyrophyllite and diaspore. No metamorphism at the contact of basic dyke and country rock. Dolerite dykes in craton spread over the massif in the form of swarms is the evidence of extensional tectonic and Last phase of magmatism in the region
	Quartz Reefs	D_5 (2300 Ma to 2000 Ma)	NE-SW trending quartz reef, formed in the brittle - ductile deformational environment. Alteration of feldspars and amphibole minerals. Development of phyrophyllite, diaspore, kaolinite, epidote, chlorite, sericite are the indication of hydrothermal activity. Sigmoidal veins developed within the main body of reef at the late stage of deformation. Quartz reefs displaced the older rocks, marks the dextral shearing. Quartzite and Pegmatite emplaced in NE-SW direction
SYM BUNDELKHAND	**Granitoids (BG)**	D_4 (2600 Ma to 2500 Ma)	Mortar texture, recrystallization of chlorite, biotite, feldspars, andalusites developed in E-W trending mylonites zone suggests local thermal metamorphism. Dextral and sinisterly shearing, E-W trending shear zones in the brittle ductile environment, augen structures and sub-horizontal lineation were also occurred in gneisses, TTG rocks of BnGC. E-W trending dextral shearing. Sub-horizontal stretching lineation, mylonites and ultra-mylonites developed along E-W in BMM. E-W trending shear zone with S-C and S-C fabrics are observed in dextral and synistral shears developed in granite BnGC and BMM. Hbl. Granite, Bio Granite, deformed granite, Leucogranite
PRE BUNDELKHAND (3500_2600MA)	**Bundelkhand metasedimentary and metavolcanics (BMG)**	D_3 (3200 Ma to 2600 Ma)	The NW-SE trending fabrics in the gneisses rotated to E-W. Prograde M_2 metamorphic rocks of green schist to lower amphibolites facies developed in BnGC (mafic and ultra mafics with volcano-sedimentary rocks). Act-Tre-schist, micasceous, quartzite, BMQ, Qtz. schist, Com- Gru. schist formed Tight to open folds with axial surface trending NW-SE to NE-SW, plunging towards north.M2 event of metamorphism recorded Deposition of banded iron formation, feruginious quartzite, mafics and ultramafics, vocanosedimentary rocks in epicontinental sea
	Bundelkhand Gniessic Complex (BnGC)	D_1 & D_2 (3500 Ma to 3200 Ma)	Hook folds, Tight to isoclinal fold F_1, F_2 folds coaxial with F_1 plunging towards NW, axial plane trending NW-SE to E-W. Tight to open fold F_3, plunging north, axial plane trending NW-SE to NE-S developed in D_2deformation.F_3 fold post date the metamorphism M_1, formed during D2 deformation. Gneisses, migmatites, granite-gneisses, streaky gneisses, biotite-hornblende gneisses, calc silicate granulites, garnet- sillimanite gneisses were formed (M_1 metamorphic).

Table 2.6: Tectono-thermal events in the Bundelkhand Massif

Litho Unit	Magmatism, metamorphism and Tectonics	Deformation	Events
Basic Dykes	General trend of dykes is NW-SE, displaced sinistrally the quartz reefs trending NE-SW. No metamorphism of host rock at the contact. Dykes mainly in southern bordering areas as single bodies and swarms, evidence of extensional tectonics and last phase of magmatism in the massif. Alteration along the shear zones, crystllised minerals like chlorite, muscovite, sericite, epidote, pyrite, pyrophyllite and diaspore.	D_6 (2200 Ma to 2000 Ma)	Mafic Emplacement
Quartz Reefs	NE-SW trending quartz reef formed in the brittle - ductile regime. Alteration of feldspars and amphibole minerals. Development of phyrophyllite, diaspore, kaolinite, epidote, chlorite, sericite along the NE-SW trending quartz reefs; pointing to hydrothermal activity. Sigmoidal quartz veins within the main body of reef at the late stage of deformation. The brittle ductile to ductile brittle shears developed in the gneisses, migmatites and lowgrade metamorphics. Quartz reefs displaced the older rocks, marks the dextral shearing in the massif. Quartz reefs and Pegmatite emplaced in NE-SW and N-S directions in the granites, gneisses and low grade metamorphics	D_5 (2300 Ma to 2000 Ma)	Granite and Pegmatite intrusion Hydrothermal activities and Quartz Reef
Bundelkhand granitoids	E-W trending dextral and sinistral shear zones in the brittle-ductile regime; augen structures and sub-horizontal lineation occurred in the rocks of BGC as well as in BMM. Sub-horizontal stretching lineation, mylonites and ultra-mylonites developed. E-W trending shear zone with S-C and S-C′ fabrics in dextral and sinistral shears developed in granite. Hornblende Granite, Biotite Granite, Leucogranites emplaced in the entire massif in collision tectonic environment.	D_4 (2500 Ma to 2400 Ma)	Granite Emplacement
Bundelkhand Meta volcanics and Meta sedimentaries	Tight to open folds with axial surface trending NW-SE to NE-SW, plunging towards north recorded D_3. The NW-SE trending fabrics in the gneisses rotated to E-W during the D3 deformation. Prograde (M_2) metamorphic rocks of green schist to lower amphibolites facies developed in BMM (mafic and ultra mafics with volcano-sedimentary rocks). The deposited metasediments and metavolcanics were subjected to low-grade (Greenschist to lower Amphibolite facies) metamorphism. Actinolite-Tremolite schist, micasceous quartzite, BMQ, Qtz schist, Cummingtonite-Grunerite schist formed. M_2 event of metamorphism. Deposition of banded iron formation, ferruginous quartzite, mafics and ultramafics, vocanosedimentary rocks in epicontinental sea.	D_3 (3200 Ma to 2600 Ma)	Sedimentation and Volcano activities Low-grade metamorphism M2
Bundelkhand Gneissic Complex	Tight to isoclinal fold F_1, hook folds, F_2 folds coaxial with F_1 plunging towards NW, axial plane trending NW-SE to E-W developed in D1deformation. Open fold F_3, plunging north, axial plane trending NW-SE to NE-SW, postdate the metamorphism M_1, formed during D2 deformation. Gneisses, migmatites, gray granite-gneisses, TTG, streaky gneisses, biotite- hornblende gneisses, calc silicate granulites, garnet-sillimanite gneisses, garnet cordierite gneisess, anthophyllite-talc gneisses (M_1 metamorphic event).	$D_1 \& D_2$ (3500 Ma to 3200 Ma)	High-grade metamorphism M1

Table-2.7

Geology of Study of Bundelkhand Craton

Quartz reefs	Quartz reefs
Mafics	Mafic Dykes and Swarms
Bundelkhand granitoids (Acid Magmatism) (12500-2600 Ma)	Fine grain leuco granite Coarse grain leucogranite Foliated biotite granite Biotite granite Hornblende granite
Pre- Bundelkhand granitoids (Bundelkhand Gneissic complex) 73300 Ma	Talc-chlorite schist, actinolite-tremolitte- talc schist, hornblende- chlorite -epidote schist Biotite- gneiss, hornblende-biotite gneisses, sillimanite gneisses, amphibolite Tonalite-trondhjemitegneisses, granite-gneisses, migmatite,
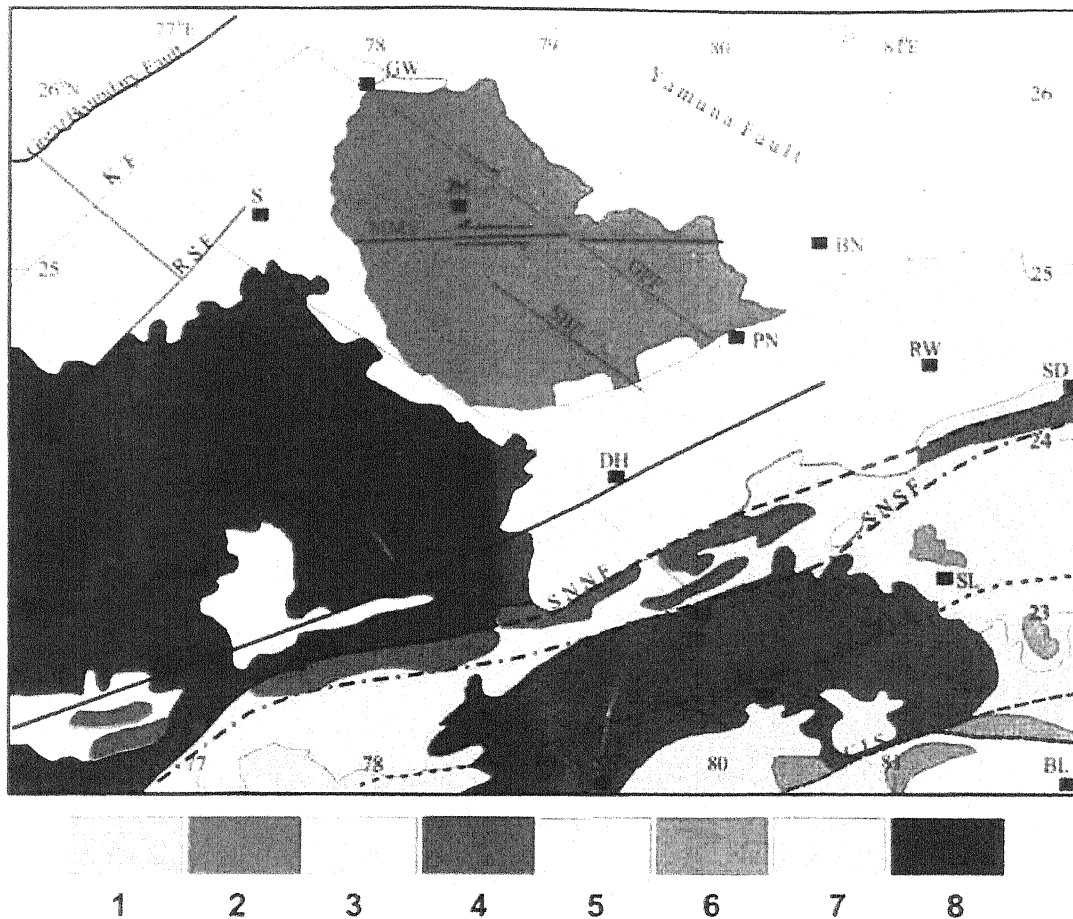
Fig-2.1: Geological and tectonic map of Central India after Yadekar *et al.* (1990), Jokhan Ram et al. (1996), Raza and Casshyap (1996) Acharya and Roy (2000), Ramchandra and Roy (2001), and Acharya (2003). 1. Gneisses and Migmatites with supracrustal rocks, 2. Bundelkhand Granitoids with BnGC, 3. Vindhyan Supergroup, 4. Mahakoshal Group, 5. Bijawar and Gwalior Group, 6. Sausor Group, 7. Gondwana Supergroup and 8. Deccan Traps. Abbreviations. BH-Bhopal, BL-Bilaspur, BLF-Balarampur Tatapani Fault, BN-Banda, CIS-Central Indian Shear Zone, DH-Damoh, GPF- Gwalior-Panna-Fault, HOS-Hosanabad, JB-Jabalpur, JH-Jhansi, KF-Kota Fault, MAN-Mandla, PN-Panna, RBN-Ratlam-Basoda-Narsingargh Fault, RSF-Ratlam-Shivpuri Fault, RW-Rewa, S-Shivpuri, SD-Sidhi, SE-Seoni, SG-Singrauli, SL-Shahadol, SNNF-Son-Narmada-North Fault, SNSF-Son-Narmada-South Fault, SBF: Sahagarh-Babina Fault MMS: Mohar-Mauranipur-Mahoba Shear.
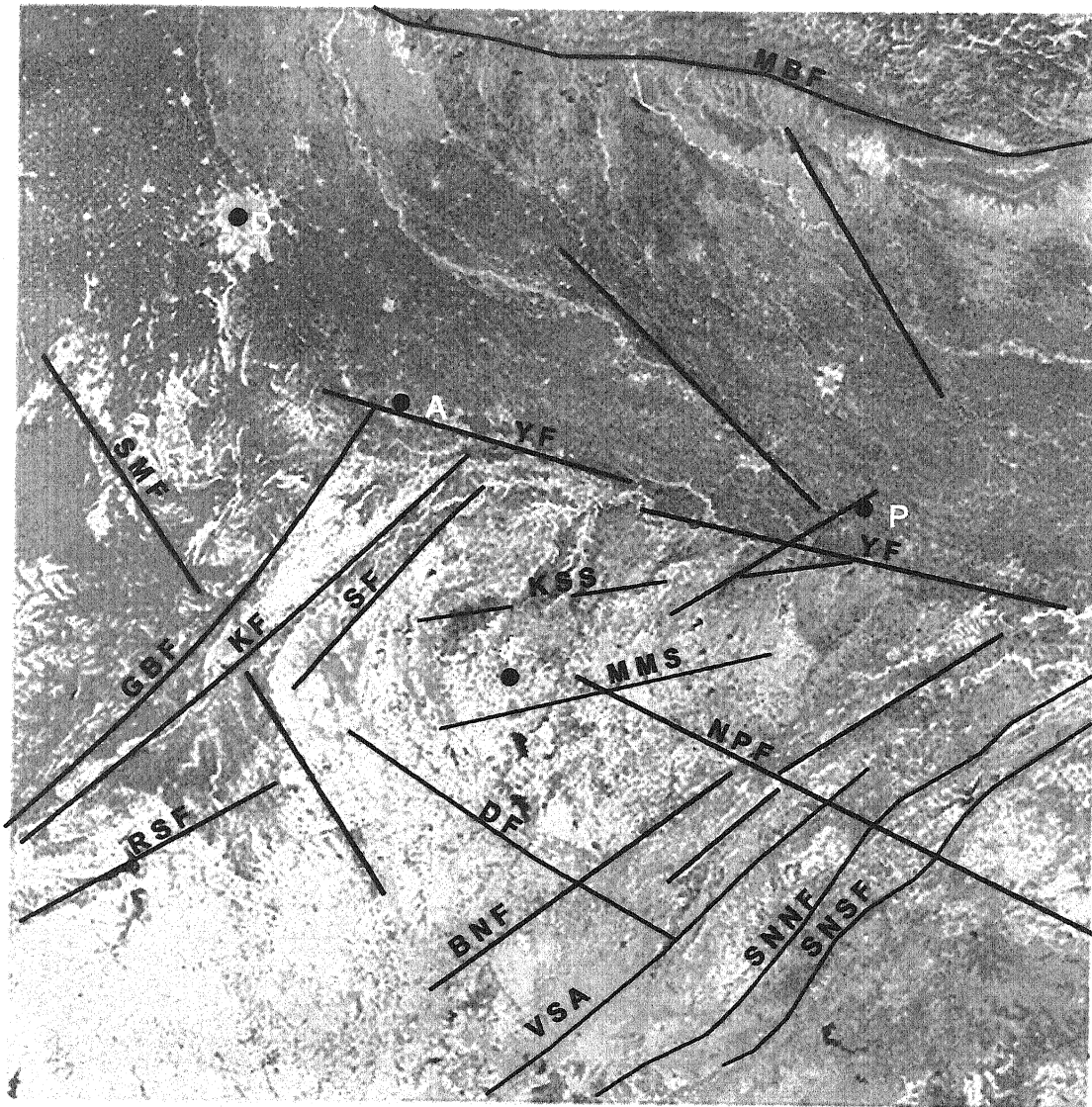
Fig-2.2: Regional Lineament map around Bundelkhand Craton interpreted from Resourcesat 1 IRS-P6 AWIFS Image FCC, 4,3,2 RGB. Abbreviations- A:Agra, D-Delhi, J: Jhansi, BNF: Basoda-Narsingargh-Fault, DF: Damoh fault, GBF-Great Boundary Fault, KF: Kota Fault, KSS: Kalpi-Shivpuri Fault, MMS: Mohar Mauranipur Mahoba Shear zone, MBF: Main Boundary Fault, NPF: Naogaon-Gwalior-Panna Fault, RSF: Ratlam-Shivpuri Fault, SF: Siivpuri Fault, SNNF: Son-Narmada-North Fault, SNSF: Son-Narmada-South Fault, VSA: Vindhyan synclinal axis, SMF: Sawai Madhopur Fault, and YF: YamunaFault
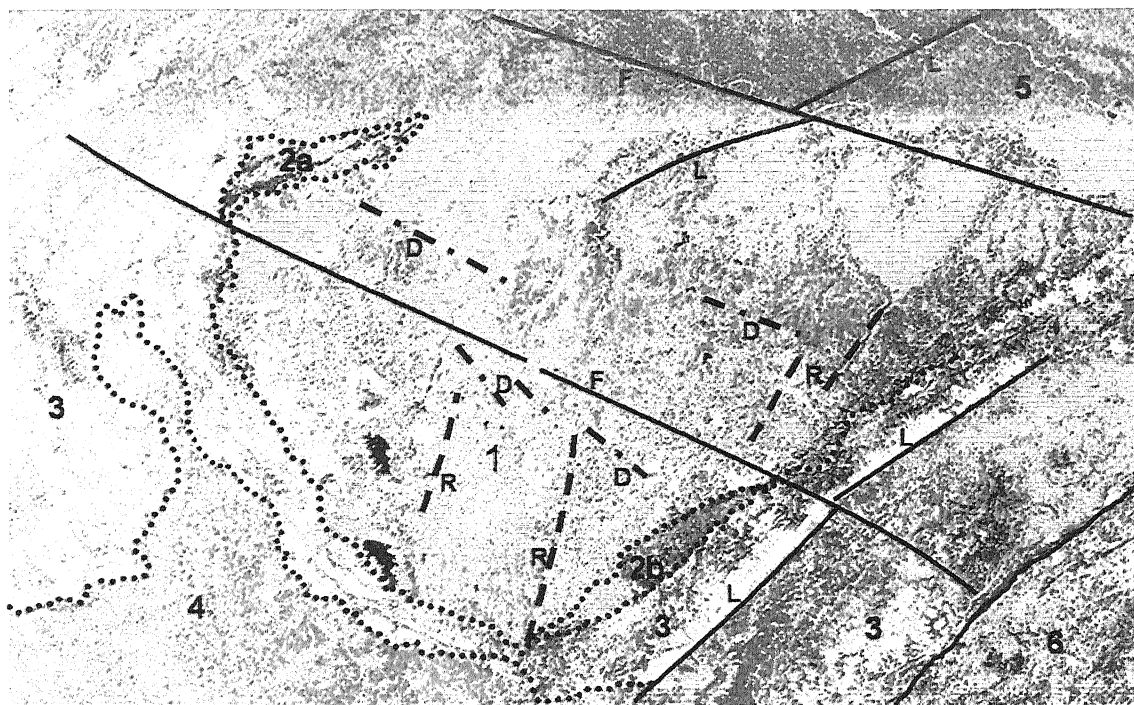
Fig.-2.3: Tectonic framework and geological map of Bundelkhand craton and adjoining areas, interpreted from Resourcesat 1 IRS-P6 (AWIFS Image FCC, 4,3,2 RGB). 1. Bundelkhand massif, 2a. Gwalior Group, 2b. Bijawar Group, 3. Vindhyan Supergoup, 4. Deccan Volcanics, 5. Gangetic alluvium, 6. Mahakoshal Group. F. Fault, L. Lineament, D. Basic Dyke, R. Reef
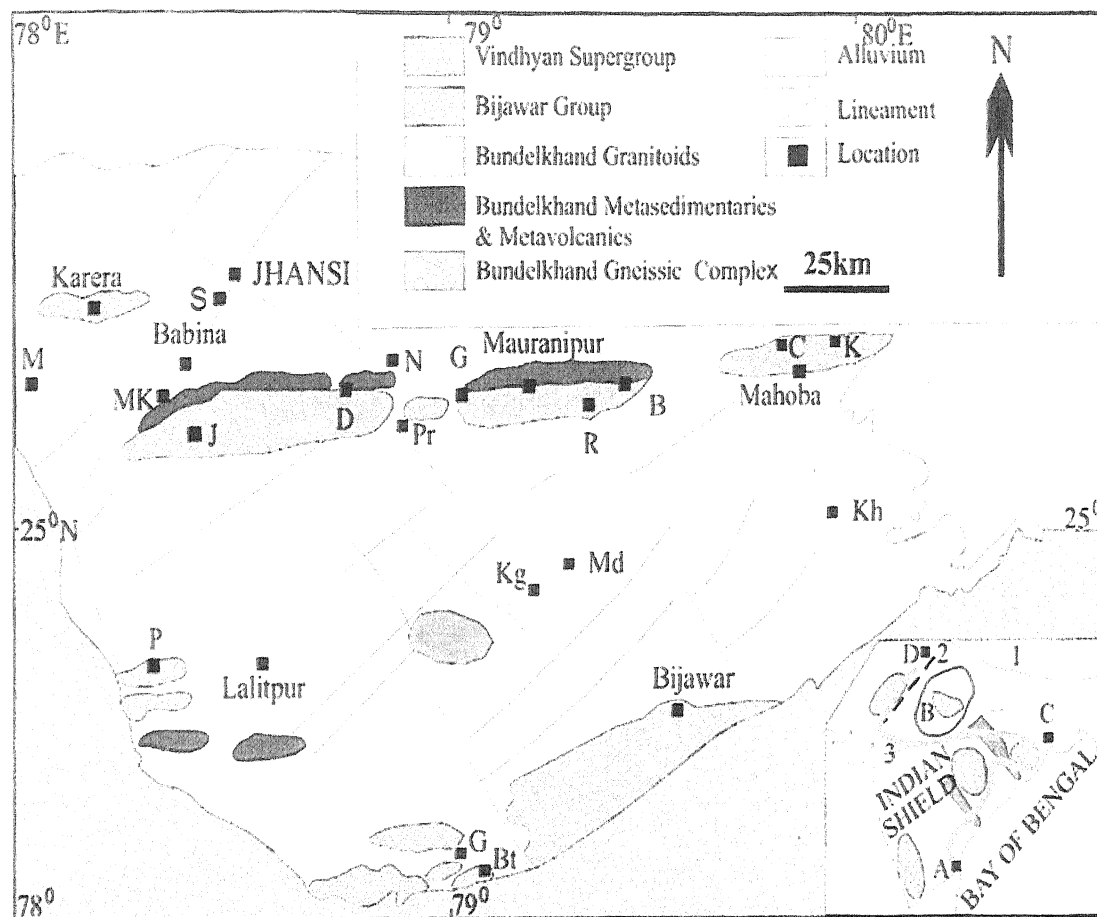
Fig.-2.4: Geological map of Bundelkhand craton (modified after Basu 1986 and Mondal et al. 2002). The metamorphic rocks (BnGC and BMM) older than Bundelkhand granitoids are mainly exposed in the central part of the massif along Mohar-Babina-Mahoba transect. Abbreviations- D: Dhaurra, G: Gora, M: Mohar, MK: Mankua, S: Shivgarh, B: Baragaon, P: Panchwara, R: Roni, Pr: Prithivipur, Kg: Khargapur, Md: Madla, G: Girar, Bt: Baraitha, Kh: Khajuraho, N: Niwari, C: Charkhari, J: Jaunpur and K: Kabrai. The inset shows the position of different cratons and nucleus in the Indian shield. The thick curvilinear line showing the trend of position of Middle Proterozoic mobile belt, passes around the Bundelkhand craton (after Radhakrishna and Naqvi 1986). Abbreviations- A: Madras. B: Bundelkhand craton, C: Calcutta, D: Delhi, 1: Himalayan folded belt, 2: Great boundary fault and 3: Son-Narmada-Lineament
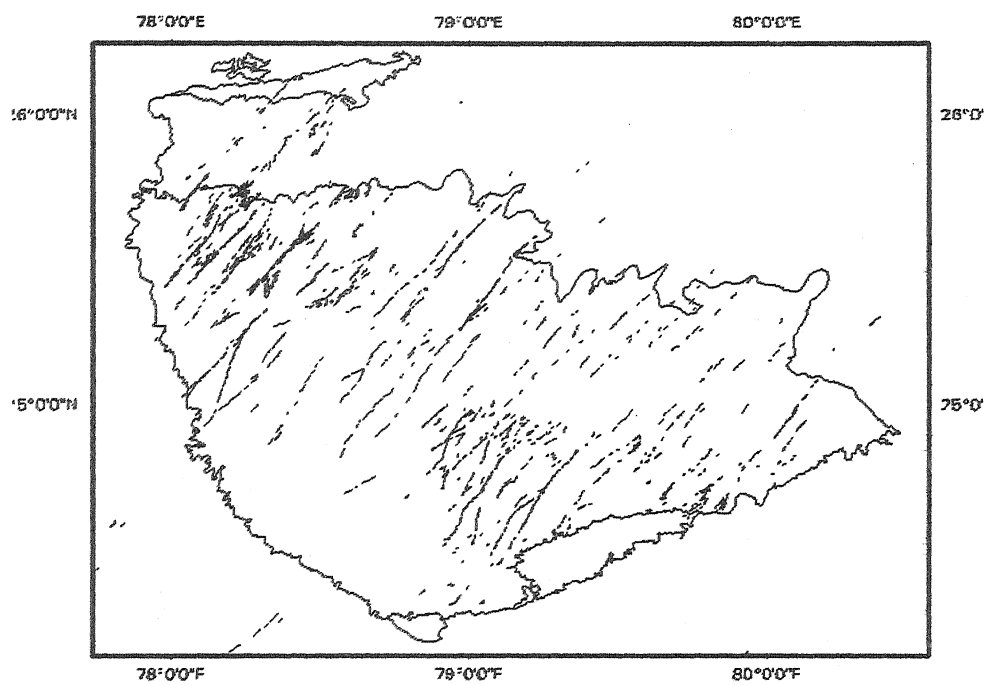
Fig.-2.5: Lineament trand of the quartz reef and maffic dykes in Bundelkhand massif based on the IRS P6.

Satellite Data of study area
IRS-1D, LISS-III
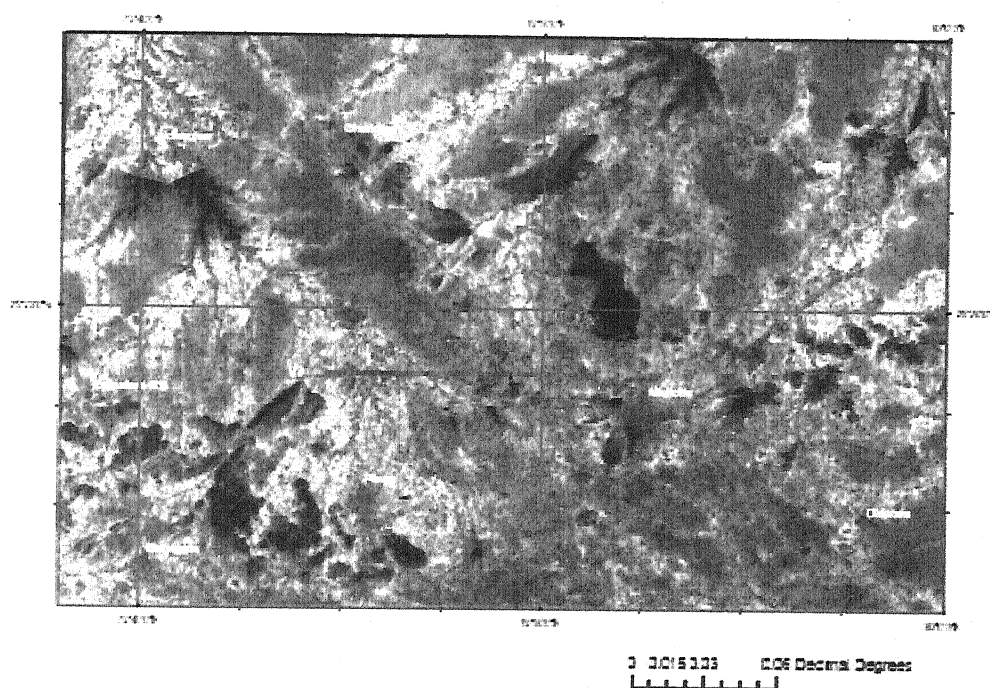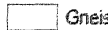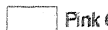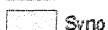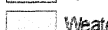
Fig.-2.6a: Imagery of the study area
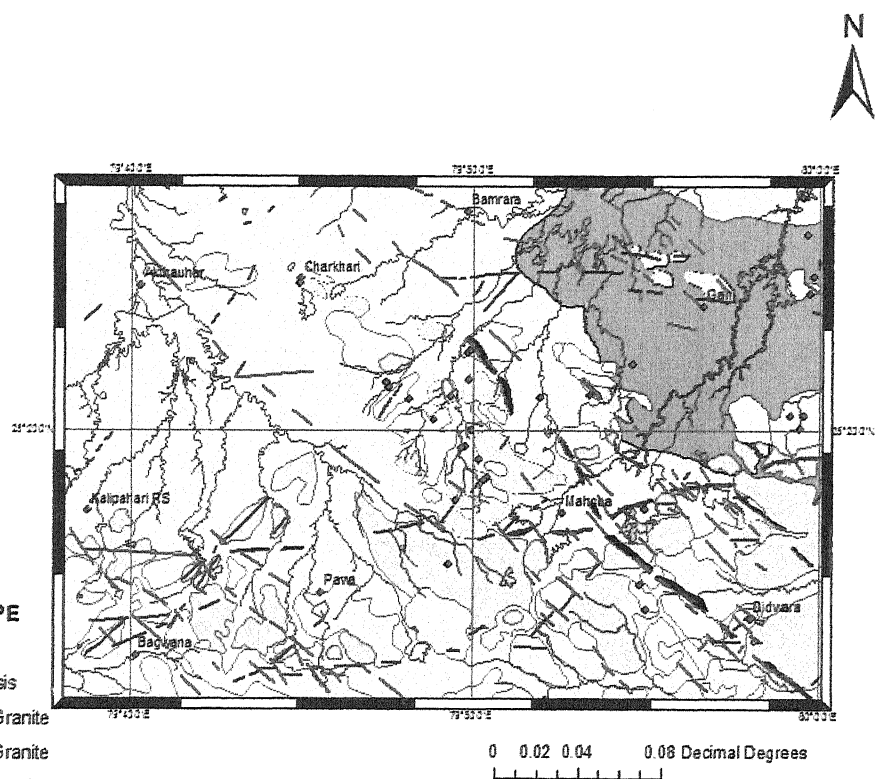
Fig.-2.6b: Geological map of the Mahoba area
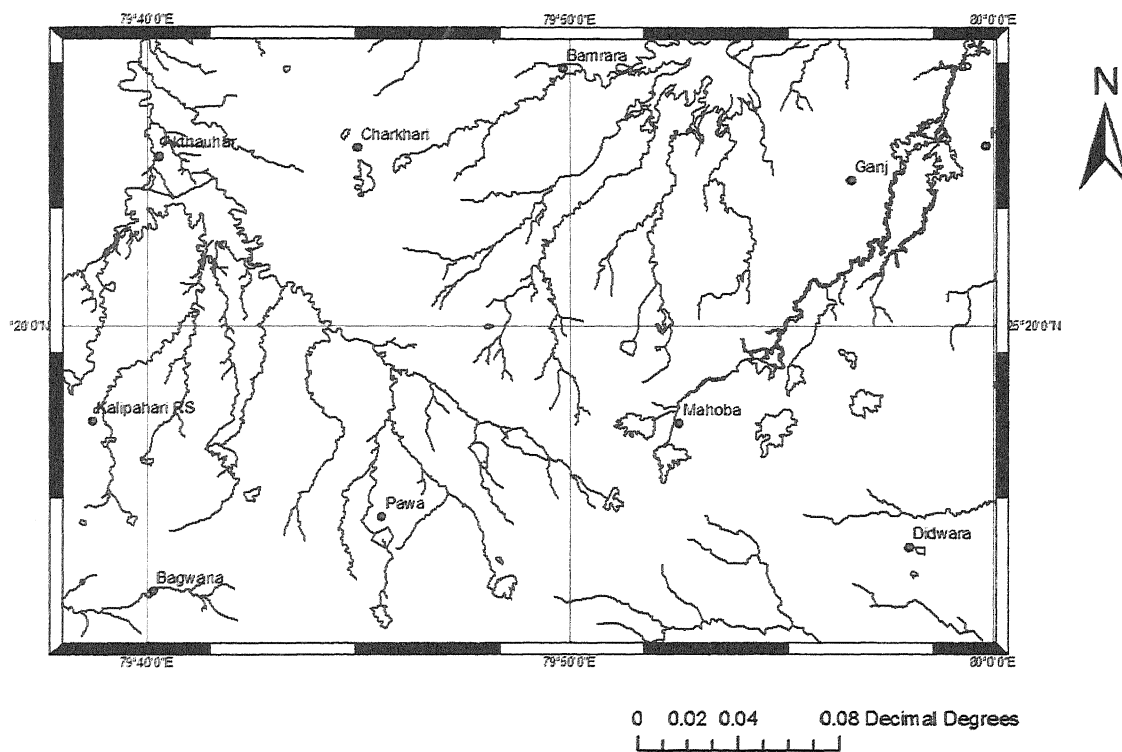
Fig.-2.7 : Drainage Map of the study area based on IRS-1D data .
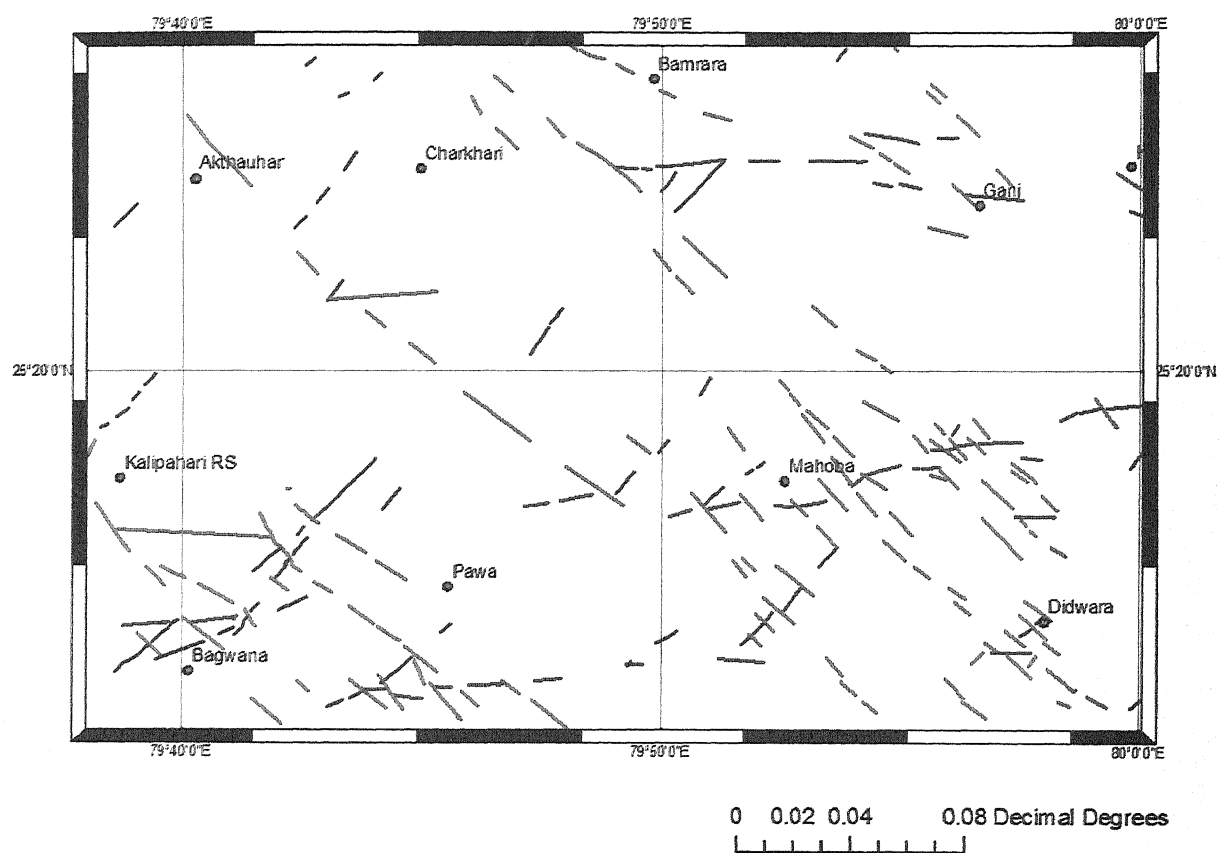
Fig.- 2.8 : Lineament map of the study area based on IRS-1D data

PLATE-1
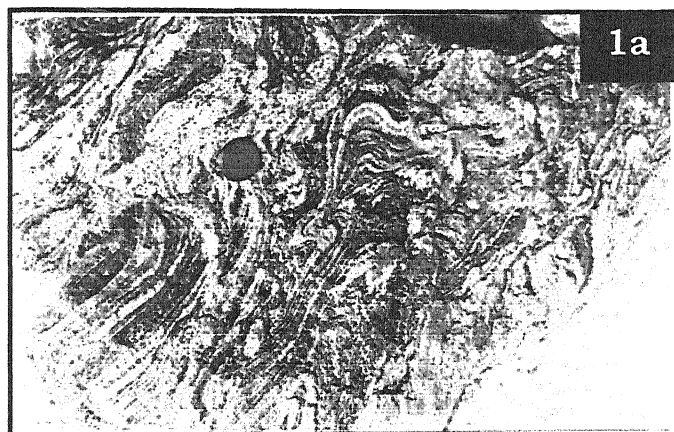
1a : Field Photograph of Gneisses exposed at Nathupura. F_1 to F_3 folding

1b : Field Photograph shows two generation of F_1 and F_3 folding in gneisses near Jankhera

1c : Photograph shows tight folding in gneissic rock and subsequently to mylonitised defined by S-C fabrics

PLATE-2
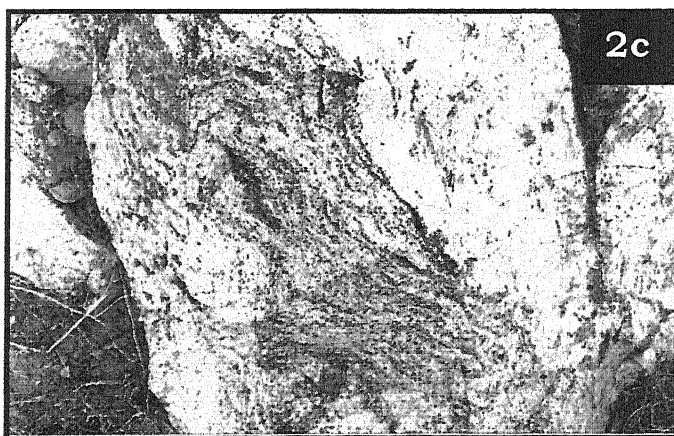
2a : Partial melting signature and ptegmatic fold in the gneisses rock exposed at village Nathupura

2b : Sharp contact of gneisses with undeformed grey granite at village Nathupura

2c: Field Photograph shows Xenolithic enclaves of gneisses in Leucogranite rock at Sahapahari

PLATE-3
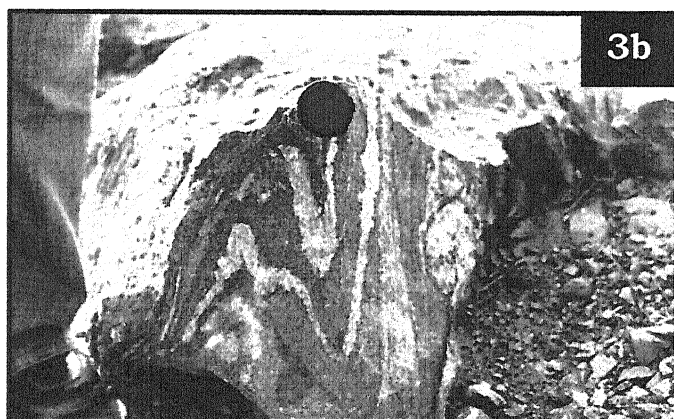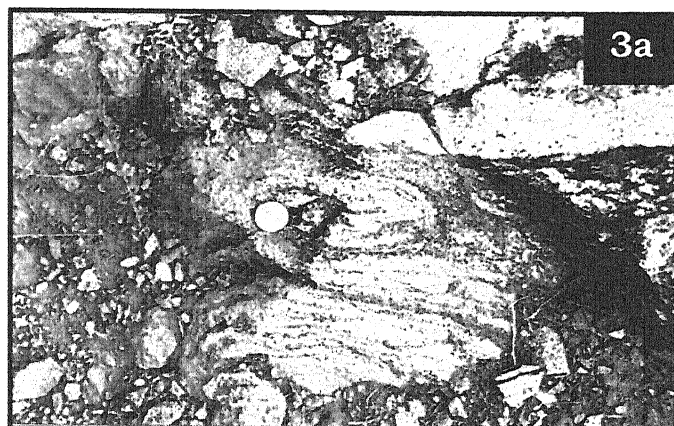
3a : Hook folds in gneisses rock exposed at Mahoba to Charkhari road

3b : Refolded structure from TTG gneisses exposed at Nathupura Village

3c : S-type shear fold in the gneisses at Nathupura

PLATE-4

4a : Magmatite bearing gneisses and F_1 fold at Nathupura

4b : High-grade gneisses exposed at S-W of Lodha-Pahar containing pegmatite vein along S-C fabrics

4c ; Photograph of gneisses showing isoclinal fold and S shear fault planes are also present
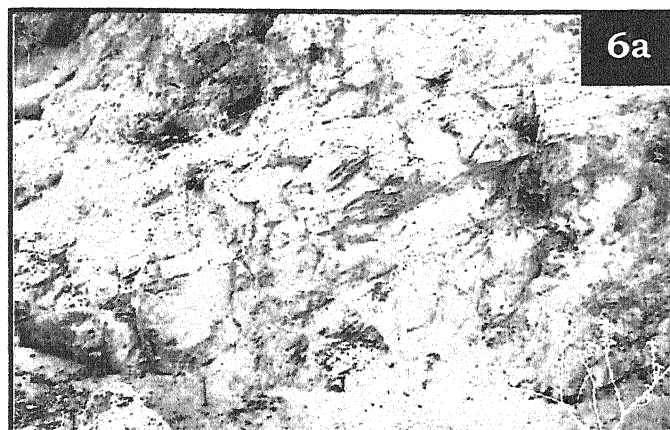
PLATE-5
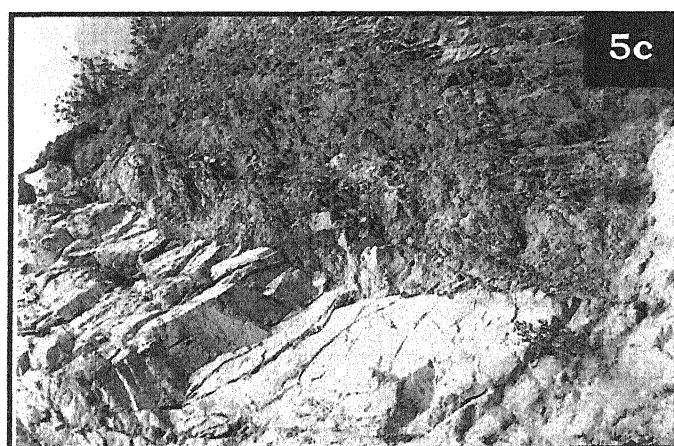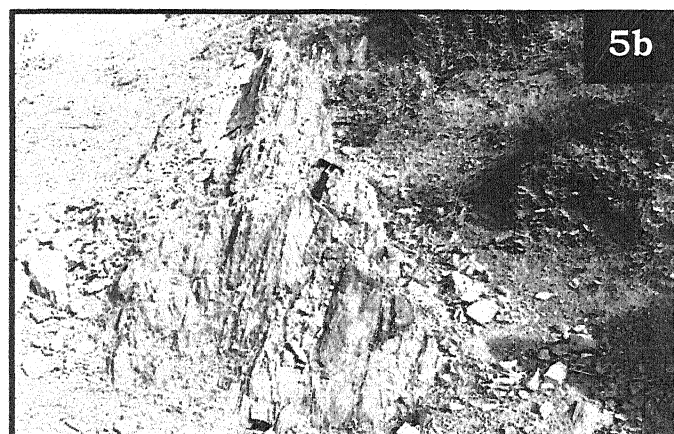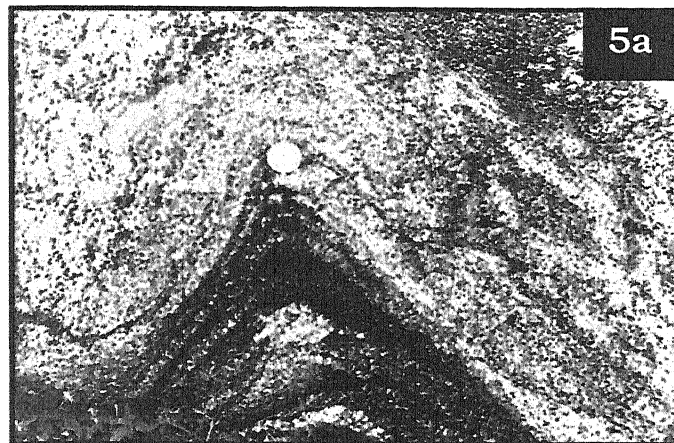
5a : Field photograph of gneissic enclave in the biotite granite, showing F1 and F2 folding and melting [The enclaves in biotite granite at Mahoba railway station].

5b : Field photograph at southern part of Lodha Pahar showing inclined shear zone. The inclined shear zone from biotite-silliminite gneisses
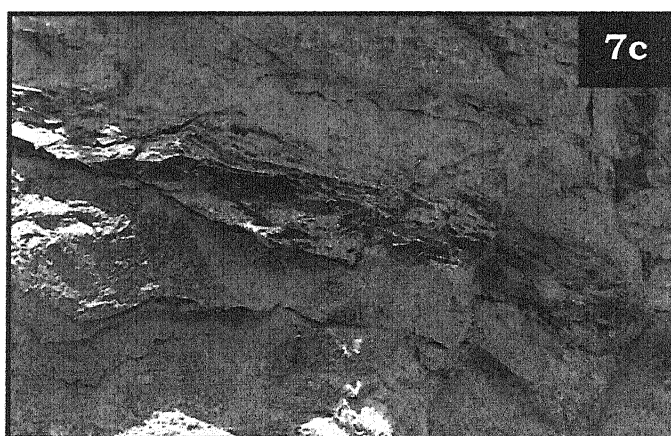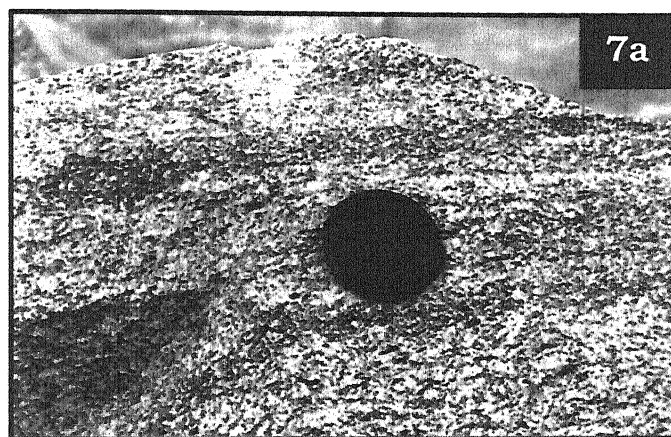
5c : Field Photograph show mylonitization in pink granite at Lodhpahar

PLATE-6
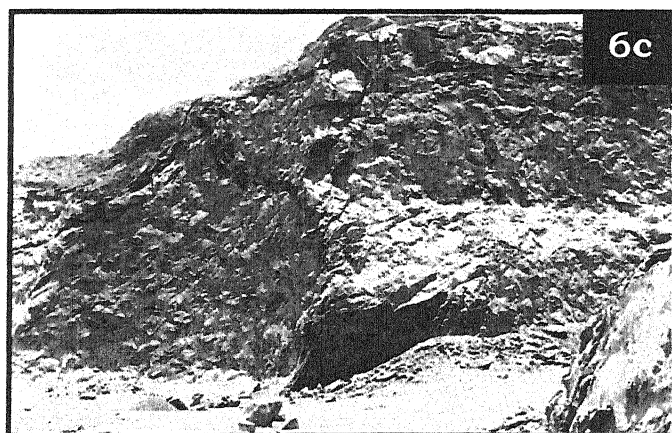
6a : Photograph shows the band of sulphide mineralization in the amphibolite of Lodha Pahar

6b : Panaromic view of Lodha Pahar

6c : Mylonitised TTG gneisses exposed at northern part of Lodha Pahar
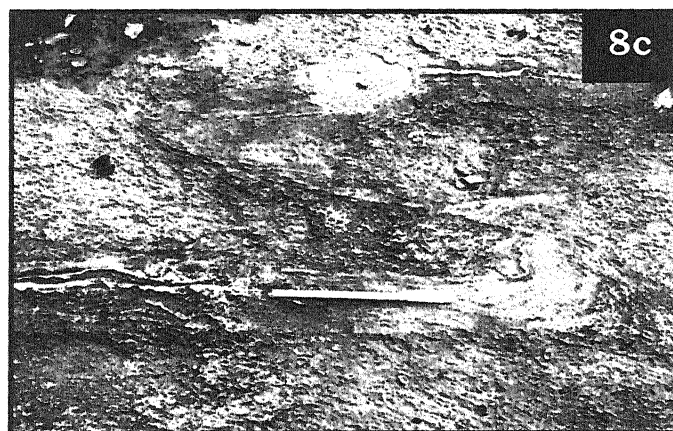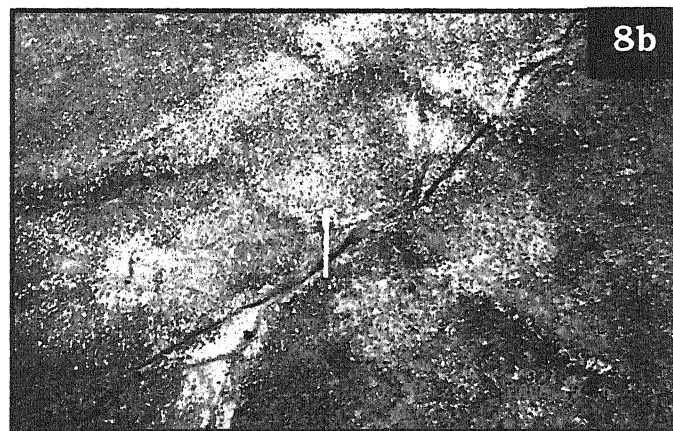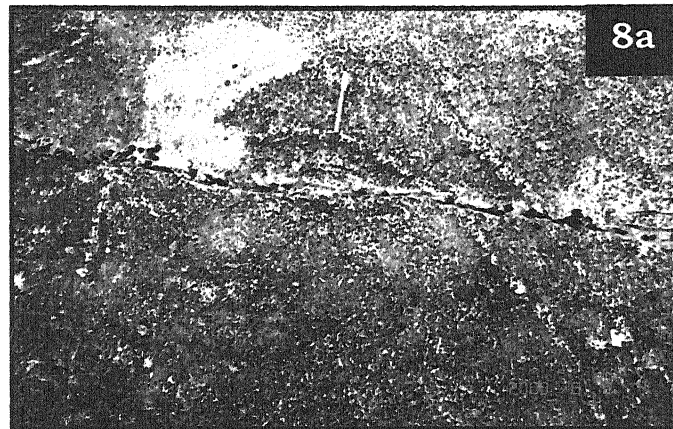
PLATE-7

7a : Streaky granite gneisses exposed at village Dahara

7b : Pegmatite & porphyritic granite emplaced along the shear zone at Lodha Pahar

7c : Field photograph shows patches of mylonitized basic rock in TTG at Lodhapahar
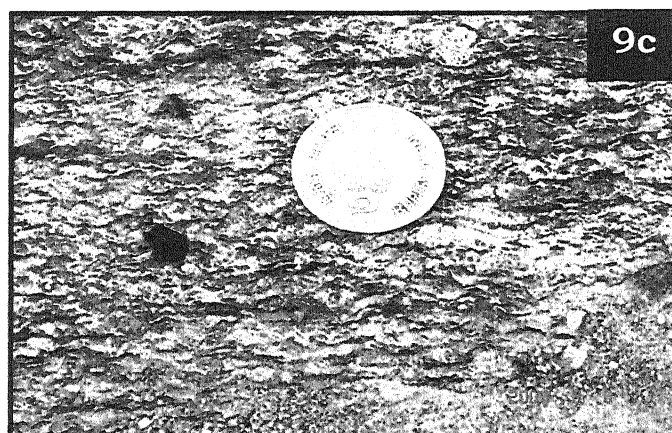
PLATE-8

8a : Field Photograph shows sheard fold in the pink granite near Bijaynagar sagar dam

8b : Field photograph shows shear fold in mylonitized pink granite near Bijanagar sagar Dam, Ratauli road

8c : S-type shear fold from granite

PLATE-9

9a : Field photograph shows E-W trending mylonitized pink granite at Bijanagar sagar Dam

9b : Photograph shows mylonitized pink granite at Bijanagar sagar Dam, Ratauli road

9c : Photograph shows oriented crystals of quartz and feldspar in pink granite near Bijanagar sagar Dam

PLATE-10
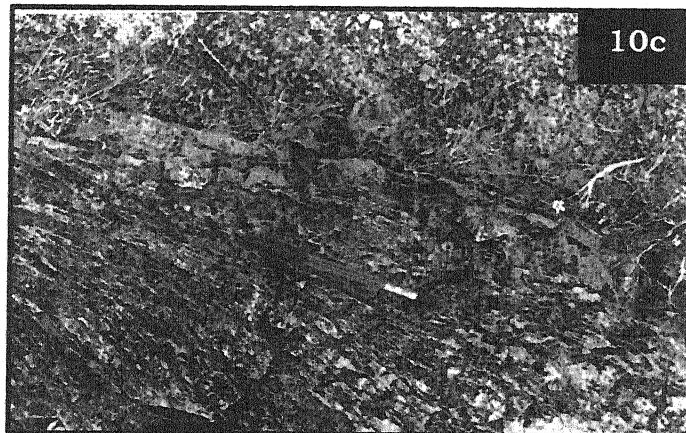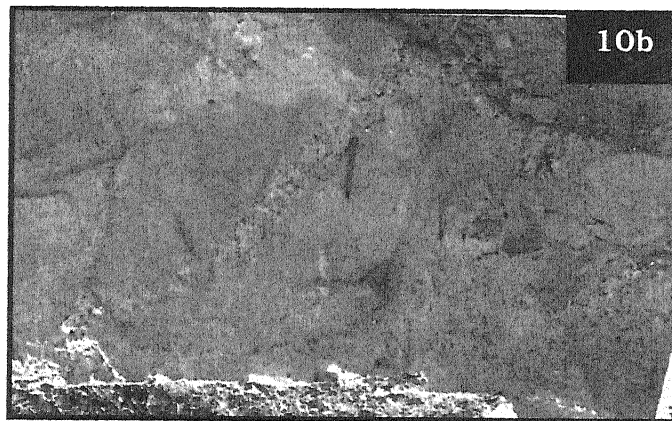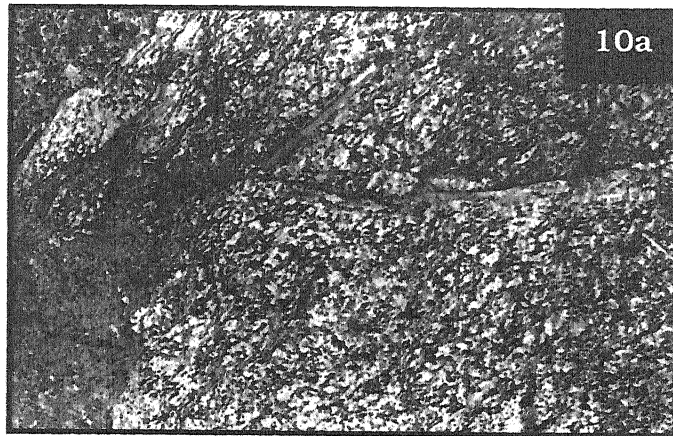
10A : Mylonitized and folded granite near Nandpura village

10B : Field Photograph showing folded pegmatite vein in gray granite at Raipura Kalan

10C : Field photographs show mylonitization in pink granite at Damaura village

PLATE-11

11a :   Panoremic view of pink granite

11b : Photograph shows E-W trending pink granite hilloks exposed in Damaura village

11c :   E-W trending pink granite exposed in Ghutwai village

PLATE-12
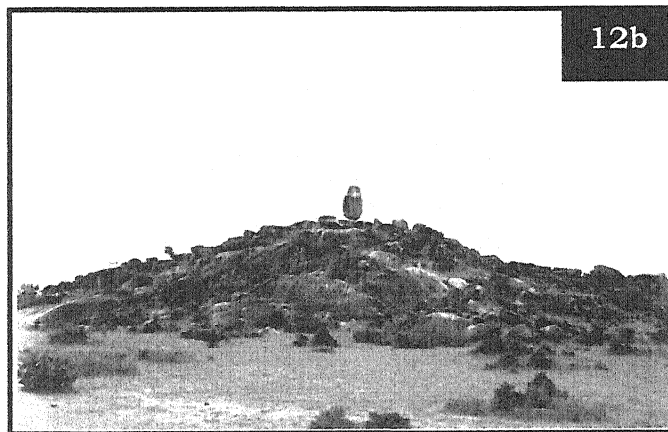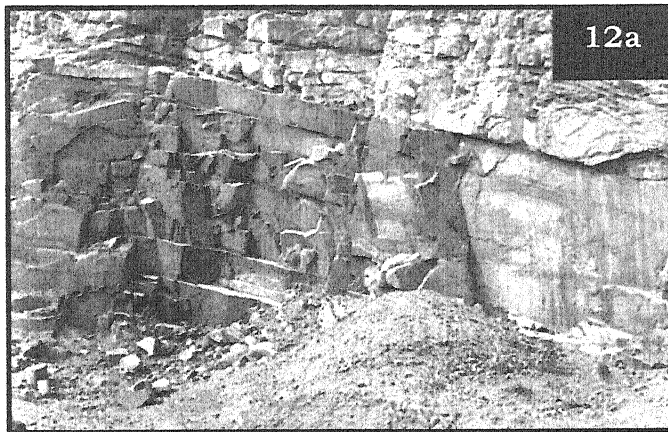
12A : The field photograph shows the highly sheared & fractured mylonitized pink granite at Kumdohra village (Mahoba to Rajpura road)

12 B : Field photograph shows balancing boulder in E-W trending pink granite

12C : Panoramic view of biotite granite.

Chapter-3

PETROGRAPHY

The textural relation of granite, biotite granite, hornblende bearing granite, granite gneisses and high grade metamorphic rocks have been described in this chapter. The geochronological study of crystallization and deformation is mainly based on relation between the time and fabrics of rocks i.e. external foliation (se) and the internal foliation (Si) with the porphyroblast. The time relation between the phases of deformation and episodes of metamorphic/ crystallinization, the rocks of the area displays textural evidences of metamorphic reaction involved in the formation of diverse minerals parageneses. The field relationship and geochronological studies suggest that rocks of Bundelkhand have been subjected to polyphase deformations and metamorphism in the Archean time. The detail petrographic studies have been discussed under the following heads (a) Bundelkhand gneisses complex (b) granitoids (c) dolerites and mafic dykes (e) quartz reefs and (f) mylonites.

3.1 BUNDELKHAND GNEISSES COMPLEX (BnGC) :

The BnGC rocks comprise of gneisses, TTG, migmatites, granite gneisses, sillimanite gneisses, amphibolites, hornblende- biotite gneisses. These rocks are exposed in low land topography, generally showing NW-SE and E-W foliation and are well exposed at Nathupura, Lodhapahar, Jankhera ridge (Fig-2.6). The small xenoliths of BnGC were also found at several places as enclave within the granitoids. They are light to dark grey coloured bands of tolanites-trondhjemite gneisses (TTG), biotite gneisses granite, sillimanite gneisses and granite gneisses. The gneisses of Lodha pahar and Nathupura are mainly composed of biotite gneisses, where altered chlorite minerals and ferromagnesian minerals are aligned to the foliation of the rocks. The accessory minerals in biotite- gneisses include euhedral crystal of the Fe-Ti oxides, large crystal of apatite and zircon minerals.

The amphibolites and biotite-rich amphibolites (biotite-hornblende gneisses) are also found to be associated with the above mentioned rock types. These rocks are exposed in the small lensoidal bodies in the gneisses. Some places sulphide

mineralized shear zone has been observed in the gneissic rocks. Highly deformed and altered peridotites and mafic schistose rocks were also present at few places which is intrusive in the trondhjemitic gneisses. The BnGC rocks have been lithologically divided into three suits (1) gneiss TTG, migmatites granite gneisses (2) amphibolites and hornblende- biotite gneisses (3) schist and quartzites.

3.1.1 Biotite gneisses, TTG and Granite gneisses :

In study area, pelitic gneisses contain general trend of NW-SE to WNW-ESE and steeply dip towards north direction. At one place, they contain the deformational event in the gneisses indicate that N-S compression, which folded the whole sequence into tight isoclinal to open fold of various generations. The presence of complex folds in the gneisses indicates that gneisses had experienced polyphase deformation. Megascopically, these rocks are light grey to dark gray in colour, medium to fine grained but some places coarse grained variety are also observed with pink colour bands. Some places the thickness of melanocratic bands is greater than leucocratic bands. In gneisses melanosomes are set in dominant leucosomes. The leucosome are largely of quartz-feldspathic with minor amount of biotite. The melanosomes are granodiorite to diorite with biotite and minor amphiboles. The waxing and wining pattern are occurred in leucocratic and melanocratic bands at several places. Partial melting signatures as aggregates of granites melt are recorded from the gneisses. A sharp intrusive relationship between grey granite and gneisses has been observed. The leucocratic bands are rich in quartz and k-feldspar while melanocratic bands are rich in quartz, plagioclase and biotite minerals. The S-C fabrics in gneisses and the (local) micro faults in the gneissic rocks have been also noted. The small euhedral crystals of Fe-Ti oxides, feldspar, quartz, scricite, silliminite, apatite, epidote, zircon, opaque etc. are found in gneisses.

Feldspar

Orthoclase, microcline and perthite feldspar are the major minerals found in the BnGC rocks. Microcline is medium to fine grained containing cross hatched twinning. Sericite orthoclase shows the twinning to the untwining nature and some places shows the Carlsbad twinning. Sericitized feldspars incurred in the granite

gneisses and deformed gneisses. Coarse size orthoclase crystals with albite lamellae represented the lamellar twining (Plate-1b) have been identified from many places. The albite lamelles are very thick but some places thin (Plate-1c, 2b). Plagioclase minerals are subhedral, medium to coarse grained in gneisses rocks. They exhibits the prismatic forms plagioclase are colourless to grey (first order interference colour mineral). The characteristic feature of plagioclase is polysynthetic twinning (Plate 2c). Plagioclase contains the inclusions of biotite, apatite and K feldspar crystals. At some places myrmekite intergrowth characterized by vermicular texture obtained from granitic melts of gneisses.

Quartz

The quartz crystals are colourless to first order grey interference colour. They exhibit euhedral to anhedral in shapes medium to fine grained minerals. It shows and close extension due to polyphase deformation and crystallization. At many thin section quartz crystals are surrounded by biotite minerals.

Biotite

Biotite is dominant mineral constituent of this rock unit. Biotite are subhedral in shape. Two variety of biotites occur in this rock unit. (1) brown coloured biotites, most common, strongly pleochroic and (II) green coloured biotite.moderately pleochroic, rarely found. Some places both are found together and characterized by the one set cleavage. The brown colour variety of biotite contains the pleochroic haloes and some times coarse crystal of zircon with in the pleochroic haloes (Plate-5c). The magnetite crystal are formed along the cleavages of biotite minerals (Plate-1b). The biotite minerals are medium to coarse grained, tabular form, subhedral in shape (Plate-1a). The green biotite mineral show the one set of cleavage and are mainly associated with the retrograded and mylinitised granite- gneisses (Plate-2a). At many places magnetite crystals occur around the biotite crystals (Plate-2b). Medium to fine grained crystal of biotite are also oriented to foliation direction of the gneisses.

Sillimanite

Silimanite usually occurs in small often minute crystals in the thin section. Prismatic, needle like crystals along the cleavages of biotite crystals are rare.

Sillimanite is usually found around the magnetite crystals (Plate-3a and 2b). It is colourless, high relief crystal and length slow. The textural study indicates that biotite is become unstable at higher temperature and responsible for the development of sillimanite. Rarely needle like crystal found as aggregates of very fine fibers at the cleavages of biotite. They are colourless, birefringence, parallel extinction fibrous habits minerals (Plate-3b).

Muscovite

Medium to fine grained they occurs in thin tabular crystals or scaly aggregates as retrograde product. Infew section characterized by second order interference colour. One set of cleavage are reported in muscovites thin section.

Garnet

Garnet is colourless, high relief, non pleochroic mineral medium to fine grained crystals. Garnet is distinguished from other mineral on the basis of high relief. Garnets are medium to fine grained colourless in thick section (Plate-6c). They does not show any cleavage and inclusion.

Zircon

They are mostly associated with biotite gneisses, coarse crystals of zircon are also observed in few sections. Small crystals are associated with pleochroric haloes (Plate-6a). Zircon is usually small prismatic crystal in thin section, characterized by high relief.

Apatite

Apatite is medium to fine grained crystals. They are well developed in sillimanite gneisses. Apatite is euhedral in shape, colourless mineral. It show the moderate to high relief, first order interference grey in colour (Plate-6a, 7c and 8a) colourless birefringence.

Sericite

Sericite is alteration product of the K-feldspar. The development of sericite has been observed in many thin sections. This is randomly oriented, flaky in nature.

Sericitised orthoclase are observed in same thin section of granite, gneisses (Plate-1c). Sericites are secondary minerals formed by the hydrothermal alteration of the K feldspar in gneisses.

Magnetite

Magnetite minerals are usually euhedral to anhedral in shape (Plate-1a, 2a an 2c). Magnetite mineral are medium to fine grained. They are arranged in the cleavages of biotite minerals. They are embedded in the biotite, quartz crystals.

Chlorite

It generally occurs as secondary product due altered of biotite. Some times occurs in patchy masses, but some places it observed as subhedral-elongated crystal. Chlorite is characterized by light green to dark green pleochroism and low interference colour

Rutile

Medium to coarse grained crystals of rutile are deep red brown in thin section. Rutile crystals in most of the thin section are euhedral in shape. The characteristic feature of the rutile minerals are simple contact twinning (Plate-4c).

3.1.2 Amphibolites and hornblende- biotite gneisses :

Amphibolites are mostly exposed at Lodha pahar, Kabrai area. They are medium to fine grained in nature & dark in colour. All the amphibolites are hard and compact in nature. The amphibolites of Lodhapahar also contain sulphide mineralization. The hornblende, biotite, plagioclase, magnetite, quartz, orthoclase, are the common mineral that occur in different proportion in the amphibolites. On the basis of mineral paragenesses, the amphibolites has been classified into two types (1) hornblende- biotite gneisses (2) hornblende-plagioclase gneisses.

Hornblende

Prismatic crystals of hornblende minerals are medium to coarse- grained in nature, subhedral in shape. Light green to dirty olive green colour is the characteristic features of the hornblende in the gneisses. Two set cleavages are presents in many thin sections (Plate-7b). The extinction angle for prismatic section of hornblende

crystals ranges 10^0 to 20^0, characterized by second order interference colour. At many places hornblende crystal are altered to chlorite crystals (Plate-8c). Inclusions of biotite, magnetite, quartz, plagioclase are common in hornblende-biotite gneisses (Plate-9b and 9c). Hornblende crystals are associated with pyroxene crystals (Plate-11a). Hornblende is inclusion in biotite found in many section. Replacement texture is common.

Plagioclase

The plagioclases are medium to fine grained subhedral in shape and is characterized by colourless prismatic crystal first order grey colour mineral. (Plate-9a)

Quartz

Medium to fine grained subhedral to anhedral and the undulose extinction due to the strain effect. Quartz crystal contains the inclusion of hornblende and biotite crystal (Plate-11b and 11c).

Biotite

It is observed as medium to fine grained crystals, brown in colour, pleochroic mineral (pleochrism are light brown to dark brown). All the biotite crystals are aliened in the schistocity plane. Some time biotite crystal shows the replacement texture with amphibole and pyroxene crystals (Plate-11a and 11c). In many thin sections, biotite crystals are oxidized form. The inclusion of the quartz magnetite and hornblende crystals are common in the coarse grained crystals of biotite minerals (Plate-10a, 11a).

Chlorite

It is an alteration product of primary crystallizing mineral of biotite and hornblende. It is present in patch masses around the biotite and hornblende crystals. Chlorite pale green in colour but feebly pleochroic (pale green to darker green). In this section chlorite is present in small irregular flakes and laths.

Pyroxene

It is medium to coarse grained euhedral, mineral. Pyroxene is distinguished other minerals on the basis of high relief (Plate 17b) and cleavage angle associated with hornblende.

Actinolite

Colourless to pale green in thin section (Plate-9a). Pleochrism usually observed from yellow to green. Typical amphibole cleavage, 56^0 to 124^0, two set cleavage texture are present in actinolite minerals. It is altered product of hornblende.

Magnetite

It is present in subhedral to anhedral in shape, medium to fine grained. They are present as accessory minerals of this rock. Magnetite minerals are black in colour, some places present in form of solid inclusion in biotite, hornblende crystals.

Calcite

Calcite euhedral in shape, fine to coarse grain aggregates. The calcite crystals are colourless to grey in thin section. The twinning is common in the calcite crystals. It altered product in amphibolites.

Epidote

In the thin section, the epidote minerals are present in the form of vein. It is also found as granular aggregates. They are high relief, colourless usually the secondary alteration product (Plate-14a) of plagioclase.

3.2 GRANITOIDS :

On the basis of field relationship, mineral compositions, textural and structural studies following type of granitoids have been obtained in the study area viz. (1) biotite granite (2) hornblende granite (3) grey granite (4) leuco granite (5) fine grain granite

Megascopically, the granite of the investigated area varying in grain size from coarse to fine grained. The porphyries of feldspar are very frequent in fine grained leucogranite rock. The leucogranite contains feldspar, quartz, biotite and rarely amount of hornblende. At some places, of granite rock contain perfect two sets of jointing and fractures. The deformed granite bands contain quartz feldspathic masses and show preferred orientation where alternate of ferromagneisium mineral band in biotite rich variety. At places, bands of mica are contain wearing and waxing pattern

along the foliation planes of quartzofeldspathic masses. Leucogranite rocks are coarse to fine grained. They are holocrystalline, equigranular hypidomorphic in texture. In many thin sections leuco granite shows porphyritic texture. The minerals constituents of granitoids are as follows

(1) predominant: quartz , feldspar minerals

(2) accessory minerals: biotite (rare), hornblende, zircon, allanite and sphence, magnetite

(3) secondary minerals : epidotes, chlorites, sericite

3.2.1 Biotite Granite :

Orthoclase

It is one of the predominant mineral of biotite-granite rock. Orthoclase minerals are medium to coarse grained in thin section. They are euhedral to anhedral in shape. It shows the intergrowth of microcline (hair like) crystal. The core of orthoclase formed perthite texture that is followed by plagioclases crystal. The orthoclase are usually found to alter in sericite minerals. The phenocrysts of fresh and unaltered characters of feldspar (Orthoclase) are also observed in few sections, they show Carlsbad twinning, low relief.

Microcline

Microcline is fine gained, euhedral to anhedral in shape. Cross hatched twinning are well developed in microcline crystals but some places of microcline crystals alteration shape from orthoclase through microcline crystals are formed. At some places microcline-perthite is also recorded. In plane polarized light cross hatched twinning are common feature of microcline minerals.

Quartz

Quartz is also one of the predominant minerals constituent of granite. It occurs as coarse to fine grained in shape, anhedral crystals. Quartz is characterized by low relief, undulose extinction but less altered minerals. The undulose extinction due to the strain effect is noted in few sections.

Biotite

It is coarse to medium grained, tabular crystals, perfect one set of cleavage are present in biotite crystals (plate-12a). Two types of biotite crystals are present in thin section. The biotite are brown in colour but some places they are green in colour. Pleochroic holoes was absent in biotite of this granite. The biotite is alloay than hornblende.

Hornblende

In thin section hornblende crystals are occurs rare or nearly absent. Hornblendes are medium to fine grained by euhedral prismatic crystals. They are light green in thin section. They shows the light green to dark green pleochroism and second order interference colour. In many of the thin section hornblende crystals of two set perfect cleavages are present.

Zircon

Zircon crystals are present in the form of inclusion in biotite granite. It is usually small prismatic crystals. They distinguished other on the basis of high relief, parallel extinction and absence of cleavages.

3.2.2 Leuco granite :

Megascopically, the granites of the investigated area are fine to coarse grained. The leucogranite are grayish to grayish pink rock. These rocks are hard and compact in nature. The large amount of phenocryst of feldspars is very frequent in the coarse grained leuco granite. The feldspar, quartz, biotite, magnetite are assecceory minerals and visible in the handspecimen. The hornblende crystals are rarely observed in leucogranite. Microscopically all these rocks are characterized by coarse to medium grained in texture. They are halocrystaline, equigranular, hypidiomorphic to allotriomorphic in texture.

Biotite

Biotite is medium to fine grained, light brown in colour, but the few crystals of biotite show the pleochroic holoes. Some time biotite also contains magnetite zircon.

Plagioclase

Plagioclase crystals are medium to coarse grained. They are subhedral in shape. It gives the lamellar twinning. Plagioclase feldspars are rare. At many places antiperthite texture are developed the contact of orthoclase crystals. At one places I have seen plagioclase feldspar. Some places orthoclase feldspars are altered to form the albite. The twin lamellae of albite are observed.

Quartz

Medium to coarse grained grains are euhedral in shape, colourless in thin section. Quartz is characterized by low relief, sharp extinction and less alteration. At places quartz show undulose extinction due to strain effect. It also observed as inclusion in feldspar, biotite, magnetite.

Hornblende

The hornblende shows light green in colour. Medium to fine grained texture. The hornblende shows the characteristic pleochrism of greenish brown to light green in colour.

Zircon

It is occasionally found as inclusion in the biotite and hornblende crystals. It is present in the form of pleochroic holoes in biotite and hornblende. Zircon is look like minute small prismatic crystal. They are low relief, and gives parallel extinction, no cleavages are present in the biotite crystals.

Magnetite

Magnetite is euhedral to anhedral in shape. They are low relief, non pleochroic, dark black in colour, no cleavage are present in the magnetite crystals. At many thin section of leucogranite rock magnetite are included in the biotite, hornblendes and quartz crystals.

3.2.3 Grey granite :

Grey granite is of dark grey coloured rock with massive fabrics. The pegmatite veins are present in grey granite rock. The weathered surface of granites forms thick alternate bands of light and dark coloured minerals. Chlorite is also present at the margin of biotite at its contact with plagioclase in the deform granite.

The granite is characterized by K feldspar, quartz, biotite, hornblende, magnetite with small amount of apatite and retrograded chlorite. The granites are dominated by minerals hornblende, zircon, chlorites, biotite, quartz, and plagioclase. Small amount of rutile, magnetite, actinolite and epidote are present.

Biotite

It is observed as coarse to fine, subhedral crystals. Coarse grained flacks of biotite show pleochroism from dark pale greenish, yellow to brown, dark brownish yellow. The parallel orientation of biotite defines the schistocity of foliation. Biotites are crystalised in two generations. The biotite of the first generation is characterized by xenoblasts. The biotite of first generation is characterized by brown to dark brown pleochroism while the biotite of later generation is light yellowish green to dark greenish brown and occurs as subidioblastic crystals. Inclusion of hornblende and quartz are present. pleochroic haloes are present in biotite crystals.

K-feldspar

Medium to coarse grained quartz crystals. At many places orthoclase is altered and form sericite minerals. Orthoclase is present in hair like structure and developed the irregular stringers of sodium rich feldspar and potassium rich feldspar. Minning of these feldspar developed the microperthite texture (Plate-12c). The subhedral to enhedral crystals of orthoclase contain the inclusion of hornblende and magnetite.

Microcline

Medium to fine grained crystals of microcline are present in grey granite rock. They are least predominant mineral constituent of this granitic rock. They are differentiated on the basis of cross hatched twinning (Plate-12c). Microcline mineral are euhedral to anhedral in shape crystals but at some alteration from orthoclase through microcliniation is also recorded (Plate-12a).

Magnetite

Medium to fine grained crystals of megnatite are present in euhedral shape. Magnetite are included in the hornblende and orthoclase crystals.

Hornblende

Hornblende crystals are coarse grained, strongly pleochroic (paleogreen to straw yellow or greenish below in colour). Magnetite crystals are present in the form of inclusion. Two set of cleavage are present in the hornblende crystals (Plate-9c). The hornblende minerals are present as one accessory minerals of which is usually present as xenoblastic form and associated with biotite and magnetite in the matrix of quartz.

Quartz

Medium to fine grained crystals of quartz are present in the grey granite. The coarse grained crystals of quartz are arranged to the foliation plane. It shows the wave extention. Magnetite crystals are included in quartz crystal.

3.2.4 Pink granite :

A coarse grained pink granite is one most dominant rock type in the study area. Pink granite is usually compact and massive in nature. The pink granite rock contains pink colour of feldspar crystals and grey colours of plagioclase crystals. NE-SW trending pegmatite veins have been found intrusive in the pink granite, which are devoid of muscovites but contains the biotite coarse grained (20cm x 15cm size), feldspar crystal, quartz (10cmx5.5cm size). The deformed pink granite rock comprises epidote as vein. Medium to coarse grained pink granite at places contains porphyroblast of hornblende and feldspar. The pink granite is also characterized by perthite texture, mymekite texture. Sphere is very common mineral and is present in large amount. Magnetite crystals are found to develop along the cleavages of hornblende crystal (Plate-10B). The pink granite consists of potash feldspar, perthite, quartz, hornblende, magnetite, sphere, rutile, hercynite, zircon, allenite, chlorite, epidote and apatite. The biotite mineral is not common in pink granite of Mahoba. The hornblende is always find greater than biotite. The microcline is greater than orthoclase.

Hornblende

The coarse grained hornblende shows strong pleochroism (pale green to strong yellow or greenish blue in colour). The medium grained hornblende contains more

magnetite crystals. The core part of the hornblende contains small granules of magnetite (Plate-15a). Sometimes hornblende alteration into chlorite have been noted. Augite crystal is surrounded by hornblende. The presence of xenoblastic type texture of hornblende is also noted in few granite where the biotite and hornblende both are found as inclusion in coarse crystals of hornblende.

Chlorite

The chlorite is medium to coarse grained light green in colour usually intermingled with biotite. Fine grained magnetite is present along the prismatic cleavage of the chlorite. It shows usually pale green and pleochroic in thin section.

Biotite

Biotite is not very frequent and low in compare to hornblende. Most of the biotite crystal are oxidized form. The exsolved texture of in biotite is very common (Plate-16a). The biotite crystals are altered and formed the chlorite mineral. At many places the magnetite crystal are present at the cleavages of biotite crystals.

Quartz

Euhedral to anhedral in shape, colourless in thin section, without cleavage characterized by first order grey interference colour. Quartz crystal shows the straight extension. They are coarse to medium grained in thin section.

Orthoclase

Orthoclase minerals are medium to coarse grained and one of the dominating mineral in this rock. They are colourless low relief minerals Orthoclase minerals are euhedral to anhedral in shape. Orthoclase minerals show the hair like structure perthitic texture is form.

Microcline

Microcline is one of the important assecceory mineral of the pink granite rock. These mineral are colourless in thin section, euhedral to anhedral in pink granite. Low relief mineral and no cleavage in microcline is visible. The characteristic feature of this mineral are cross hatched twinning (Plate-15c).

Plagioclase

They are colourless in thin section, euhedral to anhedral in shape. Plagioclase crystal shows the lamellear twining. Plagioclase mineral contain the inclusion of biotite and magnetite, hornblende mineral. The plagioclase lamellae are very thin. The interference colour is mostly first order grey in plagioclase. The plagioclase noted saussaritized (Plate-15b).

Albite

Medium to coarse grained. Albite may differentiate to plagioclase albite mineral show thin lamellae. Albite minerals shows the grey first order interference colour. Albite are low relief mineral (Plate-15c).

Magnetite

Medium to fine grained in thin section. Magnetites are present in the form of inclusion as well as parallel to the cleavage. Magnetites are the opaque, euhedral to anhedral in shape mineral. Magnetite is formed around the reaction rim of biotite crystals (Plate-17a).

Zircon

Zircon is only present in biotite mineral in the form of pleochroic holoes (Plate-5c). But many places large crystal of zircon are also found (Plate-16c).

Sphene

Sphene is usually euhedral in shape, light brown in colour (Plate-16c), feebly pleochroic mineral. The cleavage are seldom and obvious in thin section. They are appeared as secondary product which was formed by the alteration of biotite mineral.

Ilmenite

Ilmenite are deep red in thin section. In the thin section ilmenite are anhedral and long rectangular outline. At some places ilmenite are altered and formed leucoxene. Leucoxcene is a fine grained aggregates.

3.3 QUARTZ REEF :

The NE-SW trending quartz reef is the most spectacular land marks geological feature massif of the Bundelkhand. In the study area many places quartz reef cut across the granitoids and gneisses rock. At many places the quartz reef are sinistrally displaced. The two set of joints and tension joints are present that reflects the late tectonic activity in the quartz reef. Megascopically quartz reef show dominantly grayish white colored but the pinky white, milky white colored reefs are also present. They are hard, compact massive in nature. Series of milky white secondary veins of quartz traverses the greater part of quartz reef. Under the microscope quartz reef represents the very coarse grains of quartz and feldspar. The quartz reef shows the varied texture and large rectangular grains of quartz with straight borders and undulose extinction. Feldspar, magnetite and chlorite are also observed in thin section of quartz reef. Epidote veins are also observed in the thin section of quartz reef. The microcline is medium to coarse grained, colourless to cross hatched twinning are common, altered to fresh in thin section. Quartz crystals and series are common inclusion in microcline minerals. Quartz, sericite and opaque are present along the fracture plane.

3.4 DOLERITE DYKES :

The ENE-WSW trending great Mahoba dyke passes from the Mahoba town and is about 11kms in length. Dolerite dyke is also exposed at Thana. Megascopically dolerite is dark green or melanocratic in colour, hard and compact in nature. Prismatic crystal of pyroxene an orthopyroxene can be identified in hand specimen but at places grayish white leucocratic band and streaks (patches) of feldspar are also recognized.

Microscopically sub-ophitic texture is common in most of coarse and medium grained variety of dolerite dyke (Plate 17c) the following minerals are identified.

- Pyroxene, orthopyroxene (hypersthene) and clinopyroxene (augite) and plagioclase feldspar are present as essential.

- Mineral while magnetite, hornblende are present assecceory

- The secondary minerals are mostly epidote quartz, chlorite in dolerite dyke.

Clinopyroxene (augite)

Augite crystals are euhedral to anhedral to anhedral in shape. It shows the light green, colourless and short prismatic crystals. Augite crystal gives high relief, second order interference colour, high extension angle mineral. At many places the plagioclase (labradorite) crystals are embedded in the augite crystal. They form the ophitic texture (Plate 18a). According to the thin section of dolerite dyke the clinopyroxene crystals are less altered in comparison of plagioclase crystals.

Plagioclase

Plagioclase is colourless, observed as long as laths of euhedral to anhedral crystals. The anhedral crystal is often large as compared with those of other plagioclase. It shows the polysysnthetic twinning, low relief and also shows the higher extinction angle. The labrodorite crystal is embedded in clinopyroxene crystals (Plate 18b). The plagioclase grains are twinned and saurritised, saussuritised plagioclase mineral gives the epidote and quartz crystals.

Magnetite

Magnetite crystals are dark black in colour, course to medium grained in thin section. The magnetite crystal are found along the cleavage plane of pyroxene crystals.

Epidote

Epidote is present as the secondary product which is formed by the sausssoricitisation of plagioclase feldspar minerals. It is an observed as granular aggregates. Epidote is mineral of high relief, colourless in plane polarized light but under cross nicol, the epidote minerals shows second order interference colour.

3.5 MYLONITISED ROCKS :

Recrystallised protomylonites, ultramylonite and mylonite phyllonite rocks have been observed at many place. Hanuman temple and Nauranga, Chando near the Bijanagar Sagar dam. The well developed S-C mylonite are present in the pink granite rock where basic rock emplaces along E-W trending dolerite rock. They have been

found to medium to fine grained but at places coarse grained variety also observed. These rocks have diverse physical appearance texture and mineral composition. Four type of deformed mylonites have been observed at Mahoba area (1) protomylonites (2) ultramylonites (3) mylonite and (4) phyllonites. Megascopically they show medium to fine grained where quartzo feldspathic masses quartz, feldspar and flakes have developed and rotated (Plate). Mesoscopic shear also developed in mylonite and ultramylonite. Following mineral assemblage have been identified-

Chlorite

Chlorite is medium to fine grained, xenoblastic to subhedral in the mylonite. The elongated scally crystals of chlorite are weakly pleochroic. The chlorite are light green in thin section and due to the alteration of hornblende. Medium grained garnet has been found in the matrix of chlorite.

Actinolite

Actinolite crystals are fine grained, light green in colour fiberous aggregates of actinolite is generally oriented with in the schistosity plane.

Quartz

Quartz is medium to coarse grained crystals, anhedral but elongated in thin section. Quartz crystals are colourless, low relief no cleavage highly elongated are present in thin section of quartz crystals. The aggregates of quartz crystals are observed around the mylonite planes. They have commonly shows the undulose extinction due to the higher strain effects. Coarse grained crystallized crystals of quartz are observed in thin section of mylonite rocks which shows ribbon texture.

Orthoclase (K-feldspar)

Mostly euhedral to anhedral elongated and fractured, medium to coarse grained crystals of orthoclase and microcline are present in thin section of mylonitic rock. Both of the orthoclase microcline minerals are colourless and low relief minerals in thin section. In the thin section of the orthoclase crystals at many places the phenocrysts of orthoclase are rotated which indicates the sense of shear. Alloved K-feldspar changed to microcline.

Plagioclase

It is observed as medium to fine grained crystals. At many places the magnetite crystals are embedded in the plagioclase crystals. In the thin section of plagioclase crystal alteration in to epidotes & services feldspar are also recorded. Plagioclase crystals are the lamellae are very thick and thin. The thin lamellae of plagioclase defined the development of albite crystals.

Garnet Medium to coarse, ideoblactic crystal of garnet have been formed in the matrix of chlorite matrix. They are usually in granular aggregated devoid of any inclusion. The EPMA analyses showed high MNO. The aoperstite types garnet has been first time reportion from any shear zone of Mahoba area. The recrystallized plagioclase and crystallized suggest that mylonite were recrystallized at 320^0C, 2-3 Kbar P-T condition.

PLATE-1
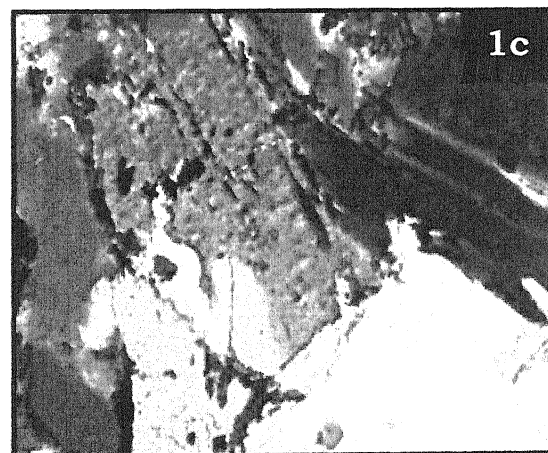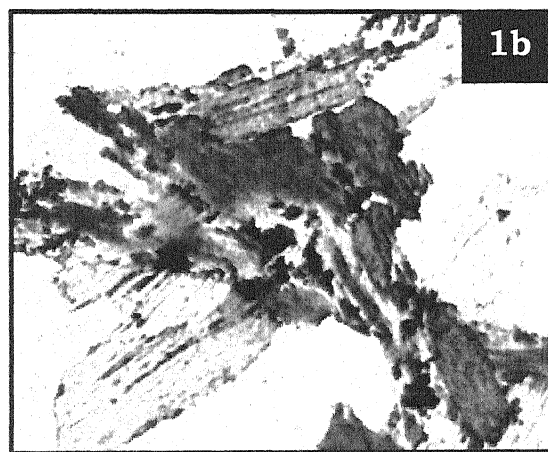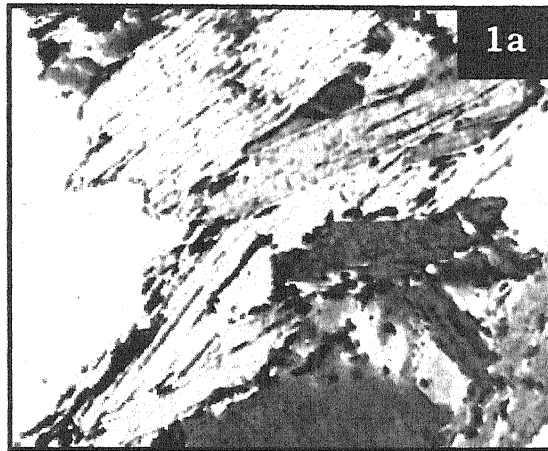
1a : Biotite Gneisses rock of Lodha pahar where the fine grained magnetite are aligned along the cleavage as well as boundary of biotite crystal.

1b : Biotite crystal are aligned along the S1 and S2 schsistosity plane.

1c : Coarse grained crystals of biotite and magnetite are aligned along the gneissosity.

PLATE-2
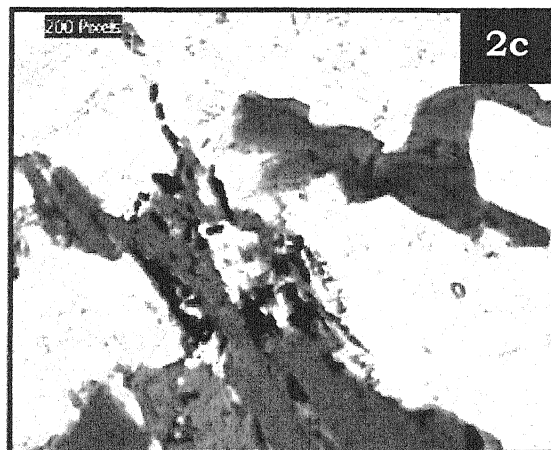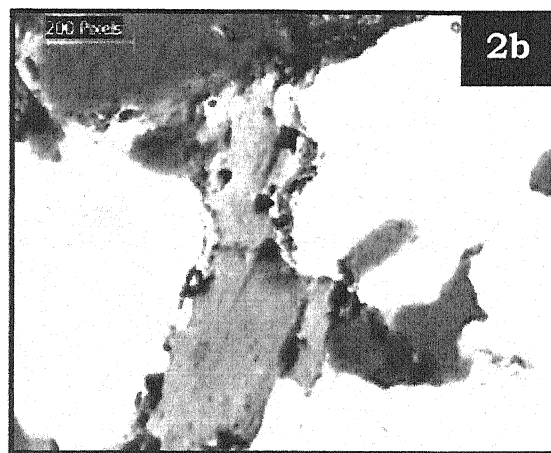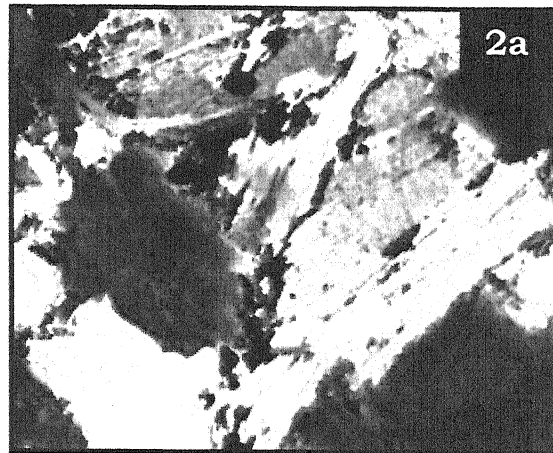
2a : Thin section of Biotite gneisses where the fine grained of magnetite are present at the boundary of biotite crystal.

2b : The biotite crystal are break along the cleavage plane and reactive with magnetite and quartz form the silliminite crystal.

2c : Biotite minerals are aligned along the gnessosity plane. Biotite are break along the cleavage plane and form radiating pattern of silliminite.
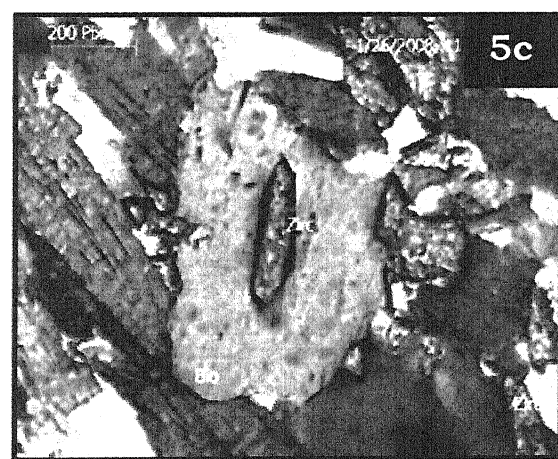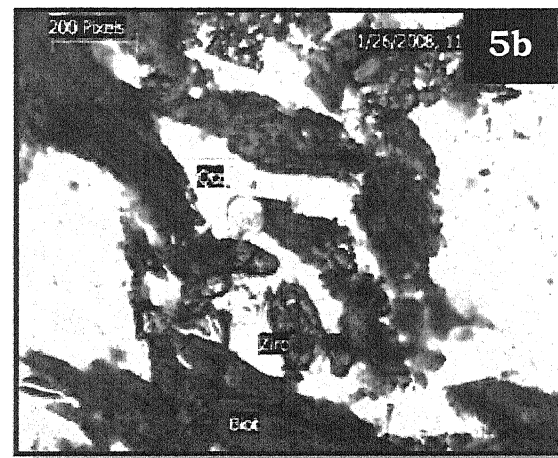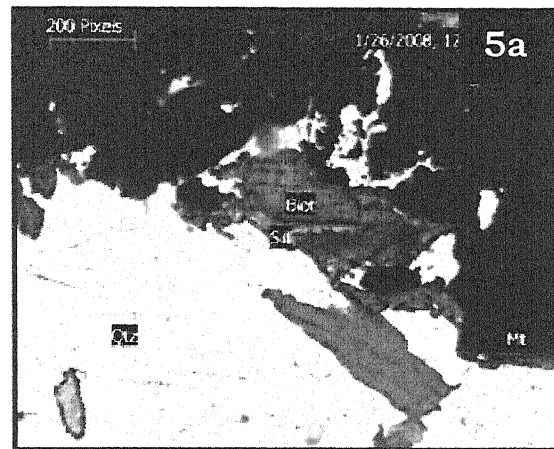
PLATE-3
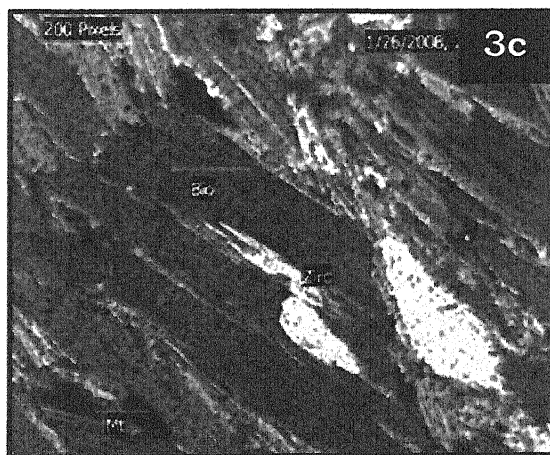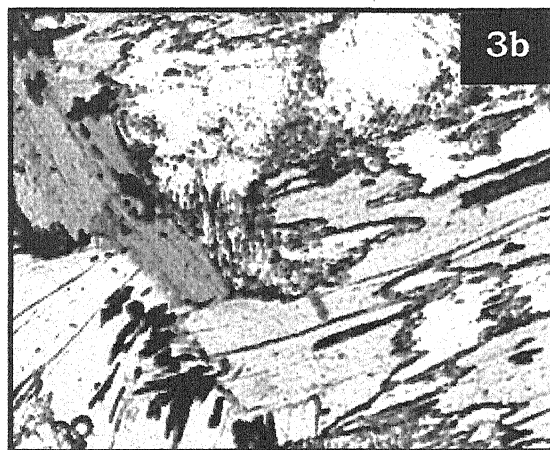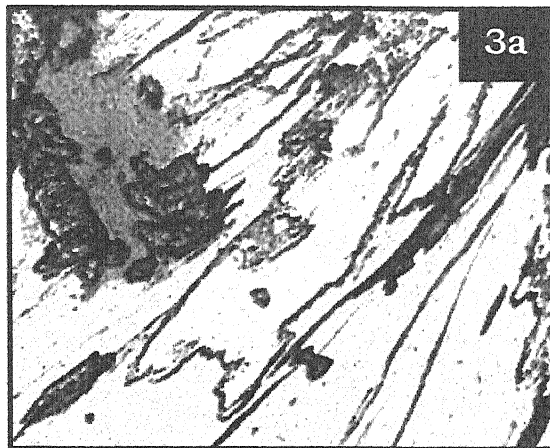
3a : Alteration of biotite and formation of sillimanite crystals. No cleavage are present in biotite

3b : Biotite silliminite gneisses, the sillimnite occurs in radiating pattern and also along the cleavage of biotite.

3c : In the biotite gneisses rock, biotite minerals altered along the cleavage plane and form the chlorite minerals.

PLATE-4
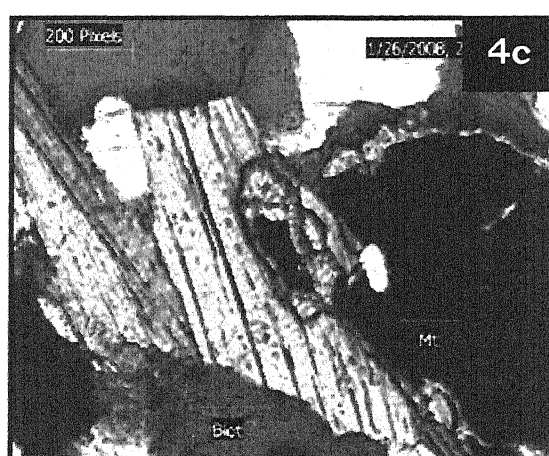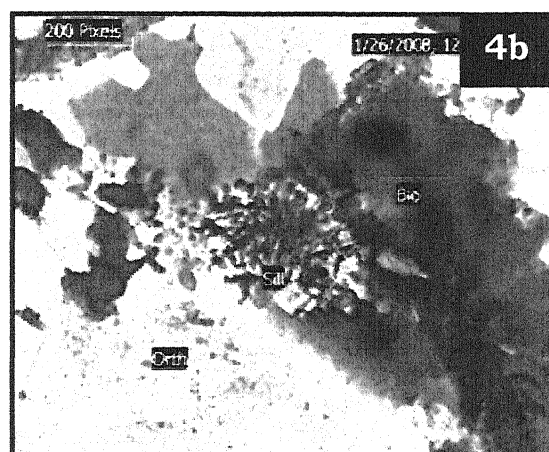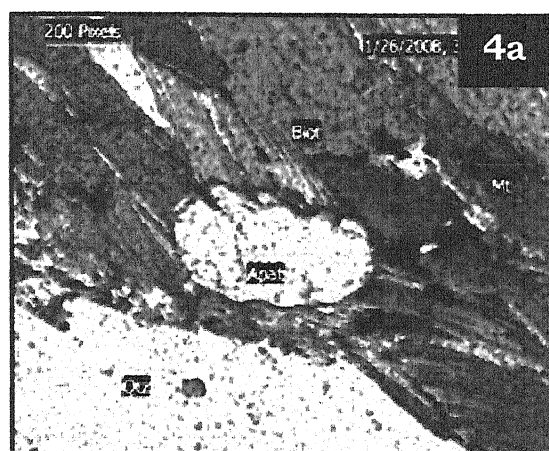
4a : The thin section shows the exsolved texture and formation of chloride. Medium grained of muscovite and elongated crystals of apatite are present in the biotite gneisses.

4b : Thin section shows the alteration of biotite along the cleavage plane, react with magnetite and quartz and form the radiating pattern of sillimanite

4c: Sillimanite rim are formed around the coarse grained crystal of magnetite. orundum are also present in the thin section.

PLATE-5

5a : Radiating pattern of sillimanite are formed by the biotite and coarse grained of magnetite.

5b : Zircon occurs in abundant in the altered biotite gneisses rock.

5c : Zircon are present in the form of pleochroic hallows in biotite.
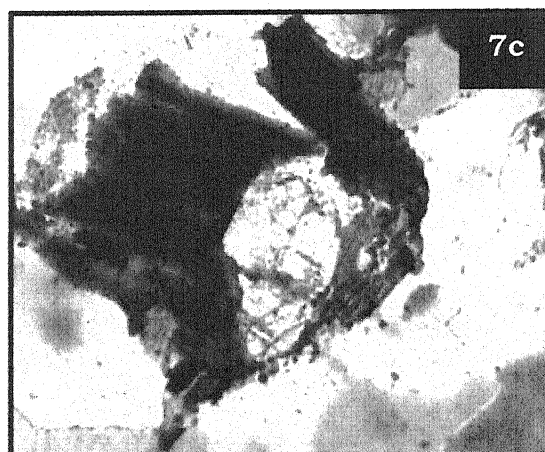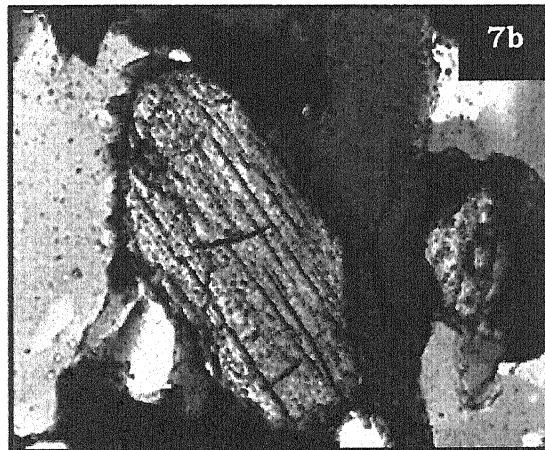
PLATE-6
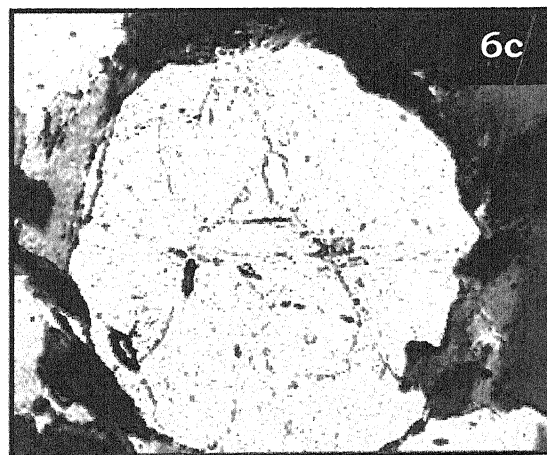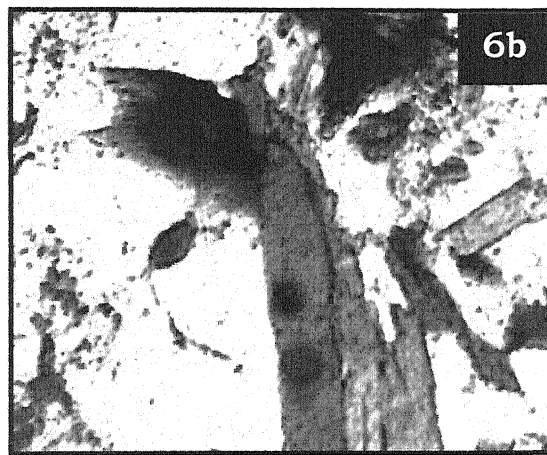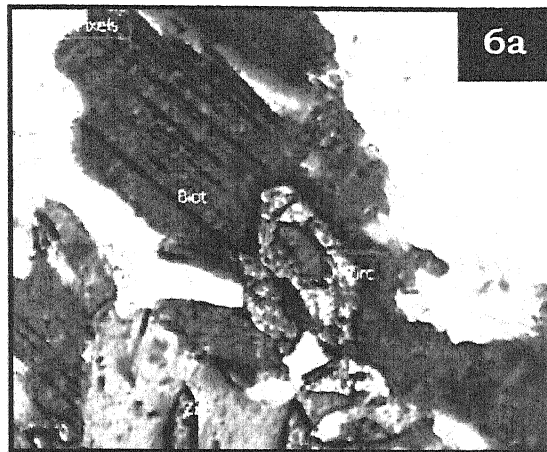
6a : Zircon and biotite are aligned along the gneissoschity plane, coarse grain of quartz crystal are also present.

6b : Two colour of biotite green and yellow , the biotite crystal are breaked along the cleavage plane. Biotite minerals goes to reaction.

6c : Coarse grained garnet crystal. Biotite crystal are aligned along the gneissosity plane.

PLATE-7
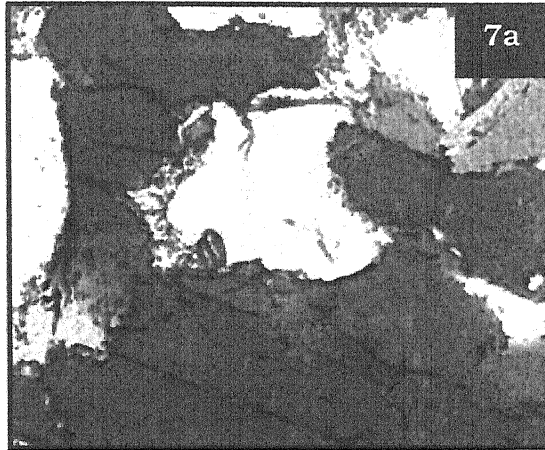
7a : Radiating pattern of sillimanite are formed by the biotite mineral.

7b : Coarse grained crystal of zircon, which is surrounded by the biotite crystals. At one place Zircon and biotite shows the corone texture.

7c : Biotite gneisses, biotite crystals are aligned along the gneissosity plane. Coarse grain crystals of apatite are also surrounded by biotite crystal.

PLATE-8
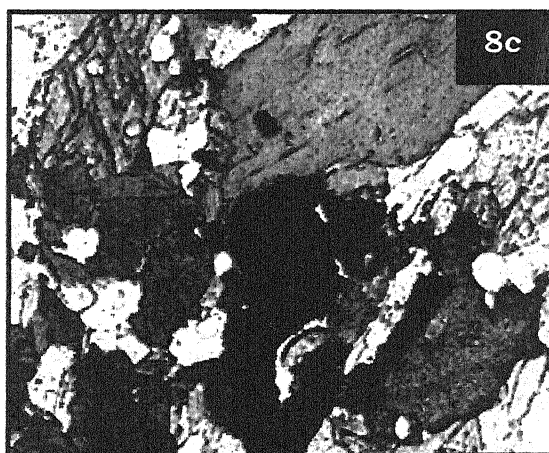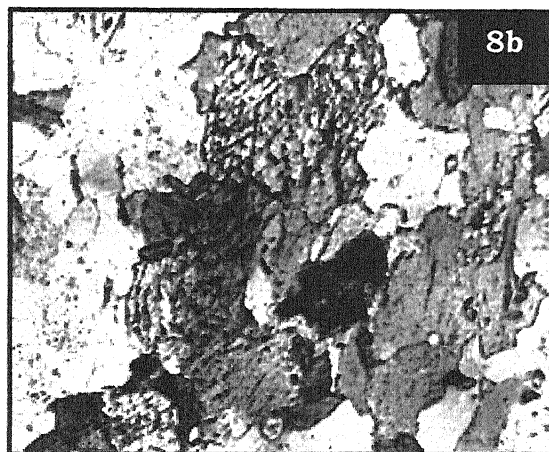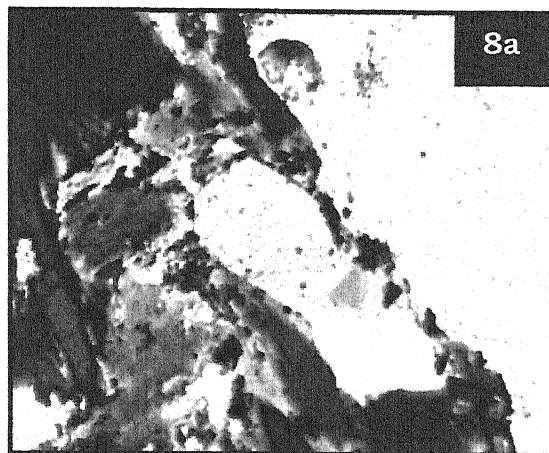
8a : Coarse grained crystal aligned along the S1 sistosity is present. One set of cleavage in biotite crystal. They are aligned along the sistocity plane. The coarse grained crystal of apatite are surrounded by the biotite crystal.

8b : Idiomorphic coarse grain Hornblende crystals . the chloritization takes place along the cleavge plane of hornblende crystal.

8c : Thin section shows the hornblende react with the magnetite and quartz crystal and form the Cpx mineral.s

PLATE-9
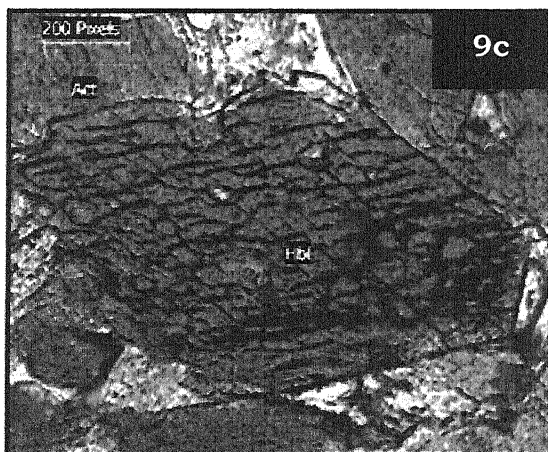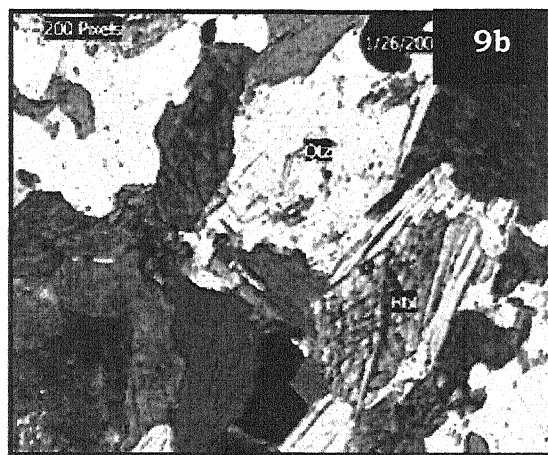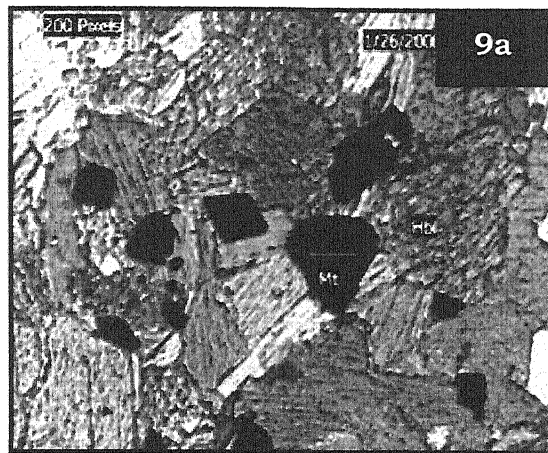
9a : Coarse grained crystal of hornblende and magnetite and amphibolite rock

9b : Corse grained crystals of hornblende magnetite and quartz crystal along the gneissosity plane.

9c : Twin perfect two set cleavage in hornblende. The hornblende crystal are altered in cleavage plane and form the actinolite and chloride crystal.

PLATE-10
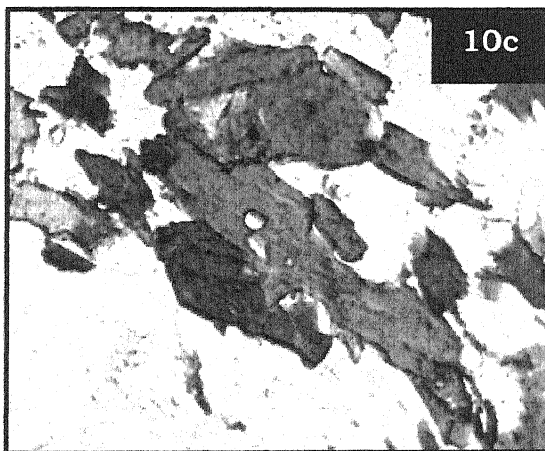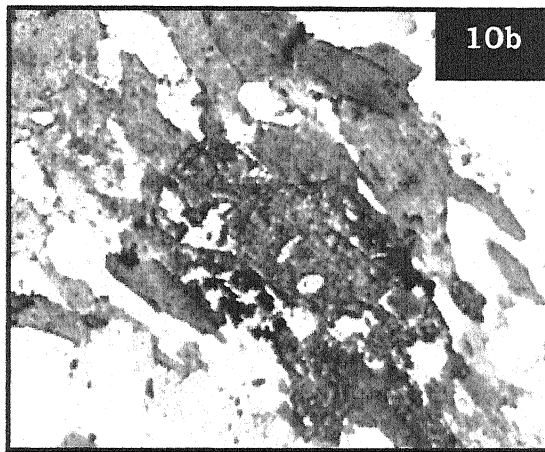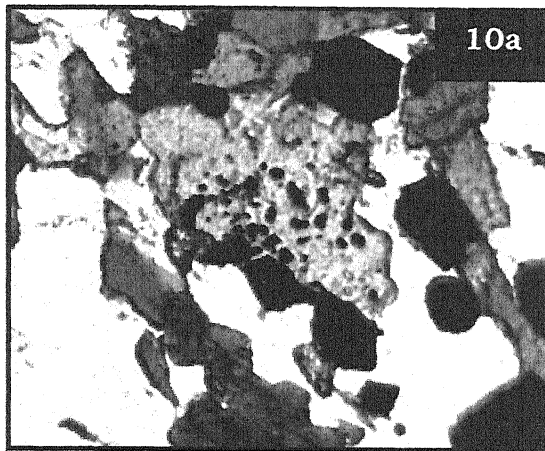
10a : Coarse grained hornblende crystal are surrounded by the medium grained magnetite crystal. No cleavage are present in hornblende crystal.

10b : Coarse grained hornblende and biotite crystals aligned in S2 plane from the biotite bearing amphibolite.

10c : Thin section shows the two colour of biotite crystal, light green and light brown. They are aligned in gneissosity plane. The hornblende crystal doesn't show any cleavage.

PLATE-11
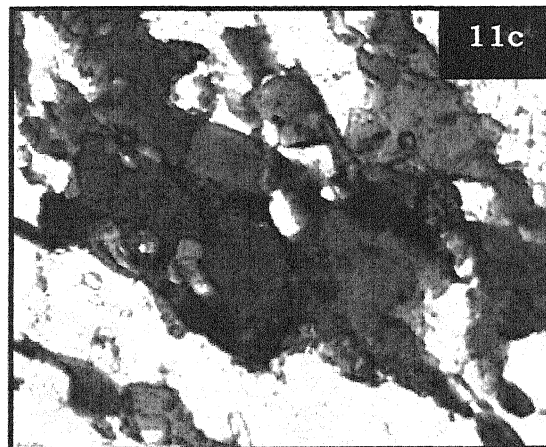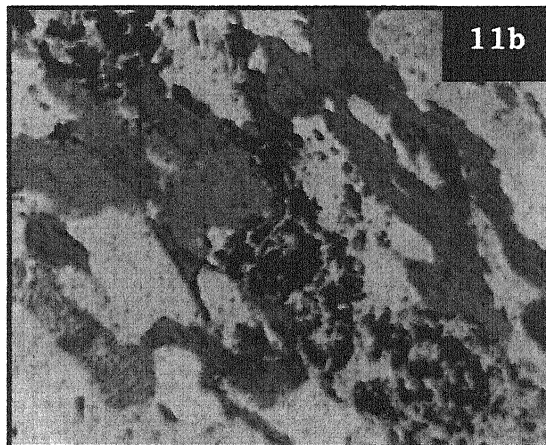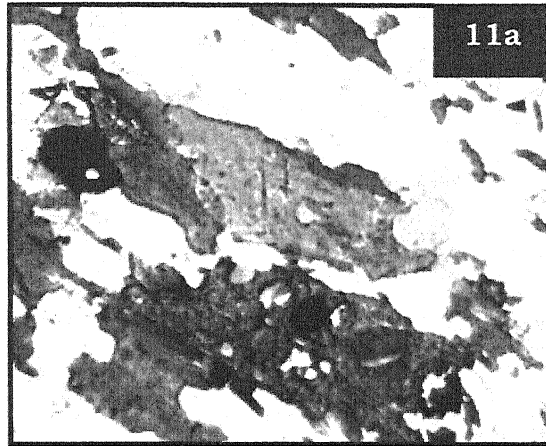
11a : Coarse grained of hornblende and magnetite are aligned in the gneissosity plane. The hbl and magnetite and quartz react and form the Cpx minerals

11b : Hbl-Opx-biotite-plagiclase-Kfs+quartz-magnetite

1c : Coarse grained of hornblende and quartz crystal are aligned in the gneissosity plane.

PLATE-12
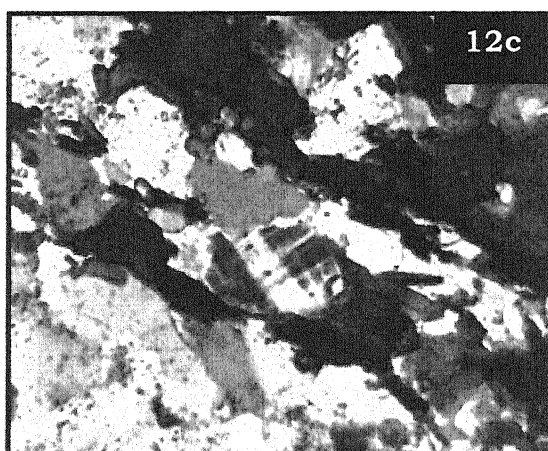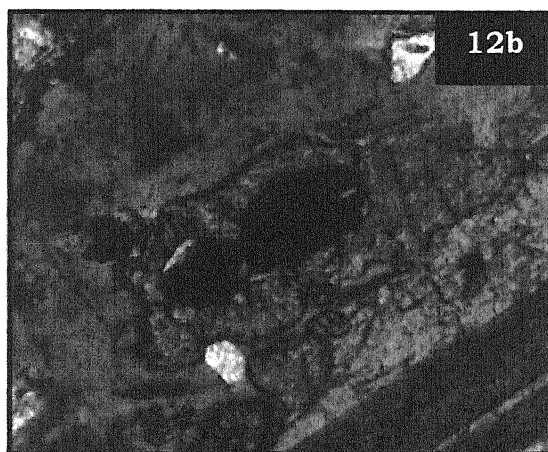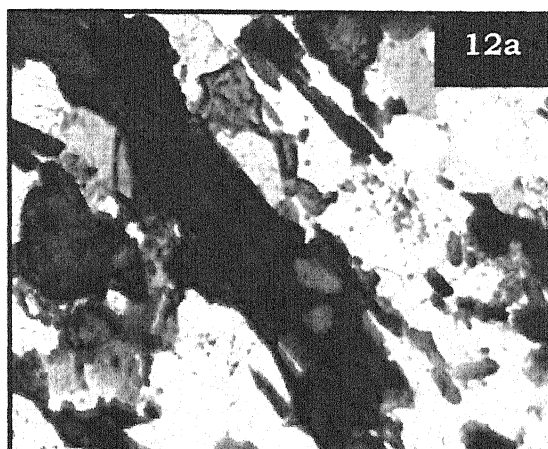
12a : All the crystal are aligned in the gneissosity plane the coarse grained of Sphene and altered orthoclase are present.

12b : Coarse grained crystals of rutile and silliminite magnetite are present in

12c : Thin section shows the crystal of hbl and orthoclase quartz microcline magnetite are aligned in the direction of gneissosity plane. The quartz is leeser than the orthoclase crystals.

PLATE-13
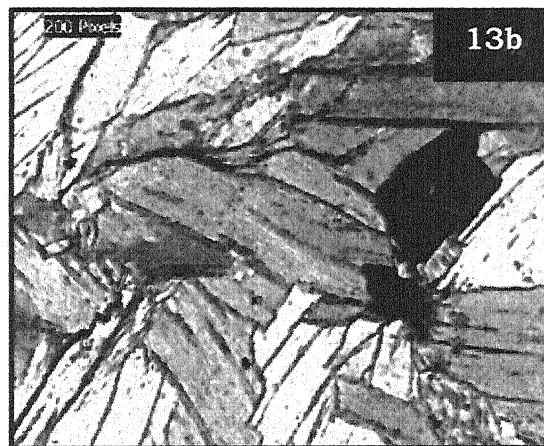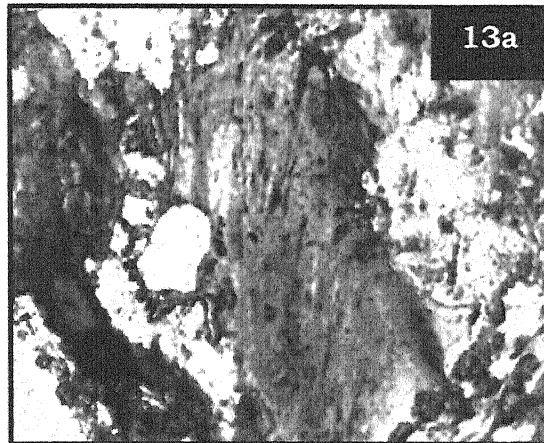
13a : Gneisses rock with Sillimanite and biotite

13b : Thin section of biotite schist. The coarse grain of magnetite also present.

13c : Coarse grained biotite are present in the thin section of schist rock. The magnetite crystals are present at the boundary of biotite.

PLATE-14
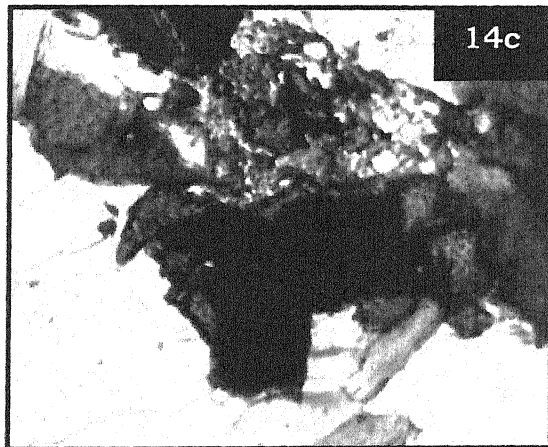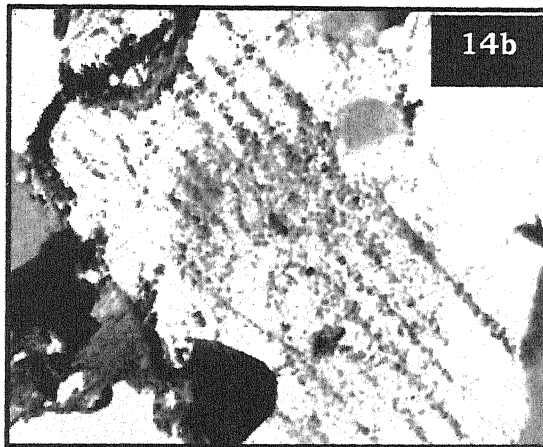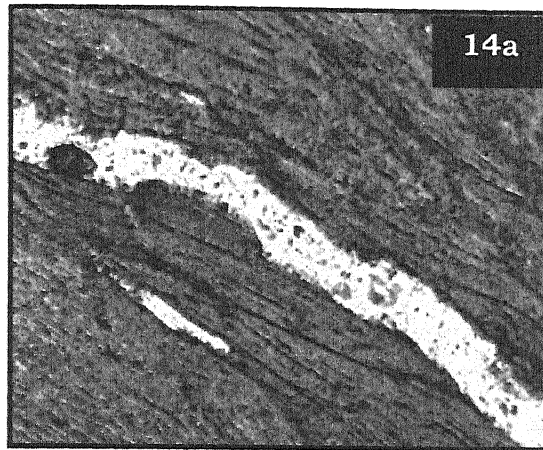
14a : Biotite crystal are aligned along the s1 sistosity plane. Secondary phase of epidote vein are developed in the biotite crystals.

14b : This section shows the exolved texture in the biotite. The rim of sillimanite is formed around the coarse grain of magnetite. Pleochroic hallows are present in the biotite crystal.

14c : Relict of the biotite in hornblende granite.

PLATE-15
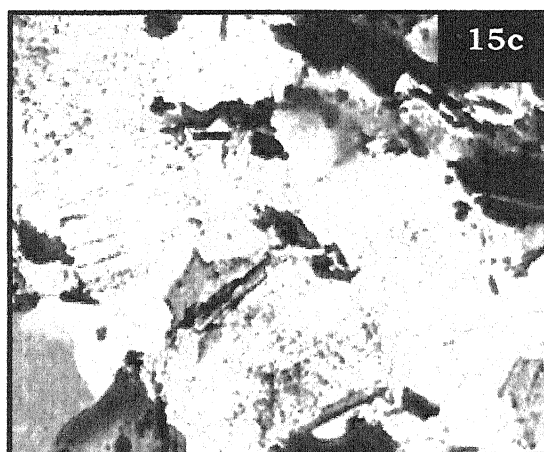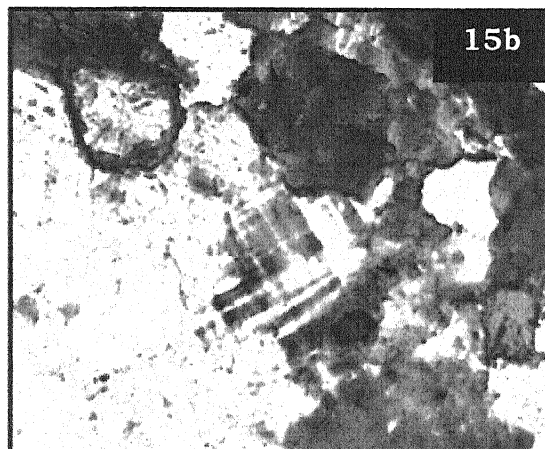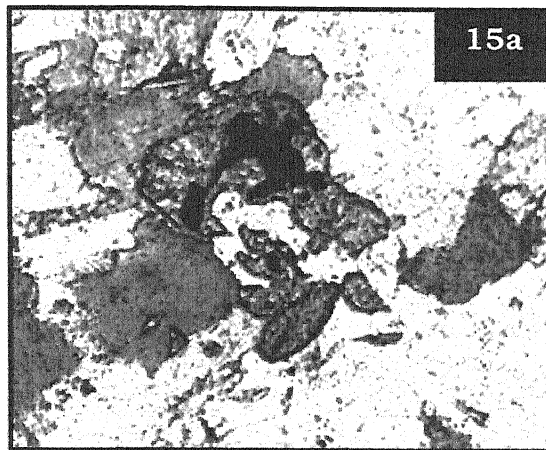
15a : Coarse grained crystal of orthoclase and microcline and hornblende and biotite are present in granite.

15b : Coarse grained crystal of orthoclase are serisetized and perthite texture are also present.

15c : Thin section shows the reaction rim of sillimanite around the biotite crystal.

PLATE-16
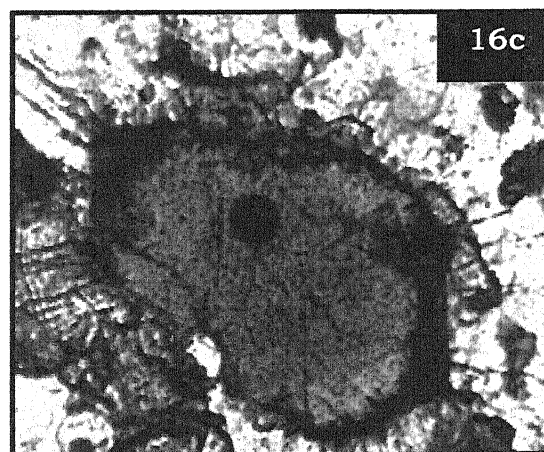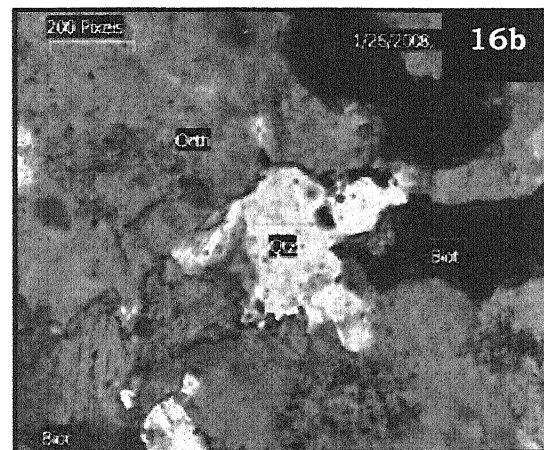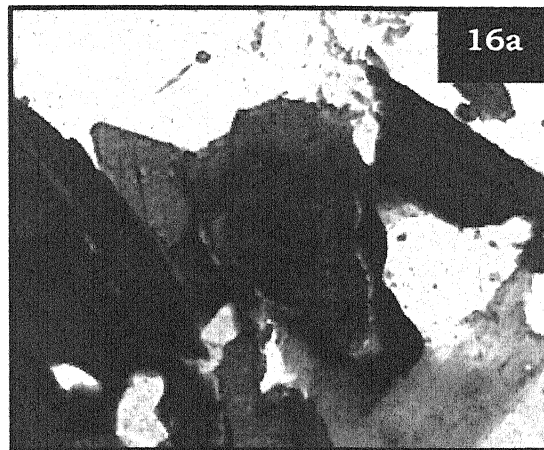
16a : Coarse grained of biotite and quartz and orthoclase are present in granitic rock.

16b : Coarse grained crystal of leucite is present in pink granite rock. The biotite crystal are present at the boundary of leucite crystal. This crystal is highly fractured.

16c : Coarse grained of sphene and biotite are present in granitic rock.

PLATE-17
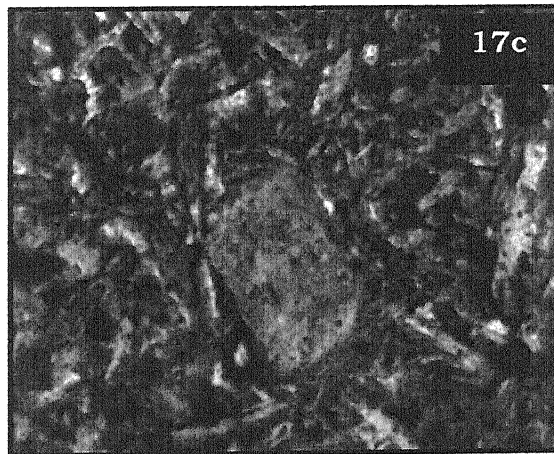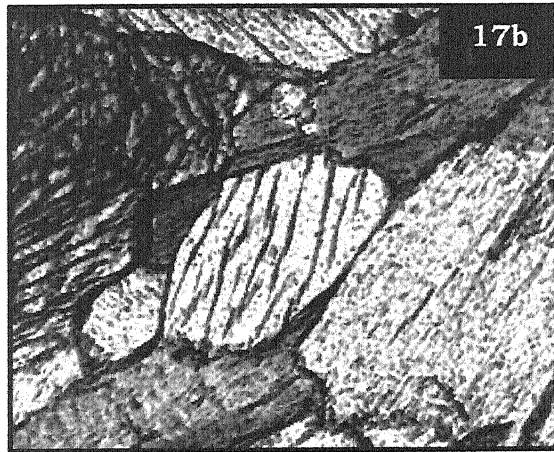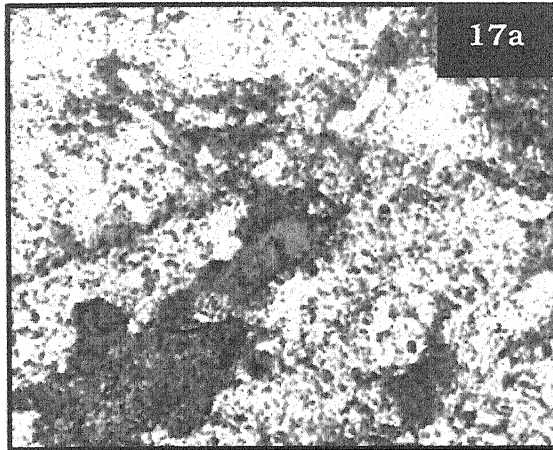
Amphibolitic rock and also coarse grained Cpx and amphiboles are present in the thin section.

PLATE-18
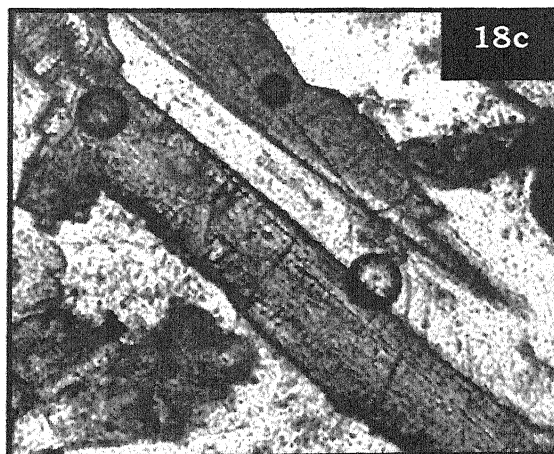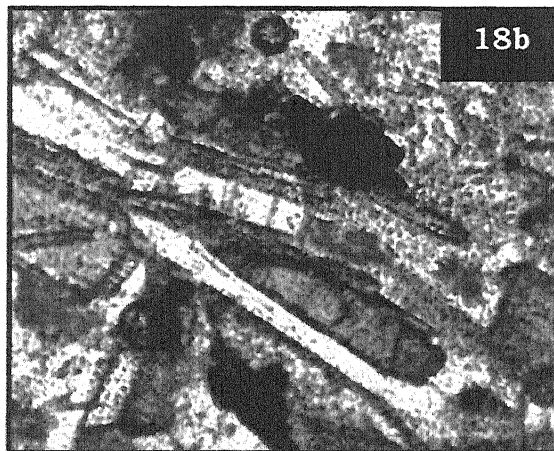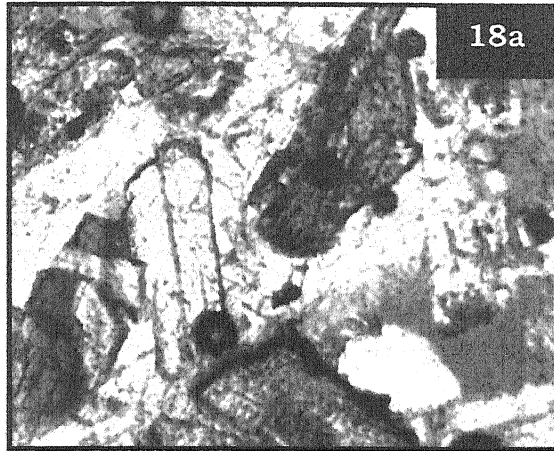
Amphibolitic rock and also coarse grained Cpx and amphiboles are present in the thin section.

Chapter-4

METAMORPHISM AND PHASE PETROLOGY

4.1 INTRODUCTION :

It has been realized that the mineral assemblages of metamorphic rock may reflect the approach of chemical equilibrium during the crystallization. The distribution of elements in the coexisting minerals should be systematic if they attained chemical equilibrium. These crystallized minerals also show a systematic chemical variation in their composition. Such variation in their mineral chemistry indeed reflects the physical conditions of metamorphism and the mineral parageneses reflect a unique phase compatibility relation in the P-T space.

The analysis of co-exiting minerals and the phase compatibility relationships in pertinent system have been used to provide data about nature and tendency of equilibrium and also help to deduce the P-T-X conditions during metamorphism. Thus, we can find out unique pigeonhole on the basis of mineral paragenesis depicted in the petrogenetic grids, which provide information's about the metamorphic evolution. Today the concept of petrogenitic grid is too advanced in comparison to Bowen (1940), who firstly proposed the concept of grid with univariant reaction curves bounding all the conceivable divariant mineral assemblages for a particular bulk chemical composition.

In the following paragraphs an attempt has been made to discuss the mineral parageneses, P-T conditions and phase compatibility relationships of different assemblages obtained from the petrography, textural relationship. The phase petrology and involved metamorphic reactions of different metamorphism along with the fluid inclusion data generated for these assemblages.

4.2 CHEMOGRAPHIC RELATIONSHIP :

The rocks of BnGC, exposed around Nathupura and other places of the study area comprise biotite gneisses, granite-gneisses, tonalite gneisses, trondhjemite gneisses, hornblende-biotite gneisses and amphibolites. These Archaean rocks were tectonically deformed and metamorphosed and subsequently emplaced by different

episodes of gray granitoids (Fig.-2.3). The detailed petrographic study on different foliation planes with chronological events of deformations reveal at least two phases of metamorphism in BnGC. The early phase metamorphism was very high-grade as evident by complete absence of prograde muscovite, chlorite, kyanite, talc, actionlite and epidote etc. minerals and presence of sillimanite, perthite, and diopside minerals. The presence of tonalite-gneisses and their intermingled relationship with other gneisses in the field points that regional metamorphism in the central part of Bundelkhand area was coterminous with migmatites and gray granite. The geochronological study points the formation of TTG around 3300 Ma (Mondal *et al* 2002}. Since the crystallized minerals of the metamorphics are aligned on S_1 and S_2 planes developed during the D_1 deformation D_2 phase and have similar structural trend of TTG, therefore, it can be concluded that a tectonothermal event should be at Mid-Archaean for the first phase of metamorphism of BnGC. Basu (2002), Sharma (1988) and Singh et al (2007) have also been suggested similar views. The second episode of metamorphism in the TTG & granite gneisses of BnGC is mainly confined to the shear zones and is low grade to very low grade may be possibly contemporaneous to east-west trending shear zone. This may be considered as retrograde event. The mylonitised and sheared rocks has been recorded from the gneisses, granite, migmatites, amphibolites and hornblende, biotite gneisses. During the mylonitisation, the chlorite-biotite microcline-albite-quartz and chlorite-biotite-epidote, chlorite-chloritoide-magnetite garnet–Chlorite –muscovite-quartz, muscovite chlorite –magnetite- feldspar-quartz assemblages were developed in shear zones trending in E-W direction and are related to D4 deformation (Table-2.6.)

The first phase of metamorphism possibly initiated at deformation D1. In general, rocks associated with the F1, F2, and F3 folds observed in the gneisses are responsible for the development of gneissic foliation in the pelitic, psammatic and mafic rocks which are defined by the orientation of flaky minerals and elongated plagioclase and needles of magnetite. This episode of metamorphism is further subdivided into two stages (i) formation of gneisses and amphibolites (ii) anatexis migmatite, granite-gneisses, granulites, tonalite, and trondhjhemite. The detailed mineral assemblages of gneisses and amphibolites are listed in detailed in chapter III.

(i)   Biotite–K-feldspar-perthite-quartz.

(ii)   Biotite-plagioclase-K-feldspar-antiperthite quartz.

(iii)   Garnet-biotite-K-feldspar-quartz.

(iv)   Biotite–K-feldspar-perthite-sillimanite-quartz

Assemblages in amphibolebiotites and hornblende- biotite gneisses:

(i)   Hornblende - clinopyroxene - biotite - plagioclase - K-feldspar - quartz.

(ii)   Hornblende – biotite – K – feldspar – plagioclase - quartz.

(iii)   Hornblende – clinopyroxene – plagioclase - quartz.

(iv)   Hornblende - plagioclase - K - feldspar - quartz.

The TTG rocks which includes both tonalite and Trondhjhemite-rocks, content significant amount of K-feldspar, antiperthite, plagioclase, perthite, biotite, and quartz with minor amount of illmanite, apatite, zircon, sphene, spinel etc. The muscovite and clinopyroxene are completely absent in TTG .The hornblende has been noticed in minor amount in most of the TTG rocks.

The gneiss contains mainly biotite, quartz, plagioclase and K-feldspars. The zircon and apatite are present in the significant amount in all the rock samples. The perthite and antiperthitic texture are also present in the gneisses. The garnet and sillimanite minerals reported by earlier workers from the Kabrai area (Saxena 1961) could not be obtained from the present investigated area. The absence of the garnet and sillimanite from Kabrai area may be possibly due to composition variation and excavation of outcrop. It is very significant that muscovite as prograde or retrograde phase is completely absent from the gneisses.

The minerals assemblages of these rocks can be portrayed in AKF diagram (Fig.-4.2) and explained through six components in the KFMASH system. The AKF diagram shows three phases fields of garnet – biotite and K – feldspar. The K-feldspar – biotite join defines the two-phase field for non-garnetiferrous gneisses. The mineral assemblages of tonalite and trondhjhemite gneisses may be treated in CaO,

Na_2O, K_2O, FeO, MgO, SiO2, Al_2O_3 and H_2O (CNKF MASH) system and portrayed in the AFM diagram (Reinhardt Projection) with FeO and MgO as separate component and as plagioclase. Thus the phase compatibility relationship can be better represented by AFM projection from plagioclase (Fig-4.3). The advantage of this projection is that the tie line connects hornblende, clinopyroxene and biotite composition of the three coexisting phases form triangle, enclosing the field of composition of three mineral associations having the fixed composition. The common presence of hornblende-clinopyroxene-biotite phase for amphibolite may be due to large field with variation in the bulk composition of amphibolite rock and these co-existing minerals may be considered as continuous reaction in the CFMASH system between hornblende and biotite at variable pressure and temperature(Fig-4.3). The presence of corroded biotite in the hornblende and clinopyroxene, and similarly presence of corroded hornblende in the biotite and clinopyroxene from the hornblende- biotite gneisses discussed in the chapter III may be attributed to the break down of the biotite and hornblende by the following continuous reaction in CFMASH system and portrayed in AFM diagram (Fig-4.3).

$Biotite_1$ + $Hornblende_2$ = $Biotite_2$ + $Hornblende_1$

Clinopyroxene + Biotite + plagioclase = hornblende +K- feldspar + V
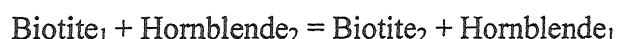
The absence of garnet mineral from all the hornblende-biotite gneisses and biotite-gneisses may be due to either low silica content or due to strong retrograde metamorphism of hornblende biotite-gneisses or in appropriate fluid activity. The absence of garnet from these gneisses may be considered due to the non-availability of appropriate bulk composition and high K_2O and Al_2O_3.

The enclaves of amphibolites are very common in the gneisses. Sometimes they are co folded with biotite gneisses. The petrography studies reveal that talc, epidote, tremolite, chlorite, actinolite, etc. are completely absent, while diopside, calcite, plagioclase, hornblende are present as medium to coarse grained texture. The absence of garnet from the basic gneisses may be due high MgO, K_2O and low Al_2O_3. The common presence of plagioclase, hornblende, and diopside assemblages can be explained in three-phase field of ACF diagram (Fig.-4.1) in CFMASH system. The

other compatible assemblages viz. hornblende-plagioclase-magnetite ± quartz and diopside – hornblende – magnetite ± quartz can be also explained in ACF diagram in six component system of CFMASH system.

4.3 P-T CONDITION :

The detailed petrographic study revealed that at least two phases of metamorphism took place in Bundelkhand gneissic Complex. The early phase metamorphism (M_1) was high-grade as evident by complete absence of prograde muscovite, chlorite, kyanite, actinolite, tremolite, talc and epidote minerals and presence of cordierite, garnet, sillimanite, perthite, diopside, hornblende, anthophyllite and gedrite minerals. The presence of tonalite-gneisses and their intermingled field relationship with other gneisses point out that regional metamorphism was more or less contemporanious with TTG. On the basis of observed mineral assemblges of MnGC rocks of Study area a pterogenitic grid has been constructed in the KFMASH system (Fig4.4) involving the Grt, Bio, Sill, Crd, Mus, Kfs, qtz. Four invariant points and The metastable points have been obtained in the AKF diagram in the KFMASH sysyem and a prograde path have been suggested

The different observed mineral assemblages viz. garnet-biotite-sillimanite-K-feldspar (Fig.4.3), biotite-garnet-K-feldspar-plagioclase-quartz (Fig. 4.2) and hornblende-clinopyroxene-plagioclase-magnetite-quartz (Fig.4.3) of the high-grade metamorphic rocks of Bundelkhand massif reveal that the rocks of Bundelkhand Basement gneissic Complex belong to upper amphibolite to granulite facies. The P–T conditions obtained from different geothermobarometric models (Singh et al 2007) reveal that all the above-mentioned mineral assemblages in gneisses were developed between $650° C$ to $725° C$ temperature and 5 to 6 kbar pressure (Fig 4.4).

4.4 FLUID INCLUSION :

4.4.1 Introduction :

Fluid inclusions are nothing but the small quantities of fluid trapped with in the mineral during the process of crystal growth. They represent actual sample or the only samples of fluid existing at the time of formation of a mineral and its growth.

This data can be used to reconstruct the geological history of a rock in combination with other features like textures and mineralogy. Thus the fluid inclusion study provide important clues in under standing the geological processes viz, the P-V-T-X (pressure, temperature, density, composition) of the rocks and the fluid that formed or traversed the rock in the geological past. There are different types of inclusions observed in mineral viz., fluid inclusion, solid inclusion, melt inclusion, gaseous inclusion.

Fluid inclusions are present as small amount of liquid vapour and gas phases or mixture of these phases. In the granite-gneisses and quartz reef the inclusion are trapped at the time of mineral formation or outwards during the change in geological condition. To understand the genetic condition of gneisses and granite of the Mahoba area, fluid inclusion study were carried out in the quartz crystals.

The small fluid filled vacuoles are present in quartz crystals. These fluid filed vacuoles are observed with a standard petrographic microscope. In the gneisses apatite and quartz in the granite rocks the quartz crystals are considered to be suitable for an investigation of the inclusion. The study shows that mineral contains many excellent fluid cavities (Fig 4.5-4.10). The inclusions reach up to 120cm in length. The inclusion are spheroidal orbalat in shapes in the gneisses (Fig-4.11-4.16). While inclusion are larger in shape in granite comparison to the gneisses. The granitic inclusions are elongated, and prismatic mode of formation of inclusion.

Various scheme of classification have been proposed. The most useful and widely applicable classification of fluid inclusion is proposed by Roebber (1976) which categorized the inclusion into primary (p), secondary (s), and pseudo secondary (ps) on the basis of their origin.

The laboratory grown crystals size, abundance and distribution of inclusion are principally a function of growth kinetics and the stability of various growing faces. The natural, processes leading to the growth and re-crystallization of minerals are diverse and complex during these processes variety of inclusion trapped in crystal which can be easily identified in the ten minerals viz. quartz, fluorite, halite, calcite, apatite, dolomite, sphalerite, barite, topaz, and casseterite. The fluid feature common

to all these minerals is that they are transparent and lightly coloured which, of course, is the most fundamental prerequisite for any optical study of inclusion. The overall abundance and distribution of inclusion in a single crystal depend partly on the primary growth condition and partly on the post crystallization history of the samples. Fluid inclusion shapes are highly variable and are partly controlled by the crystallography of the host minerals.

Mode of formation of primary inclusion :

Primary inclusion – most of the crystals grow or recrystalise in a fluid medium of any kind. During crystals growth or growth irregularities may result for trapping of small portion of the fluid in solid crystals. Such irregularities may be sealed off during growth of surrounding part of the host crystals, yielding primary inclusion (p). Primary inclusion from the granitic rocks of the study area are large prismatic and elongated in shape (plate-4.12). But in the gneisses rock the primary inclusion are usually spheriodal and orblate in shape (plate-4.35). The size of primary inclusion varies from rocks. Most of the primary inclusions are biphase (L+V) i.e. liquid + vappour phase inclusion (plate-4.29).

Secondary inclusions (s); the inclusion formed by any process after crystallization of the bulk of the host minerals. Secondary inclusions are formed by the two processes. (a) from ductile deformation (b) from brittle deformation.

The trapped fluid into these deformation lamellae may be sealed during recrysallization of the host grains commonly, after the healing process is completed. This result the formation of rows of inclusions having regular spacing with the plane with in the grains (plate-4.39).

Pseudosecondary (PS) inclusion are those that are trapped along a fractures developed in the crystals during its growth, instead of being trapped as primary inclusion in the rim of the crystals.

The choice of significant inclusions are exceedingly valuable in extracting the appropriate thermobarometry and compositional information. This is because of the possible presence of several generation of inclusion in the one sample.

It is worth to described that inclusions with sign of leakages, necking down or those abjacent to the crakes are not suitable for getting reliable data. Therefore such inclusions were not included in text. The temperature of trapping can be estimated by the heating of the sample to the point at which the bubbles disappear i.e. the temperature of homogenization. This marks a minimum temperature of formation of the minerals, provided no leakages, exists.

4.4.2 Method of sample preparation :

To calibrate the genetic condition of different type of granite, quartz reef gneisses of study area the fresh sample were collected for the fluid inclusion study. The chosen samples of fluid inclusion interest are rich in transparent minerals like quartz and apatite and taken from the various locations to cover the nature of fluid in the study area.

4.4.2.1 Sowing and Grinding :

After cutting, ideally with a small diameter saw, the surface is hand ground angles plate using progressive fiergrade of silicon carbide (sic) grit. The final grade should be at least 800 (FScale).

4.4.2.2 Polishing :

Hand polishing is carried out using a soft, napped polishing Nylone cloth mounted on a rotary lapping machine. Zirconium powder are used from the polishing of slide one side of polishing takes the 15 to 20 minuets, and the grain size is $0.3\mu m$

Reverse Mounting is essential after polishing for the fluid study. Therefore the sample mounted with the polished face down on to a glass microscope slide using a low melting point dental was once removed and polished by zorconiun power followed by polishing on zylene. The slide cleaned, using acetone or Alcohol or zylene. At the end the slide is cleaned by the fresh water. Dip the slide in fresh water in 10 to 20 minutes. The fluid inclusion slide should be doubly polished and the thickness should be section of 0.1 to 1.0mm in thickness.

Final stage of reserve mounting of the slide are (0.5 to 1mn) are thick, once removed the slide in hot plate can be clean using acetone or Alcohol and fresh water,

petrological microscope, low magnification lenceses (25 x power) identity the primary, secondary and pseudo secondary inclusion in granite waffers. The best-procedure to identifying the inclusion in the waffers to scan the sample using a low to moderate magnification. Inclusion of average size (10 in micron) will usually appears as small dark speaks or group of trails of speaks with in the small because of the strong internal reflection. The objective should then be change to one of the higher power at the same time raining the sub stage condenser close to the specimens. This should reduced the internal reflection and with an appropriate adjustment of the focus. The inclusion should be clearly visible. In the primary inclusion are large in size. They are trapped in quartz crystals in disseminated forms and primary stage of mineral formation. But the secondary inclusion are trapped at the stage of secondary intergrowth of minerals formation. They are trapped in fractures secondary inclusion are small in size they are aligned in particular directions.

4.5 FLUID INCLUSION PETROGRAPHY :

Fluid inclusion petrography is used in the determination of inclusion shapes, size, phase proportion (like monosphase, biphase), determination of degree of fill, length and width of the inclusion, types of inclusion (L+V+G+S) and abundances and distribution of the inclusion. The fluid petrography is also useful in growth zones, relationship to the crystal faces and traces the cleavages direction. The optical examination of fluid inclusion are used in determination of either metastable inclusions, heterogeneous trapping, leakage and daughter inclusion identification and necking down inclusion, their relation with other inclusion and with the host grain suggest the type and origin of the inclusion and also the relative chronology.

4.6 FLUID IN GNEISSES :

Thermodynamics concept and experimental work suggest that mineral stability is the guidelines, factors to understand mineral reaction in metamorphic. Aparts from P and T, the action of chemically active fluids is also important factor, because they promote or inhibit metamorphic reactions. Although metamorphic system is described as subsolides or solids state that virtually contains several types of a fluid phases. In

the Bundelkhand gneissic rocks, the fluid inclusion petropgraphy indicates that gneisses consisting orthoclase, quartzs and apatite have appreciable amount of fluid inclusion. They provide important insight into the composition of the fluid present, when the minerals grains formed. The experimental study reveal a variation in composition and density, with respect to change in the P-T conditions of metamorphism and thus help to record the uplift/extensional history of a metamorphic terrane.

Most of the primary fluids of the gneisses are rounded and trabular in shape and are usually biphase (L+V) in nature. The gas bubble trapped in fluid use to under the influence of gravity or due to thermal gradient with in the inclusion, when the temperature go down most of the gneisses inclusion are sink down and shows the hazy texture. Keeping this advantage, the heating and freezing stage are run to determine the phase change at appropriate time. The useful qualitative and semi quantitative composition data have been obtained. The determination of composition and density of fluid inclusion in largely based on a comparison of the behaviour of the inclusion. The cooling experiment was done below -150^0C. The primary fluid the inclusion of gneisses are found to freezed consisting at -120^0C all the bobbles upto -120^0C. That is shown by hazy texture, the heating initiated after super cooling and various kind of change texture were noted at several temperature. In the gneisses primary inclusion of the gneisses rocks melt different melting temperature. study on linkam heating and freezing stage suggested of primary inclusion of the gneisses rocks are dominated by H_2O-NaCl, H_2O-Na_2CO_3 system. The temperature clathrate melting of H_2O-NaCl;-$MgCl_2$ also noted in several samples that indicate at 1.1^0C temperatures.

4.7 DENSITY OF FLUID INCLUSION :

The relative volume of liquid and gas phases are determined at room temperature (using geometrically regular inclusions), and if the composition of the fluid inclusion is known, the density of the homogeneous inclusion can be determined using various P-V-T data. Determination of the density of the inclusion, the length and width of the liquid and bobble were calculated using the software of linkam. On

the basis of calculated length and width of the inclusion the degree of fill of the inclusion has been determined. The data of degree of fill, shape, size length and width, eutectic point taken into considerate for interpretation of fluid composition. The software has facility two plots the density and salinity diagram on the basis of these given values. The gneissic rock yield the different system inclusion for various type of shows which depends on length and width and also values of degree of fill and the basis of these values the plot the density and salinity diagram (table-4.1).

4.8 FLUID IN PINK GRANITE :

The fluid inclusion signatures in quartz of granite can also provide some compositional evidence for syn to post magmatic fluid. The later may provide evidences of major hydrothermal activity and tectonic related events in the upper crust. It is important to distinguish primary and secondary inclusion to known the temperature and chemical environment during minerals growth. Tuttle (1949), pointed that the primary inclusion is useful for tectanothermal event. He also empases that the presence and attitude of secondary inclusion are essential that can be useful to structural geologist to interprete the tectonics of the area. Fluid inclusion signature in granitic has been used to find the chemical composition fluid during and after the crystalization of granitic magma of Bundelkhand magmatites (BnGC).

The secondary fluid provide evidence of major hydrothermal convection and tectonic related events in upper crust. The Bundelkhand pink granitoid consist quartz as major minerals constituent besides the rock consist the biotite–hornblende magnatite – rutile – pottash feldspar, minerals. The minerals are medium to coarse grained. The mermekite textures are also found in many thin sections of pink granite rock. The coarse crystal of quartz have been selected for the preparation of fluid inclusion.

Most of the inclusions in the granitic rocks are biphase (L+V). In the granite rock primary inclusions are rounded and elliptical in shape. Some places they are cylindrical in shape. At the room temperature inclusion are light greenish in colour. But freezing stage inclusion are sinking down and they gives the purple colour. At 70^0C all the (L+V) phase are freeze out and both the phases are mixed, when return to

heating stage melting of Ice will start and first bubble are developed at the -11.0°C. The eutectic point of suggested that most of the inclusion are related to H_2O-KCl system. But some inclusions are developed at -35°C. They give H_2O-NaCl-MgCl system. The clathrate of the H_2O-KCl system is -1.8°C. In the case of H_2O-NaCl-MgCl system temperature is +21.5°C. The density calculation of these inclusions based on length and width of the inclusions. plot the density diagram in P-V-T-X software field and diagram.

4.9 FLUIDS IN GRANITES :

Fluid inclusion signature in quartz of the granite rock can provide direct compositional evidence for syn and post magmatic fluids. The secondary fluid can provide evidences of major hydrothermal convection and tectonic related events in the upper crust. It is important to distinguished primary and secondary inclusion because of the poacity to determining the temperature and chemical environment during mineral growth. Secondary inclusion further allow us to reconstruct part of the history of a crystal.

The granite consist the quartz biotite hornblende magnatite rutile orthoclase plagioclase and microcline are the major minerals of the pink granite. Fluid inclusion signature in quartz can provide direct compositional evidence for syn and post magmatic fluid in granite.

Two type of inclusions have been identified in the Bundelkhand granites. The size bubble is a first observation followed volatile content of the inclusion petrography of fluid inclusion. Volatile rich melt fluid may also be present with in the bubble. The density of a fluid phase that depend on the pressure and temperature at the time of trapping. The best procedure is to scan the sample using a low to moderate magnification. Inclusion of average size (15 in microns) will usually appear as small dark specks or group of trails of specks with in the sample because of strong internal reflection. They are biphase (L+V) in nature. The biphase nature of the inclusion are easily separate out. The fluid are an aqueous solution and a vappour bubble. The primary inclusion are biphase in nature. They occurred randomly but the secondary inclusions are aligned in the particular direction. They are small in length. Some

places the pseudosecondary inclusion are also noted. The quartz crystal in the granite rock are euhedral in shape white to light green in colour. The inclusion in the crystal are moderate relief mineral. Most of the primary inclusion found in the quartz are rounded and elliptical in shape, but some place they are cylindrical in shape.

The primary inclusion they are transparent to light green in colour at the room temperature that changes to dark green to purple in colour at cooling. At the room temperature the inclusion consist of liquid + vappour (L+V) two phase. On gradual cooling they developed the solid ice phase. Freezing stage the vappour phase is disappear and all the crystal are freeze out. All the crystal are freeze out and the quartz crystal show the green to purple colour the crystal are shink down at -120^0C. Gradual heating lead to melting of solid phases at the temperature. Which is the tripple point (L+V+S) phase. Complete melting of solid phase give to liquid and vapour (L+V) and the inclusion envolved along the two phase (L+V) univarient line. When the solid phase change to liquid crystal phase show many change in their shape and texture and colour. At the freezing stage colour of the fluid is purple to brown but lowering of temperature give the green to transparent in colour.

Again lowering the temperature the clathrate melting will be appear. At the room temperature appear vapour phase will moved in the liquid phase, zig –zag movement of the vapour phase are present in the clatherate melting. Again increasing the temperature above the 300^0C the water will pass from the microscope and found the Th (Temperature of Homogenization).

Secondary monophase biphase aqueous inclusion range in shape from irregular to elongated and tabular. At the room temperature inclusion consist of monophase with low degree of fill. Lowering of temperature result in the formation of hydrohalite and ice at temperature between -54^0C. On the gradual heating melting of hydrohalite and ice takes place at -30^0C which is the vappour saturated eutectic point of H_2O Nacl system. Final ice melting is observed in the temperature range of -120c, -4^0C .The density and degree of fill and salinity are calculated by the PVTX software.

Table : 4.1 : Fluid phase system in the study area

Sample No.	Rock type	No. of Experiment	Type of Inclusion	Shape	Degree of fill	Tm	Density	System
MO$_4$-12	Pink granite	1	L+V	Rounded	0.83996	-12.3	0.999	H_2O-NaCl
		2	L+V	Ellipse	0.9956	-34.8	0.997	H_2O-NaCl-$MgCl_2$
		3	L+V	Cylindrical	0.94405	-17.3	0.998	
MO$_4$-4	Pink granite	1	L+V	Rounded	0.9556	-11.0	0.997	-H_2O-KCl
		2	L+V	Rounded	0.17500	-17.3	0.997	
		3	L+V	Rounded	0.4405	-11.5	0.998	-H_2O-KCl
MO$_4$-276	Gneisses	1	L+V	Ellipse	0.8719	-21.8	0.996	H_2O-NaCl
		2	L+V	Ellipse	0.94019	-21.8	0.997	$Na_2CO_3H_2O$- NaCl Na_2CO_3
MO$_4$-184	Gneisses	1	L+V	Trabular	0.91134	-30	0.997	KCl
		2	L+V	Trabular	0.94019	-21.8	0.997	H_2O-NaCl
		3	L+V	Trabular	0.9075	-34.6	0.999	H_2O-NaCl-$MgCl_2$
BU/PM/183	Gneisses	1	L+V	Rounded	0.8828	-36.3	0.997	H_2O-Na_2CO_3
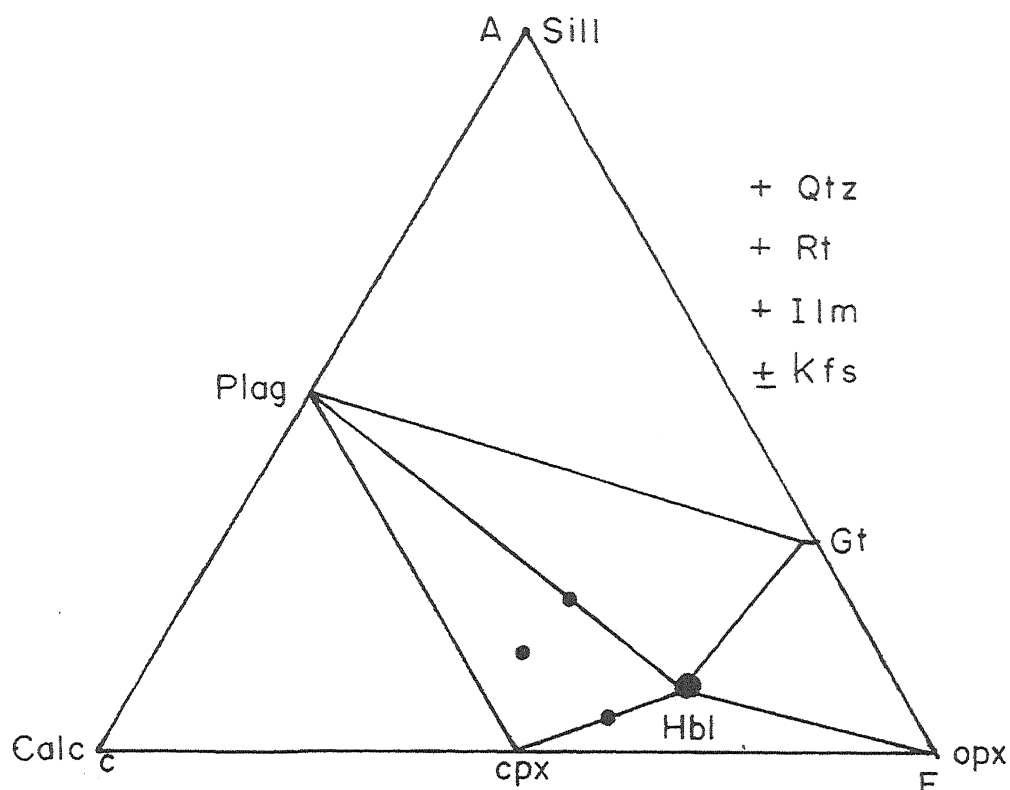
Fig 4.1: The phase compatibility relation for amphibolites portrayed in ACF diagram. The solid circles represent the observed mineral assemblages in the
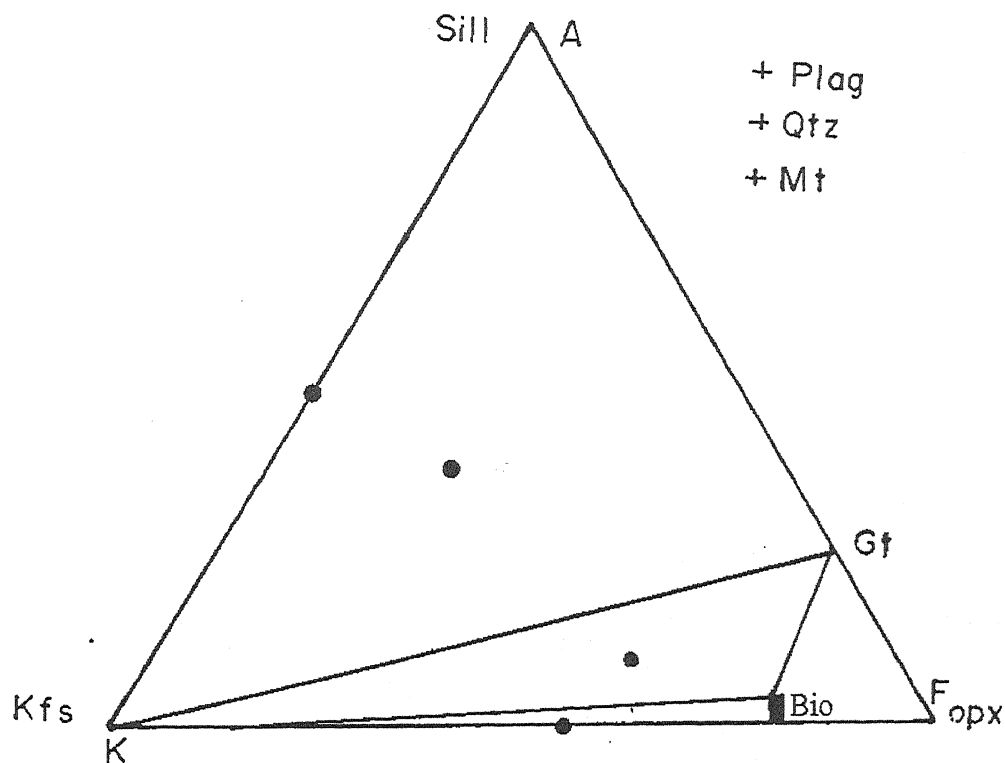
Fig 4.2: Phase relation of biotite gneisses, tonalite, garnetiferious gneisses and TTG are shown in AKF diagram in the KFMASH system. The solid circles represent the observed mineral assemblages in the study area.
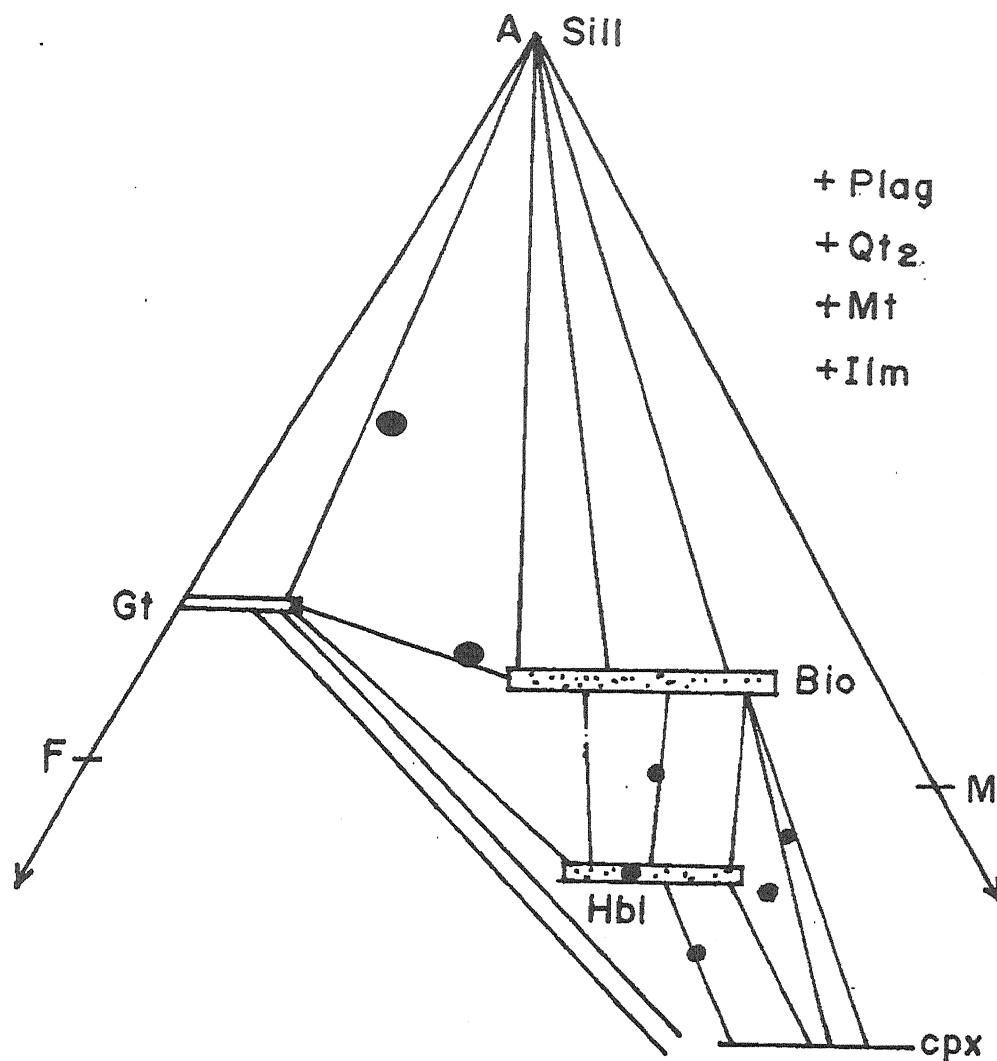
Fig 4.3: The phase relation ship for the biotite gneisses, Biotite- hornblende gneisses and amphibolites, and BnGC group of rocks in the A'F'M' projection diagram "Projection from plagioclase in the tetrahedron AKFM in the system Na2O – K2O – CaO –FeO – Al2O3 – SiO2 (NACFMASH) proposed by Reinared 1967". The solid circles represent the observer minerals assemblages.
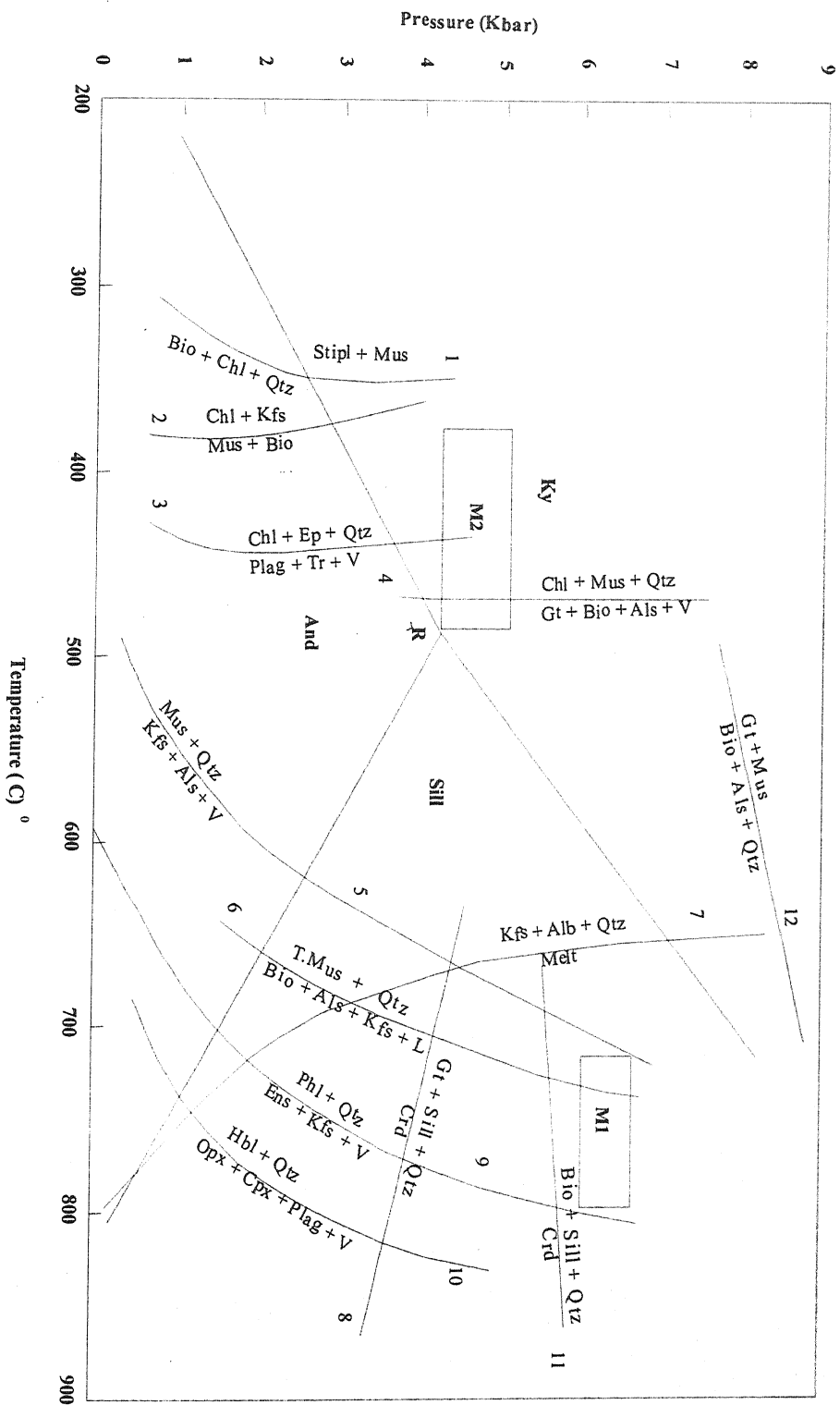
Fig.4.4a: P-T conditions of metamorphism are represented by experimentally determined equilibria of the reactions. The triple point (R) and stability of aluminosilicate is after Bohlen et al. (1991). The experimentally determined equilibrium reaction .1 Nitsch (1970), 2 and 3- Winkler (1976), 4. Hirschberg and Winkler (1968), 5. Chatterjee and Johannes (1974), 6. Thomson (1982), 7. Ebadi and Johannes (1991), 8. Holdaway and Lee (1977), 9. Valley et al. (1990), 10. Spear et al. (1981), 11. Thomson (1982) and Holdaway and Lee (1977), 12. Thomson (1982). The shaded boxes represents the P-T of the metamorphism, (i) M1 for the rocks of Bundelkhand Gneissic Complex (BnGC) and (ii) M2 for the rocks of Bundelkhand Metavocanics and Metasedimentaries (BMM) obtained from the different geothermobarometry.
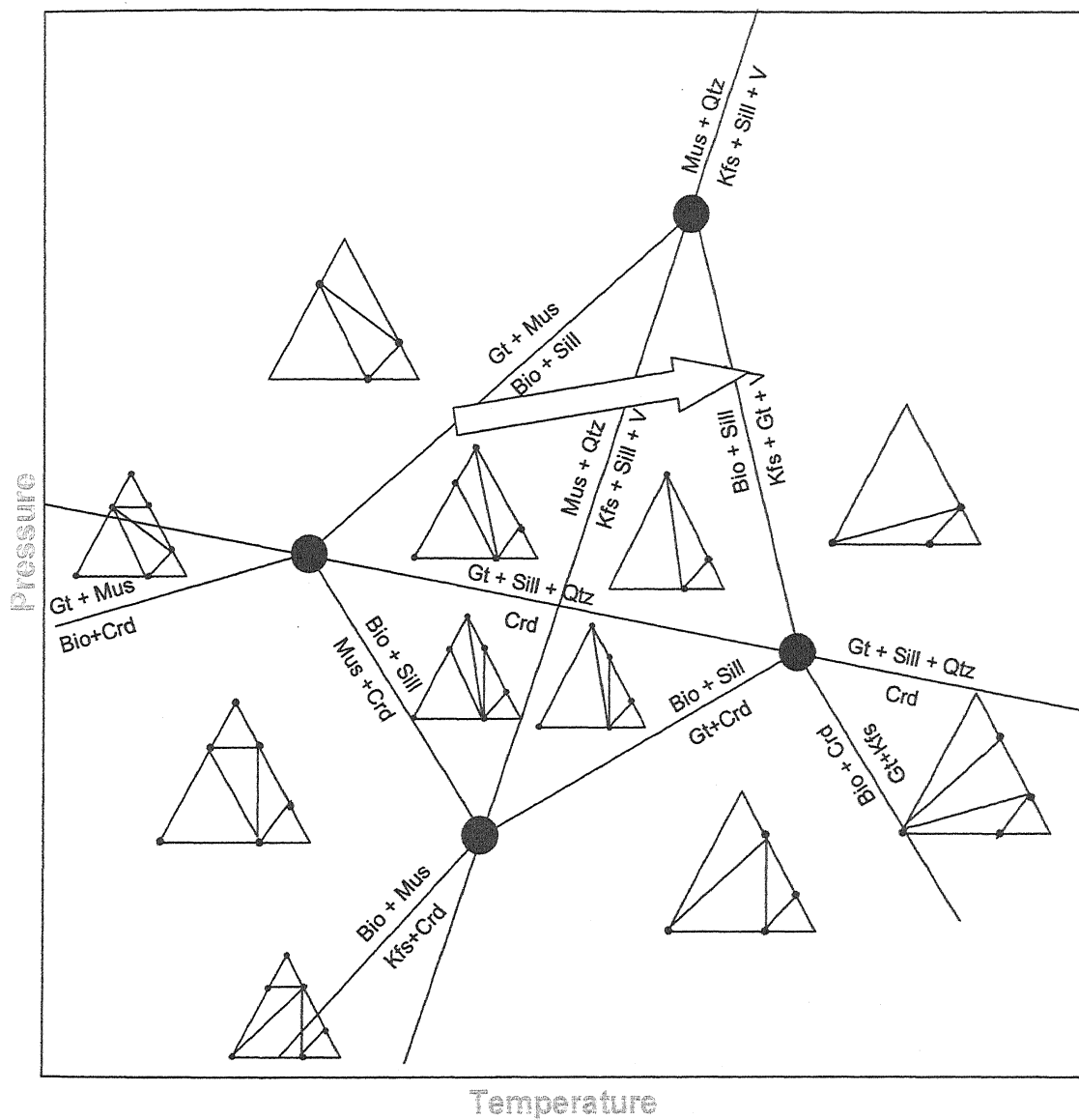
Fig 4.4 : Petrogenitic grid in the KFMASH system for the peletic rocks of BnGC group of Mahoba area. Arrow represents the P-T path.
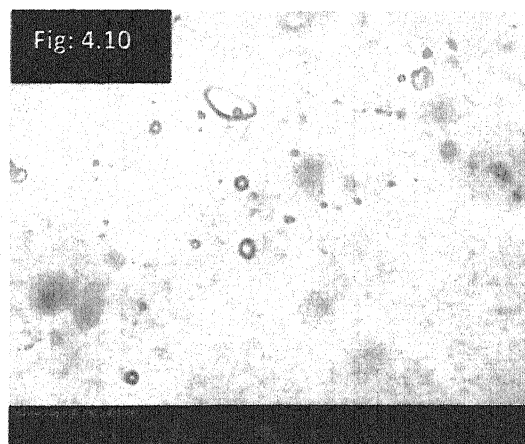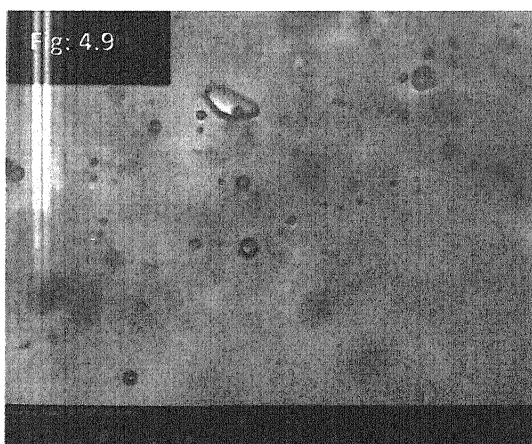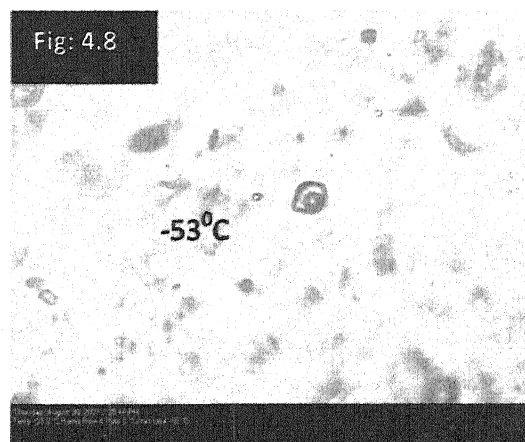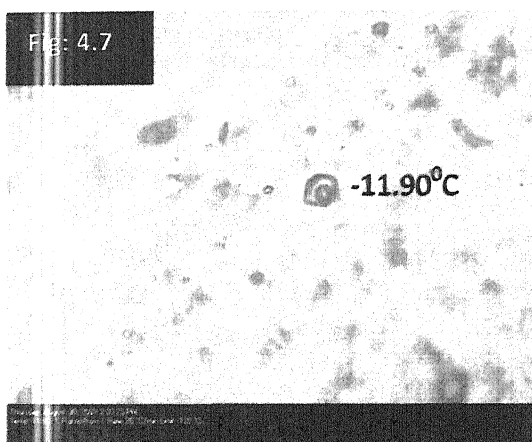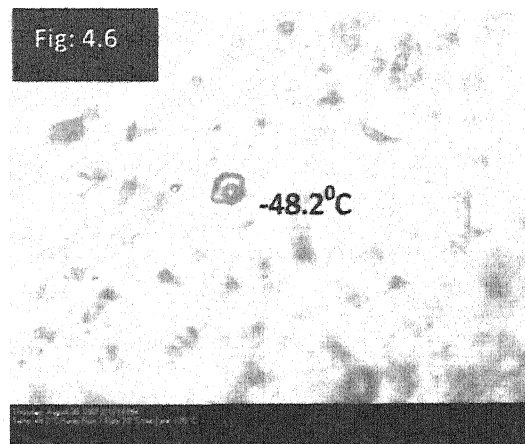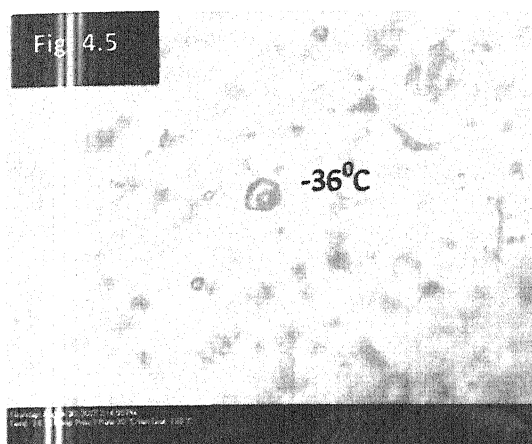
Fig: 4.5 -36^0C

Fig: 4.6 -48.2^0C

Fig: 4.7 -11.90^0C

Fig: 4.8 -53^0C

Fig: 4.9

Fig: 4.10

Fluid inclusion textures from the rocks of Mahoba area at various temperature.

Fig: 4.11 — 22°C
Fig: 4.12 — 25.8°C
Fig: 4.13 — -70.1°C
Fig: 4.14 — -94.4°C
Fig: 4.15 — -120.3°C
Fig: 4.16 — 23.8°C
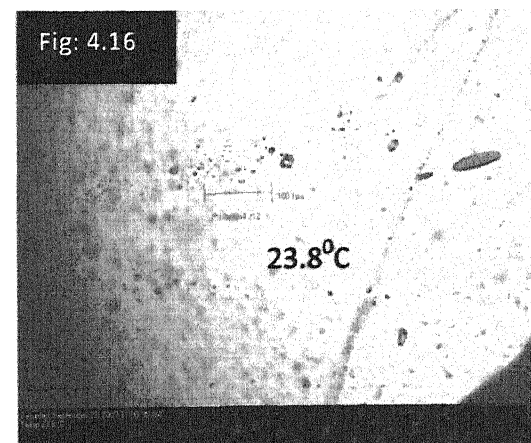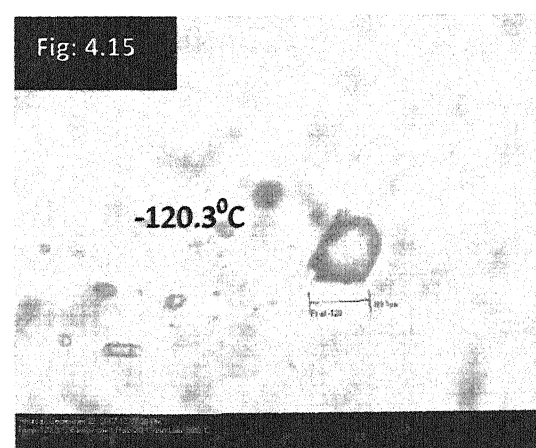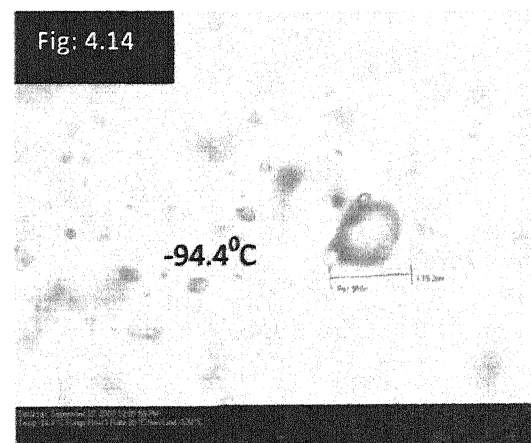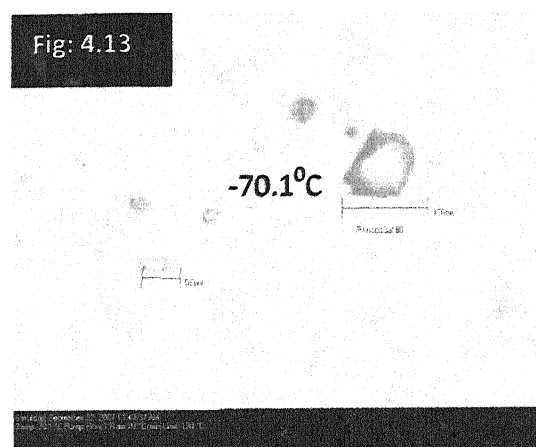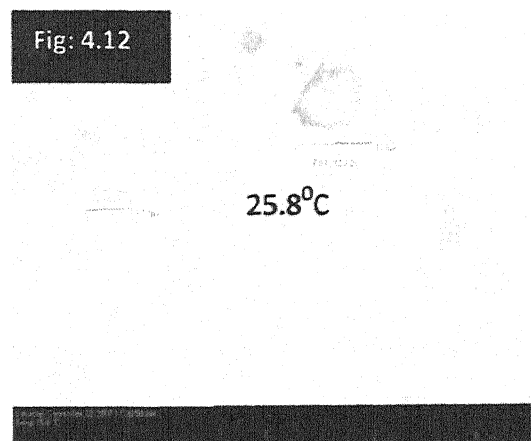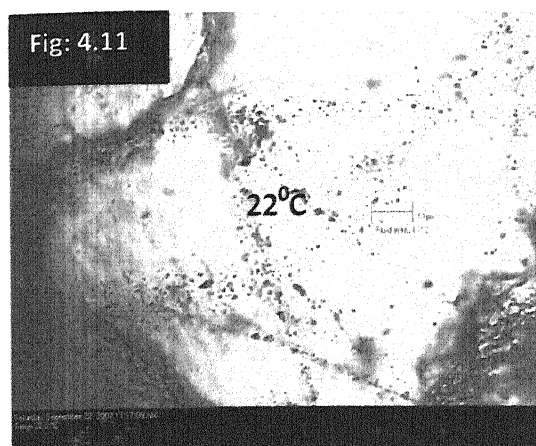
Fluid inclusion textures from the Pink Granite of Mahoba area at different heating temperature.
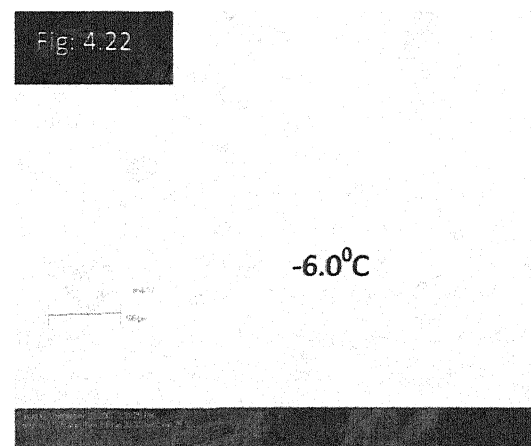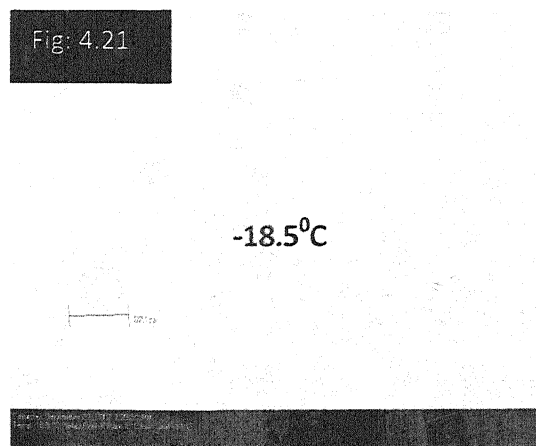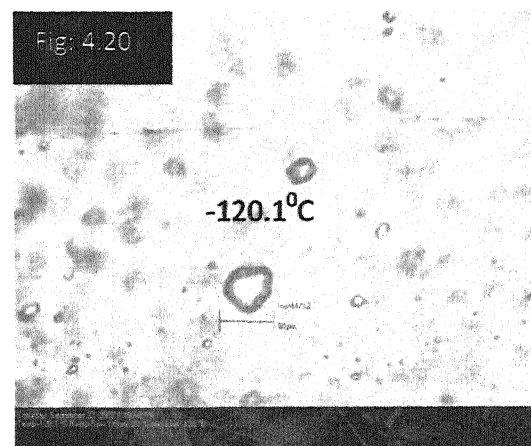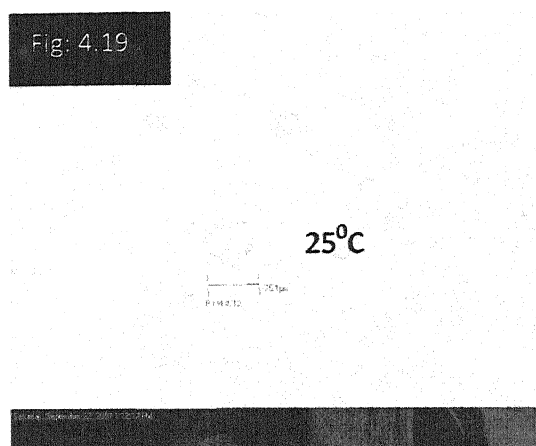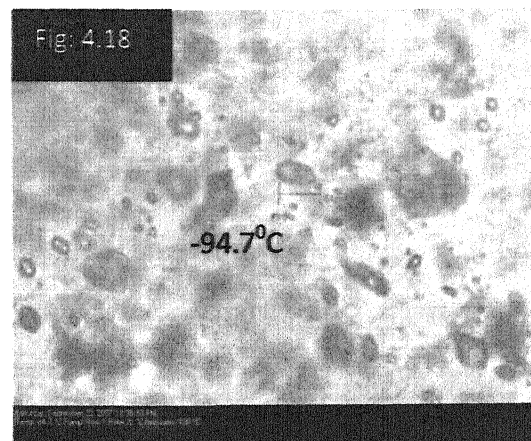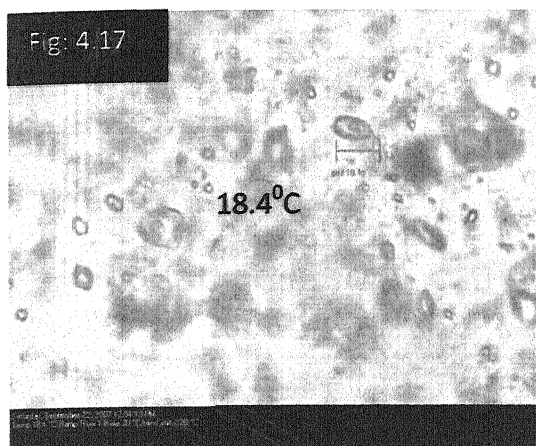
Fig: 4.17 — 18.4°C

Fig: 4.18 — -94.7°C

Fig: 4.19 — 25°C

Fig: 4.20 — -120.1°C

Fig: 4.21 — -18.5°C

Fig: 4.22 — -6.0°C

Fluid inclusion textures from the rocks of Mahoba area at various temperature.

Fig: 4.23

Fig: 4.24

-53.2^{0}C

Fig: 4.25

-97.8^{0}C

Fig: 4.26

-17.1^{0}C

Fig: 4.27

-45.0^{0}C

Fig: 4.28

-34.9^{0}C
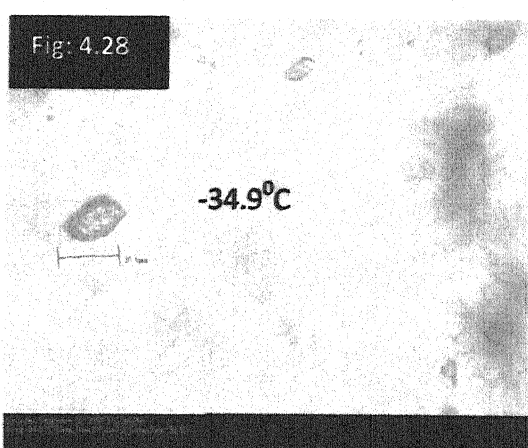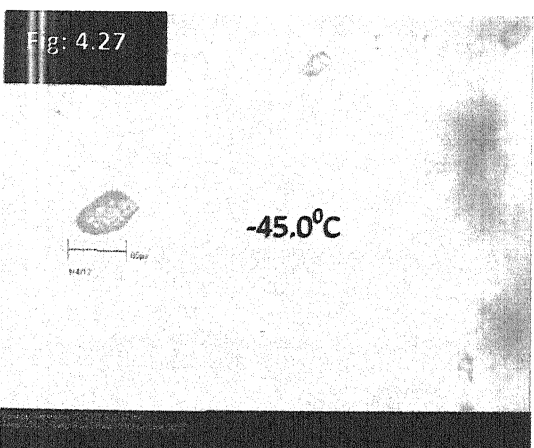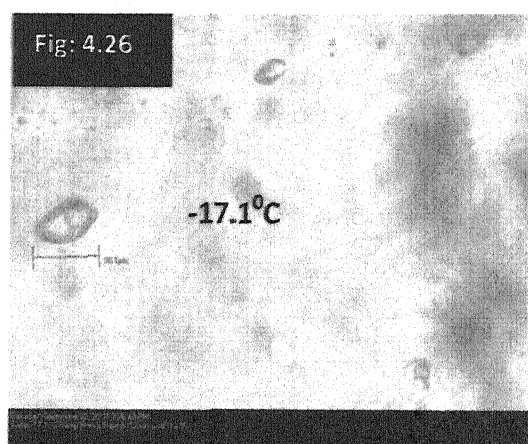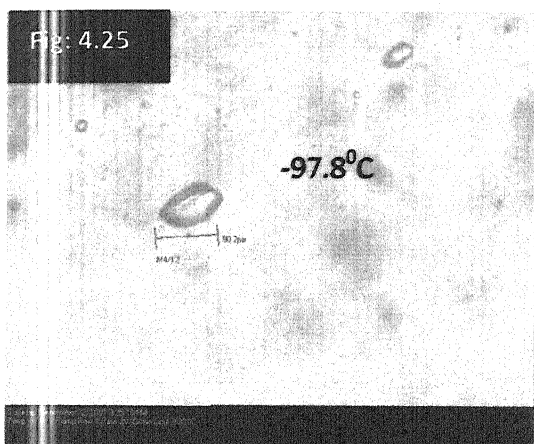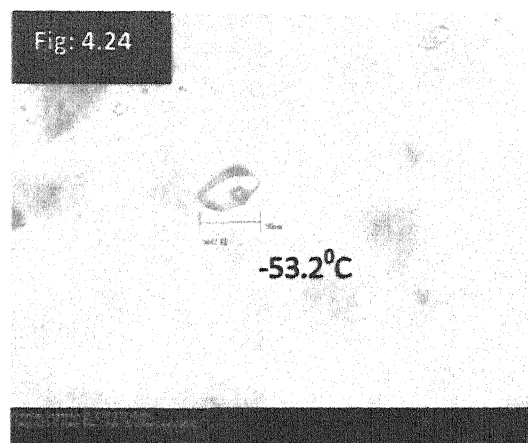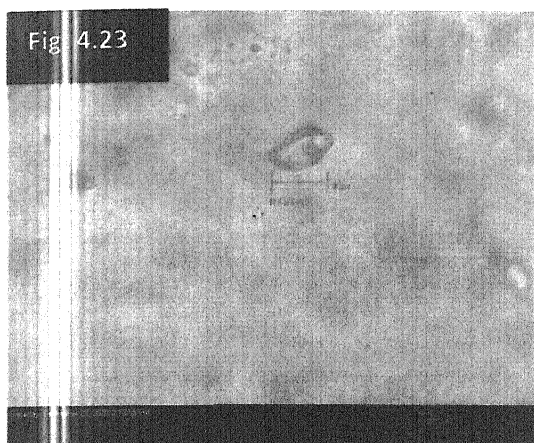
Fluid inclusion textures for the pink granite of Mahoba area at various temperature.
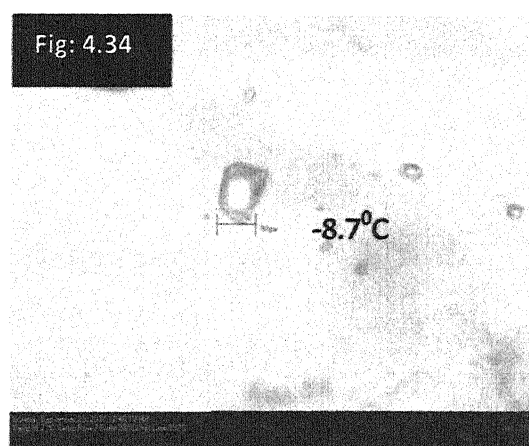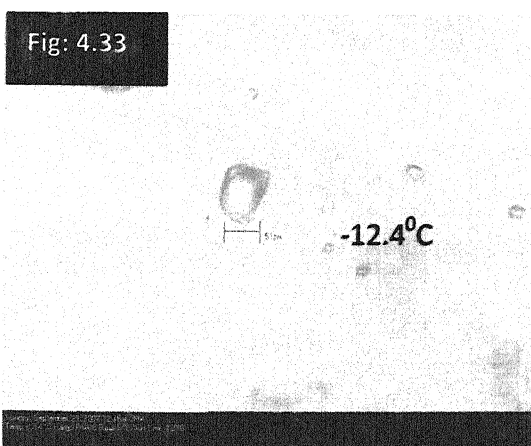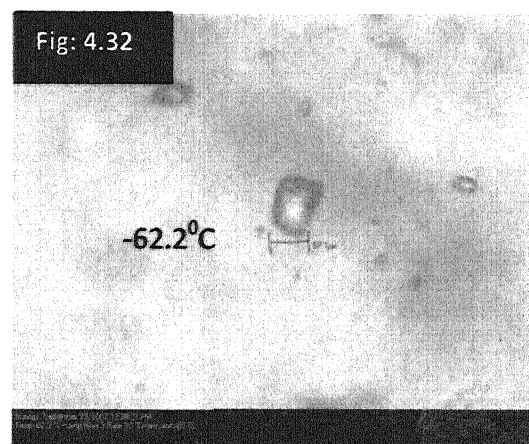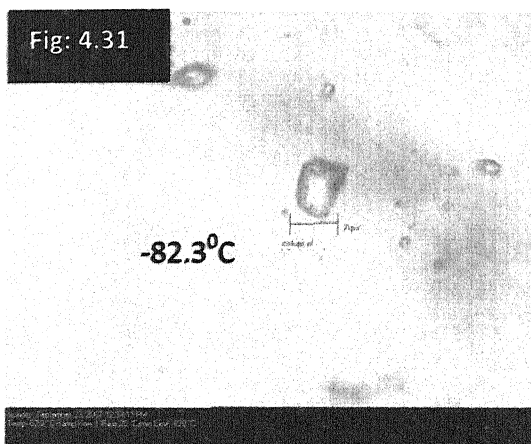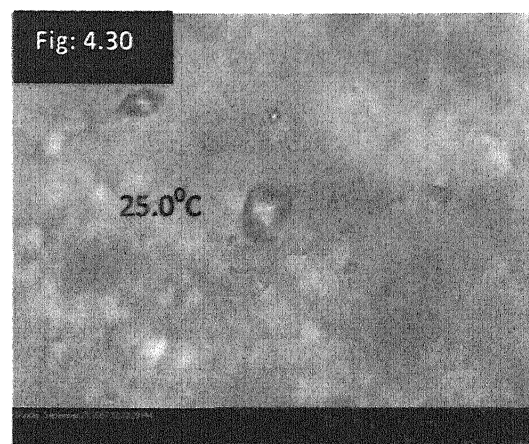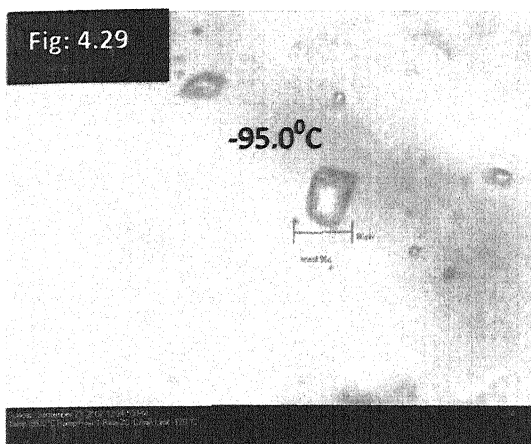
Fluid inclusion textures from gneiss of Mahoba area at various temperature.
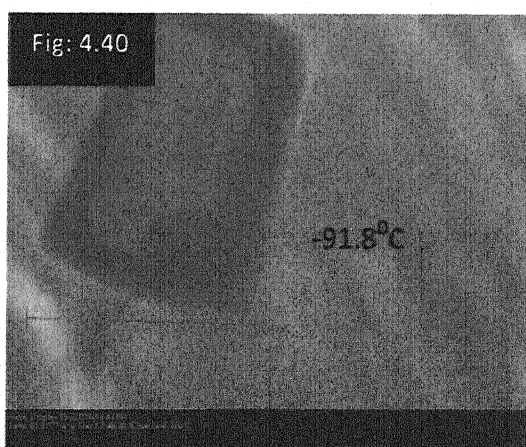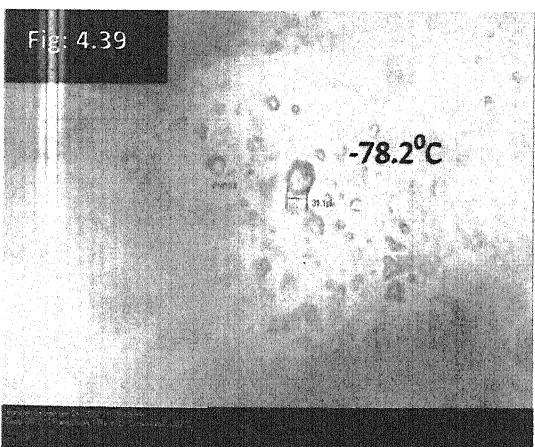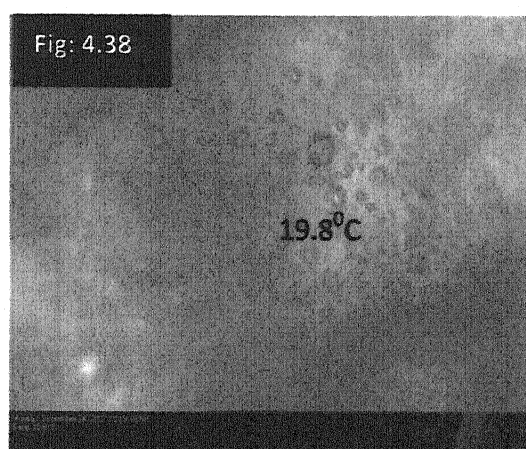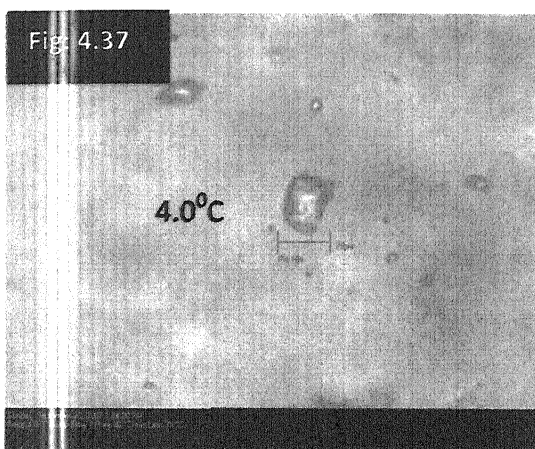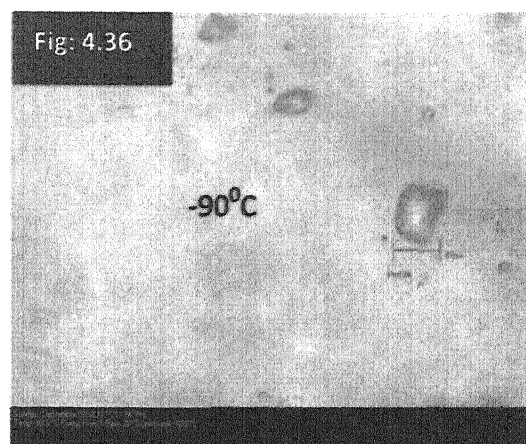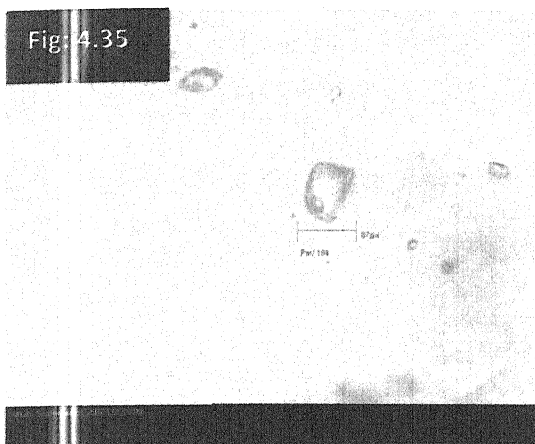
Fig: 4.35

Fig: 4.36

-90⁰C

Fig: 4.37

4.0⁰C

Fig: 4.38

19.8⁰C

Fig: 4.39

-78.2⁰C

Fig: 4.40

-91.8⁰C

Fluid inclusion textures from gneissic rock of Mahoba area at various temperature.

Fig: 4.41 −38.6⁰C

Fig: 4.42 −120.1⁰C

Fig: 4.43 −26.1⁰C

Fig: 4.44

Fig: 4.45 −90⁰C

Fig: 4.46 −26.9⁰C

Fluid inclusion textures from gneissic rock of Mahoba area at various temperature.

Fluid inclusion textures from gneissic rock of Mahoba area at various temperature.

Fig: 4.53 — 25.8⁰C

Fig: 4.54 — -70.1⁰C

Fig: 4.55 — -94.4⁰C

Fig: 4.56 — -120.3⁰C

Fig: 4.57 — -120.0⁰C

Fig: 4.58 — -16.2⁰C
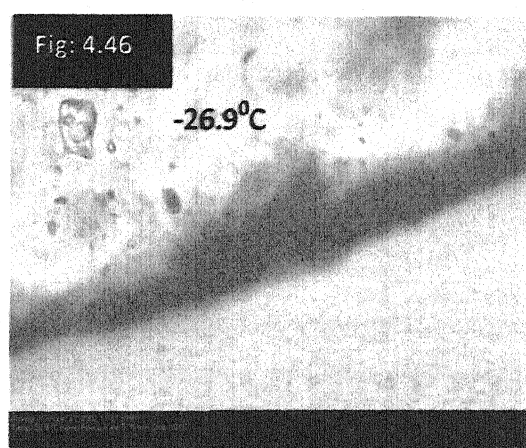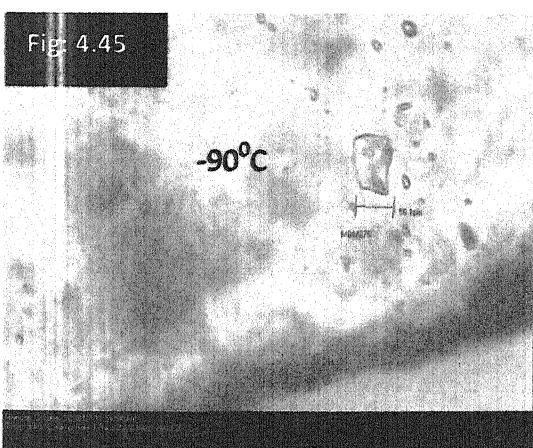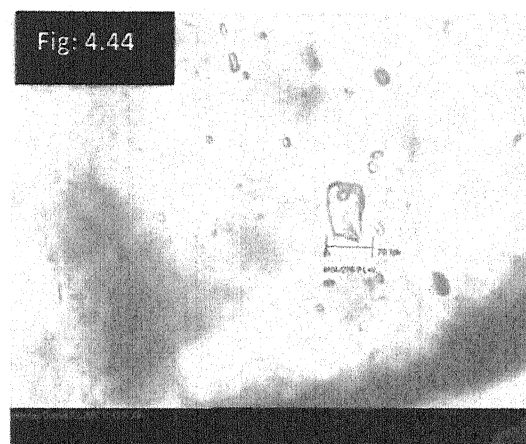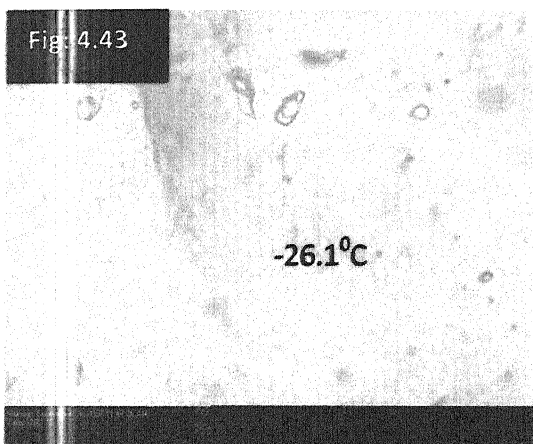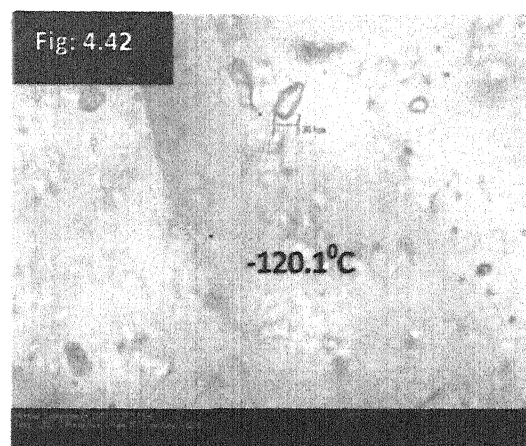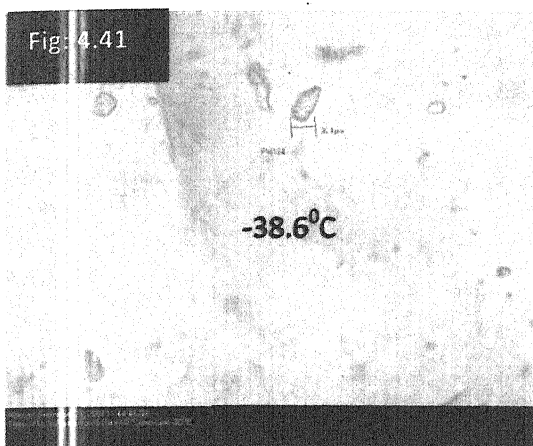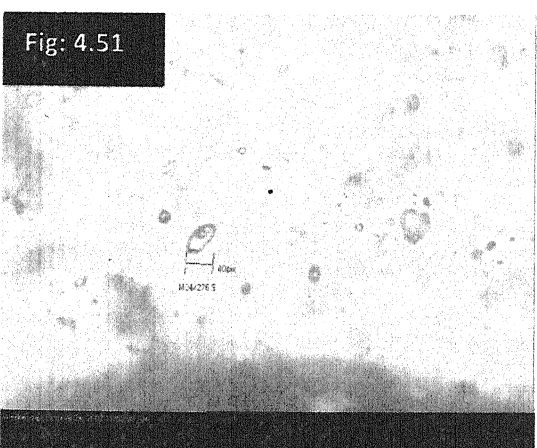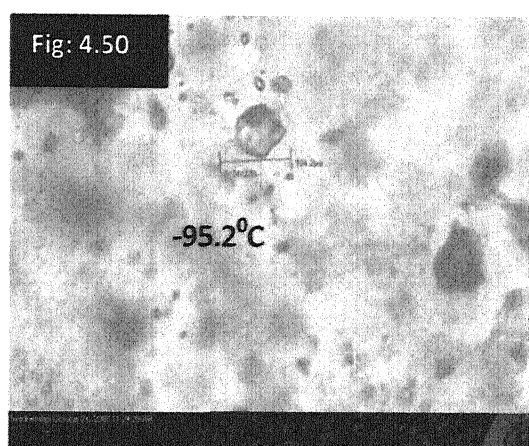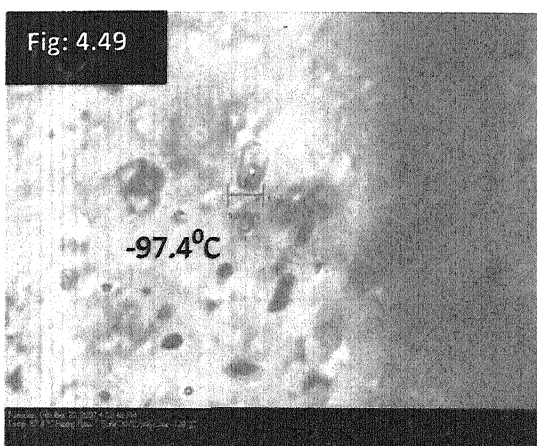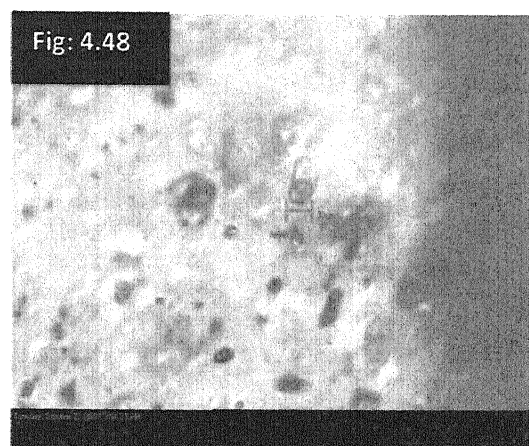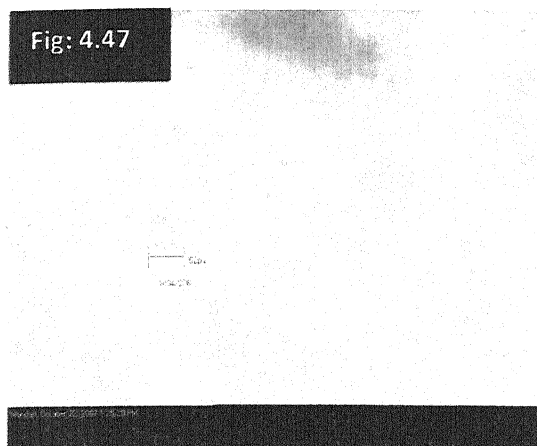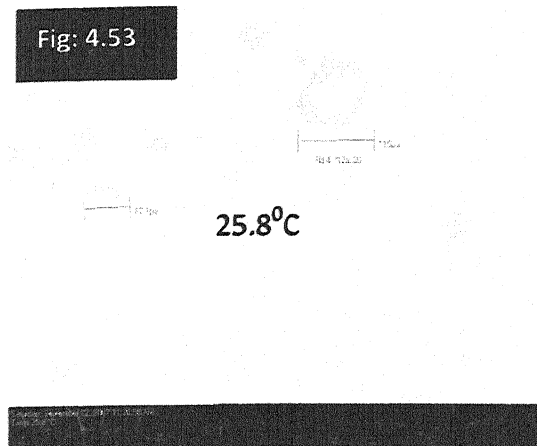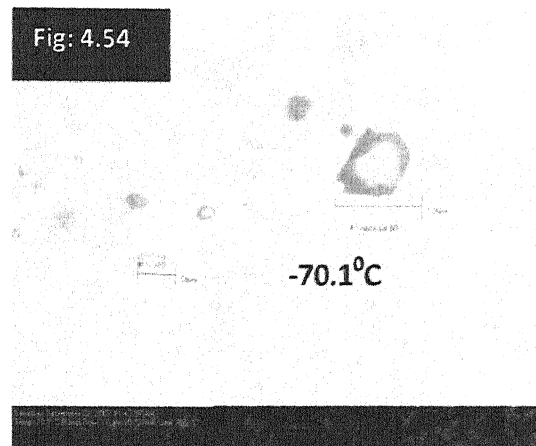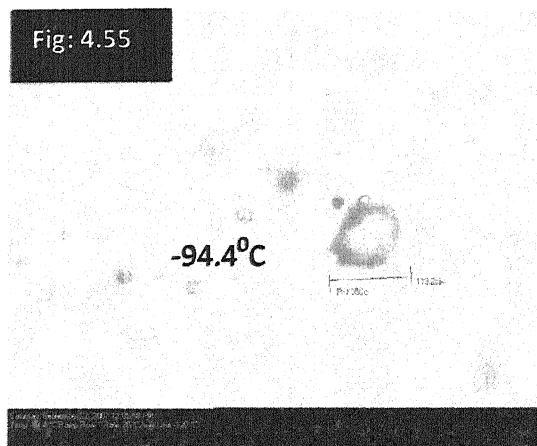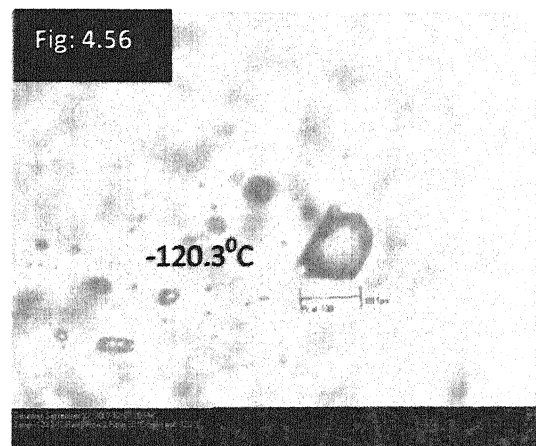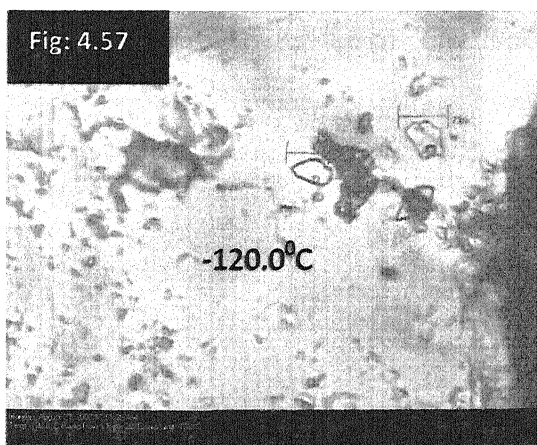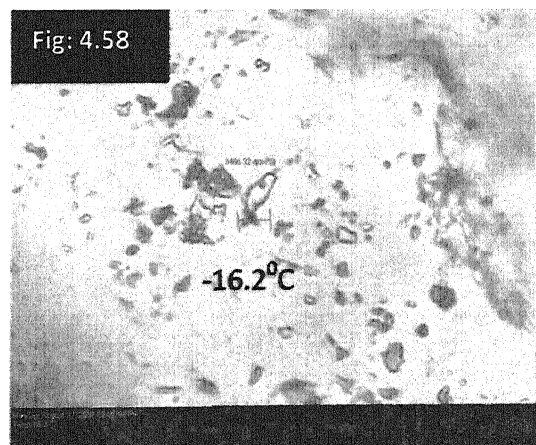
Fluid inclusion textures for the pink granite of Mahoba area at various temperature.
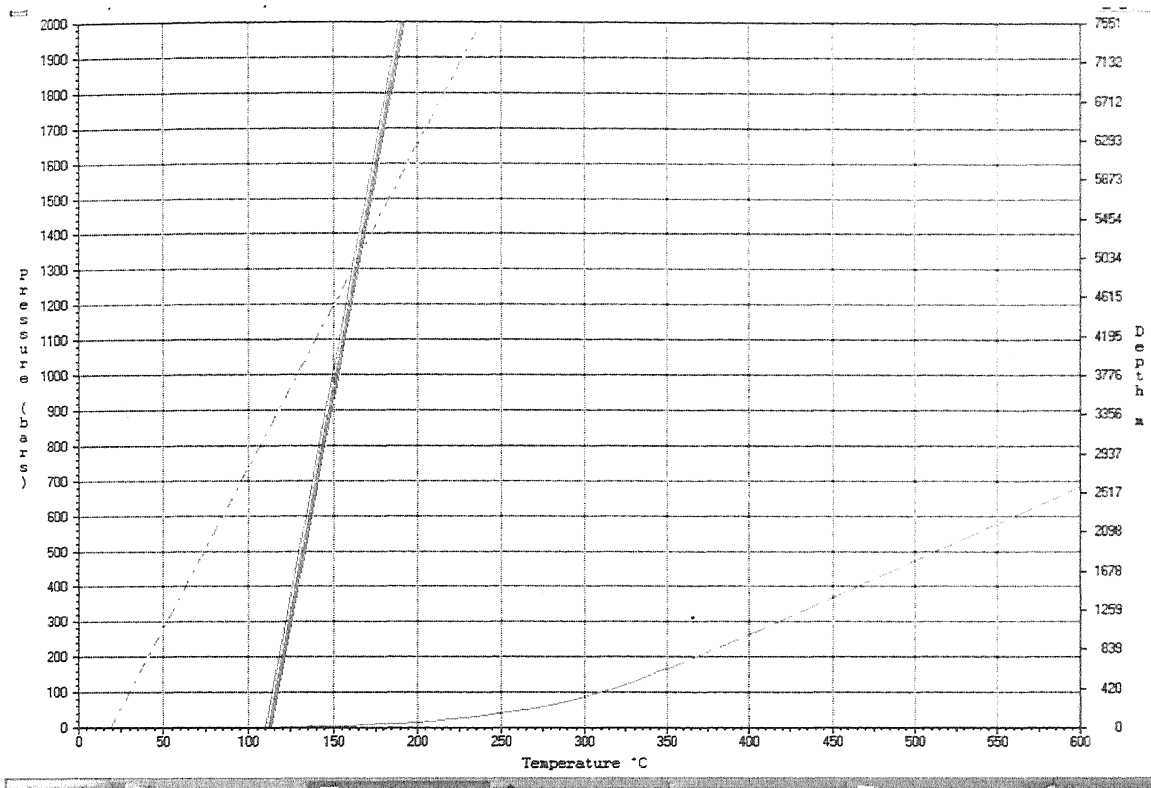
Fig 4.59
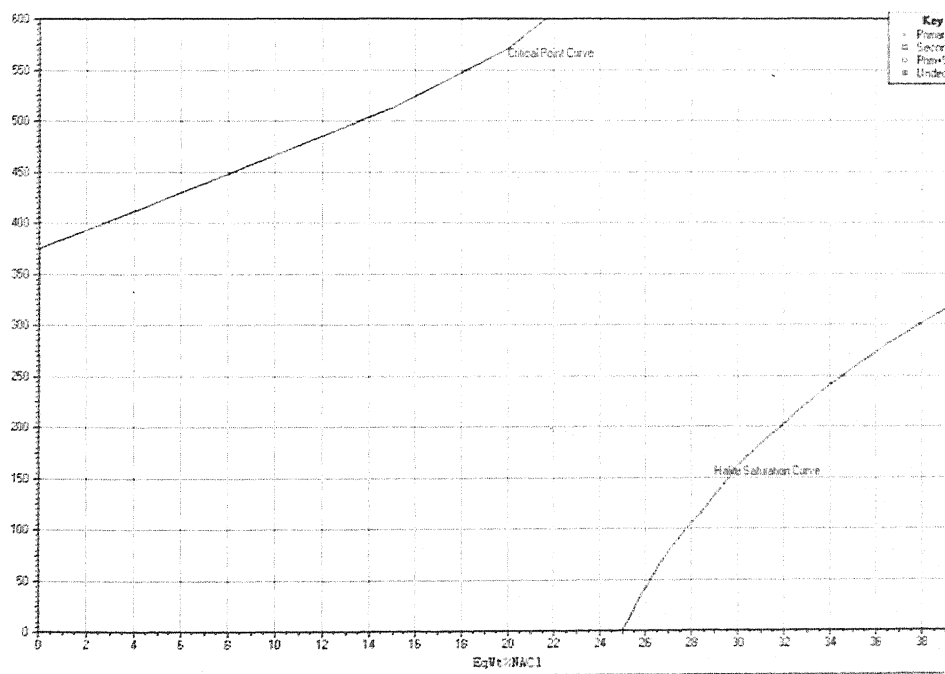
Fig 4.60

Chapter-5

GEOCHEMISTRY

5.1 INTRODUCTION :

Each granite suite has characteristic compositional features and show regular transitional internal variations in composition. When two elements are plotted against each other, the compositional changes reveal themselves as smooth curves, sometimes linear and sometimes curved (White, 2001). A granite suite will possess characteristic mineralogical features and may also have a distinctive textural character. Single suites may be comagmatic, or else may be cogenetic, both in terms of source and processes. A prime concern in studying granite suites is the process which produced the compositional variation in each case. Following various possible mechanisms for producing such variation have been suggested by following Chappell and White (2001):

1. Variation inherited from heterogeneous source rocks

2. Varying degrees of partial melting

3. Magma mixing and/or mingling

4. Assimilation or contamination

5. Restite separation and restite crystal fractionation

6. Fractional crystallisation

7. Hydrothermal alteration

These processes could operate alone, or sometimes simultaneously or in some cases sequentially (e.g. 5 followed by 6, or 6 followed by 7). They can be evaluated on the basis of observations for the different granite suits.

In order to classify the granite and granite- gneisses of the study area and further to understand their genetic relation of major, trace and rare earth elements, the geochemistry of representative litho units of BnGC and BG have been carried out. The field relations and petrographic studies of different lithounits of the petrological

interest of rocks of study area (discussed in preceeding chapter), it appears that the gray granite is primarily associated and possibly may be related to BnGC that was emplaced as the last phase of acidic magmatism during the first Tectonothermal event in Middle Archean. Therefore, special emphasis has been made to the genesis of grey granite and its possible relation with respect to the Bundelkhand pink granitoids (BG) and BnGC. An attempt has also been made to understand the relationships of TTG, biotite gneisses to biotite granites and pink granites.

On the basis of the field relationship, available geo-chronological data, structural and petrographic studies, the above-mentioned rock types have been grouped under following heads for the geochemical study.

1. Bundelkhand Gneissic Complex (BnGC): Migmatites, TTG, gneisses, gray granite and amphibolites.

2. Bundelkhand Granitoids (BG): hornblende granites, biotite-granites, coarse grain leucogranites, fine-grained leucogranite and deformed granites

Twenty eight representative samples [BnGC (N=14), Gray granite (N=7), biotite granite (N=1) and Pink granite (N=6)] from study area were analyzed by X-ray Fluorescence Spectrometer Philips at NGRI, Hyderabad. The major elements (wt%) and their calculated CIPW weight norms for the granite (PG), granite gneiss (GG) and granite-gneisses (BnGC) are represented in table 5.1a, 5.1b and 5.1c respectively using the Petrograph Software.

5.2 X-RAY FLUORESCENCE (XRF) SPECTROMETRY :

Major oxides were determined in all the samples by XRF at National Geophysical Research Institute (NGRI), Hyderabad (India). A Philips MagiXPRO-PW2440 fully automatic, microprocessor controlled, 168-position automatic PW 2540 with VRC sample changer Wavelength dispersive X-ray Spectrometer was used along with 4 KW X-ray generator for the determination of major oxides (SiO_2, TiO_2, Al_2O_3, Fe_2O_3, MnO, MgO, CaO, Na_2O, K_2O and P_2O_5) in rocks of Mahoba. The MagiX PRO is a sequential instrument with a single goniometer based measuring channel covering the complete elemental range. A Rhodium (Rh) anode is used in the X-ray tube,

which may be operated at upto 60 kV and current upto 125 mA, at a maximum power level of 4 KW. Suitable software "Super Q" was used to take care of dead time correction and inter-element matrix effects. International geochemical standard reference material (SRM) from US Geological Survey, Canadian Geological Survey, International working group, France and NGRI, India were used to prepare calibration curves for major oxides (Govil, 1985)..

5.3 BUNDELKHAND GRANITOIDS :

The granites of Bundelkhand area is represented by dominant pink granite followed by biotite granite and subordinate amount of hornblende granite and lueco granite, collectively referred here with Bundelkhand granites (BG). Beside these, the gray granite (GG) patches associated with the Bundelkhand granite and BnGC have been also encountered at several places.

The major elements data presented in table (5.1a-c) depict the following characteristics of the Bundelkhand granitoids of Mahoba area.

1. The BG and GG are highly silicic, having 68.75 to 73.65-wt% SiO_2 and 57.74 to 76.16-wt% SiO_2 respectively.

2. Alumina in BG and GG are present as moderate to high that range from 12.46 to 14.06 wt% and 11.59 to 16.47-wt% Al_2O_3 respectively but have greater than the total alkalies ($Na_2O + K_2O$ = 2.23 – 10.76 wt%).

3. The potash content in BG (K_2O= 4.43 – 6.22 wt%) and GG (2.75 – 5.52 wt%)is more than the soda content (Na_2O = 2.44 - 4.49 wt%) for GG and 3.33 – 4.10 wt% for BG rocks.

4. The low titania content in BG (TiO_2 = 0.12 – 0.42 wt%) and GG ($TiO2$ = 0.15 – 0.96 wt%).

Thus BG and GG are characterised by high silica, moderate to high alumina, higher K_2O than Na_2O and low TiO_2 contents.

5.3.1. Classification and nomenclature:

These granitoids have been chemically classified on the basis of different oxide, norm and cationic parameters. The classification schemes based on Na_2O vs

K_2O (Harpum, 1963), $CaO-Na_2O-K_2O$ (Hunter, 1974), An-Ab-Or (O'Connor, 1965), Q-A-P (Streckeisen, 1976, and Le Maitre, 1989), R_1-R_2 multicationic (De La Roche *et al*, 1980) and P-Q (Debon and Le Fort, 1983) etc have been used to find out the geochemical characters of rocks of the study area. The two softwares mainly Newpet and Petrograph were used for the graphical presentation. The Na_2O vs K_2O (Fig.-5.1) and ternary $CaO-Na_2O-K_2O$ (not shown) diagrams for Bundelkhand granitoids were plotted where the majority of the samples fall in the field of granite, but few of them are in the adamellite to granodioritic fields. The samples lie in the fields of granite to granodiorite in normative classification of ternary An-Ab-Or (Fig.-5.2) and Q-A-P (Fig.-5.12). An alternative approach based on major element criteria of various granitoids of Mahoba is proposed using cationic/molecular values such as R_1-R_2 multicationic classification (after De La Roche *et al.,* 1980) diagram (Fig.-5.4). It includes all major cations derived from a mineralogical network, the degree of silica saturation and the combined changes in Fe/(Fe + Mg) and (Ab +Or)/a ratio which express whole-rock chemistry of the granitoids. The R_1 [=4Si-11(Na + K)-2(Fe + Ti)] and R_2 [=6Ca + 2Mg + Al] parameters have been calculated from bulk chemical analyses (Table-5.1 and 5.1) as oxide weight percentage converted to millication proportions. Plotting of samples on the classification based on R_1-R_2 diagram in figure-5.18 (after De La Roche *et al.,* 1980), the Mahoba granitoids belong to granite (syenogranite and monzogranite) to granodiorite. But the gray granite (GG) plots in the field of tonalite. The P = [K –(Na + Ca)] and Q = [Si/3 –(K + Na + 2Ca/3)] (Fig.-5.5), proposed by Debon and Le Fort (1983), reveal that majority of the samples are plot in the fields of granite, adamellite and granodiorite.

Greig and Stemprok (1969) proposed a discrimination based on the oxides of $SiO2$ – (FeO + CaO + MgO) – (Al_2O_3 + Na_2O + K_2O) with the idea that stanniferous granitoid are usually high in silica, Al_2O_3 and Na_2O and depleted in ferro-calc-magnesium constituents .The specified compositional for tin- bearing granitoids ranges from 75 to 83% for SiO_2, 17 to 25% for combined Al_2O_3 + Na_2O + K_2O and less than 5% for ferro-calc-magnesium contents. The diagram has been applied (Fig. 5.6) for granitoids of Mahoba also but not found suitable for such granites.

The chemical-mineralogical study based on multicationic parameters two factors "A" and "B" proposed by Debon and Le-Fort (1982) and Debon *et al.* (1986) define the peraluminous and metaluminous characters of granitoids that depends on its positive and negative values of 'A' respectively. This plot reflects the nature and proportions of their characteristics minerals other than quartz and feldspars. The A-B diagram (Fig.-5.13), where A = [Al −(K + Na + 2Ca)] versus B = (Fe + Mg + Ti) shows clearly that the most of the Mahoba granitoids is occupied by the IIIrd and IVth fields of the metaluminous domain. This indicates that they belong to the association of biotite and biotite + hornblende respectively.

The high molar A/CNK i.e., $Al_2O_3/(CaO + Na_2O + K_2O)$ ratios of the analysed granitoid samples are plotted against SiO_2. The most of the samples fall in the field of metaluminous composition having molar A/CNK ratio less than 1.1, which suggest that the granitoids though igneous in origin but have some crustal components (Chappel and White, 1974).

Though, it is not possible to assess how much igneous/sedimentary source material was involved in a given granitic rock but it is possible to determine how much a given granitic rock appear an I-type or S-type. Presence of normative corundum and low molar concentration of Al/ (Ca + Na + K) < 1.1 also suggests I-type nature of Mahoba granitoids (BG) according to the scheme proposed by Chappel and White (1974).

The criteria used for distinguishing I-type and S-type granites (Chappel and White; 1974 and Takahasi *et al.,* 1980) are given in table, 7 and have been compared to Mahoba granitoids (BG and GG).

The comparative study reveals that Mahoba granitoids (BG and GG) are distinguished as metaluminous I-type granite. They correspond to biotite minerals and also presence of hornblende, ferromagnisian constituents (magnetite and ilmenites), relatively low to moderate K_2O (with ~ 5 wt% K_2O and < 3.95 wt% Na_2O), molar A/(CNK) < 1.1, normative corundum > 1, presence of normative minerals ilmenite, apatite, diopside, hypersthene (table-5.3) and narrow range of more felsic composition. Leucocratic syeno-and monzo-granite composition predominated with

high boitite content are locally important. The other characteristic features viz; presence of ilmenite in place of magnetite and deep brown titanium-rich biotite in place of green biotite indicate that magma was containing relatively low oxygen fugacity and low ferric ferrous ratios.

Total alkalies versus silica (TAS) diagram of Middlemost (1985) for classification suggest that most of the Mahoba granitoids samples plot in hypoalkalic field and few of them in silica field (Fig-5.3). It is very clear from this diagram that the Mahoba granitoids are mostly hypoalkalic in nature and their alkalinity (Na_2O + K_2O) does not exceed more than 10%. This study point out that the local metasomatism may not be ruled out in the study area.

Based on the log K_2O/MgO vs. SiO_2 (wt %) diagram (Fig.-5.8). Mentioned in Bhattacherjee (1993), is plotted for the Mahoba granitoids. Similarly plots based on the SiO2 Vs K2O (Fig-5.9) points that pink granites are mostly higher in K_2O and lies in the field of calc- alkali series while the gray granite showing the scattered field and mostly confined calc-alkaline. The most of the BG and GG fall in alkali granite field. Biotite granites (BG) fall in the transition zone and alkalic granite fields. These granitoids represent the calc-alkaline differentiation trend, evident from A-F-M diagram (Fig.-5.15) as given by Irvine and Baragar (1971). Though the majority of samples plots in calc-alkaline field but evolved towards alkalies corner.

5.3.2. Tectonic discrimination:

In order to characterise the tectonic environment of the Mahoba granitoids, the classification scheme proposed by Maniar and Piccoli; (1989) demands various steps to be followed in a sequential manner to arrive at the true tectonic environment of the granitoids (table-5.5). Using the different discrimination parameters as proposed by Maniar and Piccoli (1989), it has been noted that the chemical features of BG and GG granitoids (table-5.6) do not follow a single and firm tectonic environment viz; IAG/CAG/CCG/POG (figure-5.17). The ambiguity evolved in this classification scheme cannot be used for tectonic discrimination of granitoids. Nevertheless, gray granite appears an appropriate tectonic environment, which has no more resemblance with pink granitoids.

All the Mahoba granitoids falls in the field of orogenic granites, (Maniar and Piccoli; 1989) and is distinctly away from the field of anorogenic granites in the discrimination diagram and also it does not fall in the field defined for post – orogenic granitoids (POG) (Fig.-5.17). Discrimination between CCG and IAG + CAG can be made on the basis of molar A/ (CNK) ratio (Fig.-5.14). They suggested that CCG do not have A/ (CNK) values less than 1.05; whereas IAG + CAG do not A/ (CNK) values greater than 1.15. If the A/ (CNK) ratio is between 1.05 and 1.15, it is not possible to discriminate between CCG and IAG+CAG. Considering above constrains, the Mahoba granitoids represent continental collision. It is therefore suggested that Mahoba granitoids is metaluminous in nature and resulted from the partial melting of TTG rocks, possibly during the late continent collision.

5.3.3. Petrogenesis:

De La Roche's R_1-R_2 plots, the ionic proportion of major oxides (modified by Batchelor and Bowden; 1985) have been used for discrimination of tectonic environments. Most of the Mahoba granitoid samples plot in the field of pre-to-syn-continental collision in nature (Fig.-5.18)

For the partial melting vectors and metamorphic sources, (Batchelor and Bowden; 1985) proposed that the first liquids to get separated from is the fusion of felsic crustal source (gneiss, metapelite, intermediate metaigneous rocks) that will have compositions equivalent to alkali feldspar and quartz ± sodic plagioclase. The Mahoba granitoids plotted in R_1-R_2 multicationic diagram (Fig.-5.18) occupied the field away to anatectic granite. It indicates that the felsic melt generated at higher depth (Fig.-5.16) is completely mobilised in the crust and emplaced at a shallower level and its composition would be equivalent to a synogranite or granite. If it is assumed that lower crustal sources had compositions represented by A, B and C (Fig.-5.18), then increasing degree of equilibrium, partial melting would generate the compositions whose vectors could have represented by PM-A, PM-B and PM-C, respectively.

To identify the nature of the Mahoba granitoids (BG and GG), author attempted K_2O/Al_2O_3 vs Na_2O_3/Al_2O_3 (wt %) plot (Fig.-5.20) which discriminates

igneous protolith as has been outline by Garrels and Mackenzie (1971). The diagram suggests that almost all samples plot in the igneous protolith.

5.3.4 Major oxides geochemistry :

The felsic (SiO_2 + Al_2O_3 + Na_2O + K_2O) vs mafic (FeO^* + MgO + MnO + CaO) constituents appear to mark the inverse relation between Mahoba granitoids. This antipathic relationship between the silica-alumina-alkalies combination and ferro-calc magnesian of the Mahoba granitoids indicate the crystallisation differentiation pattern similar to that of the other granites of the magmatic origin

The Mahoba granitoids (BG and GG) is usually pink in nature and have higher weight percentage (average wt%) of SiO_2 (70.74), Al_2O_3 (13.16), K_2O (4.63), Na_2O (1.83), FeO^* (3.91) and lower percentage of CaO (1.73), MgO (0.89) and TiO_2 (0.3). To consider the role of differentiation processes for the formation of the Mahoba granitoids, the variation diagrams of Harker (Fig.-5.19) are plotted.

Silica versus other oxides :

Calcium and magnesium oxide: CaO and MgO show a sympathetic relationship with one another in Mahoba granitoids although CaO content is always more than MgO. CaO content in granite and granite gneiss varies from 0.51 to 6.12-wt% and MgO varies from 0.21 to 1.72 wt%. The CaO and MgO show antipathetic relationship with SiO_2 (Fig. 5.19).The BG granitoids are usually low in MgO while GG granitoids have higher MgO wt%.

Alkalies: Na_2O varies from 3.3 to 4.10-wt% and K_2O content varies from 4.43 to 6.22 wt% with the maxima and minima for the Mahoba pink granitoids. In gray granite, Na_2O varies from 2.42 to 4.49 wt% and K_2O ranges from 2.75 to 5.55wt%. The Na_2O and K_2O bear an inverse relationship to each other. Further K_2O/Na_2O ratio varies from 0.65 to 17.31 in pink granitoids whereas in gray granite varies from 0.74 to 20.83. When silica content is plotted against Na_2O and K_2O individually (Fig. 5.19), it is seen that there is a tendency for concentration of SiO_2 around 72 wt% (68 and 72 wt %), Na_2O at 3 wt% (1 and 3 wt %) and K_2O at 5 wt% (4 and 6 wt %). Broadly, there is a general trend towards increase in K_2O content with increasing

silica for the BG. In the binary variation diagram it is found whenever there is enhancement of K_2O, correspondingly there is fall of Na_2O, which indicates the dominance of microclinisation at the expense of albitisation and vice versa. Two stages of microclinisation and albitisation were noted in gray granite.

Alumina: In BG granitoids, Al_2O_3 content varies from 12.06 to 14.53-wt%, whereas in GG granitoids it ranges from 12.34 to 16.47 wt%. The alumina content increases with decreasing silica content (Fig, 5.19). The inverse relationship of Fe2O3, CaO and Al_2O_3 with SiO_2 has noted for the Mahoba granitoids. A variation diagram plotted for Cao with SiO2 yields two distinct trends for GG and BG granitoids (Fig-19b)

Total alkalies and alumina for the granitoids and gneisses bear a more or less antipathic relationship. There is no definite trend in combined alkalies or alumina though the latter shows a tendency to decrease with increase in silica.

The enrichment of Fe_2O_3 (total) in granite gneiss and its depletion in biotite granite depicts the antipathetic relation of Fe_2O_3 with SiO_2 (Fig. 5.19). Similar trends have been obtained for MnO and MgO against the SiO2 (Fig-19c)

Thus, the variation and clustering of various oxides, plotted for Mahoba granitoids in Harker's variation diagrams show more or less similar trend without gap, suggesting the two distant petrogenetic histories for them.

5.3.5 Trace Element Geochemistry :

Trace element geochemistry has been of enormous use in understanding the evolution of the Earth. As we shall see in subsequent paragraphs, a fair amount of what we know about the evolution of the core, the mantle, and the crust has come from the study of trace element abundances. Though trace elements, by definition, constitute only a small fraction of a system of interest, they provide geochemical and geological information out of proportion to their abundance (White 2001). There are several reasons for this. First, variations in the concentrations of many trace elements are much larger than variations in the concentrations of major components, often by many orders of magnitude. Second, in any system there are far more trace elements

than major elements. In most geochemical systems, there are 10 or fewer major components that together account for 99% or more of the system. This leaves 80 trace elements. Each element has chemical properties that are to some degree unique, hence there is unique geochemical information contained in the variation of concentration for each element. Thus the 80 trace elements always contain information not available from the variations in the concentrations of major elements. Third, the range in behavior of trace elements is large and collectively they are sensitive to processes to which major elements are insensitive. Thus the trace elements would better tools for the understanding the geochemical process than the major oxides.

The Mahoba granitoids, in general, appears to be enriched of several trace elements notably niobium, gallium, barium, copper, zinc, thorium, cesium, zirconium, vanadium and yttrium and conversely depletion in Chromium, tantalum, nickel, phosphorous, cobalt, and strontium. The trace element contents in different granitic rocks of Mahoba is shown in table-5.2 and 5.4 The Mahoba granitoids, however, when plotted on Rb-Sr log-log variation diagram (Fig.-5.19) of Condie (1973), the most of the samples cluster above the lines defined by Rb/Sr = 1, at the depths relevant to 30 to 40 kms.

El Bouseilly and El Sokkary (1975) pointed out the usefulness of an Rb-Ba-Sr ternary diagram in tracing differentiation trends of granitic rocks. This diagram can also be used to classify the granites, evaluate fractionation trend and also detect specialization of tin bearing nature of the granites. In the Rb-Ba-Sr ternary diagram (Fig.-5.11), the analyses of the Mahoba granitoid rocks are plotted showing considerable variation from granodiorite to normal granite for the GG. The few samples of gray granite fall in the filed of highly differentiated granite while the pink granite comes under the normal granite.

Based on Whalen *et al.,* (1987), the diagrams (Fig. 5.20,a,b) Zr + Nb + Ce + Y (ppm) vs FeO*/MgO (wt%) and Zr + Nb + Ce + Y (ppm) vs (K$_2$O + Na$_2$O)/CaO (wt%) show the nature of pink granite (BG) as fractionated felsic granites (FG) whereas gray granite (GG) and gneiss represent the orogenic granite type (OGT) of the unfractionated I-type granites but fall away from the field (Fig 5.20).

The selective trace elements characteristics of the Mahoba granitoids can not be assigned collectively of any one tectonic regime when plotted on Y + Nb vs Rb log-log (ppm) and Y vs Nb log-log (ppm) diagrams (Fig. 5.21 a,b) based on scheme of Pearce *et al.,* (1984). The samples cluster near the tripple junction demarcating lines of volcanic arc granitoids (VAG), syn-collisional granitoids (syn-COLG) and within plate granitoids. The (WPG) fields for the gray granite and VAG for the pink granitoids (BG) have been found.

Recently, Frost *et al.* (2001) has proposed three tier geochemical classification scheme for granitoids in a view to decipher; (i) differentiated history of granite magma determined by $FeO^*/(FeO^* + MgO)$ ratio of these rocks; (ii) source of magma based on alkali-lime index of the rock ($Na_2O + K_2O$ - CaO) and (iii) sources and conditions of the melting based on aluminous saturation index (ASI). The granites (BG) and granite gneiss (GG) have been plotted based on $FeO_{(t)}/(FeO_{(t)} + MgO)$ vs SiO_2 (Fig. 5.23) which suggest that the BG is typically ferroan whereas GG has affinity with ferroan and some of them related to magnesian type which is much depleted in $FeO_{(t)}/(FeO_{(t)} + MgO)$ ratio. The magnesian and ferroan-differentiated series of granitoids are indeed equivalent to tholeiitic and calc-alkalic magma types respectively as originally discriminated by Miyashiro (1974). However, a little overlapping in the fields of magnesian and ferroan have been noted towards high silica content of rocks which is more likely related to the late-stage compositional evolution of granitoids during their differentiation. What so ever the reason may be but BG is apparently distinct from GG. But both have experienced different degree of chemical differentiation in different episodes (Fig.-5.24). It is more likely that the magnesian enrichment trend of GG may be responsible high fractionation in the study area.

Modified alkali-lime index (MALI) plotted against K_2O weight percentage (Fig. 5.24) show compositional affinity of GG with Mesozoic Cordilleran granitoids, though scattered calcic to calc-alkaline. In order to discriminate the various igneous series $Na_2O + K_2O$ – CaO vs SiO_2 wt.% diagram (Fig. 5.24) was plotted show a specific trend for both BG and GG, rather spread over calcic to alkalic fields through

calc-alkaline and alkalic-calcic, which suggest that the processes other than crystal-liquid separation might have played an important role in the evolution of BG and GG. The molar A/(CNK) ratio of BG and GG points in nature similar to as meta aluminous granites (I-type).

5.3.6. Trace element variation :

Table-5.4 shows the average distribution of trace elements of Mahoba granitoids of the study area. The gray granitoids have higher Rb (152-512 ppm), Ba (293-1391 ppm), Zr (231-960 ppm), Nb (16-56 ppm), Th (15-97ppm), Ce (122-174 ppm) and lower values for Cu (1.3-5 ppm), Sr (42-308 ppm), Cs (3-15 ppm),), Co (6.14 ppm), Ni (3.37 ppm), and Y (35-82 ppm). The increase in Rb, Ba, and decrease in Sr and phosphorous with increase in SiO_2 content of the Mahoba granitoids, suggest the role of differentiation in the formation of these granitic rocks.

However, when the trace elements for Mahoba granitoids are plotted against SiO_2 in Harker's variation diagrams (Fig. 5.20), they show some genetic features. Ba, Sr, V, Ce and Nb increases with decreasing SiO_2 showing the differentiation trend. This supports the view that these granitoids were of the same in nature and possibly have got same petrogenetic history. Cu and Rb show inverse relation with SiO_2 and increase from granite to granite gneiss rocks. Ga and Y do not show any marked variation with increasing SiO_2, but form it clusters for the granites and granite gneisses, which also support their same nature.

5.4 RARE EARTH ELEMENTS (REE) :

The rare earths are the two rows of elements commonly shown at the bottom of the periodic table. The first row is the *lanthanide* rare earths; the second is the *actinide* rare earths. However, the term "rare earths" is often used in geochemistry to refer to only to the lanthanide rare earths. The rare earths are infact transition metals. In the transition metals, the *s* orbital of the outermost shell is filled before filling of lower electron shells is complete. In atoms of the period 6 transition elements, the *6s* orbital is filled before the *5d* and *4f* orbitals. In the lanthanide rare earths, it is the *4f* orbitals that are being filled, so the configuration of the valence electrons is similar in

all the rare earth, hence all exhibit similar chemical behavior. Ionic radius, which decreases progressively from La3+ (115 pm) to Lu3+ (93pm), is thus the characteristic that governs their relative behavior. Because of their high charge and large radii, the rare earths are incompatible elements. The degree of incompatibilities varies, however, highly charged U and Th are also highly incompatible elements, as are the lightest rare earths. The heavy rare earths (HREE) have sufficiently small radii so that they can be accommodated to some degree in many common minerals. The heaviest rare earths readily substitute for Al3+ in garnet, and hence can be concentrated by it. Eu, when in its 2+ state, substitutes for Ca2+ in plagioclase feldspar more readily than the other rare earths. Thus plagioclase is often anomalously rich in Eu compared to the other rare earths, and other phases in equilibrium with plagioclase become relatively depleted in Eu as a consequence.

Rare earth elements are progressively becoming an important and useful tool in petrogenetic studies because they are geochemically very similar to those of its nearest atomic neighbor, but differing from Ce and Eu which have tendency of change REE with greater or smaller atomic valency state depending upon the geological environment.

Rare earth elements (REE's) are a group of 15 (trace) elements with atomic number from 57 Lanthanum (La) to 71 Lutetium (Lu), 14 of these elements (except Promethium-Pm) occur naturally. For convenience the REEs are divided into two sub-groups: (i) from La to Sm (i.e., lower atomic numbers and masses) are referred to as the light rare earth elements (LREE) and (ii) from Gd to Lu (higher atomic numbers and masses) are referred to as the heavy rare earth elements (HREE). Very occasionally the term middle rare earth elements (MREE) is loosely applied to the elements from about Sm to Ho (Handerson; 1984). In nature all of the rare earth elements exhibit a 3^+ oxidation state (trivalent), except Ce^{4+} (oxidised) and Eu^{2+} (reduced) under most geological conditions.

The ionic radii of the REE are all approximately 1Å. There is a regular decrease in the ionic radii (for the trivalent REE from 1.03 for La to 0.86 Å for Lu) with increasing atomic number (The Lanthanide Contraction). Eu is both divalent and

trivalent in igneous system, the Eu^{2+}/Eu^{3+} ratio depending on the fugacity of oxygen (fO_2). Divalent Eu is geochemically very similar to strontium ionic radius: Eu^{2+} = 1.17Å, Sr^{2+} = 1.18Å, thus it is strongly partitioned into feldspars. Ce may be tetravalent under highly oxidizing conditions such as during weathering or hydrothermal alteration (Hanson, 1980).

5.4.1. Methodology of REE determination :

Analytical methods

The chemical composition of the representative samples of granite gneisses, gray granite etc. are given in table 1. Representative samples were collected so as to avoid vein fillings and alteration rinds, cleaned and then powdered using an agate mortar. Whole rock major elemental analysis were carried out by XRF, and trace, REE and PGE analysis were carried out by ICP-MS, the details of which are given below.

Inductively coupled plasma-mass spectrometry (ICP-MS)

Trace, rare earth (REE) and platinum group elements (PGE) were determined by ICP-MS using the national facility available at NGRI, Hyderabad. The powdered rock samples were digested using acid mixtures for determination of trace and REE following Zahida et al., 2006. The analysis of PGE and Au were carried out by following NiS-fire assay with Te co-precipitation and ICP-MS method, the details of which are given in Balaram et al, 2006. The samples were introduced into the PerkinElmer SCIEX ELAN DRC-II, inductively coupled plasma mass spectrometer (Concord, Ontario, Canada) with a conventional pneumatic Meinhard nebulizer, using a peristaltic pump with a solution uptake rate of about 0.8 mL/min. The instrument was run in peak hopping mode, and all the samples were analyzed for 34 trace elements, including all REEs and all the PGE including Au. For trace and REE determination, ^{103}Rh at 20 ng/mL was used as an internal standard while for PGE determination Cd & Tl was used as an internal indicator at 20 ng/ml in order to compensate for the signal drift caused by the changes in nebulizer efficiency, gradual clogging of the torch and interface, and to compensate for the matrix-induced suppression or enhancement effects. Matrix-matching standard reference material

(procured from United States Geological Survey, USA, Canadian materials technology lab-CANMET) was used for calibrating the instrument since this standard has certified values for all of the elements studied. Other details, such as instrument operation and data acquisition parameters, are given in Balaram and Gnaneshwar Rao, 2003 and Balaram et al., 2006. Single isotopes were used for all elements and were selected based on their abundance levels and the freedom from interferences from other elements usually present in rock samples. The detection limits of most of the elements including PGE were about 0.01mg/ml, and the precision is better than 6% for trace and REE, and is <10% for PGE analysis.

5.4.2 REE data presentation :

Though all igneous geochemists normalize rare earth abundances to some set of chondritic values, there is no uniformity in the set chosen. Popular normalization schemes include the CI chondrite Orgueil, an average of 20 ordinary chondrites reported by Nakamura (1974), and the chondritic meteorite Leedy (Masuda et al., 1973). Although the absolute values of the normalizing values vary (for example, the Nakamura values are about 28% higher than those of Orgueil), the relative abundances are essentially the same. Thus the normalized rare earth *pattern* should be the same regardless of normalizing values. Some sets of normalizing values are listed in Petrograph and many other softwares. A more complete tabulation can be found in Rollinson (1993).

Rare earth element concentrations in rocks are usually normalised to a common reference standard, which most commonly comprises the values for chondritic meteorites. Chondritic meteorites were chosen because they are thought to be relatively unfractionated samples of the solar system dating from the original nucleosynthesis. The REE data (ppm) and their chondrite normalised value of analyzed samples are given in table (5.5). In order to compare graphically rare earth elements (REE) are represented by the spider diagram for the Mahoba granitoids (fig.-5.28). The concentrations for the individual rare earth element is generally normalized to their abundance in chondrite by dividing the concentration of a given element in the rock by the concentration of the same element in chondritic meteorites.

The ratio Eu/Eu* is a measure of the europium (Eu) anomaly and a value of greater than 1.0 indicates a positive anomaly whilst a value of less than 1.0 is a negative anomaly. The Eu/Eu* ratio in the Mahoba granitoids varies from 0.38 to 0.57, which indicates negative Eu-anomalies. Taylor and McLennan (1985) recommend using the geometric mean in this case $Eu/Eu^* = Eu_N/\sqrt{[(Sm_N).(Gd_N)]}$. Europium anomalies may be quantified by comparing the measured concentration (Eu) with an expected concentration obtained by interpolating between the normalized values of Sm and Gd (Eu^*). The variation of Eu/Eu* is also limited (0.18 to 0.57) suggesting a source signature rather than feldspar fractionation (Norman *et al.,* 1992).

5.4.3. Rare earth element geochemistry :

Rare earth elements of seven selected samples of the gray granites and granite gneisses and six samples of pink granites (BG) were analyzed and chondrite normalised patterns by Taylor and Mclennan, 1985 (1.5 x values of Evensen *et al;* 1978) are shown in figure-5.25, 5.26 and 5.27. All the suites exhibit enriched LREE patterns relative to HREE along with variable negative Eu anomalies. In figure-5.25, the most of the granitoid samples show steep by inclined pattern and are highly fractionated. They are enriched in LREE and depleted in HREE showing moderate and large negative Eu-anomalies for pink granite.

The samples of pink granite and gneiss show almost a flat HREE pattern with pronounced negative Eu-anomaly (Fig.-5.28) but shows enriched LREE, most probably due to presence of accessories such as zircon and magnetite. The flat HREE pattern might have resulted due to presence of ample amount of apatite, which is mostly entrapped within large feldspar grains. The strong negative Eu-anomalies indicate that this rock is highly evolved during differentiation processes.

Presence or absence of the Eu-anomaly is usually related to the presence or absence of feldspar in the magma. This may be controlled by the fractionation of feldspar during the differentiation or melting of either feldspar bearing or depleted protolith (s). Small negative Eu anomaly indicate the removal of Calcic-plagioclase from the magma (i.e. probably at initial stage) and the increasing size of negative Eu-

anomalies indicate the gradual increase in the removal of relatively more calcic-plagioclase attaining the last stage i.e., the magma is more evolved.

The degree of fractionation of a REE pattern can be expressed by the concentration of LREE (La or Ce) ratio to the concentration of HREE (Yb or Y). The Mahoba granitoids is characterized by high LREE abundances (chondrite normalised ranges from 259-480 for GG and 277 -228 for the pink granites). The HREE (as Yb) abundances vary between 43-19 for GG and 16 -26 for BG. All the LREE shows positive correlation with FeO*. The most iron-rich sample shows the lowest abundance of SiO_2 and highest abundance of LREE with total REE content (343.71 ppm). The REE patterns of the Mahoba granitoids are moderately to strongly fractionated characterized by an increase of ΣREE and $(La/Yb)_N$ (2.74-6.17) and a consistent pattern of fractionation $(La/Sm)_N$ = (3.67-6.78), $(Gd/Yb)_N$ = (1.35-7.54).

All the suites exhibite enriched LREE pattern relative to HREE along with variable negative Eu anomalies. The most of the granitoid samples show steep by inclined pattern and are highly fractionated. The ΣREE of BG ranges between 280 – 501 for GG and 245-578 for BG 277.99 ppm are significantly different but continuous to decreases from GG to BG. This feature can be very well illustrated when LREE (La + Ce + Nd) and ΣLREE are separately plotted against B (Fe + Mg + Ti) content for BG and GG. B components calculated other Debon *et al*, 1986) whole rock data actually represent ferromagnesian minerals of granitiods. In present study, the ferro-magnesian minerals in KG and KGG are mostly represented by biotite and hornblende, which is relatively more in GG compared to BG.

Rare earth elements of seven selected samples of GG (n=2) and BG (n=6) of the study area were analyzed at Hyderabad (table-5.2). All the suites exhibited enriched LREE pattern relative to HREE along with variable negative Eu anomalies. The most of the granitoid samples show steep by inclined pattern and are highly fractionated.the pink granite shows distrinct pattern. The HREE are found to eluster at Yb and Lu which have wide gap for LREE concentration (Fig.05.28). on the other hand the Gray Granit is yield narrow range for the LREE and wide spread zone for

HREE especially for Yb and Lu (see Fig.-3.28). the gneisses show uniform pattern with plate pattern or HREE.

The ΣREE of BG ranges between 245-578 ppm and GG 280 – 501 ppm are significantly different but continuous to decreases from GG to BG. This feature can be very well illustrated when LREE (La + Ce + Nd) and ΣLREE are separately plotted against B (Fe + Mg + Ti) content for BG and GG. B components calculated (Debon *et al*, 1986) for whole rock data actually represent ferromagnesian minerals of granitiods. In present study, the ferro-magnesian minerals in BG and GG are mostly represented by biotite and hornblende, which is relatively more abundant in BG compared to GG. In +ve correlation noted between LREE vs B and ΣREE vs B for the samples of BG and GG indeed reflect that BG variation can be explained in terms of varying degree of melting of GG source but an internal differentiation within BG by fractionation cannot be fully ruled out. The striking chondrite normalized REE pattern is similar where REE pattern is inclined composed to the relatively flatter HREE pattern with some degree of negative Eu anomalies with all samples. This feature strongly suggests that BG melt could be derived by partial melting of protolith of GG having feldspar depleted signature source. A limited range of Eu – anomalies noted for BG (Eu/ Eu* = 0.45) reflects the source character whether than fractionation (feldspar) during its evolution. The HREE pattern of BG are distinctly depleted in Tm and Yb compared to that of GG points the mechanism of melt separation from the probable sources GG.

5.5: GEOCHEMICAL MODELING OF BG AND GG MELT GENERATION:

Several lines of field photographic and bulk geochemistry of BG, and GG reveal with origin from crustal anatexis i.e.; partial melting of crustal source generating the metaaluminous BG and GG melts. Therefore, it is now pertinent to model the partial melting in terms of Rb, Sr content where Rb is incompatable in acid igneous system. The partial melting model of bulk continental crust (Taylor and Mc Lennan, 1985) as calculated and presented by Gasparon *et al* (1993) have been used to explain variation of BG and GG. The partial melting model suggests that the

variation of BG as well as GG can be explained by varying degree of partial melting (5 to 50%) of bulk continental crust but distribution coefficient for Sr (d_{Sr}) must be very low i.e. $<<10$. The anorthite content of feldspar is very sensitive to determine the distribution coefficient of Sr, therefore, a small changing D_{Sr} will shift the vertical trend of partial melting of source towards higher or lower sides of Sr content. The result of partial melting modeling at least suggests that the differentiation of BG and GG melt are more governed by partial melting of bulk crust rather than fractional crystallization. The estimates upper limit of partial melting i.e., 50 % of bulk crust noted for BG and GG are consistent with required rheological, critical melt percentage to leave the source region has decreased granite melt.

5.6: TECTONIC ENVIRONMENT:

In order to characterize the tectonic environment for the genesis of Bundelkhand granites (BG) and Gray granite (GG) rocks are classified on the basis of major oxides criteria based on the fields of the Maniar and Piccoli (1989) and also have been compared to inferr the tectonic environment for Bundelkhand granite (BG) and gray granite granite and gneiss (GG). For this study the discriminants functions given in table 5.3b have been also applied.

All the BG and GG fall in the field of orogenic granites which is distinctly away from the field of anorogenic granites in the discrimination diagram (Fig.-5.17) by the weight percentage of SiO_2 vs K_2O. Further classified on the basis of the projection diagrams (Fig-4.10b and c) among the MgO (wt%) vs FeO* and CaO (wt%) vs FeO* + MgO (wt%), it does fall in the field defined for post- orogenic granitoids (POG) for gray granite while most of sample of BG occurs in POG. The BG and GG are originated by the continental collision with metaluminous nature, which is clearly evident on the basis of the discriminate variation diagram of molar A/(CNK) Vs A/(NK). Petrogenetic modeling demonstrates that the observed discrimination diagram based on Pearce *et al* (1984) can be explained by the volatiles induced enrichment in Th, Ba and LREE during the genesis of collision granites. It is apparent that the Th, Ba, La, V, Ce and Sm enrichment is a likely consequence of K-silicate and sericitic alteration due to growth of secondary biotite and hornblende and

sphere respectively and Rb depletion is likely consequence of chloritisation and argillic alteration due to the breakdown of feldspar and mica. Using classical system in terms of Qz – Ab- Or (Tuttle and Bowen, 1958, Manning *et al*, 1980) diagram (Fg.- 5.22) in the presence of water. The emplacement of BG can be estimated at moderate level (5 Kb) plotting on the quartz – orthoclase cotectic close to the granite thermal minima. However, the average GG plots into the quartz saturated granite melt field, therefore its unsuitability estimates its physical conditions of emplacement.

5.7 BUNDELKHAND GNEISSIC COMPLEX :

Due to the highly insoluble and immobile nature, rare earth patterns often remain unchanged during metamorphism may be applicable for rock of BnGC. Hence rare earth patterns can provide information on the premetamorphic history of a rock. Indeed, even during the production of sediment from crystalline rock, the rare earth patterns often remain little changed, and rare earth patterns have been used to identify the provenance, i.e., the source, of sedimentary rocks. Rare earth patterns have also become useful tools in chemical oceanography, now that modern analytical techniques allow their accurate determination despite concentrations in the parts per trillion range.

The extent of compositional variation of major, trace and REEs within individual gray granite plutons or a granite suite and their field associated with high grade metamorphics of Mahoba area have been determined from the analysis of whole rock samples and is portrayed and evaluated using different graphical methods (e.g., variation diagrams, chondrite normalized REEs diagrams). The algebraic methods (e.g., least squares regression, Rayleigh fractionation) are also used to model sample to sample differences in the abundance of any element and evaluate different processes thought to produce geochemical variation during crystallization. The variation trends defined by modeled compositions are compared to the variation trends in the actual data set. The goodness of fit is used to accept or reject the likelihood of the modeled process being significant in producing the actual geochemical variation observed in the data set.

The migmatites, gneisses, amphibolites, are the main rocks of the study area grouped under the BnGC. The major element data (Table No.-5.2) of the gneisses and the granites of the study area consist the following characteristics signature:

1. Both, the gneisses and gray granites are the highly silicic having 65.07 to 74.4-wt% SiO_2 and 57.74 to 76.16-wt% SiO_2 respectively.

2. The alumina content in gneisses is moderate and ranging from 11.59% to 16.47wt%Al_2O_3 while in granites it is present as low to moderate, ranging from 8.08 to 15.39wt% Al_2O_3 in gneisses. Alumina content (Av. 13.25-wt% in gneiss and 12.95wt% in granite) is greater than the total alkalies (K2O +Na_2O) (Av. 6.84wt% in gneiss and 8.26 wt% in granite) in gneisses and granite-gneisses.

3. The potash content in gneisses ranges from 0.8 to 6.22 wt%K_2O while in gray granites ranges from 2.44 to 4.49wt%K_2O. Potash content is less than the soda content (2.22 to 6.23 -wt% Na_2O) in majority of the gneisses but in contrast to this the K_2O content is greater than the Na_2O content (2.22 to 4.49-wt% Na_2O) in majority of the granite samples.

4. The Titania (TiO_2) content in gneisses and granites are low ranging from 0.1 to 1.8wt% TiO_2 and 0.13 to 0.96wt% TiO_2 respectively.

5.7.1: Classification and nomenclature:

The gneisses and granites have been geochemically classified on the basis of different oxides, norms and cationic parameters keeping in view that these rocks are the metamorphosed product of igneous protolith. The classification scheme based on Na_2O vs K_2O, An-Ab-Or (O'Connor 1965), Q-A-P (Streickeisen, 1969 and 1968), TAS Le Maitre (1989), P-Q (Debon and Le Fort, 1983) etc. have been considered for the geochemical classification of granites and gneisses of the present study area.

The variation diagram on Na_2O vs K_2O (Fig-5.1), the majority of gneissic rocks occur in the tonalite field while granite plots lie in the field of adamellite and granodiorite.

Majority of the gneisses are fall in tonalite, trondhjemite fields while majority of granite are fall in granite field of An-Ab-Or diadram (Fig-5.2). Pressure boundaries suggested by Whitney (1975) points that average composition of gneisses are plotted in the field above 10 Kb pressures, while granites plot in the field between 4 and 10 Kb. The variation in positions of granites plots between 1.5 to 12 Kb may be due to multiphase of emplacement of acid magmatism and their crystallization at different depths.

The normative Q-A-P triangular diagram (Fig. 5.12) developed by Le Maitre (1989) has been also considered for classification of gneisses and granitoids. The potted values on this diagram show that the majority of gneisses fall in the granodiorite and tonalite fields while the gray granites fall in the monzogranite and granodiorite fields. Gneisses forms a poor calc-alkaline trend, on the other hand granite forms a typical intermediate K_2O and Na_2O rich trend.

The P-Q diagram proposed by Debon and Le Fort 1983 (P=[K - (Na+ Ca)] and Q=[Si/3 - (K+Na + 2Ca/3)]) for the classification of gneisses rocks reveals that majority of the gneisses are fall in the tonalite field (Fig-5.7) while majority of granites are plot in the field of granite and adamellite (Fig.-5.7) Similar view have been obtained from the plot of SiO_2 vs-Zr/TiO_2 (Fig.-5.5) and NaO_2+H_2O vs SiO_2 (Fig.-5.4).

A=[Al-(K + Na + 2Ca)] versus B=(Fe + Mg + Ti) diagram proposed by Debon and Le Fort (1982) and Debon *et. al.* 1986 describes the chemical-mineralogical changes on multi-cationic parameters. The plot in the field of peraluminous and metaluminous mainly depends on its negative value of 'A'. The A-B diagram (Fig.-5.13) clearly shows that most of the gneisses occupy the delineated IVth fields of the metaluminous domain. This view also supported by the presentation of geochemical data of gneisses in Shand's alumina Saturation Index diagram (Fig.-5.14). The geochemical data of granites in A-B diagram indicates that they belong to the association of biotite ± hornblende ± clinopyroxene ± orthopyroxene ± olivine (Fig.-5.13).

Total alkalies verses silica diagram plotting (Fig.-5.2) developed by Middle Most (1985) point out that majority of the granites lie in alkali granite field. Alkalinity (Na_2O+K_2O) of these samples never exceed more than 10%, which reveals that local metasomatism may not be ruled out in the study area.

The analyzed granite samples were plotted in the A-F-M diagram, (Fig. 5.15) developed by Irvine and Baragar (1971). This diagram clearly depict that the granite samples collected from the emplaced part of the shear zone rocks are represented in the calc-alkaline differentiation trend and evolved toward the alkali corner. Most of the samples lie in the calc-alkaline trend. Rahman and Zainuddin (1993) also described that the Bundelkhand granites are probably have calc- alkaline affinity.

The analyses of gneisses and granites are plotted on the SiO_2 versus K_2O diagram (Fig.-5.10) proposed by Irvine and Baragar (1971). The diagram indicates a distinct fields calc-alkaline trend.

5.7.2: Tectonic discrimination:

Mid to early Archean age (3200-3500 Ma) have been proposed for the TTG and migmatite, gneisses (BnGC) around Kabrai area (Mondal *et al* 2002) while Paleoproterozoic age (2600. to 2500 Ma) have been proposed for the Bundelkhand granitoids (BG). Singh *et al* (2007) suggested two episodes of metamorphism for the Bundelkhand granite-gneisses.

To classify the tectonic environment of the granites and granite gneisses of the study area, different discrimination parameters proposed by Maniar and Piccoli (1989) are applied. They distinguished seven types of granitoids based on their tectonic setting:

Viz. Island Arc Granitoids (IAG), Continental Arc Granitoids (CAG),Continental Collision Granitoids (CCG), Post Orogenic Granitoids (POG), Rift-Related Granitoids (RRG),Continental Epeirogenic Uplift Granitoids (CEUG) and Ocean Plagio granites.

Among them, IAG, CAG, CCG and POG are considered as organic granitoids, whereas RRG CEUG and OP are believed to anorogenic granitoids. Thus can be

grouped into two groups according to tectonic setting as IAG, CAG, CCG (group-1) and RRG, CEUG and POG (group-2).

All the granites sample are fall into the field of orogenic granites distinctly away from the field of anorogenic granites in the discrimination diagram (Fig.-5.17) and also majority of the granite of the study area are fall in the orogenic granite field (Fig.-5.17). Shand's alumina Saturation Index diagram (Fig.-5.14) points that majority of granite are fall in metaluminous field where A/CNK value ranges from 0.9 to 1.15 It suggests that granites of the study area were resulted from magmatic origin of POG.

5.7.3: Petrogenesis:

De La Roche's R1-R2 plots, cationic proportion of major oxides (modified by Batchelor and Bowden; 1985) have been used for discrimination of cationic environment. Majority of granites of the study area plots in the syn-continental collision field (Fig.-5.18). The values of the molar ratio Al_2O_3 /(Cao+Na_2O) of granites of the study area in Shands index diagram, have metaluminous composition (A/CNK= 0.9-1.05) suggest that granites were derived from igneous sources (I type granites). Zanuddin *et. al.* (1992), Mondal and Zainuddin (1996) suggested that Bundelkhand granites is characterized by I type affinity.

5.7.4: Major oxide variation :

To consider the role of differentiation process in the formation of gneisses and granites of the study area based on the variation diagrams of Harkers (Fig.-5.19).

Silica Versus other oxides :

Calcium and magnesium oxides: CaO and MgO show a sympathetic relationship with one another in gneisses of the study area but CaO contents is always more than MgO. Same trend is also observed in granites. CaO contents in gneisses varies from 0.2 to 6.01-wt% while in granite varies from 0.43 to 6.72-wt%. MgO contents varies from 0.12 to 4.54-wt% in gneisses while in granites in varies from 0.17 to 3.72-wt%. In both gneisses and granites, CaO and MgO shows antipathic relationship with SiO_2 (Fig.-5.19).

Alkalies:

In gneisses Na_2O varies from 2.44 to 4.49wt% while in the granite it varies from 2.28 to 6.23wt% and K_2O content varies from 0.8 to 6.22 wt% and 2.75 to 5.52 wt% respectively. In both gneisses and granites Na_2O and K_2O bear an inverse relationship to each other. Further K_2O/Na_2O ratio varies from 0.14 to 1.82 in gneisses while this varies from 0.8 to 1.53 in granites when silica content is plotted against Na_2O and K_2O individually (Fig.-5.19). It is seen that there is a tendency for concentration of SiO_2 around 70wt% in both gneisses and granites but Na_2O around 5wt% in gneisses and 3 to 4wt% in granites. In gneisses of the study area, K_2O concentrates around 1.5wt% while in granites concentrates around 4wt%.

Alumina:

In gray granite of the study area, Al_2O_3 content varies from 11.59 to 16.48wt % while in gneisses varies from 8 to 15.4wt%. Alumina content increases with decreasing silica content (Fig.-5.19) and the rations of the Al_2O_3 and SiO_2 shows inverse relationship. Total alkalies and alumina for both gneisses and granites bear a more or less antipathic relationship. There is no definite trend in combined alkalies or alumina though the later show a tendency to decrease with increase in SiO_2. P_2O_5, CaO, Fe_2O_3, TiO_2, and MgO has a tendency to increase with decreasing SiO_2 contents (Fig.-5.19).

Al_2O_3- (Na_2O+K_2O+CaO)-$(FeO+MgO+MnO)$ -triangular diagram :

The gneisses and granites of the study area were plotted on a triangular Al_2O_3 - $(Na_2O + K_2O + CaO)$ - $(FeO + MgO + MnO)$ diagram indicates the distinct field viz. anatectic and magmetic nature. The majority of the analyzed gneisses and granites sample are plotted in the field of magmatic region (magma of anatexis origin), which shows affinity towards cotectic. This means that the granite rocks of the study area have been formed due remobilization and partial melting of these gneisses where exposed as lensoidal patches within the granite.

Rubidium versus potassium diagram :

The Rb-K_2O contents of granites of the study area plotted on Rb Vs K_2O diagram (Fig.-4.16 and 5.19), which shows positive correlation as they have similar

ionic behavior. This type of behavior is called the pegmatitic-hydrothermal trends emphasizes the part played by the field phase (Shows 1968). It is concluded that alkali field circulation has taken an important during the crystallization of magma.

5.7.5: Trace element geochemistry :

The trace element geochemistry is very useful for understanding the evolutionary history of the rocks especially the metamorphic rocks. The distributions of trace element are similar to those of major elements and their proportion in the rocks depends on mineralogy, fluid composition, and volume of fluid and pressure-temperature conditions (Hanson 1978; Rollinsion, 1993, 2007).

The granite plot in normal granite field (Fig 4.13b) point that high Ba concentration is typically associated with high temperature (least differentiate) K-feldspar (Taylor et. al. 1960). Here the increase in Ba is accompanied by decrease in Rb. Granite plot in strongly differentiated granite field is indicated by the Ba/Rb ratio, which characterizes the change from normal granite to strongly differentiated type. Rubidium enrichment has been known to occur in highly differentiated granite (Ahrens et. al. 1952, Taylor et. al. 1956).

Condie (1973) has developed Rb vs Sr (log-log) variation diagram (Fig. 5.16) to estimate the crustal emplacement depth for granites. The gneisses and the granites of the study area are plotted in this diagram. All plots of gneisses lies between 0.3 and 2.0 while granite scattering started 0.3 and above 10.0 on the defined line. It is noted that the granite melt might have been generated at depths around 23-35 Kms. Temperature of about 750° C can be expected at such depth it considering, a generally accepted geothermal gradient of about 30°C per km.

Pearce et. al. (1984) described the discrimination of granite in Rb-Y-Nb and Nb-Y (in ppm) space. The relative trace element characteristic if granite of the study area can not be assigned collectively of any one tectonic regime when plotted on Y+Nb versus Rb log-log (ppm) and Y versus Nb log-log (ppm) diagram (Fig.5.21), all the samples cluster near the triple junction demarcating lines of volcanic arc granitoids (VAG), syn-collisional granitoids (syn-COLG) and within plate granitoids (WPG) field.

Behavior of potassium –rubidium –strontium :

The high grade metamorphics and granite shows high K, Rb, Sr. Th K, Rb. The plot in general shows a positive correlation with wide variation in K /Rb ratios (Fig.-5.19). In the majority of the cases, the data shows that K/Rb ratio of the amphibolite zone have value greater then 100. It is generally accepted that this is related to the upper amphibolite facies metamorphism (Heier, 1973; Tarney and Windley, 1977; John Thang, 1984). However the granite are enriched in Rb (maximum up to 417 ppm) as compared with the value of 150 ppm given by Taylor (1965) for granite. This suggests that these granites were subjected to late stage differentiation.

The plot of Rb Vs Sr (Fig. 5.19) points that the gneisses and granites of the study area show the positive relations. Rb concentration ranging from 89 to 330 ppm in gneisses while ranging from 152 to 517 ppm in granite .The Rb/Sr value of gneisses (4.62) and granite (5.28) are much higher than the value of the continental crust as a whole (0.12) and lower crust (0.047) (Taylor and Mc Lehmann, 1985).

The high Rb/Sr ratio of the metamorphic may be due to chemical variation during metamorphism of feldspar minerals appears to be the dominant controlling factor for the abundance of Sr. This is quite evident from the positive correlation shown by gneisses of the study area when Sr plotted against normative plagioclase. The granite of the study area has also positive correlation.

The average distribution of trace elements of gneisses and granites of the study area are shown in Table 5.4 and 5.5. The gneisses have higher Rb (90-330ppm), Ba (141-1163ppm), Sr (50- 495ppm), Zr (156 to 577ppm) and Y (4.9 to 59.2 ppm) content while in granite, Rb ranges from 156 to 517 ppm, Ba (292 to 1391 ppm), Sr (43 to 308), Zr (231 to 960ppm) and Y (35 to 82ppm).

The gneisses and granites of the study area is plotted on Harkers variation diagrams (Fig. 4.19). The trace element of gneisses and granites plotted against SiO_2 shows some generic similar relationship with gneisses and gray granites. However majority of them does not shows a distinct trend. Ga, Zr, and Nb show a tendency to

increase with decreasing SiO_2. However Ga shows distinct trend. Y, Cu, Rb, Ba and Sr do not shows any marked variation with increasing SiO_2 in the gneisses and granites.

5.8: EARLY CRUSTAL EVOLUTION OF BUNDELKHAND COMPLEX :

It was merely described that Bundelkhand massif complex mainly comprises multiphase granitoids (Jhingran, 1958; Sharma, 1982; Sarkar *et. al.* 1984; Basu, 1986) an intrusion of early Proterozoic age (Mondal *et al.;* 2002) and remnants of metamorphics of low and high- grade rocks of Archean as rare remnants. Five phases of granite emplacement have been suggested for this massif by Rahman and Zainuddin (1993), Mondal and Zainuddin (1996) and many others. The hornblende-bearing granitoids characterized by metaluminous composition is attributed to the oldest phase (Phase I) and is followed by biotite granites. It is supposed that granitic magma was perhaps generated by the partial melting of the early formed alkali felsic crust i.e. TGG (Mondal *et al*; 2002,). The coarse-grained porphyritic granite belongs to the third phase of emplacement ast intrusive into the older phases of granitoids. The leucogranites attributed to fourth and fifth phases of granite emplacement and are the youngest phase, characterized as per aluminous and monzo-to-syno-granites (Mondal and Zainuddin 1996). It is suggested (Mondal *et. al;* 2002) that the first three major phases of above granitoids were emplaced around 2500 Ma within a short time span. The discrimination diagrams (Fig-5.15, 5.17, 5.18 and 5.19) and geochemical behaviors discussed in the preceeding paragraphs suggest that Bundelkhand granitoids are assigned to subduction and collision related mechanisms. Mondal et. al., (1998) and Mondal *et. al* (2002) also indicated similar opinion and suggested that this event may be related to as continental welding and an event of cratonic growth and it's stabilization phase in Bundelkhand (Sharma 1999).

The granitoids occur about 70% of total area of craton, therefore more attempts have been made for the evolution of Bundelkhand granitoids. The early geological records are nearly meager or nearly absent due to huge emplacement of granitoids. It is the fact that no serious attempt has been given for early geological history of the craton viz. what was before the granitoids and how was the continental

crust evolved in Bundelkhand massif. Perhaps Basu (1986) first time has described in detailed about the older xenoliths/ enclaves (metasedimentaries and metamafics) from the Bundelkhand craton. Later on Basu (2001) suggested that the older metamorphics present as a lensoidal body are aligned in specific orientation within the Bundelkhand granite. Sharma and Rahman (1999) first time described a complex evolutionary history of the Bundelkhand region extending from early Achaean to palaeoproterozoic in the systematic chronological order with little documents. They divided the cratonic history of Bundelkhand into three parts: (i) the highly deformed older gneissic-greenstone crust comprising amphibolites, quartzite, banded –magnetite- quartzite and calc-silicates rocks emplaced by syn-to-late alkaline to tonalitic granites around 3.2Ga, and 2.7Ga. (ii) Undeformed multiphase granitoid plutonic batholiths (2.5-2.4Ga) emplaced into the early crust (granite-greenstone) and marks the cratonization of Bundelkhand blocks and (iii) mafic dyke swarms, marked the tectonic rifting and extension as last phase of magmatism in the tectonically stabilized Craton.

This is established that primitive continental crust gradually and gradually thickened and enlarged during the Archaean by rapid intrusive and extrusive mafic and ultra mafic activities. At the early Proterozoic time the continents were started to stabilize on the earth. As a result, about three quarters of the present area and volume of continents were formed by this time (Condie 1976).

It has been also postulated by many workers (Windely 1982, Condie 1994) that first continents appeared in the Archaean were possibly small plates, which eventually converged to form the larger continent. Most of the exposed rocks of Archaean age in shield are metamorphics, reflecting the removal of the upper Archaean crust that once overlaid them. In many instances, these ancient metamorphic rocks preserve the faint signatures of sedimentary and volcanic features also, such as cross bedding, ripple marks, pillow structure (Gillen 1985). It is also supposed that tectonic activity then (at Archaean) may have been more marked, i.e. orogenic cycles more be completed relatively more rapidly than in more recent periods of earth history.

The Phanerozoic was a period of earth's history when large continents broke up, drifted apart and collided. Modern plate tectonic processes probably seems to

become established during the Proterozoic but it's mechanism in Archean can't be ignored (Condie1976; Kroner and Cordani 2003; Viewer 2002). Mountain chains and metamorphic belts were formed in collision zones and progressively younger organic belts were attached to the Precambrian cores or cratons as nucleous. Thus continents started to grow outwards as sedimentary basin around the early phase of cratonic event (Micro-continent/Proterozoic cratons) and subsequently, they closed, compressed and welded together. Archean mountain belts contain metamorphics of mafic & ultramafic throughout the Archean terrain. The tectonic activities are related to high heat flow, which is the driving force of the earth's activity and heat generation. This was very high in the early stage and started to decline during the Proterozoic.

The recent geological studies (Gillen 1985, Nagui, 2005) reveal that Precambrian shields rocks were formed in two different metamorphic environments. The first is so called "green-stone belt" which were deformed and metamorphosed at relatively low grade and, secondly, the contrasting gneissic terrain, which is made up of granulites, granite-gneisses and migmatites that were formed at high temperature and pressure. The gneisses of these high-grade terrains were intensively deformed and crystallized at moderate to high pressure and temperature at the nucleous of shield of the Achaean. The greenstone belts have been reported from most of the cratonic areas of world, which were formed during the period 3500-3000/2700 Ma ago. This belt is usually considered as a long, narrow synform and marginal basin containing thick sequences of metamorphosed mafic and ultramafic, volcano sedimentaries and overlying sediments (Gillen 1985). There are three major litho-units in all the green stone belts: (a) upper part: gray rocks, conglomerates, sandstones, banded iron-stones (b) Middle part: antiseptic volcanic rocks,(c) lower part : basic to ultrabasic lavas. The ultra mafics lavas were probably derived from the mantle and are komatiite in composition and characterised by spenifex texture. Mafic rocks of greenstone belt are mainly basalt, andesite and dacite, similar in composition to lavas of modern island arcs. The sedimentary of green stone belts were derived from granite- gneisses and volcanics.

In the Indian shield, the green stone has been reported from Dharwar, Singbhum and Rajasthan cratons. Recently, it is assumed that Bundelkhand craton is another nucleus in the north of Sonata, which has its own continental growth and Precambrian crustal evolution (Singh *et al.*, 2007). The available geo-chronological data, field evidences, various discrimination diagrams and geo chemical behaviors of major and trace elements discussed in the adjoining area (Singh 2005) suggest that crustal growth of Bundelkhand craton occurred between middle Archaean to early Proterozoic i.e. 3300-2500 Ma and was related to green stone belt. The present study are is the eastern part of this balt. That comprises mainly the gneisses of BnGC.

In the older metamorphic group (BnGC) tight to isoclinals, coaxial folds (F_1 & F_2) were developed possibly during the deformation D_1 and first phase of metamorphism that is followed by D2 deformation (F_3 open fold) marks the post metamorphism. The first phase of metamorphism (M_1) was high- grade as evidenced by the complete absence of muscovite, chlorite, talc, kyanite, stautolite, tremolite, epidote etc. from the gneisses and pelitic rocks of the study area. These rocks (BnGC) are characterized by granulose texture where clinopyroxene, hornblende, perthite, biotite, sillimanite, orthopyroxene, garnet etc minerals were developed. M_1 metamorphism can be further be subdivided into two stages (i) formation of gneisses and amphibolites and (ii) migmatite stage anatexis, granulites, tonalite and trondhjhemitic.

The TTG contains significant amount of K-feldspar, plagioclase, biotite and quartz, and Minor amount of ilmanite, apatite, zirocon, sphene. The biotite gneisses contain biotite, quartz, plagioclase and K-feldspar with significant amount of zircon and apatite. Sexena and Mishra (1962) reported garnet and sillimanite from Kabrai area but it could not found in the study area, possibly may be due to composition variation. It is worth to mention that prograde muscovite, chlorite, staurolite, actinolite could not be recorded from these rocks. Mineral assemblages in gneisses are biotite – K-feldspar – antiperthite + quartz, biotite-plagioclase – K-feldspar – quartz and in amphibiotites and hornblende-gneisses are hornblende – clinopyroxene – biotite – plagioclase – K-feldspar – quartz and hornblende – clinopyroxene –

plagioclase – K-feldspar – quartz. The P–T conditions reveal that all the above mineral assemblages yield 650° C to 750° C temperature and 6 to 7 kbar pressure (Singh *et al.*, 2008).

The observed mineral assemblages, petrochemistry and field relations from the study area are similar to other older crust. The geochronological study points that high- grade gneisses and granulite comprising meta-sediments and ultrabasic to basic igneous rocks along with tonalitic gneisses were crystallized at 3500-3200 M.a. It can also be inferred that the crystallized minerals of older metamorphics aligned on S_1 and S_2 planes in the gneisses and the mesoscopic structures viz. F_1 and F_2 folds formed during D_1 is the pre-tectonic M_1 metamorphism while F_3 folds developed in the D2 deformation is post date the M_1.

The signature of second phase of metamorphism (M_2) is well preserved in the adjoining area near Mauranipur along with the gneisses terrain (Singh 2005). The field relationship shows that mafics and ultramafics are trending ENE–WSW to E–W parallel to the banded iron formation. The foliation planes generally striking ENE–WSW, steeply dips north westerly while towards the south of these schistose rocks, exposure of BnGC rocks are observed trending WNW–ESE. Thus it can be concluded that they have an angular relationship with each other. The BMM rock comprises mafics and ultramafics, banded magnetite quartzites and metavolcanics. In BMM rocks tight to open folds trending in E–W direction were observed especially in metasedimentary rocks, axial surface trending NW–SE to NE–SW plunging towards north. The S_1 and S_2 schistosity developed in BMM are related to D_1 and D_2 deformations. Intense schistosity at the contact between meta-sedimentary and metavolcanics within BMM indicate sinistral shearing.

The first phase of metamorphism in mafics and ultramafics and metavolcanosedimentaries is possibly initiated at the D_4 deformation due to load pressure and rise in temperature. Tight to open F_1 folds were developed in mafics and ultramafics and metasedimentaries are the responsible for the development of S_1 foliation, which is defined by the flaky minerals viz. muscovite, chlorite, talc, biotite amphibole and epidote. The appearance of talc, chlorite tremolite, actinolite in the

ultramafic rocks and actinolite, hornblende, epidotic, garnet chlorite, biotite in the mafic rocks points that metamorphism has reached up to the green schist to lower amphibolites facies conditions.

The minerals assemblages observed in the BMM are epidotic – chlorite – actinolite / tremolite – albite – magnetite – quartz, chlorite – actinolite – tremolite – magnetite $\pm$ quartz $\pm$ albite, actinolite - tremolite – talc – chlorite$\pm$ quartz $\pm$ serpentine $\pm$ biotite, talc – tremolite $\pm$ quartz and talc – chlorite$\pm$ magnetite $\pm$ phlogopite is related to green schist.

The field relationship, textural study, phase relationship and geochemical studies reveal that the exposed metamorphic rocks in the central part of Bundelkhand massif is definitely older to the paleoproterozoic granite (BG) and has been divided into two groups: (i) Bundelkhand Gnessic Complex (BnGC) (3500 to 3200Ma), which comprises TTG gneisses, migmatites, amphibolites, hornblende-biotite gneisses and granite- gneisses, and (ii) Bundelkhand metasedimentaries and metavolcanics (BMM) (3200-2600Ma) which comprises mafic-ultramafics, banded magnetite quartzite, quartzite and meta-volcanics. These two groups of rocks were invaded by Bundelkhand granitoids (BG) intrusions in different episodes (2500-2300Ma). In the later phase NE – SW trending quartz reefs, tending NE-SW offsetting the above said older litho units, were emplaced around 2000-2300Ma. The last phase episode in the craton is related to an evidence of extensional tectonic and thermal relaxation that is marked by the emplacement of mafic dykes trending in NW-SE around (2000-1800Ma).

Table-5.1 : A chemical analysis of major oxides of rocks of Mahoba area.

Samole and Name	SiO2	Al2O3	Fe2O3	MnO	MgO	CaO	Na2O3	K2O	TiO2	P2O5
BU/PM/169GG	72.71	14.03	1.47	0.03	0.38	0.43	3.79	5.22	0.15	0.04
BU/PM/175GG	62.98	11.59	8.63	0.14	1.69	3.29	2.91	3.93	0.94	0.34
BU/PM/179GN	70.5	15.42	2.29	0.05	0.49	2.6	6.27	0.84	0.28	0.1
BU/PM/184GN	70.13	13.93	0.41	0.01	0.15	0.17	3.56	3.35	0.04	0.01
BU/PM/185GN	73.68	14.1	0.87	0.02	0.34	0.16	4.73	2.78	0.1	0.02
BU/PM/191GN	68.51	10.08	7.73	0.1	4.36	1.85	2.19	2.7	1.18	0.25
BU/PM/193GN	69.28	11.09	5.27	0.09	4.02	1.51	2.77	2.07	0.88	0.08
BU/PM182GN	60.34	15.33	5.77	0.09	2.89	6.44	5.33	1.52	0.68	0.31
KM/1GN	72.22	12.94	2.69	0.04	0.68	1.43	3.75	4.43	0.33	0.09
MO4/306GG	72.92	13.86	1.37	0.04	0.14	0.8	3.59	5.52	0.13	0.01
MOU/02GG	64.59	16.47	3.99	0.08	1.06	2.52	4.01	5.06	0.63	0.2
MOU/03PG	70.46	13.65	2.78	0.06	0.87	1.51	4.3	4.72	0.31	0.1
MOU/06PG	73.4	13.54	0.93	0.01	0.14	0.42	3.39	6.22	0.05	0.08
MOU/07PG	72.63	14.1	1.15	0.02	0.22	1.18	3.82	4.91	0.14	0.03
MO4/11PG	71.82	14.05	1.93	0.03	0.44	0.61	3.37	5.79	0.34	0.05
MO4/12PG	70.48	13.5	3.33	0.06	1.24	1.5	3.97	4.47	0.42	0.11
MOU/172GN	73.65	13.21	1.46	0.03	0.6	0.27	3.56	5.59	0.15	0.02
MOU/270AGG	57.74	14.08	8.22	0.16	4.18	6.72	3.47	2.75	0.77	0.31
MOU/277GN	68.07	12.9	5.94	0.1	2.6	1.95	3.7	2	0.88	0.11
MOU/278GN	65.19	12.9	7.15	0.17	4.51	2.74	2.46	2.48	0.65	0.21
MOU/279GN	79.04	7.62	3.8	0.06	2.33	1.39	2.37	1.39	0.64	0.07
MOU/283GG	70.52	10.09	6.08	0.11	3.72	1.22	2.44	3.48	0.96	0.5
MOU/285GG	64.54	15.47	4.65	0.08	1.53	3.34	3.96	3.78	0.57	0.2
MOU/291PG	68.75	14.29	3.52	0.06	1.31	2.34	3.65	4.43	0.37	0.13
MOU/299GN	67.07	15.7	3.69	0.08	1.18	2.73	4.97	2.25	0.39	0.1
MOU/301GN	69.48	15.07	2.97	0.05	0.83	1.85	4.1	4.16	0.31	0.11
MOU/304GN	71.75	14.53	1.42	0.03	0.22	1.3	4.28	4.35	0.11	0.02
MOU10GG	76.16	12.43	0.98	0.01	0.37	0.17	4.49	4.05	0.08	0.01

Table-5.2 : Chemical analyses of trace element and REE from the rocks of study area.

Samole and Name	Sc	V	Cr	Co	Ni	Cu	Zn	Ga	Rb	Sr
BU/PM/169GG	1.386	14.467	5.672	47.231	2.264	1.145	50.381	19.606	256.897	89.7
BU/PM/175GG	10.62	201.037	45.602	29.784	6.235	2.401	101.208	37.19	451.437	134.606
BU/PM/179GN	1.127	24.898	5.233	19.256	2.715	1.755	42.957	25.742	89.573	449.661
BU/PM/184GN	0.871	18.615	8.682	51.131	3.653	1.455	39.605	16.381	164.945	75.943
BU/PM/185GN	0.755	17.65	9.808	48.181	2.423	1.139	56.589	22.386	127.983	161.531
BU/PM/191GN	8.681	126.4	3.502	15.197	1.733	1.295	77.02	23.11	187.422	50686
BU/PM/193GN	7.63	87.683	10.991	13.407	4.33	2.446	162.061	27.606	247.526	52.172
BU/PM182GN	5.021	130.049	16.962	35.344	6.037	5.379	43.398	23.386	16.605	495.642
KM/1GN	2.199	35.276	5.847	22.033	2.474	1.412	88.215	22.941	231.691	100.38
MO4/306GG	1.323	10.901	5.472	38.061	2.871	1.187	42.447	22.273	517.804	38.164
MOU/02GG	3.384	58.115	5.578	16.346	2.221	1.468	68.236	25.042	232.973	278.342
MOU/03PG	2.363	43.096	10.922	21.62	3.966	1.37	35.694	20.565	257.018	103.265
MOU/06PG	0.687	18.22	4.157	54.2	1.902	1.316	32.222	25.798	329.511	21.903
MOU/07PG	0.994	18.823	5.258	38.318	6.03	2.578	189.777	22.198	252.129	98.501
MO4/11PG	1.479	26.31	6.16	23.377	2.7	1.434	33.177	24.028	314.355	80.327
MO4/12PG	2.507	49.552	11.038	28.886	3.444	1.206	57.08	22.703	218.354	103.804
MOU/172GN	1.079	19.365	5.196	34.319	2.724	1.566	38.676	18.264	308.649	32.442
MOU/270AGG	9.376	214.92	24.843	34.177	5.95	2.519	133.197	24.75	173.515	308.677
MOU/277GN	6.927	65.448	4.845	12.417	2.161	2.029	95.451	25.842	158.486	82.496
MOU/278GN	14.944	119.572	12.614	22.637	4.694	0.877	126.804	21.422	209.814	93.077
MOU/279GN	5.3	43.824	7.822	24.416	3.179	1.147	51.655	16.638	99.369	66.116
MOU/283GG	7.46	101.241	3.972	13.404	2.996	3.412	104.296	27.25	343.365	42.934
MOU/285GG	3.926	100.6	5.683	20.535	2.212	1.268	58.968	24.509	153.128	214.294
MOU/291PG	3.086	65.289	8.467	17.283	3.05	1.531	65.175	22.671	224.669	143.521
MOU/299GN	3.463	60.313	8.873	21.461	2.767	2.55	49.928	25.536	221.962	174.734
MOU/301GN	2.048	37.193	5.409	27.385	2.392	1.22	73.804	22.874	212.774	115.176
MOU/304GN	1.161	17.757	6.587	29.335	3.241	2.594	56.398	23.033	306.41	67.556
MOU10GG	0.511	5.721	5.497	9.027	0.842	1.301	17.129	4.021	54.483	13.624

Samole and Name	Y	Zr	Nb	Cs	Ba	La	Ce	Pr	Nd	Sm
BU/PM/169GG	35.057	231.091	16.313	6.683	1380.47	155.988	221.88	21.072	70.026	10.276
BU/PM/175GG	69.112	690.052	44.105	15.688	513.419	75.232	174.667	20.852	81.514	14.596
BU/PM/179GN	14.045	234.467	11.328	6.283	497.348	73.438	121.756	12.285	43.204	6.24
BU/PM/184GN	36.746	170.744	2.732	1.883	1163.444	14.526	44.499	3.727	15.444	4.237
BU/PM/185GN	4.971	114.902	4.1	0.674	398.512	12.227	21.133	1.878	6.061	0.883
BU/PM/191GN	38.611	436.262	28.744	10.456	283.78	46.09	88.543	9.855	40.6	8.61
BU/PM/193GN	58.484	577.924	33.297	19.803	351.731	82.31	159.533	17.816	72.89	14.435
BU/PM182GN	19.141	247.892	19.342	0.537	622.57	32.562	72.485	8.511	33.354	5.191
KM/1GN	37.136	288.648	24.421	1.935	529.731	85.984	159.727	16.125	55.672	8.73
MO4/306GG	54.643	255.337	49.132	11.609	293.202	85.514	166.453	16.555	55.885	9.617
MOU/02GG	40.703	396.922	19.603	3.326	1391.799	84.795	159.955	17.018	64.122	10.575
MOU/03PG	32.245	275.091	21.896	1.325	833.472	74.417	133.136	13.423	47.394	7.667
MOU/06PG	11.233	33.614	16.652	2.131	141.354	5.006	10.505	1.132	4.065	0.957
MOU/07PG	42.648	209.824	25.905	2.32	603.074	63.185	120.777	11.968	41.537	7.344
MO4/11PG	44.48	381.388	29.081	2.271	656.309	149.61	279.609	25.81	83.56	12.086
MO4/12PG	28.677	319.761	22.513	2.595	729.874	64.25	121.37	12.144	43.792	6.936
MOU/172GN	16.472	152.928	16.415	2.236	468.247	27.772	48.483	4.68	16.04	2.858
MOU/270AGG	36.19	273.499	15.978	6.702	703.509	58.057	122.072	13.666	53.921	9.356
MOU/277GN	43.81	487.012	34.29	12.154	301.186	37.345	71.047	7.553	29.318	5.861
MOU/278GN	38.498	250.06	16.811	1.18	341.976	28.634	55.302	5.912	23.824	4.55
MOU/279GN	59.286	388.505	22.25	3.71	290.279	84.383	163.803	77.755	70.994	13.788
MOU/283GG	82.434	934.136	56.544	20.645	507.587	66.065	135.08	14.587	59.084	12.272
MOU/285GG	34.553	266.126	16.113	4.086	1217.346	73.048	132.408	13.497	50.134	8.446
MOU/291PG	23.185	276.968	15.175	3.987	926.051	63.004	110.891	10.702	37.128	5.755
MOU/299GN	31.565	288.729	21.069	9.35	996.154	87.601	147.294	14.042	47.485	7.388
MOU/301GN	30.491	272.919	19.181	4.653	929.31	26.424	48.401	5.065	19.371	4.174
MOU/304GN	25.959	155.945	16.736	4.005	400.668	33.342	63.121	6.354	22.554	3.988
MOU10GG	5.806	12.791	2.462	0.348	80.653	14.687	23.662	2.882	9.726	1.414

Samole and Name	Eu	Gd	Tb	Dy	Ho	Er	Tm	Yb	Lu	Hf
BU/PM/169GG	1.224	8.383	1.085	5.987	0.574	1.889	0.221	2.247	0.364	7.032
BU/PM/175GG	1.59	11.417	1.67	10.174	1.098	3.902	0.527	5.886	1.025	20.476
BU/PM/179GN	1.327	4.759	0.519	2.556	0.249	0.854	0.095	1.004	0.153	0.644
BU/PM/184GN	0.967	3.729	0.748	5.705	0.689	2.403	0.342	3.53	0.588	7.048
BU/PM/185GN	0.407	0.795	0.104	0.698	0.085	0.32	0.046	0.537	0.111	4.971
BU/PM/191GN	1.567	7.682	1.24	7.507	0.784	2.447	0.296	3.137	0.557	11.638
BU/PM/193GN	2.149	11.452	1.675	9.988	1.092	3.818	0.516	5.722	0.981	15.133
BU/PM182GN	1.42	4.058	0.539	3.059	0.338	1.19	0.149	1.688	0.295	6.031
KM/1GN	0.95	7.175	0.992	5.874	0.64	2.276	0.302	3.089	0.502	9.444
MO4/306GG	0.596	7.921	1.229	8.001	0.926	3.44	0.493	5.667	0.943	8.689
MOU/02GG	2.17	8.318	1.155	6.181	0.739	2.558	0.322	3.39	0.555	10.533
MOU/03PG	1.036	6.101	0.878	5.23	5.567	2.001	0.257	2.67	0.424	8.351
MOU/06PG	0.123	0.863	0.176	1.393	0.185	0.736	0.129	1.645	0.293	2.501
MOU/07PG	0.804	6.097	0.948	6.157	0.712	2.567	0.371	4.233	0.718	7.555
MO4/11PG	0.971	9.73	1.26	7.388	0.792	2.875	0.367	3.928	0.613	11.378
MO4/12PG	0.973	5.537	0.765	4.497	0.489	1.719	0.219	2.429	0.403	9.353
MOU/172GN	0.464	2.418	0.382	2.346	0.26	0.945	0.128	1.447	0.258	5.94
MOU/270AGG	2.074	7.529	1.044	6.289	0.673	2.265	0.289	3.055	0.501	7.196
MOU/277GN	1.207	5.187	0.923	6.496	0.793	2.898	0.401	4.43	0.784	12.214
MOU/278GN	1.049	4.32	0.792	5.752	0.709	2.486	0.347	3.704	0.644	5.968
MOU/279GN	2.242	11.279	1.732	10.596	1.136	3.862	0.493	5.383	0.887	9.815
MOU/283GG	1.851	10.44	1.832	12.755	1.524	5.581	0.788	8.897	1.546	25.553
MOU/285GG	1.767	6.905	0.951	5.531	0.581	1.965	0.256	2.649	0.444	7.193
MOU/291PG	1.123	4.759	0.66	3.798	0.413	1.432	0.185	2.012	0.335	8.112
MOU/299GN	1.268	6.259	0.88	5.272	0.571	1.914	0.249	2.49	0.412	7.907
MOU/301GN	1.008	3.786	0.675	4.676	0.521	1.772	0.228	2.34	0.378	7.94
MOU/304GN	0.565	3.303	0.516	3.429	0.401	1.537	0.232	2.714	0.475	5.791
MOU10GG	0.185	1.144	0.147	0.852	0.091	0.331	0.042	0.507	0.084	0.667

Samole and Name	Ta	Pb	Th	U
BU/PM/169GG	1.365	46.807	64.298	9.053
BU/PM/175GG	3.415	33.382	61.841	17.316
BU/PM/179GN	0.737	30.849	18.585	4.844
BU/PM/184GN	0.474	34.65	28.224	10.271
BU/PM/185GN	0.42	32.38	19.897	30.461
BU/PM/191GN	1.226	24.255	14.908	6.058
BU/PM/193GN	1.342	36.938	26.906	6.014
BU/PM182GN	1.397	23.489	9.489	5.998
KM/1GN	2.283	40.9	72.555	15.531
MO4/306GG	5.115	56.284	97.509	66.744
MOU/02GG	0.145	32.902	30.917	8.576
MOU/03PG	1.555	32.519	46.774	10.512
MOU/06PG	1.784	31.922	8.911	15.078
MOU/07PG	2.876	49.138	62.169	33.157
MO4/11PG	1.985	50.838	110.225	19.24
MO4/12PG	1.405	33.228	47.419	11.796
MOU/172GN	1.388	24.437	37.536	19.499
MOU/270AGG	0.706	25.097	15.895	4.105
MOU/277GN	1.483	45.517	14.79	6.314
MOU/278GN	1.129	33.999	6.785	1.58
MOU/279GN	1.013	22.38	23.394	3.797
MOU/283GG	2.214	31.352	32.112	12.266
MOU/285GG	1.176	27.039	28.768	7.442
MOU/291PG	1.182	32.272	38.752	9.699
MOU/299GN	1.725	32.771	38.402	6.848
MOU/301GN	1.398	30.517	16.892	7.899
MOU/304GN	2.386	41.223	39.403	37.052
MOU10GG	0.314	13.816	20.509	4.236

Table-5.3. Normative Minerals and CIPW weight Norm calculation for the rocks of Mahoba area.

Samole and Name	Apatite	Zircon	Ilmenite	Orthoclase	Anorthite	Corundom	Magnetite	Hypersthene	Quartz	Rutile
BU/PM/169GG	0.09	0.05	0.06	30.85	2.18	7.58	1.47	0.95	51.21	0.12
BU/PM/175GG	0.81	0.14	0.29	23.22	14.25	2.11	8.63	4.21	39.22	0.79
BU/PM/179GN	0.24	0.05	0.11	4.96	12.49	9.93	2.29	1.22	61.14	0.22
BU/PM/184GN	0.02	0.03	0.02	19.8	0.8	10.01	0.41	0.37	56.73	0.03
BU/PM/185GN	0.05	0.02	0.04	16.43	0.8	10.8	0.87	0.85	62.18	0.08
BU/PM/191GN	0.59	0.09	0.21	15.96	19.53	0	7.73	10.69	42.31	0
BU/PM/193GN	0.19	0.12	0.19	12.23	7.06	6.26	5.27	10.01	52.28	0.78
BU/PM182GN	0.73	0.05	0.19	8.98	30.21	2.61	5.77	7.2	37.15	0.58
KM/1GN	0.21	0.06	0.09	26.18	6.65	5.71	2.69	1.69	51.36	0.29
MO4/306GG	0.02	0.05	0.09	32.62	3.98	6.43	1.37	0.35	49.85	0.09
MOU/02GG	0.47	0.08	0.17	29.9	11.57	6.75	3.99	2.64	38.62	0.54
MOU/03PG	0.24	0.06	0.13	27.89	7.04	5.96	2.78	2.17	48.04	0.24
MOU/06PG	0.19	0.01	0.02	36.76	1.6	6.22	0.93	0.35	48.7	0.04
MOU/07PG	0.07	0.04	0.04	29.02	5.81	6.66	1.15	0.55	50.99	0.12
MO4/11PG	0.12	0.08	0.06	34.22	2.86	6.74	1.93	1.1	47.75	0.31
MO4/12PG	0.26	0.06	0.13	26.41	6.9	6.13	3.33	3.09	48.52	0.35
MOU/172GN	0.05	0.03	0.06	33.03	1.31	6.68	1.46	1.49	50.78	0.12
MOU/270AGG	0.73	0.05	0.34	16.25	30.3	0	8.22	10.41	27.61	0.23
MOU/277GN	0.26	0.1	0.21	11.82	9.04	7.42	5.94	6.48	52.6	0.77
MOU/278GN	0.5	0.05	0.36	14.66	12.32	5.7	7.15	11.23	43.64	0.46
MOU/279GN	0.17	0.08	0.13	8.21	6.52	3.73	3.8	5.8	67.41	0.57
MOU/283GG	1.18	0.19	0.24	20.56	2.91	5.26	6.08	9.26	50.34	0.84
MOU/285GG	0.47	0.05	0.17	22.34	15.58	5.67	4.65	3.81	41.05	0.48
MOU/291PG	0.31	0.06	0.13	26.18	10.99	5.47	3.52	3.26	45.08	0.3
MOU/299GN	0.24	0.06	0.17	13.3	13.15	8.45	3.69	2.94	51	0.3
MOU/301GN	0.26	0.05	0.11	24.58	8.68	7.38	2.97	2.07	48.55	0.25
MOU/304GN	0.05	0.03	0.06	25.71	6.42	7.47	1.42	0.55	51.99	0.08
MOU10GG	0.02	0	0.02	23.93	0.8	7.75	0.98	0.92	59.76	0.07

Table 5.4. Ratio of Trace elements analysis and REE of Mahoba Area.

Samole and Name	K/Na	K / Rb	Rb / Sr	Ba/Rb	A/CNK	Σ LREE	Σ HREE	ΣREE
BU/PM/169GG	1.3773	0.020319	2.863958	5.373632	1.486229	480.466	20.75	501.216
BU/PM/175GG	1.3505	0.008706	3.353766	1.137299	1.144126	368.451	35.699	404.15
BU/PM/179GN	0.134	0.009378	0.199201	5.552432	1.588054	258.25	10.189	268.439
BU/PM/184GN	0.941	0.02031	2.171958	7.053527	1.967514	83.4	17.734	101.134
BU/PM/185GN	0.5877	0.021722	0.792312	3.113789	1.838331	42.589	2.696	45.285
BU/PM/191GN	1.2329	0.014406	0.003698	1.514123	1.495549	195.265	23.65	218.915
BU/PM/193GN	0.7473	0.008363	4.744422	1.420986	1.746457	349.133	35.244	384.377
BU/PM182GN	0.2852	0.091539	0.033502	37.49292	1.153499	153.523	11.316	164.839
KM/1GN	1.1813	0.01912	2.308139	2.286368	1.346514	327.188	20.85	348.038
MO4/306GG	1.5376	0.01066	13.56787	0.566241	1.398587	334.62	28.62	363.24
MOU/02GG	1.2618	0.021719	0.837003	5.974079	1.421053	338.635	23.218	361.853
MOU/03PG	1.0977	0.018364	2.488917	3.242855	1.296296	277.073	23.128	300.201
MOU/06PG	1.8348	0.018876	15.0441	0.428981	1.34995	21.788	5.42	27.208
MOU/07PG	1.2853	0.019474	2.559659	2.391926	1.422805	245.615	21.803	267.418
MO4/11PG	1.7181	0.018419	3.913441	2.087796	1.438076	551.646	26.953	578.599
MO4/12PG	1.1259	0.020471	2.103522	3.342618	1.358149	249.465	16.058	265.523
MOU/172GN	1.5702	0.018111	9.513871	1.517086	1.402335	100.297	8.184	108.481
MOU/270AGG	0.7925	0.015849	0.562125	4.054456	1.088099	259.146	21.645	280.791
MOU/277GN	0.5405	0.012619	1.921136	1.900395	1.686275	152.331	21.912	174.243
MOU/278GN	1.0081	0.01182	2.254198	1.629901	1.679688	119.271	18.754	138.025
MOU/279GN	0.5865	0.013988	1.502949	2.921223	1.479612	412.965	35.368	448.333
MOU/283GG	1.4262	0.010135	7.997508	1.478272	1.413165	288.939	43.363	332.302
MOU/285GG	0.9545	0.024685	0.71457	7.949859	1.396209	279.3	19.282	298.582
MOU/291PG	0.0197	0.019718	1.565409	4.121846	1.371401	228.603	13.594	242.197
MOU/299GN	0.4527	0.010137	1.270285	4.487948	1.577889	305.078	18.047	323.125
MOU/301GN	1.0146	0.019551	1.847381	4.367592	1.490603	104.443	14.376	118.819
MOU/304GN	1.0164	0.014197	4.535645	1.307621	1.463243	129.924	12.607	142.531
MOU10GG	0.902	0.074335	3.999046	1.480333	1.427095	52.556	3.198	55.754

Table 5.5. Major oxide criteria for tectonic environment. (After Maniar and Piccoli, 1989).

Discriminant Function	Orogenic				Anorogenic		
	IAG	CAG	CCG	POG	RRG	CEUG	OP
SiO$_2$ range wt%	60-68	62-76	70-76	70-78	72-78, 60-63	71-77, 60-62	61-78
	----------Unimodal----------				----------Bimodal----------		Unimodal
Alkali-lime Index	Calcic to calcalkaline	Calc-alkaline	Calc-alkaline to alkali calcic	Alkali calcic	Alkalic	Alkalic	calcic
Shand's Index	Predominantly metaluminous	Metaluminous Peraluminous	Peraluminous	Peraluminous Metaluminous Peraalkaline (minor)	Peraluminous (minor) Metaluminous peralkaline	Peraluminous (minor) Metaluminous Peralkaline	Peraluminous Metaluminous
Na$_2$O/CaO wt%	~ 1.0	~ <4.0	~2.0 – 10.0	~2.0–18.0	~ 2.0–25.0	~1.0–12.0	~ <4.0
Na$_2$O/ K$_2$O wt%	0.4 – 3.0	0.4 – 2.0	0.4 – 1.5	0.6 – 1.2	0.7 – 1.0	0.6 – 1.0	0.0 – 50.0
MgO/FeO (T) wt%	03 – 0.85	0.1 – 0.5	0.05 – 0.6	0.02 – 0.3	0.0 – 0.2	0.0 – 0.12	0.0 – 0.7
MgO/MnO wt%	12–28	2–38	2–45	2–18	0.0–7.5	0.0–7.5	0.0–50
Al$_2$O$_3$/ Na$_2$O+K$_2$O (Molar)	>1.5	>1.1	>1.1	0.9-1.4	<1.15	<1.15	>1.0

Table 5.6. Inferred Tectonic Environment for BG and GG based on discriminant functions given in table 5.5.

Discriminant Function	Orogenic			
	Granite (BG)		Gray Granite (GG)	
	Inferred types		Inferred types	
Silica Range (wt %)	68.75 – 73.65 unimodal	IAG/CAG/CCG/POG	57 – 76	IAG/CAG/CCG
Alkali-lime Index	Calc-alkaline to alkali calcic	IAG/CAG/CCG/POG	Calc-alkaline to alkali calcic	CCG
Shand's Index	Metaluminous	CCG	Peraluminous to Metaluminous	CAG/CCG
Na$_2$O/CaO (wt %)	2.6 – 8.0	CAG/CCG	0.51 – 2.0	CAG/CCG
Na$_2$O/K$_2$O (wt %)	0.54 – 0.91	CCG	0.65 -1.05	CCG
MgO/FeO (t) (wt %)	0.15 – 0.37	CAG/CCG	0.1 - 0.61	CAG/CCG
MgO/MnO (wt %)	11 – 21.83	CAG/CCG	3.5 - 37	CAG/CCG
Al$_2$O$_3$/Na$_2$O+K$_2$O (molar)	1.41 – 1.77	IAG/CAG/CCG	1.15 – 2.26	IAG/CAG/CCG
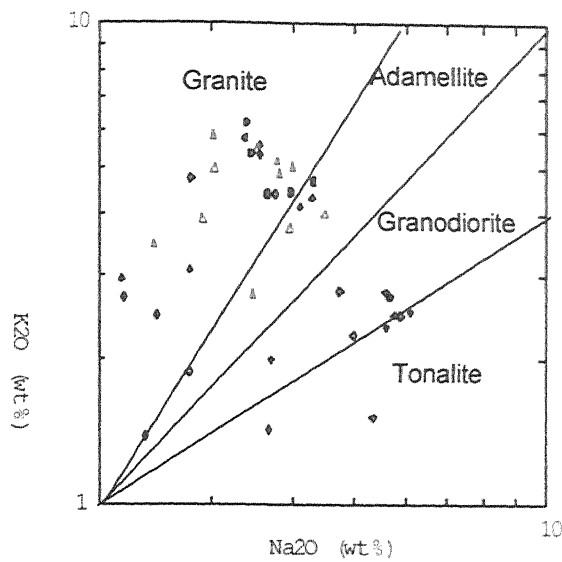
Fig: 5.1
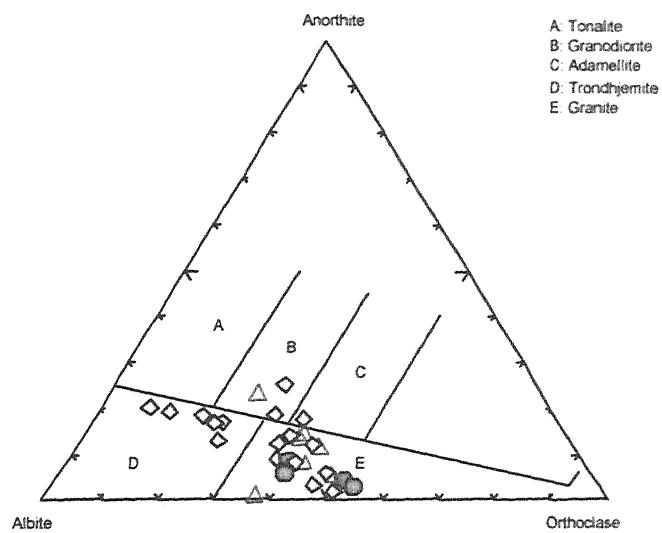
Fig: 5.2
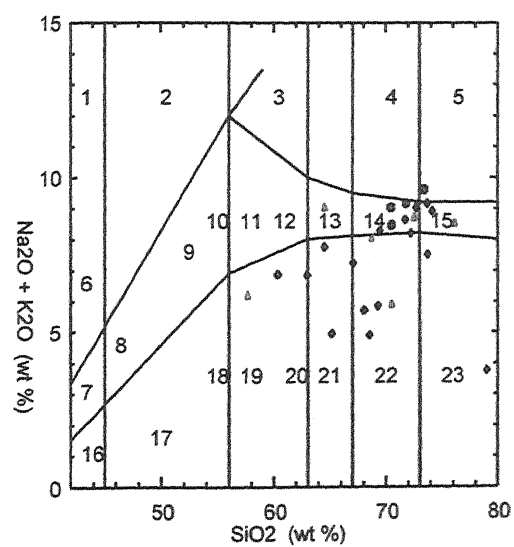
Fig: 5.3

Fig.-5.1 : Na2O vs K2O (wt%) plots for the Mahoba (Harpun 1963),
Fig.-5.2 : Normative An-Ab-Or plots for the Mahoba area (O'Connar, 1965)
Fig.-5.3 : Na2O vs SiO2 plot for Mahoba area (Middle Most, 1985)
Symbols - Circle represent : BG, Diamond Shape : BnGC, Triangle : GG
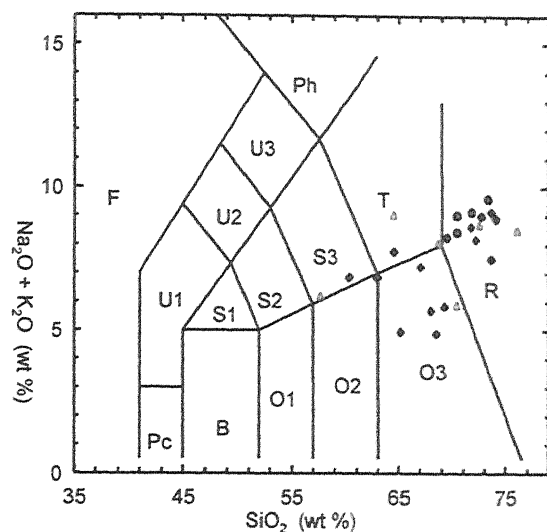
Fig: 5.4
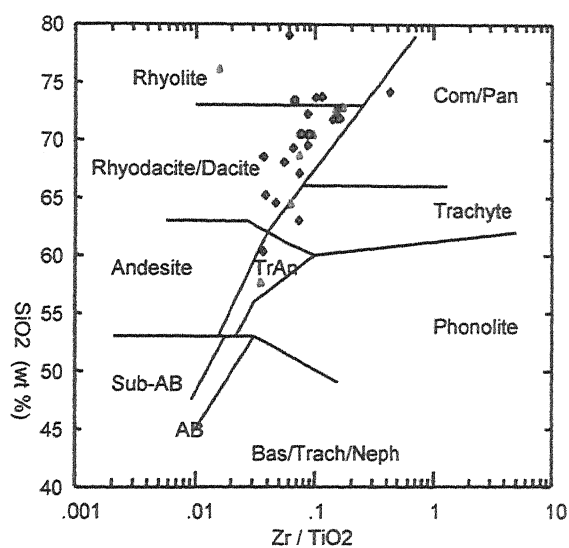
Fig: 5.5
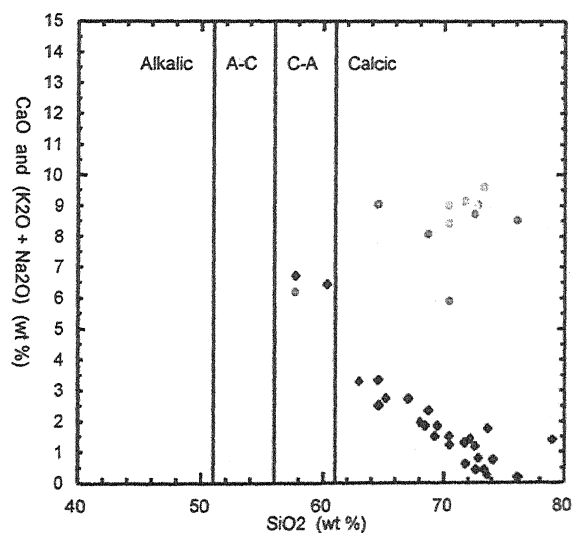
Fig: 5.6

Fig.-5.4 : Classification of granitoids of Mahoba area (TAS) after Le Maitre (1989).

Fig.-5.5 : Classification of granitoids of Mahoba area Winchester & Fbyd, (1977).

Fig.-5.6 : Classification of granitoids of Mahoba area.

Symbols : Circle represent: BG; Diamond: BnGC; Triangle: Gray Granite
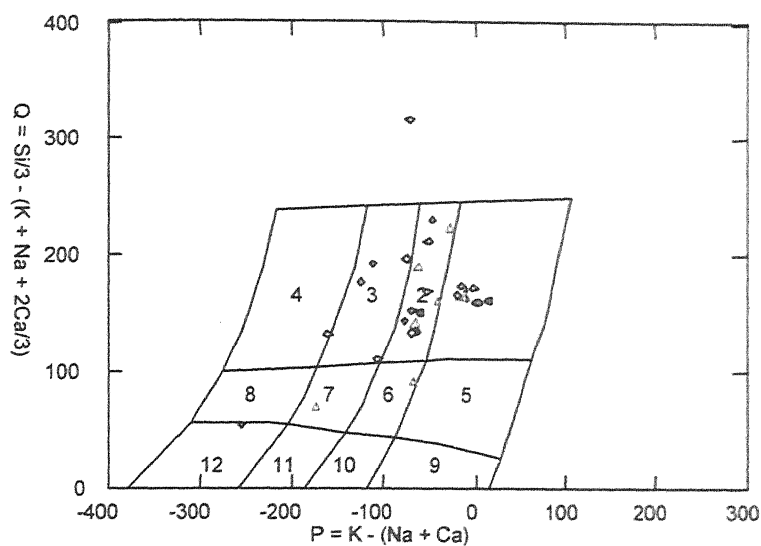
Fig: 5.7
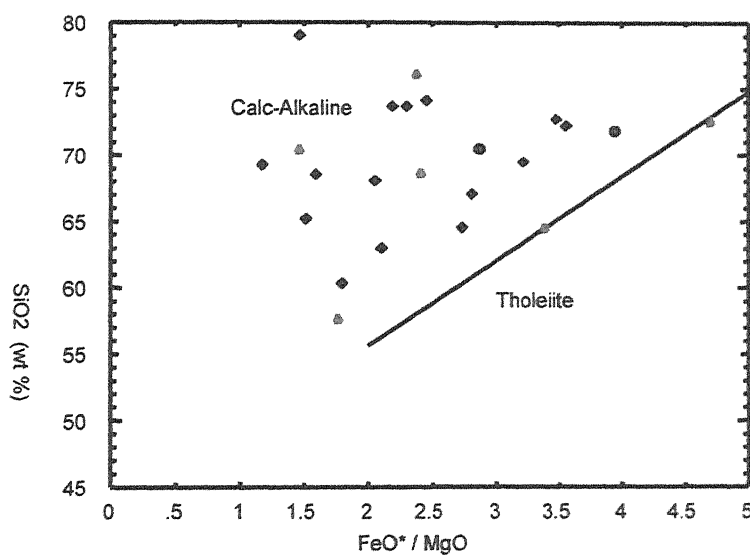
Fig: 5.8
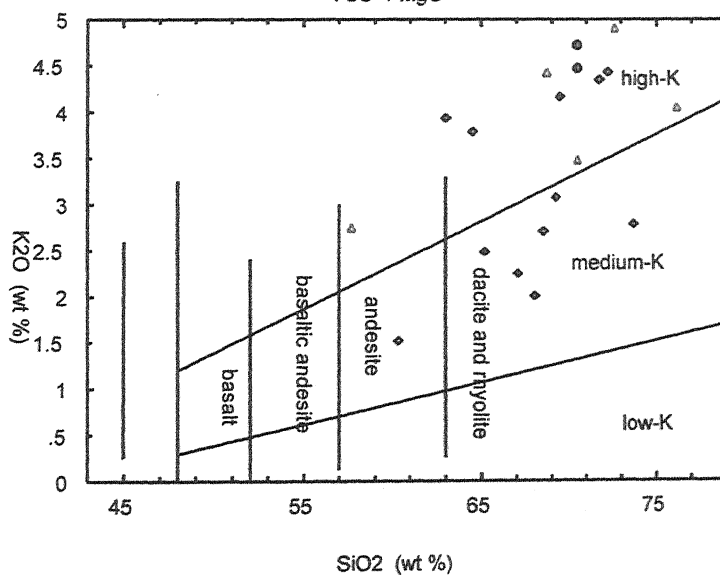
Fig: 5.9

Fig 5.7: P-Q diagram after Debon & Le fort 1983.
Fig 5.8: SiO2 vs FeO/MgO after Miyashiro 1974.
Fig 5.9: K2O vs SiO2.
Symbols: Circle: BG; Diamond: BnGC (Gneisses); Triangle: GG
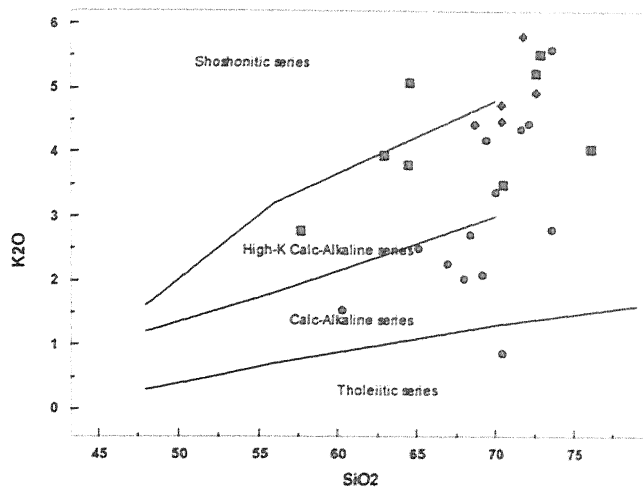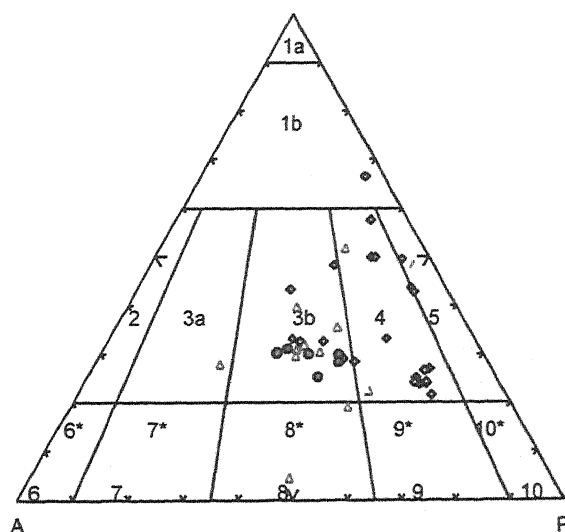
Fig: 5.10
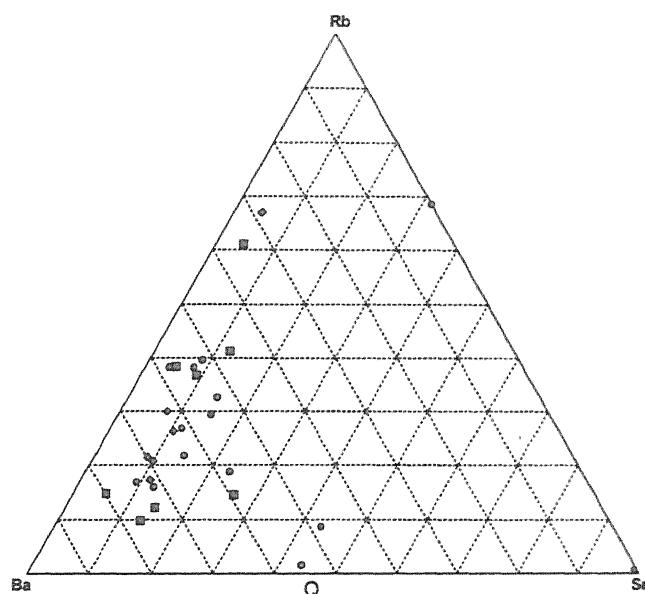
Fig: 5.11

Fig: 5.12

Fig 5.10: Classification of the granitoids of Mahoba area based on the SiO2 vs K2O; Sym.: Square: GG; Cricle: BnGC; Diamond: BG

Fig 5.11: Rb-Ba-Sr ternary diagram after El-Bouseilly and El-Sokkary(1975); Sym.: Square: GG; Cricle: BnGC; Diamond: BG

Fig 5.12: The normative Q-A-P variation diagram after LeMaitre(1989); Sym.: Circle: BG; Triangle: GG; Diamond: BnGC
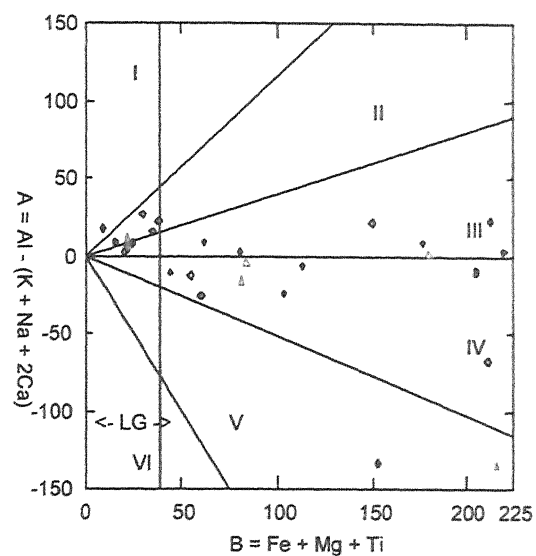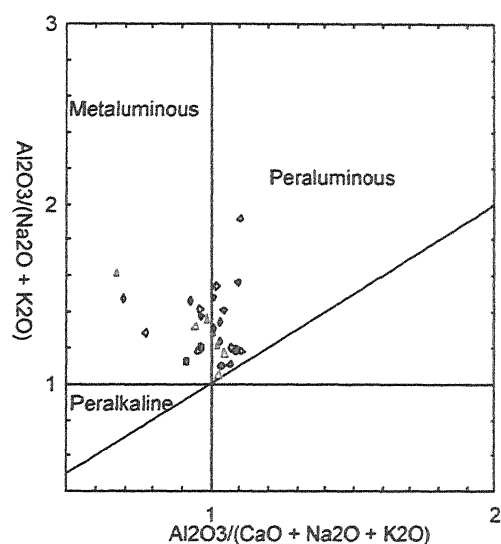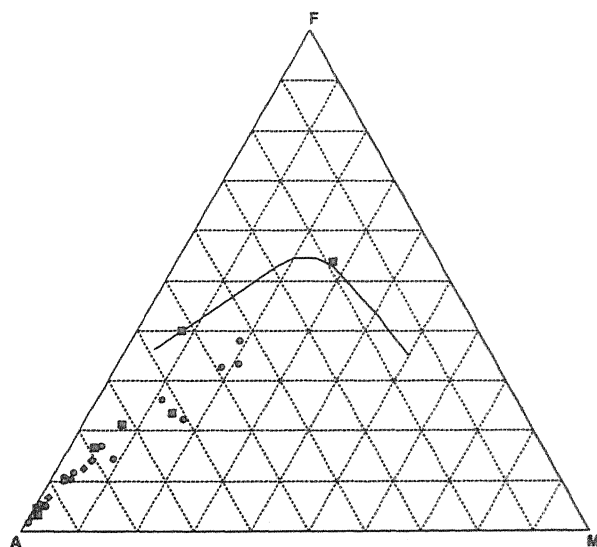
Fig: 5.13

Fig: 5.14

Fig: 5.15

Fig 5.13: A-B Diagrame for the Mahoba granotoids after Debon et. al. 1986; Sym.:
Circle: BG; Triangle: GG; Diamond: BnGC

Fig 5.14: Alumina Saturation index after Maniar and Piccoli 1989; Sym.: Circle: BG;
Triangle: GG; Diamond: BnGC

Fig 5.15 : AFM Diagram for the Mahoba granotoids (after Irvine & Banager, 1971);
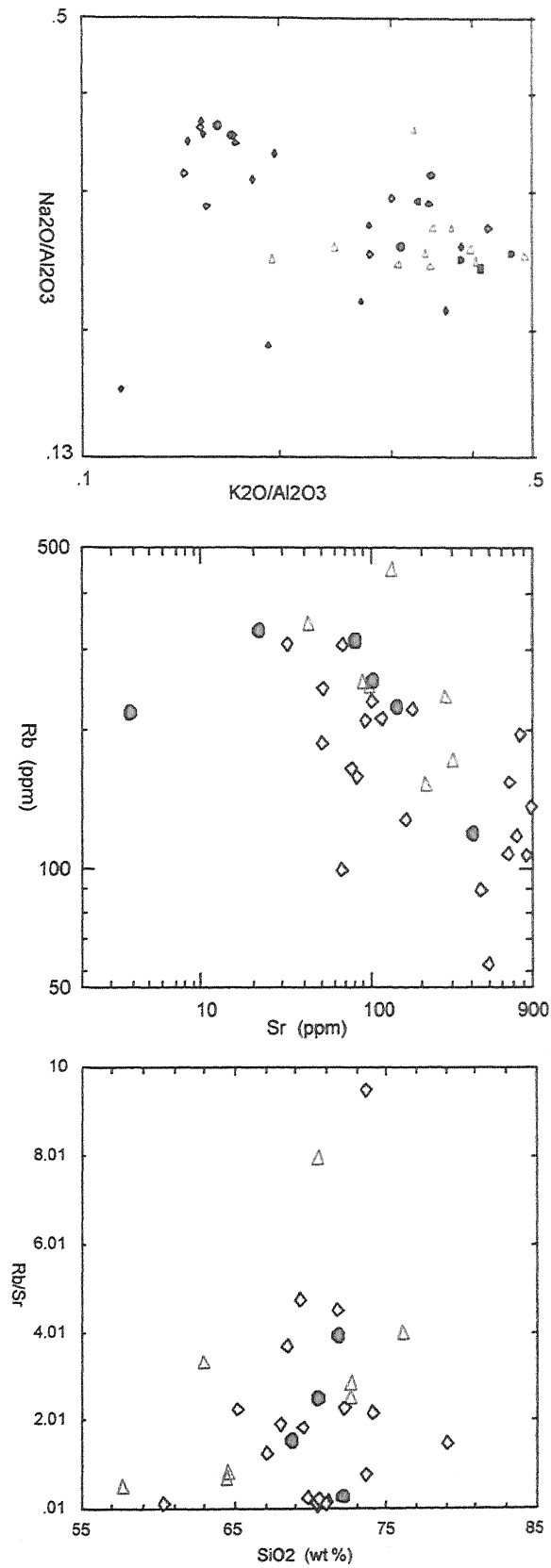Sym.: Square: GG; Cricle: BnGC; Diamond: BG

Fig: 5.16

Binary variation diagram of the Trace element for the Mahoba granotoids.

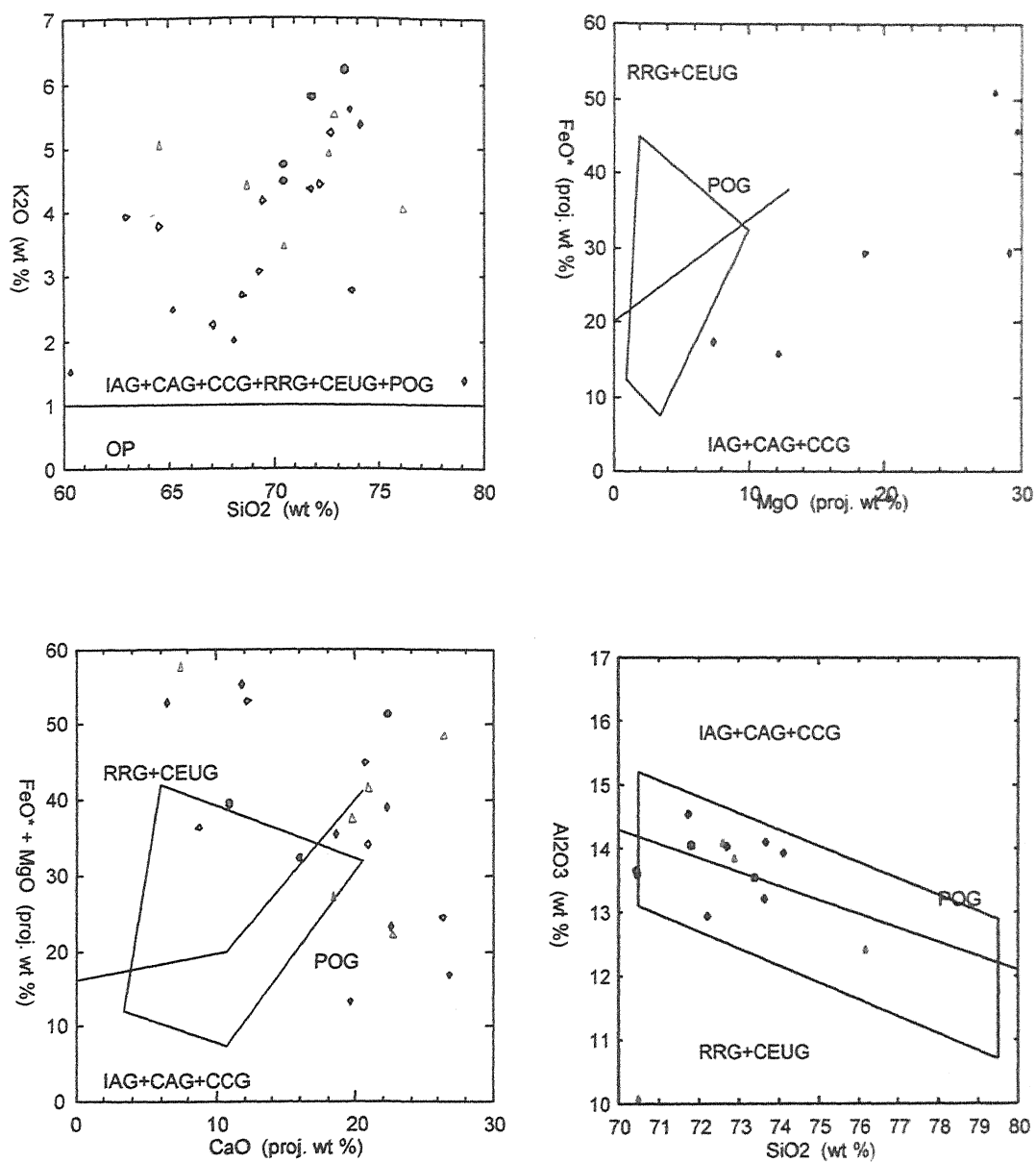Symbols: Circle: BG; Triangle: GG; Diamond: BnGC

Fig: 5.17

Fig 5.17: Discrimination Diagram for the Mahoba Granitoids (Field after Maniar and Piccoli, 1989)
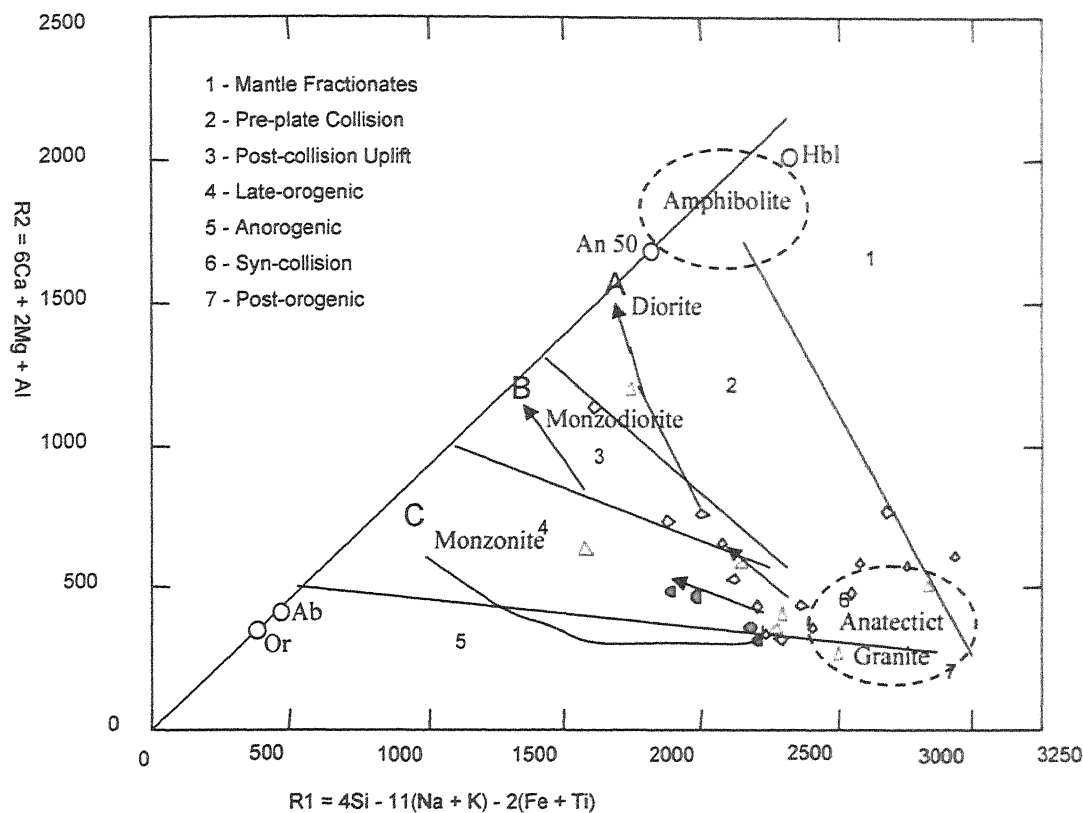
Symbols: Circle: BG; Triangle: GG; Diamond: BnGC

Fig: 5.18 a

Fig: 5.18 b

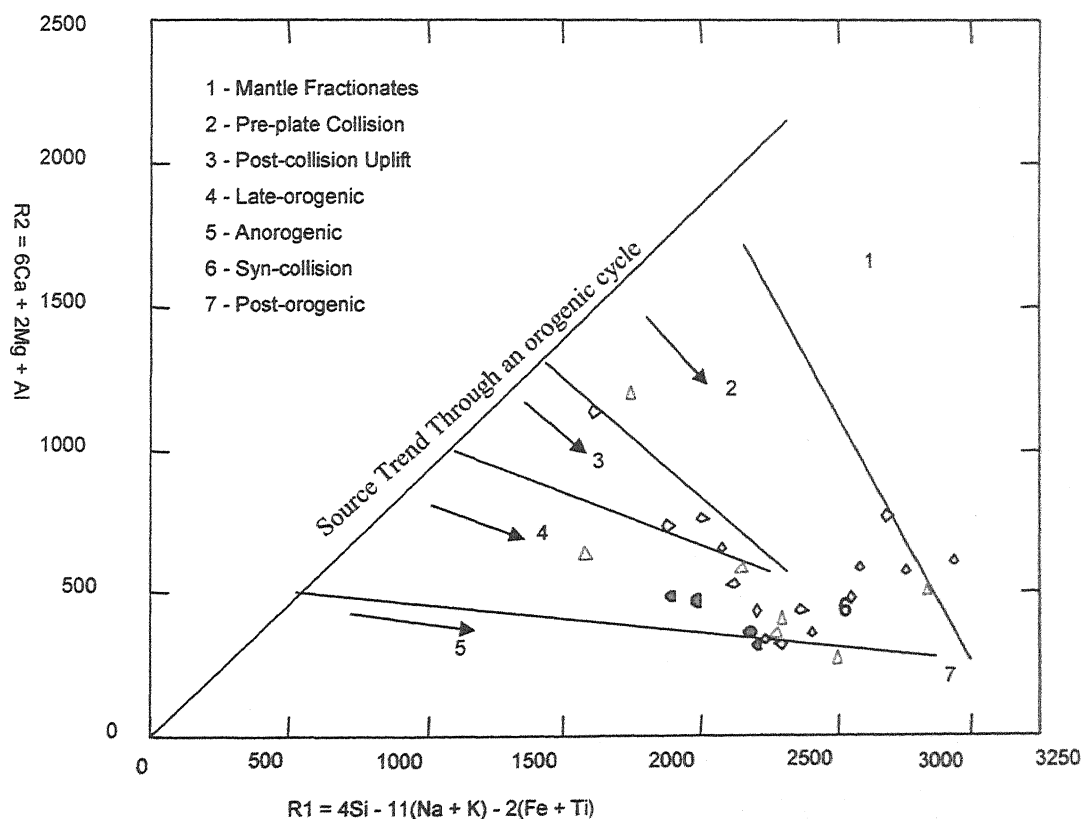Fig 5.18: R1 & R2 multicationic plots (a and b) of the mahoba granitodies (after De La Roche, 1964; Modified by Batchelor and Bowden, 1985)

Symbols: Circle: BG; Triangle: GG; Diamond: BnGC

Fig: 5.19a

Harkers variation diagram for the Mahoba granotiods.

Symbols: Square: GG; Cricle: BnGC; Diamond: BG

Fig: 5.19b

Harkers variation diagram for the Mahoba granotiods.

Symbols: Square: GG; Cricle: BnGC; Diamond: BG

Fig: 5.19c

Harkers variation diagram for the Mahoba granotiods.

Symbols: Square: GG; Cricle: BnGC; Diamond: BG
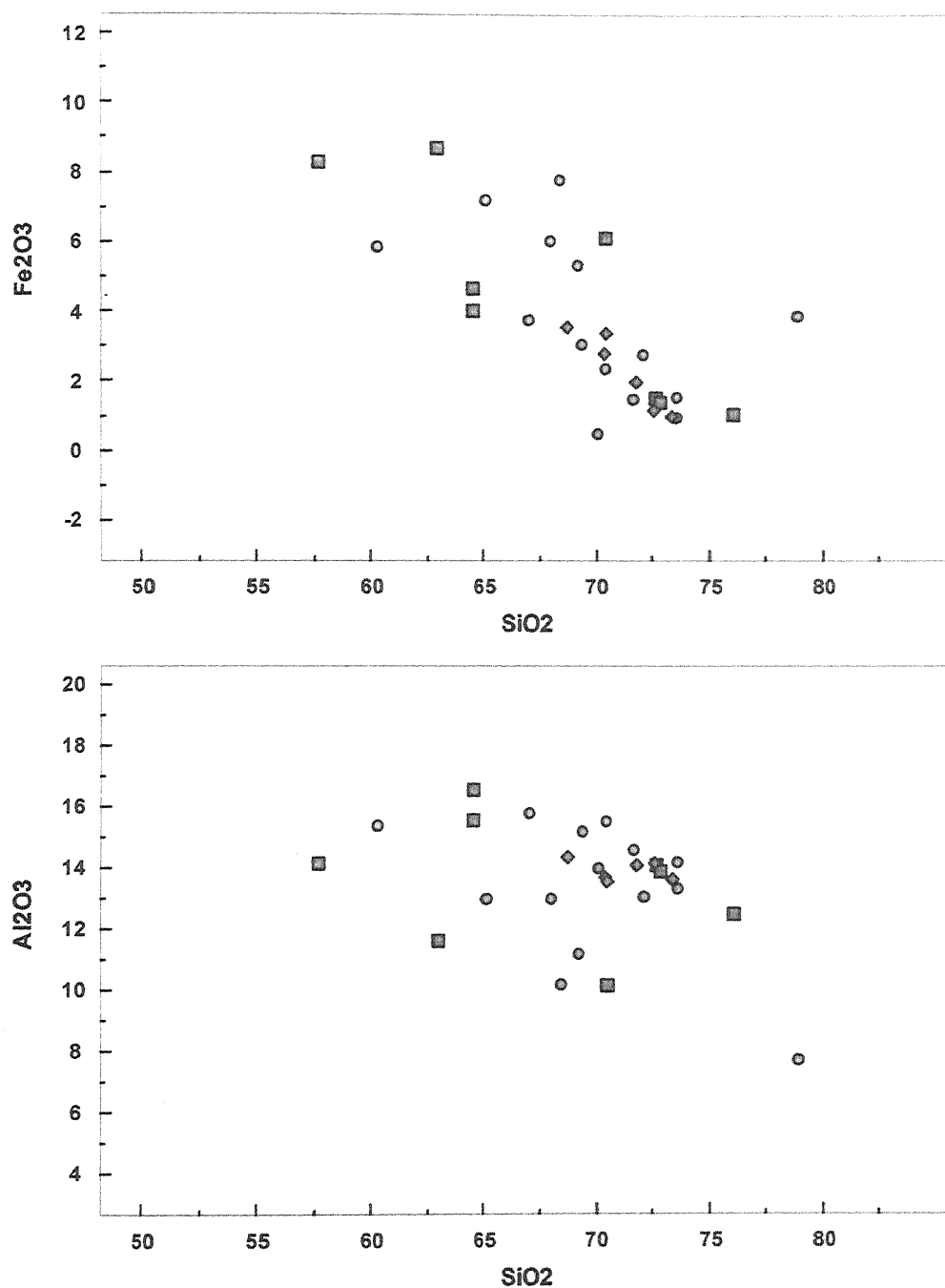
Fig: 5.19d

Harkers variation diagram for the Mahoba granotiods.

Symbols: Square: GG; Cricle: BnGC; Diamond: BG
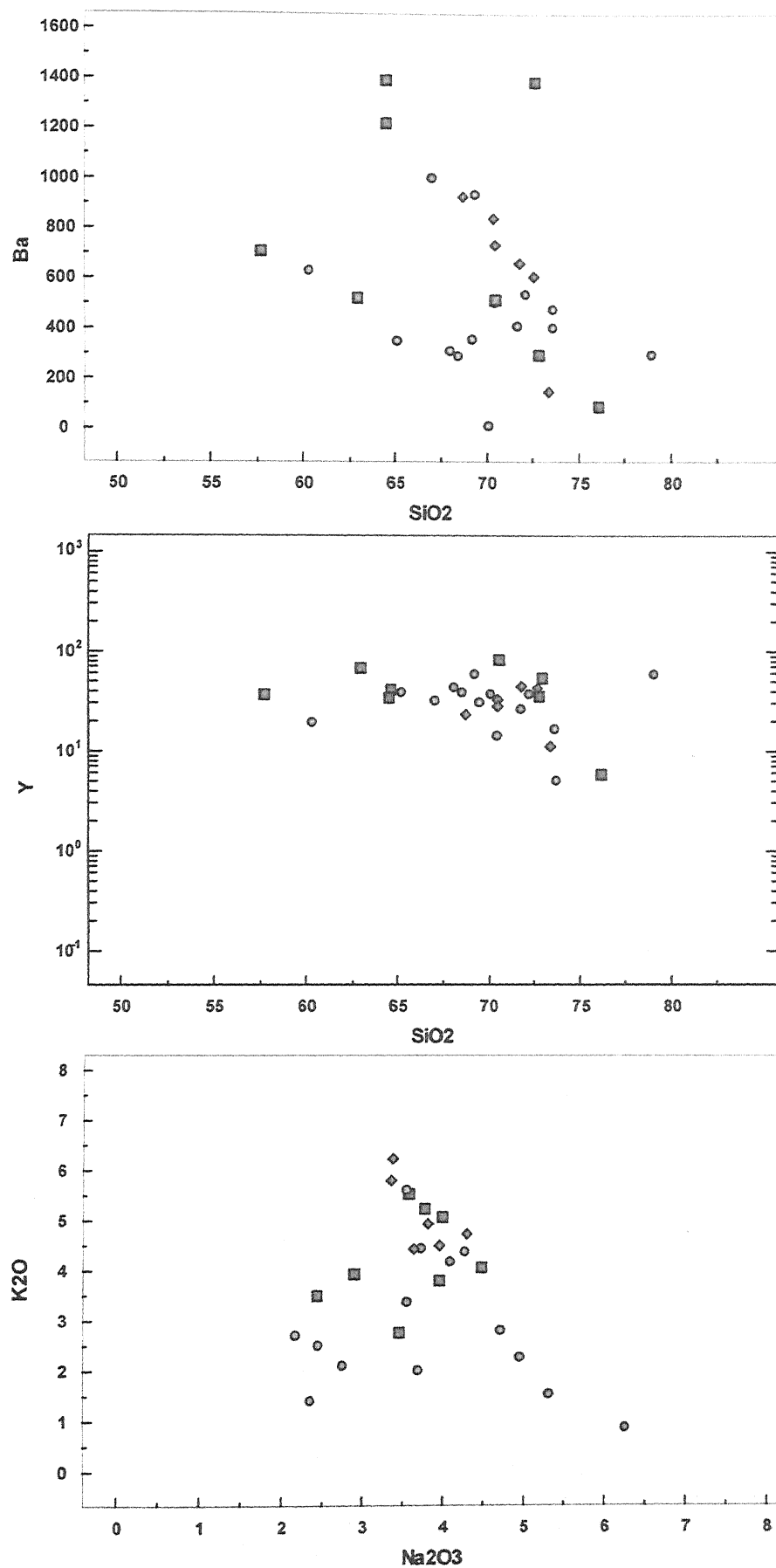
Fig: 5.19e

Harkers variation diagram for the Mahoba granotiods.

Symbols: Square: GG; Cricle: BnGC; Diamond: BG
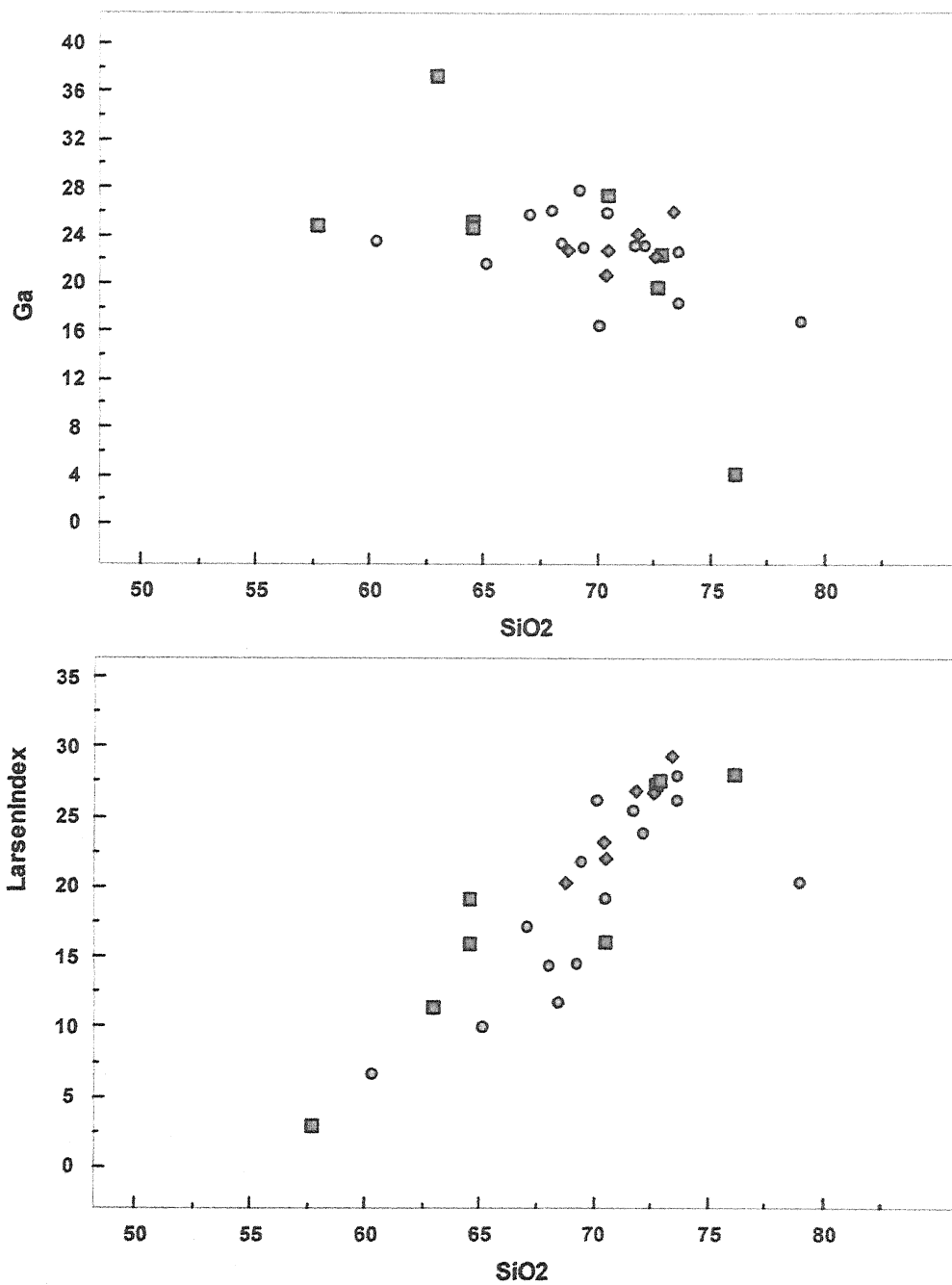
Fig: 5.19f

Harkers variation diagram for the Mahoba granotiods.
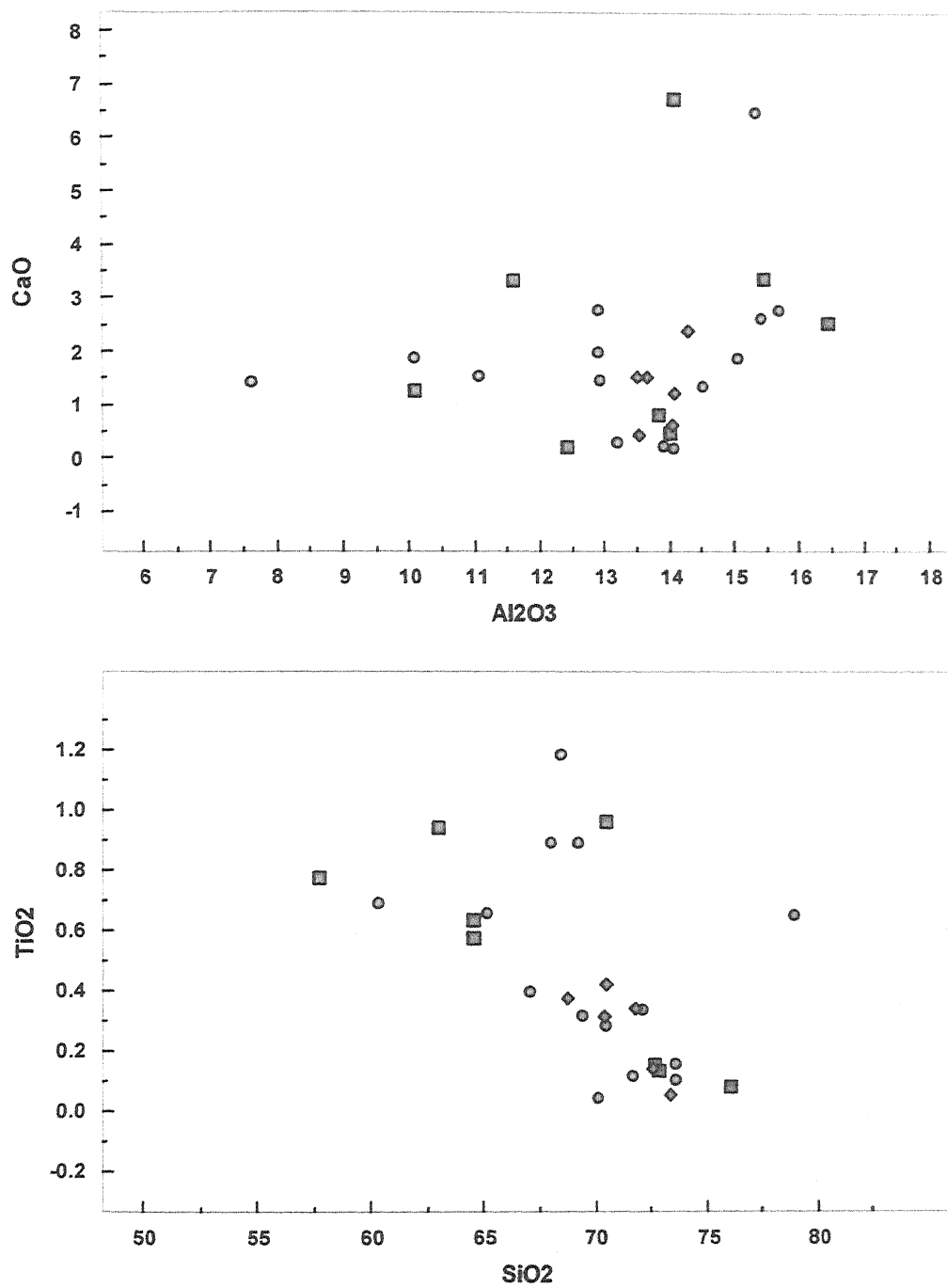
Symbols: Square: GG; Cricle: BnGC; Diamond: BG
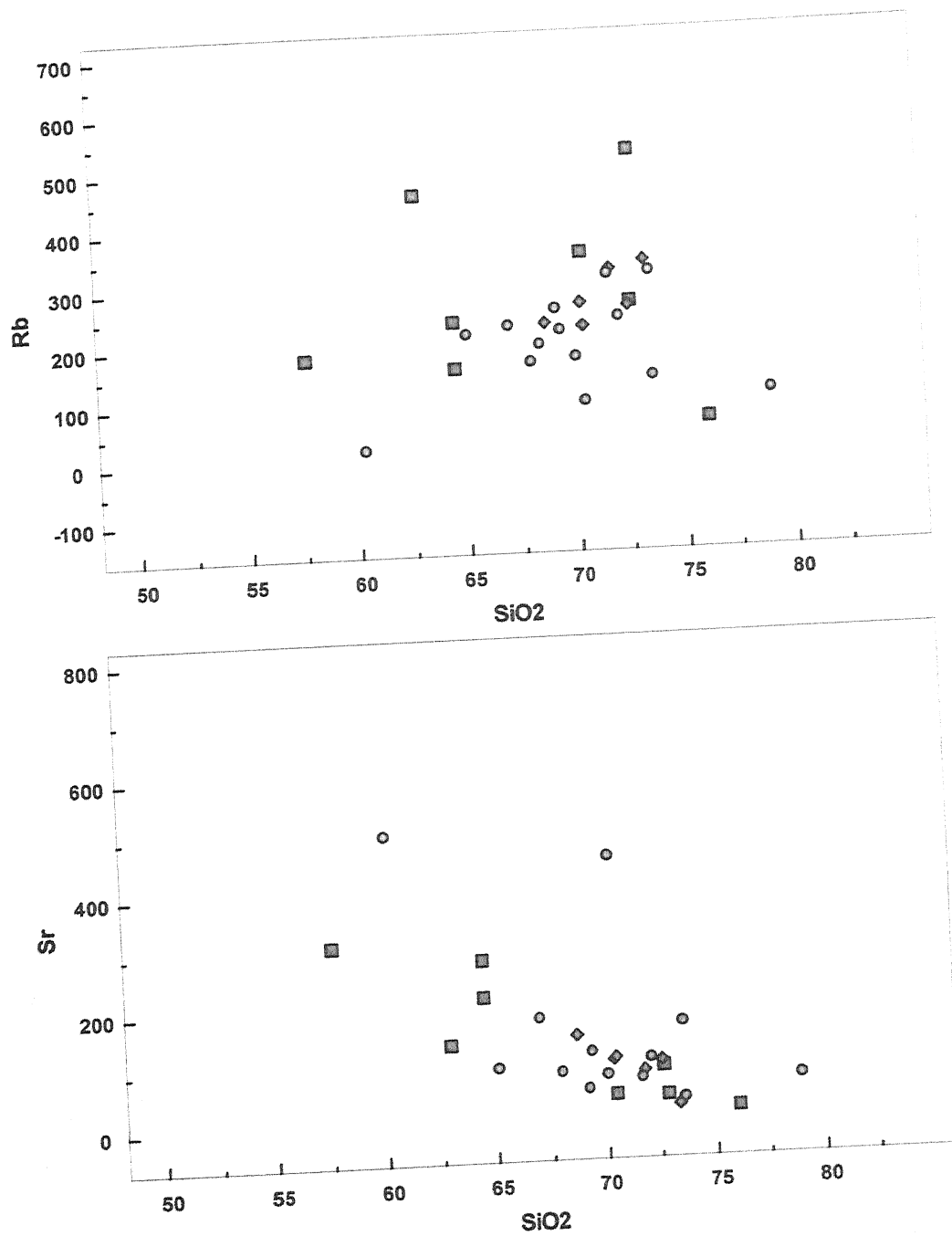
Fig: 5.19g

Harkers variation diagram for the Mahoba granotiods.

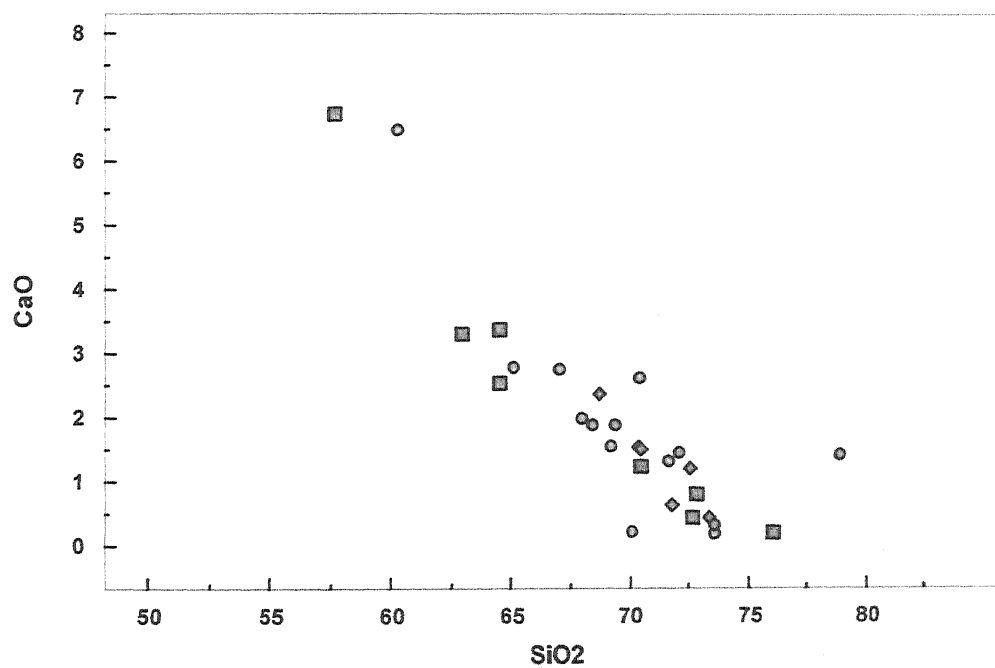Symbols: Square: GG; Cricle: BnGC; Diamond: BG

Fig: 5.19h

Harkers variation diagram for the Mahoba granotiods.

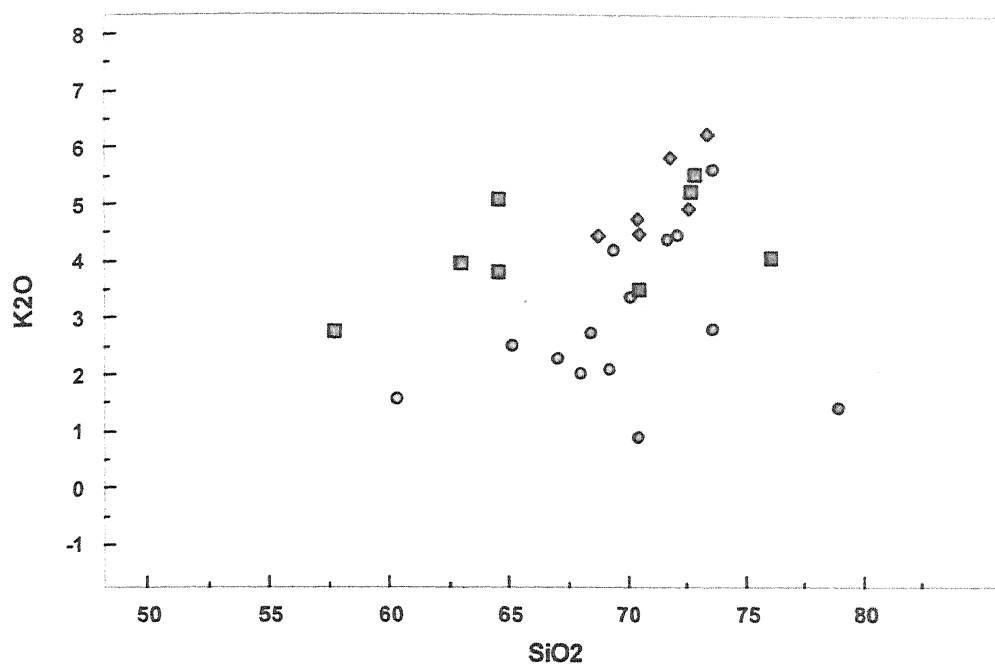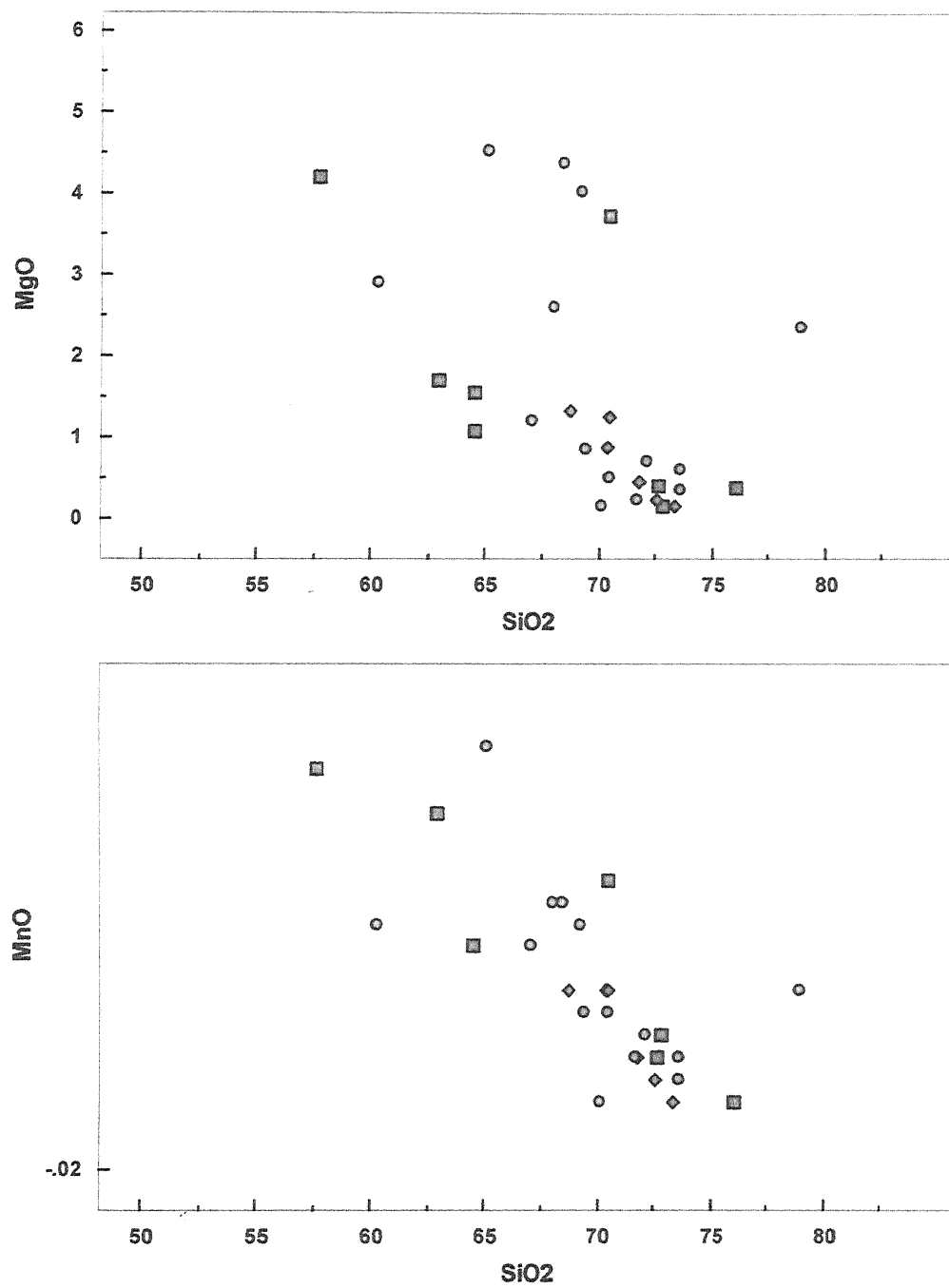Symbols: Square: GG; Cricle: BnGC; Diamond: BG
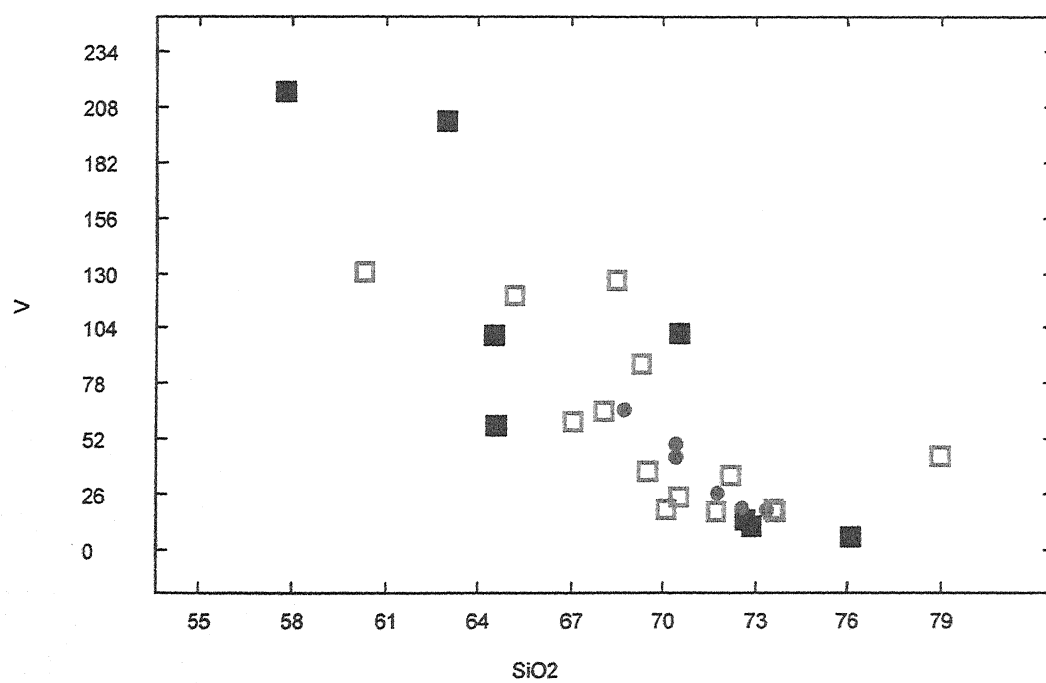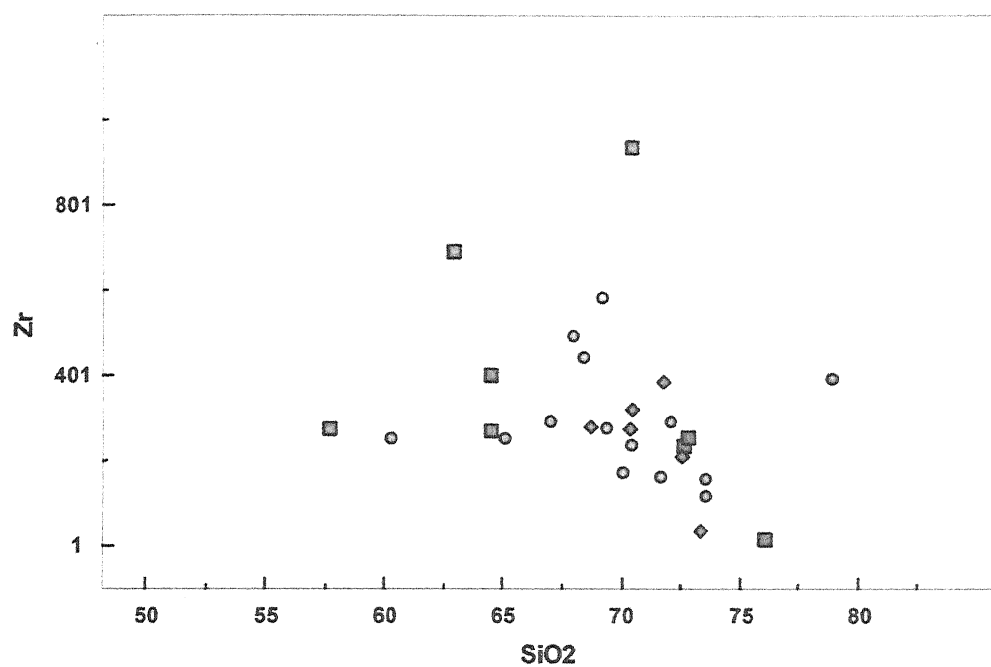
Fig: 5.19i

Harkers variation diagram for the Mahoba granotiods.

Symbols: Square: GG; Cricle: BnGC; Diamond: BG
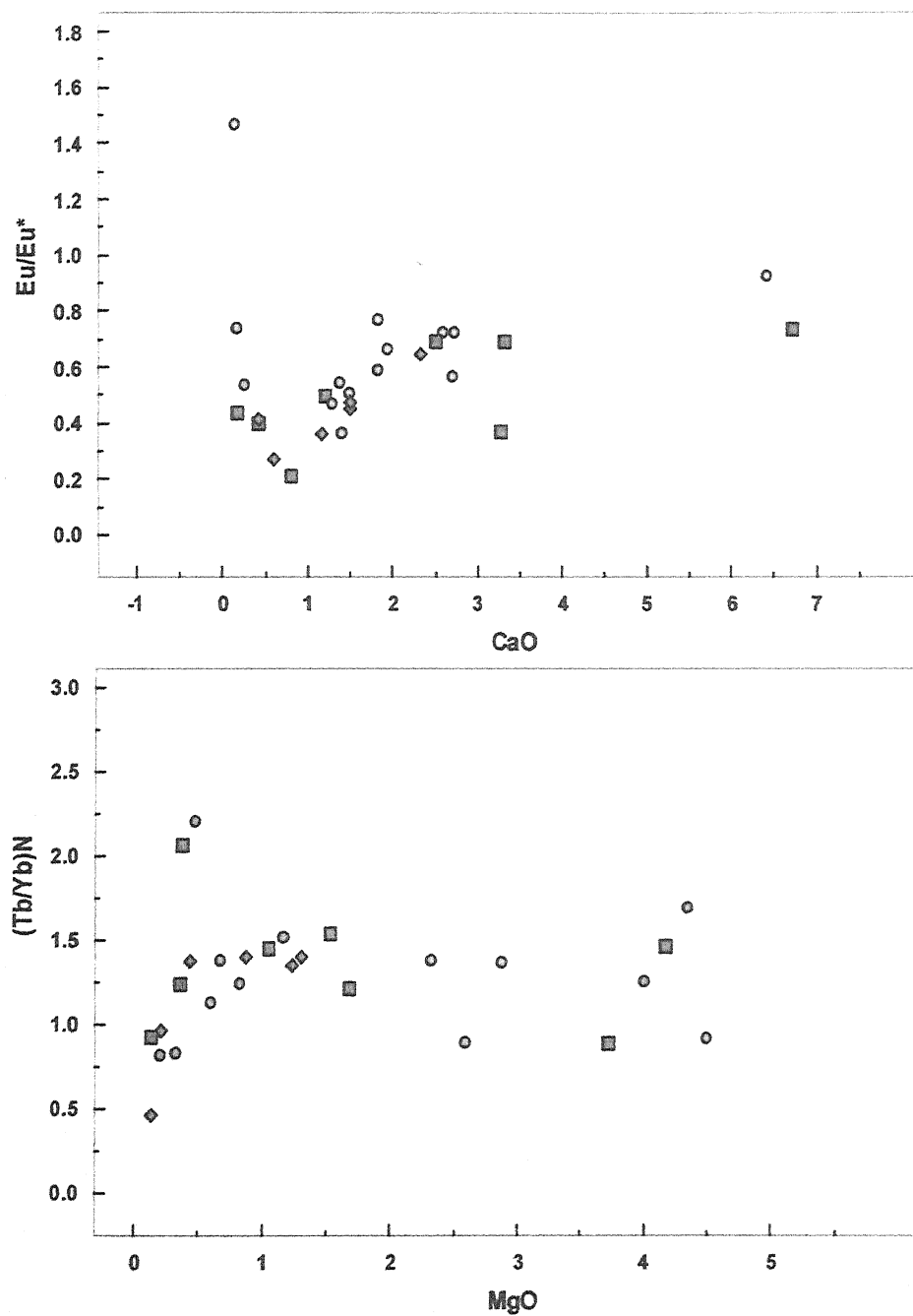
Fig: 5.19j

Harkers variation diagram for the Mahoba granotiods.

Symbols: Square: GG; Cricle: BnGC; Diamond: BG

Fig: 5.20

Binary variation diagram after whalen et. al. 1987

Symbols: Circle: BG; Triangle: GG; Diamond: BnGC
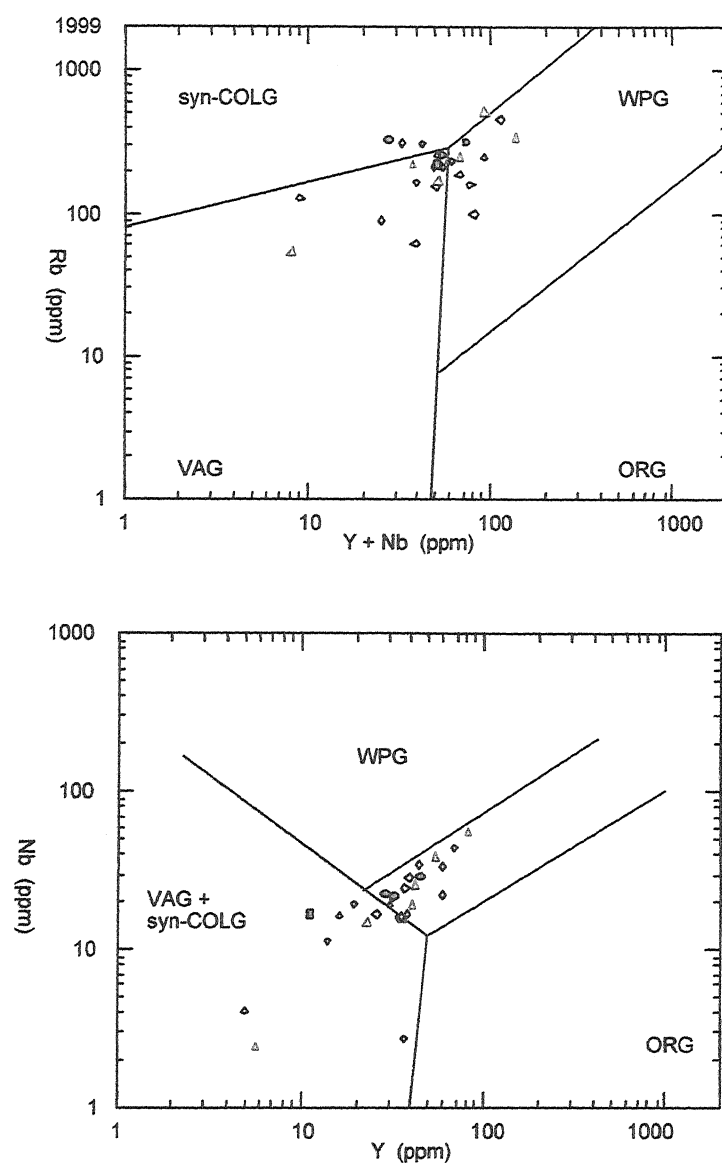
Fig: 5.21

Discrimination diagram for the Mahoba granotiods.

Symbols: Circle: BG; Triangle: GG; Diamond: BnGC
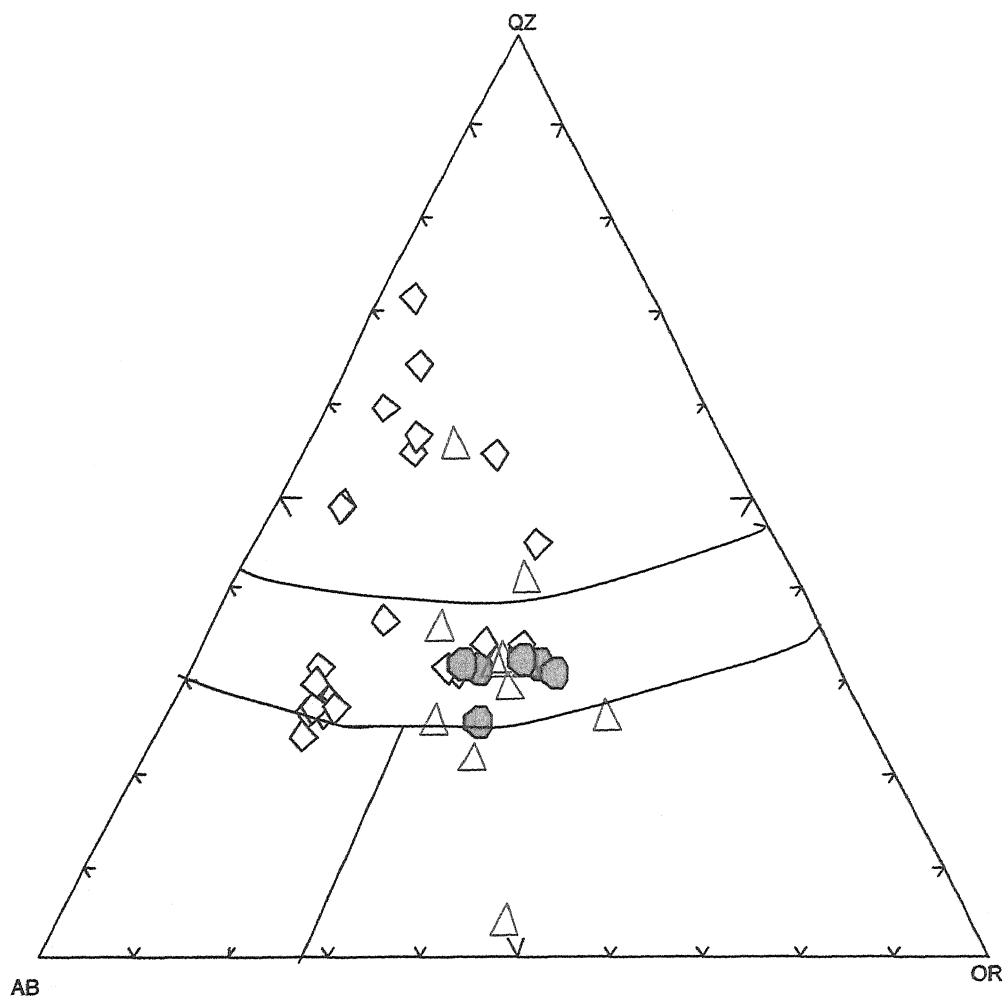
Fig: 5.22

Plots averages for Mahoba granitods in the Quartz-albite-orthoclase-H2O system
(Tuttle & Bowen, 1958; Manning et. al. 1980)

Symbols: Circle: BG; Triangle: GG; Diamond: BnGC
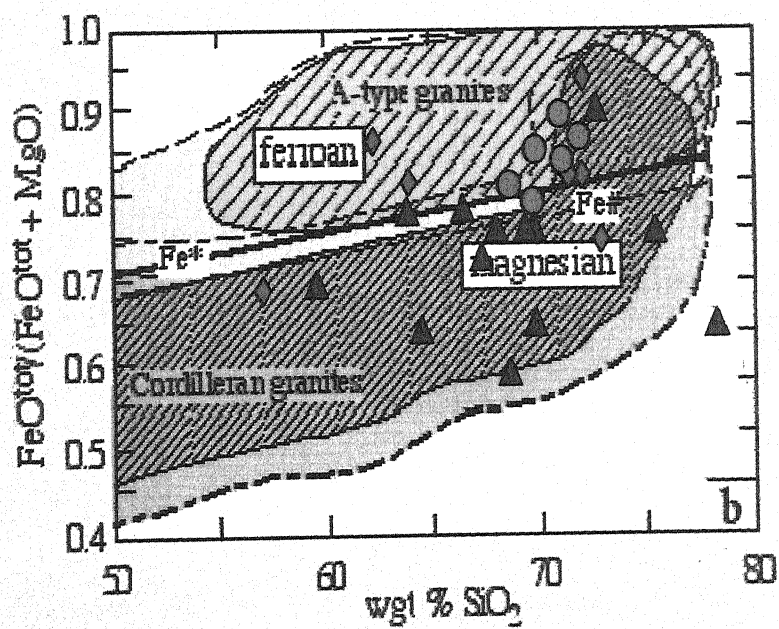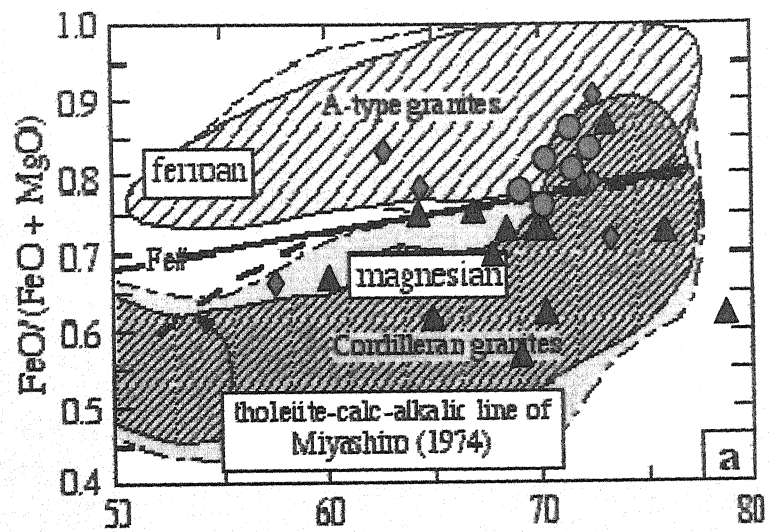
Fig: 5.23

Classification of granitoids of Mahoba based on the scheme proposed by
Frost et. al. 2001.

Symbols: Circle: BG; Diamond: GG; Triangle: Gneisses
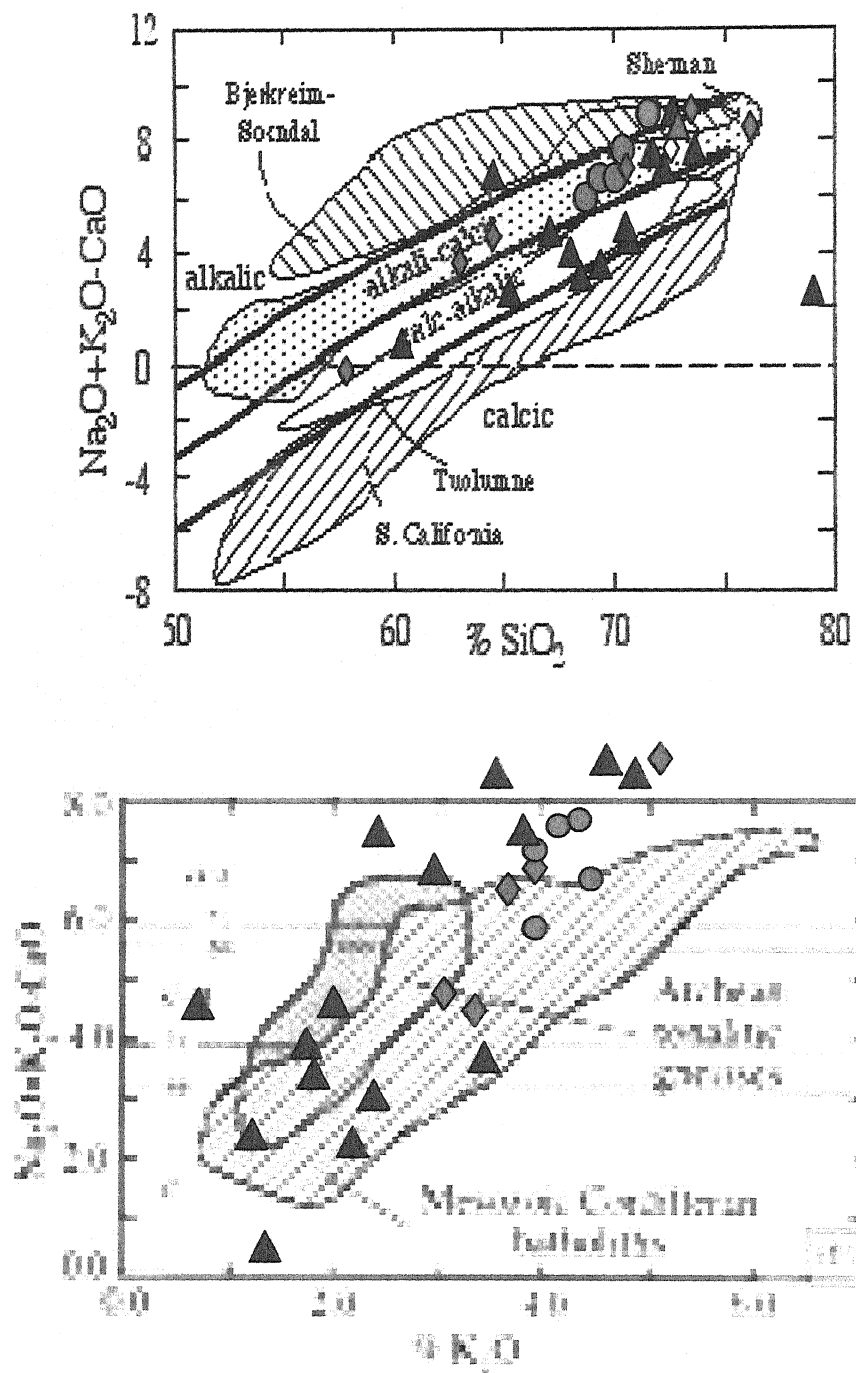
Fig: 5.24

Classification of granitoids of Mahoba based on the scheme proposed by Frost et. al. 2001.

Symbols: Circle: BG; Diamond: GG; Triangle: Gneisses
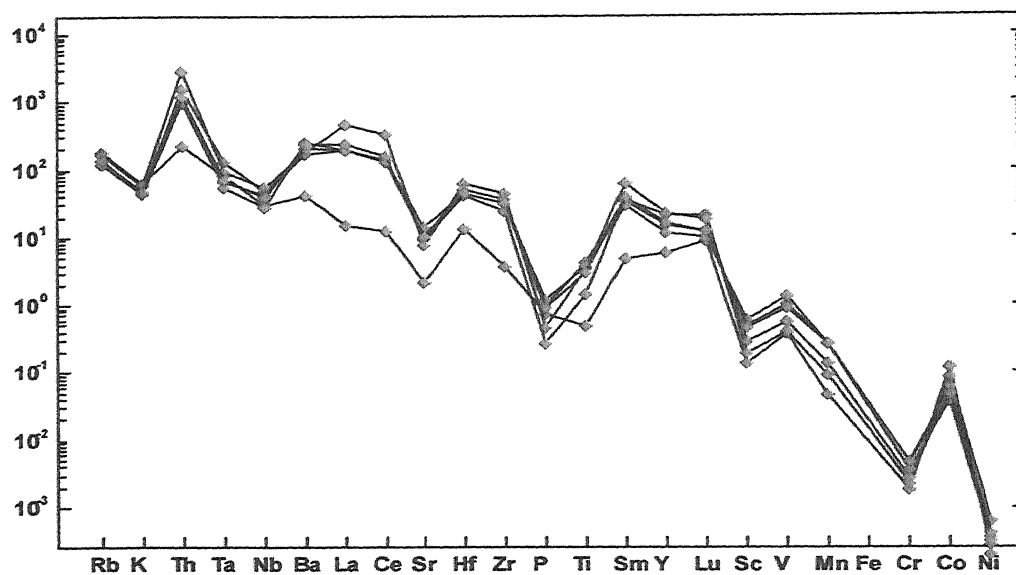
Fig.-25a : Spider diagram of Mahoba Granite (Pink Granite)
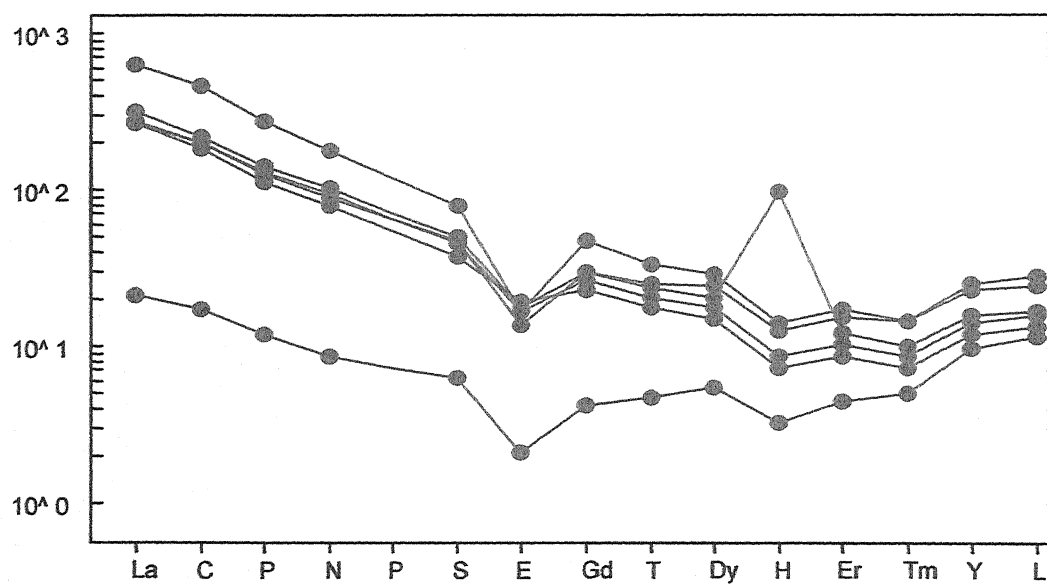
Fig.-25b : REE pattern of Mahoba Granite (Pink Granite) .
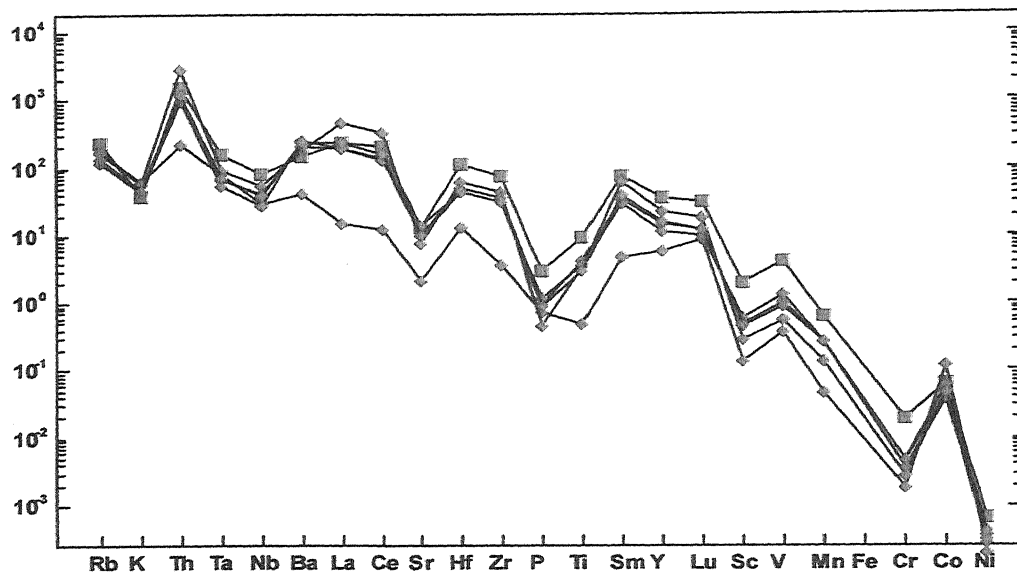
Fig.-26a : Spider diagram (Chondrite normalized) for Biotite Granite and Pink
Granite of Mahoba area.
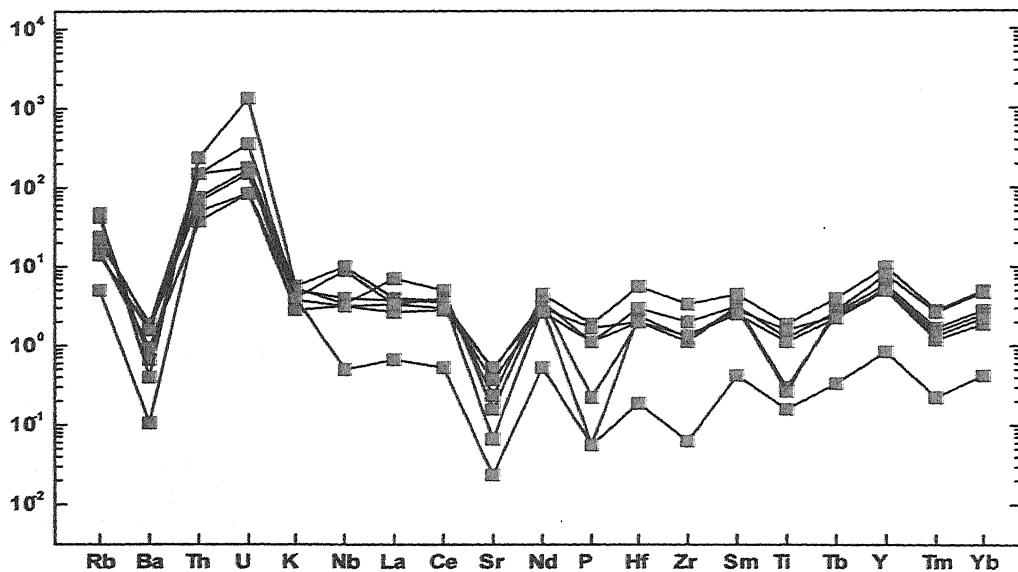
Fig.-26b : Lower continental crust normalized spider diagram for Grey granite
of Mahoba area
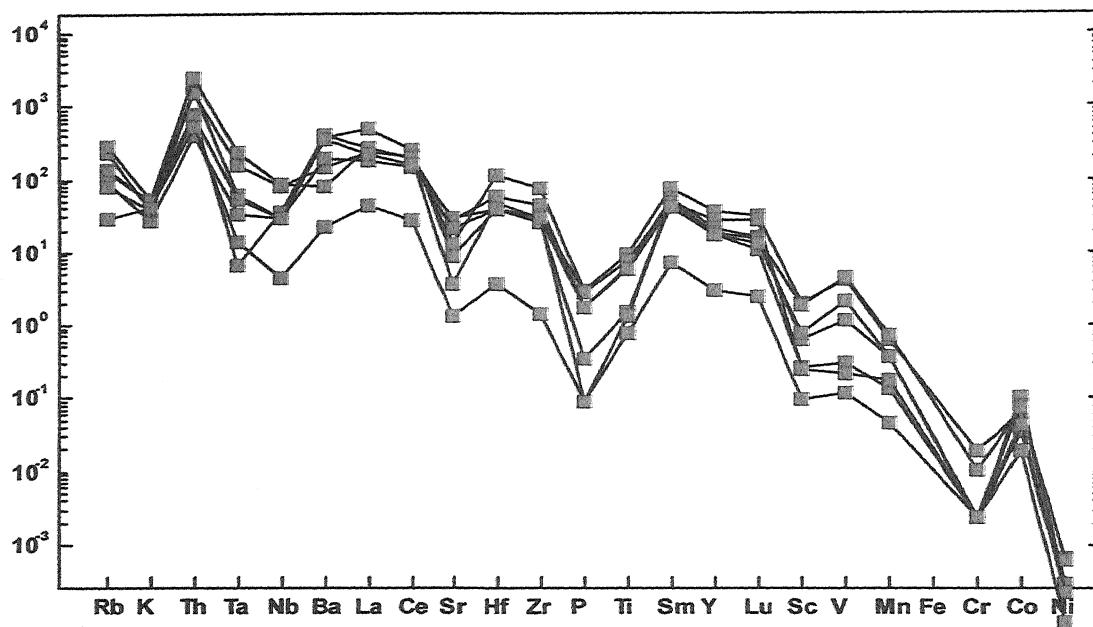
Fig.-27 : Chondrite normalized spider diagram for Grey Granite
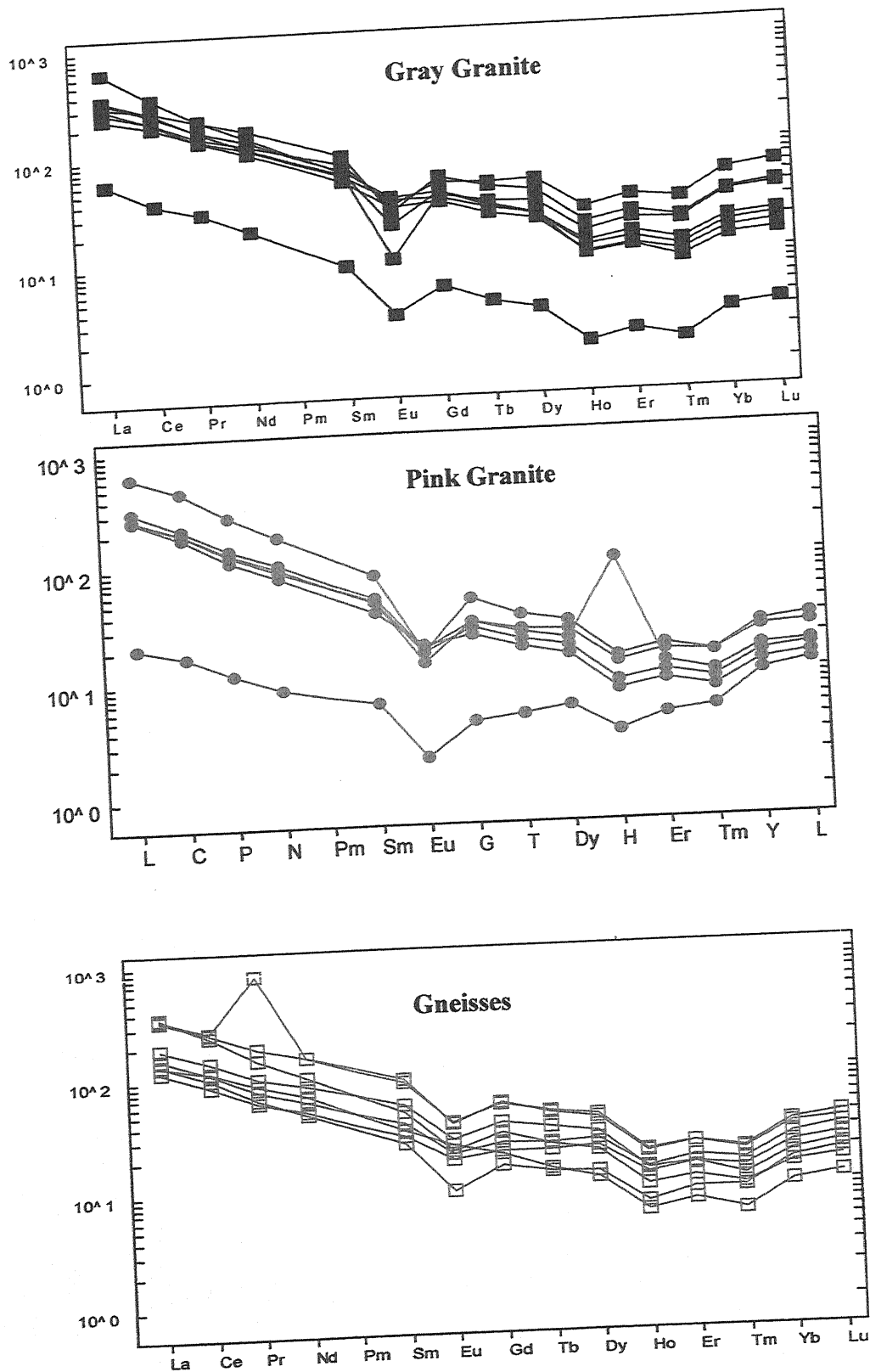
Fig.-28 :

Chapter-6

CONCLUSION

The recent geological studies (Mondal *et al.,* 2003, 2006) reveal that Bundelkhand massif is one of the oldest nuclei in the northern part of the Indian Peninsula. Like other cratons of Indian shield areas, the Bundelkhand massif also comprises extensive outcrops of granite- gneisses and granitoids in association with meta-sedimentaries and meta-volcanics of older supracrustal mass in the central part of craton (Singh *et al* 2007). The relationship of different episodes of metamorphite and granitoid events have been depicted on the basis of published geochronology data and evidences from field relationship,regional structures, petrological, geochemical and phase petrological studies of metamorphites of the Bundelkhand Massif.

The Bundelkhand craton is delineated from Aravalli-Rajasthan craton by Great Boundary Fault (GBF) in the west, from gangetic fore deep basin of Himalaya by Yamuna Fault in the north and is also delineated from Baster-Chhotanagpur craton by E-W trending Son Narmada Lineament (SNL) in the south and south east. The craton comprises rocks of Bundelkhand massif of Archean which is covered by Bijawar and Gwalior Groups and subsequently by Vidhyan Supergroup of Proterozoic and at the last by the Malwa Traps of Cretacious at several places. The Bundelkhand massif is exposed as semicircular out crop, which consists of mainly granitoids of different episodes, low to high-grade metamorphics of pelitic, calc silicates, mafic and ultramafic, BMQ and emplacement of dolerite and quartz reefs. The Central part of Bundelkhand massif has the signatures of greenstone belt that is represented by thick sequences of metavolcanics and ultramafics and volcano sedimentary rocks.

The Bundelkhand craon is known as the classical terrain for the early Proterozoic and Archean rocks (Basu 2007). It is true that most of the early to mid Archean geological records are diminished due to emplacement of Bundelkhand granitoids on the large scale. On the basis of presence relics of rocks within granitoids and followed by several geological activities subsequent to Bundelkhand granitoids the stratigraphy of Bundelkhand Craton has been classified as Pre Bundelkhand granitoids, Bundelkhand granitoids and post Bundelkhand granitoids.

The detailed regional studies of structures, rock types and their field relationship crystallines of pre Bundelkhand granitoids (BG) has been divided into two Groups viz. Bundelkhand Gneissic Complex (BnGC) and Bundelkhand metasedimentary and metavolcanics (BMM). The study area is the eastern part of Bundelkhand massif where BnGC rocks occur as small patches with in the Bundelkhand granitoids.

The BnGC rocks have been found as sporadic bodies in E-W linear trend in the central part. Besides this, it also encountered at lowland areas at several places. They comprise mainly TTG, biotite gneisses, migmatites, amphibolites etc. Similarly BMM rock also exposes in E-W trending small hillocks and comprises mafics and ultramafic, banded magnetite quartzite and meta-volcanics, where metamorphosed mafics and ultramafic unit represent actinolite-chlorite schist, hornblende-epidote-chlorite schist, talc-chlorite schist, garnet-chlorite-actinolite schist, tremolite-talc-actinolite schist. Banded iron formation comprises banded magnetite schist etc. and meta-volcanics comprises felsic and mafic volcanics. These rocks are mainly found in the western part of the study area, near the Mauranipur.

The structural studies of gneisses and migmatites point out that rocks of BnGC have experienced six phases of deformation (Singh *et al.,* 2007, Bhatt *et al* 2008) while the rocks of BMM have experienced the four phases of deformation (Prasad *et al* 2003). Tight to reclined F_2 folds of the gneisses are co-axial and co-planer with tight to isoclinal and reclined F_1 folds that were formed during the D1. Tight to open F_3 folds have NW-SE to NE-SW trending axial plane and plunging towards north and were formed during the D3 deformation (Sharma 1982).

On the other hand BMM Group of rocks received four phases of deformation (Singh 2005). Tight to open folds axial surface trend NW-SE to NE-SW, folds axes plunging towards north, are recorded in banded iron formation (BIF). Folds of BIF are trending ENE-WSW direction and steeply dip towards north. In meta-sedimentaries and meta-volcanics the sinistral shearing is at encountered several places.

The granitic batholith of Bundelkhand Granitoids (BG) has been found as intrusive in these metamorphites into different stages. Hornblende granite is

considered as the earliest phase of magmatism and is followed by biotite granite. The leucogranite is the last phase of granitoids in the massif. Coarse grain prophyritic granite is intrusive into foliated biotite granite. Coarse grained leucogranite is intruded into coarse grain porphyritic granite (Singh 2005). The fine-grained leucogranite is the youngest in massif and thus is intrusive into all the older granites. Bundelkhand granitoids are look like massive but three phases of deformations have been countered at many places. The E-W trending dextral and sinistral shear zones and S-C fabrics are observed in granitoid at several places. The presence of shear indicators viz. rotation of porphyroblats, S-C fabrics, sheath folds from gneisses and migmatites infrafolial folds and "S" type folds of BMQ, S-C fabrics in the granites from E-W trending mylonites and ultra mylonites indeed indicates that a N-S compression was prevailed after the granitic emplacement (Singh *et al* 2007). The recrytallised mylonites/ phyllonites were developed due to emplacement of porphyritic granitoids into the E-W trending mylonites zones which point out that vertical shears were dominating component at that time.

The NE-SW quartz reef is found to emplace in all earlier rocks of the massif. Quartz reefs displaced the older rock unit sinisterly and at several places the granitoids were also mylonitised and deformed. At many places earlier structure were displace of quartz reefs along NW-SE is several Kms and is related to D5 deformation. Dolerite dykes in the form of swarms emplaced along NW-SE direction and displaced the NE-SW quartz reef, granitoids, and BMM rocks and is related to D6 phase of deformation.

The present study area covers about 600 sq. km. of the central part of the eastern block. The coarse to medium grained biotite- gneisses (BnGC) of high-grade metamorphics are mainly exposed at the Nathupura. Quartz reefs are found usually to high above the granitoids which are characterized by dirty white coloured rocks but at places grey, milky white, pinkish white colour varieties are also found in the investigated area. The great dolerite dyke of Mahoba is observed as dark green or melanocratic in colour, medium grained, hard and compact and passes to Mahoba town. Grannular black prismatic crystals of pyroxenes are identified in hand specimen, at places white patches of feldspar are observed. Pyroxenes, plagioclase,

magnetite, hornblende, epidote, biotite, epidote, quartz and chlorite minerals are identified from this rock. The S-C fabrics were found to the southern part of Mahoba dyke.

The tectonothermal stratigraphy of Mahoba area has been also proposed on the basis of regional field relationship, structural data, chronological information's, metamorphism (BnGC), and igneous activities. The BMM component of Pre Bundelkhand was not found any where in the study area. It is concluded that the high-grade metamorphics viz. TTG, gneisses and amphibolites etc. were formed at first episode of metamorphism and can be assigned as part of Bundelkhand Gneissic Complex (3500-3200 Ma). These metamorphics are intruded by the granites of different episodes i.e. Bundelkhand granitoids (2500-2300). The quartz reef (2300 Ma) and mafic dykes (1800 Ma) were the last thermal events in the study area.

The rocks of older metamorphic group (BnGC) are divided into (i) gneisses, TTG, migmatites, granite-gneisses, and (ii) amphibolites and hornblende-biotite gneisses. Biotite –gneisses, TTG, migmatite, and granite-gneisses observed in the investigated area are medium to coarse grained, gray to tight gray in colour and show gneissose structures. Based on minerals constituents the following minerals assemblages have been obtained:

The TTG, which includes both tonalite and Trondhjhemite-rocks, content significant amount of K-feldspar, antiperthite, plagioclase, perthite, biotite, and quartz with minor amount of ilmanite, apatite, zircon, sphene, spinel etc minerals. The muscovite and orthopyroxene are completely absent in TTG .The hornblende has been noticed in minor amount in most of the TTG rocks along with biotite mineral.

The biotite-gneisses consists mainly biotite, quartz, plagioclase and K-feldspars. The zircon and apatite are present in the significant amount in all the rock samples. The perthite and antiperthite texture are also present in the gneisses. The garnet and sillimanite reported by earlier workers from the Kabrai area (Saxena 1961) could not be obtained in the present investigated area. The absence of the garnet and sillimanite may be possibly due to composition variation. It is very significant that muscovite as prograde or retrograde phase is completely absent from the gneisses.

In the BnGC rocks the first phase of metamorphism possibly initiated at deformation D1 and culminated in the advanced stage of partial melting and granulite formation. The following assemblages have been obtained in the KFMASH system.

(i)   Biotite–K-feldspar-perthite-quartz.

(ii)   Biotite-plagioclase-K-feldspar-antiperthite quartz.

(iii)   Garnet-biotite-K-feldspar-quartz.

(iv)   Biotite-plagioclase-K-feldspar-antiperthite-sillimanite- quartz.

Assemblages in amphibiotites and hornblende biotite gneisses:

(i)   Hornblende - clinopyroxene - biotite - plagioclase - K-feldspar - quartz.

(ii)   Hornblende – biotite – K – feldspar – plagioclase - quartz.

(iii)   Hornblende – clinopyroxene – plagioclase - quartz.

(iv)   Hornblende - plagioclase - K - feldspar - quartz.

(v)   Hornblende – garnet – plagioclase – K – feldspar - quartz.

The AKF diagram shows three phases fields of garnet – biotite and K – feldspar. The K- feldspar – biotite tie line defines the two-phase field for non-garnetiferrous gneisses. The mineral assemblages of tonalite and trondhjhemite gneisses may be treated in K_2O, FeO, MgO, $SiO2$, CaO, Al_2O_3 and H_2O (NKCF MASH) system and portrayed in the AFM diagram (Reinhardt Projection) with FeO and MgO as separate component and as plagioclase projection. The advantages of A'FM projection is that the tie lines connecting hornblende, clinopyroxene and biotite composition of the three coexisting phases form triangle, enclosing the field of composition of three mineral associations. The common presence of hornblende-clinopyroxene-biotite phase may be due to large field with variation in the bulk composition of rock. The minerals in these three co-existing phases may be considered as continuous reaction in the KCFMASH system between hornblende and biotite at variable pressure and temperature and composition. The presence of corroded biotite in the hornblende and clinopyroxene, and similarly presence of corroded hornblende in the biotite and clinopyroxene from the hornblende-biotite gneisses may be attributed to the break down of the biotite and hornblende by the following continuous reaction in CFMASH system.

Biotite$_1$ + Hornblende$_2$ = Biotite$_2$ + Hornblende$_1$
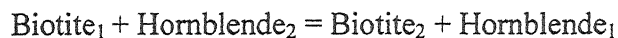
The composition of the hornblende lies between the biotite - clinopyroxene lines. Therefore, the appearance of hornblende in biotite and vice versa may be due to the following reaction in the CFMASH system.

Clinopyroxene + biotite + plagioclase = hornblende + K- feldspar + V
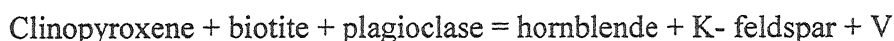
The composition of the orthopyroxene lies on the tie line of the biotite – clinopyroxene in the A'-F-M projection in the system KCFMASH (Reinhardt 1967). The absence of this mineral from all the hornblende-biotite gneisses and biotite-gneisses may be due to either quartz deficient composition or due to strong retrograde metamorphism of gneisses or inadequate CO_2 fluid activity. The absence of garnet from most of gneisses may be considered due to the non-availability of appropriate bulk composition and high K_2O and Al_2O_3.

The enclaves of amphibolites are very common in the gneisses. Sometimes they are co folded with biotite gneisses. The petrographic studies reveal that phlogopite, epidote, tremolite, chlorite, actinolite, etc. are completely absent while diopside, calcite, plagioclase, hornblende are present as medium to coarse grained texture. The absent of garnet from the basic gneisses may be due high MgO, K_2O and low Al_2O_3. The common presence of plagioclase, hornblende and diopside assemblages can be explained in three-phase field of ACF diagram in CFMASH system.   The other compatible assemblages hornblende-plagioclase- magnetite $\pm$ quartz and diopside – hornblende – magnetite $\pm$ quartz have been explained in ACF diagram in six component system of CFMASH system. The metamorphic - conditions based on experimental determined curves and geothermobaromatric result of the surrounding area yield 720^{0}C temperature and 4-5 Kbar pressure. A clockwise P-T path has been suggested (Singh and Dewdi).

Twenty- nine representative rock samples of gneisses and granites and granites of petrological interest from investigated area were chosen for analysis. The major oxide and REE including trace element were carried out at NGRI Hyderabad.

Based on Na_2O vs K_2O diagram, ternary (An-Ab-Or) diagram, Q-A-P triangular diagram, P-Q diagram, the plots of gneisses show tonalite, trendhjemite

affinity while gray granites show granite, granodiorite and adamellite affinity. These diagrams also suggest that gneisses and granitites exhibit sub alkaline nature.

Alumina content of gneisses (14.25 wt%) and granites (12.95 wt%) are greater than the total alkalies ($K_2O + N_2O$) of average value 6.84 wt% and 8.26 wt% in gneisses and granites respectively.

The tectonic environment of the granite of the study area is classified according to different discrimination parameters proposed by Maniar and Piccoli (1989) and is has been noted that the chemical signatures of granites of the study area do not follow a single and firm tectonic environmental but are related to the orogen granites of late stage. Shand's alumina saturation index diagram points that majority of the granites are related to metaluminous characters which suggest that granites of the study area were resulted from magmatic origin of CAG to POG. The BG magma was formed due to paertial melting of TGG and gneisses in the volcanic Arc granite system. Discrimination diagram of Pearce *et. al.* (1984) suggests that granites of the study area are related to syn collision type emplaced in volcanic arc granite tectonic.

The milti-cationic parameters proposed by De La Roche's suggest that granites of the study area should be related with syn to late continental collision tectonic. Majority of the granites of study area were formed due to remobilization and partial melting of these gneisses of BnGC as evidence by triangular $Al_2O_3 -$ ($Na_2O + K_2O + CaO$) – ($FeO + MgO + MnO$) diagram. The Rb Vs Sr (log-log) diagram suggested that granite melt might have been generated at depth around 23 to 35km and temperature of about 750^0C.

Trace element analyzed by El Bouseily and El Sokkaray (1975) in Rb-Ba-Sr turnary diagram reveals that granites of the study area is magmatic source and have been emplaced and crystallized at different depth with varying physiochemical conditions. Ba/Rb ratio characterizes the change from normal granite to strongly differentiated type for the GG while normal granite field for BG.

The high value of Rb (209ppm) suggests that these granites were subjected late stage differentiation. The high Rb/Sr ratio of the gneisses may be due to chemical variation during metasomatism of feldspar minerals that appears to be the dominant

controlling factor for the abundance for Sr. It is evident from the positive correlation shown by gneisses of the study area when plotted against normative plagioclase. The granite of the study area has also positive correlation. The positive correlation shown by Pb with normative orthoclase in gneisses suggests that the elements preferentially occupy in the lattice of K-feldspar in the rock.

The Bundelkhand granitoids have been chemically classified on the basis of different oxide, norm and cationic parameters. On these parameters, majority of the samples plot in the fields of granite, adamellite and granodiorite.

The chemical-mineralogical typology based on multicationic parameters delineated by Debon and Le-Fort (1982) defined the peraluminous and metaluminous characters depending on its positive and negative values respectively, reflect the nature and proportions of their characteristics minerals other than quartz and feldspars. The A[Al-(Na +K +2Ca)] - B(Fe +Mg +Ti) diagram shows clearly that Bundelkhand granitoids (BG and GG) occupy the delineated III and IV fields of the metaluminous domains which indicate that they belong to the association of Biotite>hornblende and presence of Cpx and magnetite and may be related to hybrid calc – alkaline (HCA) proposed by Barbarin (1990). The low molar A/CNK i.e., $Al_2O_3/(CaO +Na_2O + K_2O)$ ratio against SiO_2 indicate metaluminous compositional field. The molar A/CNK ratio less than 1.1 suggests that the granitoids is mainly igneous origin with least mixing of crustal components (Chappel and White, 1974). Presence of normative corundum and low molar concentration of A/CNK (<1.1) is also suggestive of I-type nature of Bundelkhand granites.

The other characteristic features, viz. low ferric/ferrous ratios and appearance of ilmenite mostly in place of magnetite and deep brown titanium-rich biotite in place of green biotite, indicate that the magmas was evolved in the conditions of relatively low oxygen fugacity. The alkalinity (Na_2O+K_2O) not more than 10% exceed, which is evident from the TAS (Na_2O+K_2O Vs SiO_2 wt%) diagram (Middlemost 1985). Most of the granitoids (BG and GG) are hypoalkalic but few of them as silicic nature. This indicates that the possibility of local metasomatism may be possible in the present area. The AFM ($Na_2O+K_2O-FeO_T-MgO$) diagram (Irvine and Baragar, 1971)

indicates that most of the BG and GG granitoids represent the calc-alkaline differentiation trend, which were evolved towards alkalies corner. The mineralogical composition and geochemical trend suggest hybrid type continental to transitional type magmatism (Barbarin 1990).

The SiO_2 versus $Na_2O + K_2O$ variation diagram for the Mahoba granite (BG) and granite gneiss (GG) and compared with granite compositional variations of Tischendorf (1985) suggest that GG is much more evolved in their silica and alkali contents.

In order to compare the characteristics of the inferred tectonic environment for the Mahoba granitoids (BG and GG), the classification scheme proposed by Maniar and Piccoli (1979) have been followed. The granitoids fall in the field of orogenic granites distinctly away from the field of the view of anorogenic granites in the discrimination diagram due to the presence of K_2O content of BG (av. 5.08 wt%) and GG (av. 3.94 wt%) being greater than one does not support anorogenic oceanic plagiogranite (OP). It concludes that the Mahoba granitoids represent continental collision and metaluminous in nature.

Considering the geochemical pattern, based on selective trace elements (Y, Nb and Rb) criteria most of the Bundelkhand granitoids can not be assigned collectively of any one tectonic regime but cluster near the triple junction demarcating lines of VAG, syn-COLG and WPG fields, when plotted on Y + Nb vs Rb log-log (ppm) and Y vs Nb log-log (ppm) based on Pearce *et al* (1984). Nevertheless, syn-COLG appears an appropriate tectonic environment due to the presence of highly content of Rb and Ta during the genesis of syn-COLG for the Bundelkhand granitoids. It is apparent that Rb enrichment is a likely consequence of K-silicate and sericitic alteration due to the growth of secondary biotite and muscovite respectively. Discriminated tectonic environment for the granitoids of the study area based on R_1 [4Si- 11(Na+K) –2(Fe +Ti)] and R_2 [6Ca +2Mg +Al] is the supporting evidence for the syn to late -COLG (Pitcher, 1982 and Harries *et al,* 1986).

Most of the granitoids (BG and GG) occupied the anatectic granite field which indicates the first liquids to get separated from the fusion of felsic crustal source

(gneiss and metapelite) would have compositions equivalent to alkali feldspar and quartz $\pm$ sodic plagioclase. This felsic melt was completely mobilized in the crust and was emplaced at a higher level and its composition will be equivalent to a syenogranite or monzogranite.

Based on Zr+Nb+Ce+Y(ppm) vs FeO*/MgO (wt%) and Zr+Nb+Ce+Y (ppm) Vs K_2O+Na_2O/CaO (wt%) diagrams of Whalen et al;(1987). The Mahoba granitoids represent the fractionated felsic granite (FG) of the biotite granite (BG) whereas granite gneiss (GG) as unfractionated orogenic granite type (OGT) in nature. Besides these, author has attempted to find out the BG and GG as the igneous protolith based on K_2O/Al_2O_3 vs Na_2O/Al_2O_3 (wt%) diagram (Garrels and Mackenzie, 1979). The Rb-Sr log-log variation diagram (Condie, 1973), the granitoid samples were found to cluster between the lines defined by Rb/Sr = 1, which is equivalent to the depth relevant to 20-30 Kms. But few samples are emplaced at depth greater than 30 Kms. Rb-Ba-Sr ternary diagrams, (El Bouseilly and El Sokkary 1973), the BG and granite gneiss (GG) fall in the fields of granodiorite and normal granite respectively. But the biotite granite (BG) falls in the normal granite field chiefly due to its relatively lower Rb levels as compared to that of the anomalous granites. Thus studies of these individual granitoids (BG, and GG) represent their own characteristics. The changes in major and trace element chemistry towards more felsic granitoids indicate fractional crystallization processes. The variation between felsic ($SiO_2+Al_2O_3$ $+Na_2O+K_2O$ wt %) and mafic ($FeO_t+CaO+MgO+MnO$ wt %) constituents, it appears to marked inverse relation in the Mahoba granitoids (BG and GG).Based on Tultle and Bowen's (1958) ternary system of normative quartz, albite and orthoclase, most of the Mahoba granitoids fall within true granitic field.

The calculated normative quartz, albite and orthoclase value of Mahoba granitoid are plotted in the Qz-Ab-Or system (Manning et al, 1980) and it is observed that the plotted points fall in a restricted and evolved compositional field approaching the thermal granitic minima but slightly deviated towards quartz-orthoclase joint. The pressure of crystallising fluid observed from this diagram can be constrained more or less 2 kb and the final temperature of crystallization about 650 ^{0}C. This depict about the occurrence of shallow level of pluton emplacement.

Rare earth elements (REEs) of the Bundelkhand granitoid (BG, and GG) are analyzed and it chondrite normalized patterns by Taylor and McLennan, 1985 (Petrograph Software used). All the granitoids have enriched LREE pattern relative to HREE along with variable negative Eu anomalies. The variation in LREE/HREE ratio can be interpreted by the presence or absence of accessory phases like monazite and zircon. The Mahoba granitoids contain variable amounts of apatite, zircon and monazite as accessory minerals. Most of the LREE are controlled by monazite (Mittle fehldt and Miller, 1983). Hanson (1978) suggested that middle rare earth element (MREE) is controlled by apatite while zircon controls the HREE (Chary, 1986). These minerals are soluble in a peraluminous melt, and they are mostly inherited from the original source rocks and included in early-formed minerals like hornblende/biotite.

For the identification of the nature of the genetic relationship of the Mahoba granitoid (BG, and GG), LREE (La+Ce+Nd) reflecting monazite control are plotted against B parameter (B=Fe+Mg+Ti) corresponding to the amount of biotite (B) values are calculated after Debon and LeFort, 1983 and Debon et al, 1986). There is some significant variations among these granitoids, because of the scattered distribution of GG rocks probably implies that the initial amount of LREE was different from granite gneisses (GG) to BG granites, perhaps represent the different segments source of the same crustal materials.

The Σ REE of BG ranges from 245 to 578 ppm (av. 302 ppm) and GG range 280 to 501ppm (av. 340.83 ppm) are significantly different but continuous to decrease from GG to BG. The striking chondrite normalized REE pattern of BG and GG are similar where REE patterns are inclined composed to the relatively flatter HREE patterns with same degree of negative Eu anomalies. This feature strongly suggests that BG granitic melt could be derived by partial melting of protolith of BnGC and GG (having feldspar-depleted signature in the source). The overall REE feature of BG and GG has close resemblance with that of Mahoba granitoids reported elsewhere.

The REE patterns of the granitoid rocks to show steeper pattern and highly fractionated. It is enriched in LREE and depleted in HREE and show moderate and large anomalies. The flat pattern of HREE in the GG might have resulted due to the

presence of ample apatite that are entrapped within large feldspar grains. The increase of size of negative Eu anomalies indicates the rock is highly evolved during differentiation processes. The observed similarities in REE pattern among all the granitoids of the Mahoba area.

From the above discussion the Mahoba granitoid (BG, and GG) represent the product of meta-aluminous melt generated by the partial melting of somewhat heterogeneous older crustal rocks perhaps the quartz- feldspathic psammatic to pelitic composition or gneiss with the saturation of Al_2O_3 as indicated by low normative corundum value, being well comparable with those for I-type granitoid (White and Chappel, 1988). The significant changes in measure in trace element towards more leucocratic granitoids with inverse relationship between felsic and mafic constituents and also evident by the relative enhancement in SiO_2, K_2O and Rb as well as Rb/Sr ratio and decrease in FeO*, MgO, CaO, TiO_2, Sr and Zr from granite gneisses (BG) to granite (GG) indicate the fractional crystallization processes with the initial crystallization of biotite and plagioclase followed by hornblende to biotite, quartz and K-feldspar. From the geochemical data, it shows very clearly that the decrease in REE content with enhanced SiO2, moderate $\Sigma LREE/\Sigma HREE$ ratio (av. 27.45) and more pronounced negative Eu anomalies (av. 0.85) are also support the fractional crystallization processes.

The granite (BG) and granite gneiss (GG) have been plotted in $FeO^{tot}/FeO^{tot}+MgO$ vs SiO_2 diagram proposed by Frost et al. 2001, which suggest that the BG is typically magnesian except a few one whereas GG has affinity with ferroan type. The magnesian and ferroan-differentiated series of granitoids are indeed equivalent to tholeiitic and calc-alkalic magma types respectively as originally discriminated by Miyashiro (1974). However, a little overlapping in the fields of magnesian and ferroan have been noted towards high silica content of rocks which is more likely related to the late stage compositional evolution of granitoids during their differentiation. Whatsoever the reason may be but BG is apparently distinct from GG and both have experienced different degree of chemical differentiation in different episodes.

Several lines of field petrographic and bulk geochemistry of BG, GG reveal with origin from crustal anatexis i.e. partial melting of crustal source generating the meta aluminous BG and GG melts. The partial melting model shows that the variation of GG as well as GG can be explained by varying degree of partial melting (5 to 50%) of bulk continental crust but bulk distribution coefficient for Sr (D_{Sr}) must be low i.e. <<10. The anorthite content of plagioclase feldspar is very sensitive to determine the distribution coefficient of Sr, therefore, a small changing D_{Sr} will shift the vertical trend of partial melting of source towards higher and lower sides of Sr content. The result of partial melting modeling at least suggests that the differentiation of BG and GG melt is more governed by partial melting of bulk crust rather than fractional crystallization.

The gneisses of the study area contain significant amount of K-feldspar, plagioclase, biotite, quartz and minor amount of ilmanite, apatite, zircon and sphene. The petrological phase relation points that mineral assemblages in gneisses are biotite - K-feldspar – antiperthite - quartz, biotite – plagiclase – K-feldspar – quartz and in amphibolite, hornblende gneisses are hornblende-clinopyroxene-biotite-K-feldspar-plagioclase-quartz and hornblende-clinopyroxene-biotite-K-feldspar-quartz reveal that the above mineral assemblages were formed above 710^{0} C in upper amphibolite to lower amphibolite conditions and 5-6 Kbar pressure. The observed mineral assemblages, petrochemistry, field relationship and P-T condition point that the high grade gneisses and granulite comprises the metasedimennts and mafic to ultramafic rock rocks along with tonalitic gneisses were recrystallised around 3200Ma. It is also inferred that crystallized minerals of BnGC were aligned in S1 and S2 plane in the gneisses and mesoscopic structure viz. F1 and F2 folds were formed during the D1 is pretectonic to M1 episode of metamorphism while the F3 folds were developed during the D1 deformation and are postdate the M1 episode of metamorphism. A disconcordent relationship between the BnGC and gray granite have been marked on the basis of change in the structural trend, grade of metamorphism, mineral chemistry, mineral assemblages. The presence of the relicts of E-W trending linear pattern in the rocks of gray granite within the BnGC represents a large scale folding and their emplacement. The presence of E-W trending mylonites structures formed by vertical

and their offset relations and the sinistral displacement with the NE-SW trending quartz reef. Another structure of mylonites and ultramylonites rocks suggest that atleast two phases of the shearing have been taken place after the crystallization of the gtranitic batholith. It is indeed worth to describe that mylonites trending in the E-W direction comparatively thicker and prominent in the investigated area indicate that they were subjected to further recrystallization possibly during the late phase of the granite emplacement along the shear zones. However NE-SW trending shear zones along quartz reefs and pegmatites were found to emplaced and sinistrally rotated as evidence by the sigmoidal structures obtained in the core part of the quartz reefs.

Thus on the basis of field relationship, geochemical data, structural, petrological and fluid chemistry it has been concluded that gneisses, migmatite and gray granite are much older phases Bundelkhand massif. The different phases of Bundelkhand granitoids were emplaced in the highly deformed BnGC, rocks. The BnGC rocks evolved in the Archean time have been characterized by clock wise. P-T-path. The fluid inclusion study suggest that Middle Archean rocks, of Bundelkhand are usually dominated by $H_2O-NaCl-NuCo_3$ system white pink granitoids (BG) were dominated by $H_2O-NaCl-MgCl_2$ system.

REFERENCES

Acharya, S.K. (2003): The nature of Mesoproterozoic central Indian tectonic zone with exhumed and reworked older granulites. Gondwana Research, V. 6, No.2, pp. 197-214.

Agarwal, B.N.P., Das, L. K., Chakraborty, K. & Sivaji Ch. (1995): Analysis of the Bouguer anomaly over Central India. a regional perspective, Mem. Geol. Soc. Ind., 31, 469-493.

Ahrens, L.H., Pinson, W.H. and Kearns, M.M., (1952): Association of rubidium and potassium and their abundance in common igneous rocks and meterorites, Geochim. Cosmochim. Acta, V.2 pp.229-242.

Balaram. V., (2008). Recent Advances in the Determination of PGE in Exploration studies – A Review Geol. Soc. Vol. 72.

Basu, A. K. (2001): Some characteristics of the Precambrian crust in the northern part of Central India. Geol. Sur Ind., Spl. Pub. 55, 182-204.

Basu, A. K. (2005): Precambrian crustal evolution and tectonism in central and west-central India. Abstract, International conf on PCGT, Bundelkhand University, Jhansi, India. 140-141

Basu, A.K. (1986): Geology of parts of the Bundelkhand granite massif, central India; Rec. Geog. India. V.117, pp. 61-124.

Basu, A.K. (2007): Role of the Bundelkhand Granite Massif and the Son – Narmada megafault in Precambrian crustal evolution and tectonism in central and western India., J. Geo. Soc. India. V 70, pp 745-770.

Basu, A.K., (1970-71): A report on geological mapping around Jhararghat, Jhansi dist.,U.P. Unpublished Progress Report, G.S.I.

Basu, A.K., (1986): Geology of parts of the Bundelkhand Granite Massif. Rec. Geol. Surv. Ind. 117 (2), pp. 61-124.

Batchelor, R.A. and Bowden, P. (1985): Petrogenetic interpretation of granitoid rock series using multicationic parameters. Chem. Geol., V. 48, pp. 43-55.

Battacharya, A.R. (1986) : Wavelength – amplitude characteristics of polyphase fold in the Precambrian Bundelkhand complex, India, Techno physics, vol.128, pp.121-125.

Beckinsole, R.D., Drury, S.A. & Holt, R.W. (1980). 3360M.yr. old gneisses from south Indian craton. Nature London, 283, 469-470.

Chappel S.W. and White, A.J.R. (1974): Two contrasting granite types. Pacific Geology, v. 8, pp. 173-174.

Chappell, B.W. & White, A.J.R. (2001). Two contrasting granite types: 25 years later. *Australian Journal of Earth Sciences* 48, 489-499.

Choundial, D.P. Paul, D.K. Sarkar Amitabha, Trivedi, J.R. Gopalan, K. and Potts, P.J. (1987): Geochronology and geochemistry of Precambrian grenitic rocks of Goa, SW India, precamn. Res., v.36, (287-302).

Condie K.C. (1976): Plate tectonics and crustal evolution. Pergamon Press, London. 288 pp.

Condie, K.C. (1973) : Archaean magmatism and crustal thickening. Geol. Soc. Am. Bull. v. 84, pp. 2981-2992.

Condie, K.C. (1994):Archean crustal evolution. Elsevier, Amsterdam, The Netherlands. Tectonophysics, vol. 257, issue 2-4, pp. 297-298

Condie, K.C., (1983): Plate tectonic and crustal evolution. 2nd edtn., Pergamon Press, 310 p.

Crawford, A.R. (1970): The Precambrian geochronology of Rajasthan and Bundelkhand, Northern India. *Can. J. Earth Sci., v. 7*, pp. 91-110.

Das, A.S. (1959-60): – A report on geological mapping of the Bundelkhand Granites and Gneisses in parts of Jhansi district. U.P. and intervening parts of Tikamgarh district, Madhya Pradesh. Unpublished Progress Report, G.S.I.

De La Roche, H., Leterrier, P., Grandclaude, P. and Marchal, M. (1980): A classification of volcanic and plutonic rocks using R_1-R_2 diagrams and major element analyses - its relationship with current nomenclature. Chem. Geol., v. 29, pp. 183-210.

Debon, F. and Le Fort, P. (1982): A chemical - mineralogical classification of common plutonic rocks and associations. *Trans. Royal Soc. Edinburg, (Earth Sci.), v. 73*, pp. 135-149.

Debon, F. and Le Fort, P. (1983). A chemical-mineralogical classification of common plutonic rocks and associations.

Debon, F., Sheppard, S.M.F. and Sonet, J. (1986): The four plutonic belts of the Transhimalaya-Himalaya: A chemical, mineralogical, isotopic and chronological synthesis along a Tibet-Nepal section. Jour. Petrol. v. 27, pp. 219-250.

Dhoundial, D.P., Paul, D.K., Amitabha Sarkar, Trivedi, J.R., Copalan, K. and Potts, P.J. (1987): Geochronology and Geochemistry of Precambrian granitic rocks of Goa, *SW India. Precamb. Res., v. 36*, pp. 287-302.

El Bouseilly, A.M. and El Sokkary, A.A. (1975): The relation between Rb, Ba and Sr in granite rocks. Chem. Geol., v. 16, pp. 207-219.

Evensen, N.M., Hamilton, P.J. and O'Nions, R.K. (1978): Rare earth abundances in chondritic meteorites. *Geochim. Acta 42*, pp. 1199-1212.

Fermor, L.L. (1935): General Report for the year 1933. *Rec. Geol. Surv. Ind., v. 68*. Pt. 1, pp. 85-88.

Frost R. B., Bornes C. G., Colling W. J., Arculus R. J., Ellis D. J. and Frost C. D. (2001): A Geochemical classification for granitic rocks. Jour. Petrology, v-42, pp. 2033-2048l.

Garrels, R.M. and Mackenzie, F.T. (1971): Evolution of sedimentary rocks, W.W. Norton, New York, 394 p.

Gasparon, M., Inuocentri, F., Hanneti, P., Peccerillo, A. and Tsegaye, A. (1993): Genesis of the Pliocene to Recent biomodal mafic- felsic volcanism in the Debrezeyt area, Central Ethiopia: Vocanological and Geochemical constraints. JOUR. African. Earth Sci., vol. 17, pp. 145-165.

Gillen, C., (1985): Metamorphic Geology: An introduction to tectonic and metamorphic processes. London, George Allen & Unwin.

Hacket, C.A., (1870): Geology of Gwalior and vienity, Rec. Geol. Surv. Ind., V. III, Pt. 2, pp. 33-62.

Hanson, G.N. (1980): Rare earth elements in petrogenetic studies of igneous rocks. Ann. Rev. Earth Planet. Sci., 8, pp. 371-406.

Harpum, J.R. (1963): Petrographic classification of granitic rocks by partial chemical analysis. Tanganyika Geol. Surv. Rep., v. 10, pp. 80-86.

Hunter, D.R. (1974): Crustal development in Kaapvaal Craton, I – the Archean, Precambrian Res., v. 1, pp. 259-294.

Hussain et al, (2004). Geodynamic evolution and crustal growth central Indian shield: Evidence from geochemistry of gneisses and granitoids. Indian Acad. Sci. (Earth Planet. Sci.) Vol-113, pp-. 699-714.

Irvine, T.N., and Barager, W.R.A., (1971): A guide to the chemical classification of the common volcanic rocks, Canadian Journal of Earth Sciences, vol.8, pp.523-548.

J.S. Martin, MW, Mark W. Martin, Janveizer and Samuel A. Bowring (2002). U-pb zircondating and Sr. Isotope systematics of the Vindhyan. Supergroup India. Geology V. 30 No.-2, pp.131-134.

Jain, S.C. Nair, K.K. and Yedekar, D.B., (1995): tectonic Evolution of the Son-Narmada –Tapti lineament zone. In: Geoscientific studies of the Son-Narmada – Tapti lineament zone. Geol. Surv. Ind. Spl. Pub. 10, pp. 188-197.

Jensen,L.S., (1976): A New Cation Plot for Classifying Subalkalic Volcanic Rocks, Ontario Division of Mines, MP 66, 22p.

Jhingran, A.G., (1958): The problem of Bundelkhand Granites and Gneisses : Presidential Address, Section Geology and Geography, 45th. Ind. Sc. Cong., Madras.

Jokhan Ram, Shukla, S. N., Pramanik, A. G., Varma, B. K., Chandra, G. & Murthy, M. S. N. (1996). Recent investigations in the Vindhyan basin. Implications for the basin tectonics. J. Geol. Soc. Ind., No. 36, 267-286.

Kroner, A., and Cordani, U., (2003): African, southern Indian and South American cratos were not part of the Rodinia supercontinent: Evidence from field relationships and geochronology. *Tectonophysics*, 375: (1-4) 325-352.

Le Fort, P., Cuney, M., Deniel, C., France-Lanord, C., Sheppard, S. M. F., Upreti, E. N. & Vidal, P. (1987). Crustal generation of the Himalayan leucogranites. *Tectonophysics* 134, 39–57.

LeMaitre, R.W (1989): A classification of Igneous Rocks and Glossary of Terms (with P.Bateman, A. Dudek, J. Keller et al). Blackwell Scientific Publication, Oxford, 193 pp.

Mallet, F.R. (1869): Vindhyan rocks in Bundelkhand. Mem Geol. Surv. Ind., 7.

Malviya, V.P., Arima, M., Pati, J.K. and Kaneko, Y. (2006): Petrology and Geochemistry of metamorphosed basaltic pillow lava and basaltic komatiite in the Mauranipur area: subduction related volcanism in the Archean Bundelkhand craton, central India. Journal of Mineralogical and Petrological Science, V. 101, pp. 199-217.

Mani, G., and Bhattacharyya, S.N., (1969-70): Report on the Investigation for copper-ore in Hirapur – Tighara – India area, Sagar, Chhattarpur and Tikamgarh district. U.p. Unpublished Progress report G.S.I.

Maniar, P.D. and Piccoli, P.M. (1989): Tectonic discrimination of granitoids. Geol. Soc. Am. Bull. v. 101, pp. 635-643.

Manning, D.A.C., Hamilton, D.L., Henderson, C.M.B. and Dempsey, M.J. (1980) : The probable occurrence of interstitial Al in hydrous, F-bearing and F-free aluminosilicate melts. Contrib. Mineral. Petrol. Springer-Verlag, v. 75, pp. 257-262.

Martin, H. (1986): Petrogneisses of Archean trondhjemites, tonalite and grandiorities from eastern Finland : Major and trace element geochemistry. J. Petrol.V., 28 pp.921-953.

Martin, H. (1993): The mechanisms of petrogneisses of the Archean continental crust – Comparison with modem processes. Lithos, 30,pp 373-388.

Mathur, P.C., (1954): A note on granitisation of quartzites in Bundelkhand. Sc. and Cult. 20 (5), pp. 242 – 243.

Medlicott, H.B. (1859): On the Vidhyan rocks, and their associates in Bundelkhand. Mem. Geol. Surv. Ind., V. II, Pt. 1, pp. 1-95.

Middle Most E.A.K., (1985). Magma and Magmatic Rocks, Longman Group Limited. Essex.

Middlemost, E.A.K. (1985): The potassic rocks. Their nomenclature, origin and evolution with examples from Australia. IAVCET Scientific Assembly Abst.

Mishra, R.C. & Saxena, M.N 1959. A Keratophyre-like rock from Mata Tila Dam site. Geol.Min.Met. Sc. Ind. 402, 115-119.

Mishra, R.C. & Sharma, R. P. (1974). Petrochemistry of Bundelkhand Granites and associated rocks of central India. Indian Mineralogist, 15, 43-50.

Mishra, R.C. (1975). New data on the geology of the Bundelkhand complex of central India. Recent Researches in Geology, II, Hindustan Publishing Corp. India, 311-346.

Miyashiro, A. (1974). Volcanic rock series in island arcs and active continental margins, American Journal of Science, vol.274, pp.321-355.

Miyashiro. A & Shido. F. (1975): Tholeitic and Calc-alkalic series in relation to the behaviour of titanium, vanadium, chromium and nickel. Am. J. Sci. V.275, pp265-277.

Mondal M.E.A., Hussain, M.F. and Ahmad, T. (2006). Continental Growth of Baster craton, Central Indian Shield during Precambrian via Multiphase subduction and Lithospheric Extension/Rifting : Evidence from Geochemistry of Gneisses, Granitoids and Maffic dykes. Jour. Geosciences, Japan. 49: 137-151.

Mondal, M.E.A., Sharma, K.K., Rahman, A. & Goswami, J.N.(1998). Ion microprobe $^{207}Pb/^{206}Pb$ zircon ages for the gneisses-granitoids rocks from Bundelkhand massif: Evidence for the Archaean components. Cur. Sc., 74, 70-75.

Mondal, M.E.A., Zainuddin, S.M., (1996): Evolution of the Archean – Paleoproterozoic Bundelkhand massif, central India-evidence from graniatoids geochemistry. Terra Nova V.8, pp.532-539.

Mondal, M.E.A., Zainuddin, S.M., (1997): Geochemical characteristics of the granites of Bundelkhand massif, central India. J. Geol. Soc. India V.50, pp.69-74.

Mondal. M.E.A, Goswami, J.N., Deomurari, M.P. and Sharma, K.K. (2002): Ion microprobe $^{207}Pb/^{206}Pb$ ages of Zircons from the Bundelkhand massif, northern India, implications for crustal evolution of the Bundelkhand-Aravalli Proto Continent. Precambrian Research. V 117, pp 85-110.

Mukherji, A., (1973-74): Geology of parts of Kharaha – Maror Area, Jhansi distt-U.P. & Tikamgarh distt., M.P. Unpublished progress Report. G.S.I.

Nakamura, N., (1974): Determination of REE, Ba, Fe, Mg, Ba and K in the carbonaceous and ordinary chondrites, Geochim. Cosmochim. Acta, 38; 7577-775.

Naqvi, S. M. (2005): Geology and evolution of the Indian plate. Capital Publishing Company, New Delhi, India, 450p.

Norman, (2001). A quick basic programme for petrochemical re-calculation of whole rock major element analyses on IBM PC J. Czech Geol. Soc. 46, pp-9-13.

O'Connor, J.J. (1965): A classification for the quartz-rich igneous rocks based on feldspar ratios. U.S. Geol. Surv. Prof. Pap, pp. 525.

Pandey, B.K., Chabria, T. and Gupta, J.N., (1995): Geochronological chracterization of the Proterozoic terrains of Penisular India : relevance to the first order target selection for uranium exploration. Expl. and Res. Atomic Minerals, V.8,pp. 187-213.

Pascoe, E.H., (1950): A manual of the Geology of India and Burma. V. I., Geol. Surv. Ind. Calcutta.

Pati, J.K. and Shukla, R. (1999): the specialized thematic study of older enclaves (Migmatites gneisses and Supracrustals) within the Bundelkhand granitoids complex in Southern U.P. Geol. Surv. India. Records,V 132 pp. 132-137.

Pati, J.K., (1996): A note on the occurrence of Orbicular Rocks in Bundelkhand Grnaitoid Complex. Geol. Soc. India, Vol. 48, pp. 345-348.

Pearce, J., Harris, N.B.W. and Tindle, A.G. (1984): Trace element discrimination diagrams for the tectonic interpretation of granitic rocks. Jour. Petrol, v. 25, pp. 956-983.

Prakash, Ravi, Singh, J.N. & Saxena, P.N. (1975). Geology and mineralization in the southern parts of Bundelkhand in Lalitpur dist., U.P. J. Geol. Soc. Ind., 162, 143-156.

Prasad, M.H., Hakim, A. & Rao, B.K. (1999). Metavolcanic and metasedimentary inclusions in the Bundelkhand Granitic Complex in Tikamgarh District, Madhya Pradesh. J. Geol. Soc. Ind., 54, 359-368.

Radhakrishna, B.P. 1989. Suspected tectono-straitigraphic terrane elements in the Indian Sub-continent. J. Geol. Soc. Ind., 34, 1-24.

Rahman, A. and Zainuddin, S.M. (1993): Bundelkhand Granites : an example of collision related Precambrian magmatism and its relevance to the evolution to the Central Indian Shield. Jour. Geol., V.101, pp. 413-419.

Rao, J. M., Rao, G. S. P., Widdowson, M. & Kelley, S. P. (2005). Evolution of proterozoic mafic dyke swarms of Bundelkhand Granite Massif, Central India. Curr. Sc., 88 No.3, 502-506.

Rasmussen, B. Bose P.K. Subirsarkar, Santanu Banerjee Ian R. Fletcher and Neal J. McNaughton (2002). 1.6 Ga U-Pb zircon age for the chorhat sandstone, lower vindhyan. India: possible implications for early evolution of animals Geology, vol-230, pp. 103-106.

Roday, P.P. & Singh, S. (1998). Palaeostrees analysis of heterogenous fault sets in the central Indian Bundelkhand Granitoids. separation into homogenous subsets, stress rations and comparison with finite strains. In. Paliwal, B.S. Ed., the Indian Precambrians, Scientific Publishers India, Jodhpur, 44-60.

Roday, P.P. Diwan, P. & Singh, S. (1995). A kinematic model of emplacement of quartz reef and subsequent deformation pattern in the central Indian

Bundelkhand batholith. Proc. Indian Acad. Sc. Earth Planet. Sc., 104 (3), 465-488.

Rogers, J.J.W. and Santosh, M., (2004). Continents and Supercontinents. Oxford University Press, New York.

Rogers, J.J.W., Callahan, E.J., Dennen, K.O., Fullagar, P.D., Stroh, P.T. & Wood, L.F. (1986). Chemical evolution of Peninsular gneiss in the western Dharwar craton, southern Indian. J. Geol., 94, 233-246.

ROLLINSON H.R. (2007). Early Earth Systems: a geochemical approach. Blackwell Publishing, Oxford, UK. 296 pp.

ROLLINSON H.R., (1993), Using Geochemical Data: Evaluation, Presentation, Interpretation, Longman, UK. 352 pp.

Roy, A., Devarajan, M. K. & Prasad, M. H. (2002). Ductile shearing and syntectonic granite emplacement along the southern margin of the Palaeoproterozoic Mahakoshal supracrustal belt. Evidence from Singrauli area, Madhya Pradesh. J. Geol. Soc. Ind., 59, 9-21.

Sarkar, A. Trivedi, J.R. Gopalan, K. Singh, P.N. Das, A.K. & Paul, D.K. (1984). Rb/Sr geochronology of Bundelkhand granitic complex in the Jhansi-Babina-Talbehat sector. U. P., CEISM seminar volume, Ind., J. Earth. Sc., 64-72.

Sarkar, A., Bhalla, J.K., Paul, D.K. Potts, P.J., Bishni, P.K., Gupta, S.N. & Srimal, N. (1989). Geochemistry and geochronology of the early Proterozoic Bundelkhand granitic complex, Central India. Symp. Precam. Granitoids, Helsinki, Finland, Geol. Surv. Finland, Spl. Paper, 8, 117.

Sarkar, A., Paul, D.K. and Potts, P.J. (1995): Geochronology and geochemistry of the Mid-Archaean trondhjemitic gneisses from the Bundelkhand craton, Central India. Recent Researches in Geology, v.16, (Ed.) A.K. Saha, Hindustan Publ. Co. pp. 76-92,

Sarkar, A., Paul, D.K. and Potts, P.J., (1996): Geochronology Geochemistry of Mid-Archean Trondhjemitic gneisses from the Bundelkhand craton. Rec. Res. Geol., V.16., pp. 76-92.

Sarkar, A., Paul, D.K., Potts, P.J., (1996): Geochronology and geochemistry of Mid. Archean trodhjemitic gneisses from the Bundelkhand Group. In : Valdia, K.S. Bhatia, S.B. Gaur, V.K. (Eds.), Geology of Vindhyanchal Hindustan, India, pp. 30-46.

Sarkar, A., Sarkar, G., Paul, D.K. and Mitra, N.D. (1990): Precambrian geochronology of the Central Indian Shield – review. *Geol. Surv. India, Spl. Pub. 28*, pp. 453-482.

Sarkar, G. and Gupta, S.N. (1989): Dating of early Precambrian granite complex of Bastar district, Madhya Pradesh, *Rec. Geol. Surv. Ind., v. 122, pt. 2*, pp. 22-30.

Sarkar, G., Paul, D.K., McNaughton, N.J., De Laeter, J.R. and Misra, V.P. (1990): A geochemical and Pb, Sr isotopic study of the evolution of granite gneisses from Bastar Craton, Central India. *Jour. Geol. Soc. India, v. 35(5)*, pp. 480-496.

Saxena, M.N. 1961. Bundelkhand granites and associated rocks from Kabrai and Mau Ranipur areas of Hamirpur and Jhansi districts. Ind., Res. Bull. Punjab University, 12, I &II, 85-107.

Sharma, K. K. (1998). Geological evolution and crustal growth of the Bundelkhand craton and its relict in the surroundings regions, northern Indian shield. In. Paliwal, B.S. Ed., The Indian Precambrian. Scientific Publishers India, Jodhpur, 33-43.

Sharma, K.K. (2000). Evolution of Archaean Palaeoproterozoic crust of the Bundelkhand craton, northern Indian shield. Research Highlights in Earth System Science. In. Verma, O.P and Mahadevan, T.M. Eds., DST's Spl. 1, Ind. Geol. Cong., 95-105.

Sharma, K.K. and Rahman, A., (1995): Occurrence and petrogenesis of the Loda Pahar trodhjemitic gneiss from Bundelkhand craton, central India : Remnant of an early crust. Curr. Sci., V.69, pp.613-617.

Sharma, K.K. and Rahman, A., (1996): Bundelkhand craton, Northern India Shield Geochemistry, petrogenesis and tectonomagmatic environments. Deep Continental Studies News Letter, DST, New Delhi,V. 6,pp12-19.

Sharma, R.P., (1982). Lithostratigraphy, structure and petrology of the Bundelkhand group. In. Valdia, K.S., Bhatia, S.B. & Gaur K. Eds. Geology of Vindhyanchal, 30-46.

Shukla, R. and Pati, J.K. (1999): The specialized Thematic study of older enclaves (migmatites gneiss and supracrustals) within the Bundelkhand granitoid complex in southern U.P. Geol. Ind. Records, V. 132. pp. 132-136.

Singh S.P. and Dwivedi S.B. (in press) Garnet – Sillimanite – Cordierite bearing assemblages from early Archean supra-crustal rocks of Bundelkhand Massif, central India : A New Report, Current Sciences.

Singh S.P. and Singh M.M. (2008). Geochemistry of Archean Mafic and Ultramafics Rocs from central part of Bundelkhand craton : Implication in the Archean crustal Evolution Jour. Eco. Geol. Georesources. Mgt. Vol. 8. ppt-15.

Singh, M. M. 2005. Petrology of supracrustal rocks of Bundelkhand massif, Babina-Mauranipur transect, Uttar Pradesh. Ph. D. thesis, Bundelkhand University, Jhansi.

Singh, M. M., Singh, S. P. and Srivastava, G. S. (2005). Crustal evolution in Bundelkhand massif Central India. Abstract, International conf on PCGT, Bundelkhand University, Jhansi, India. 242-243

Singh, S.P., and Singh, M. M., Srivastava, G.S., and Basu, A.K. (2007): Crustal evolution in Bundelkhand area, Central India. Journal of Himalayan Geology, V. 28(2), pp. 79-101.

Srivastava S.K., Nambiar K.V. and Gaur V.P. (2004): Orbicular Structures in Bundelkhand granitoid complex near Pichhore, Shivpuri District, Maydhya Pradesh., J. Geo. Soc. India. V 64, pp 667-684.

Srivastava, K.K., (1970-71). The Geology around Babina, Jhansi distt., U.P. unpublished progress report, G.S.I.

Streckeiscn, A., (1976) To each plutonic rocks its proper name, Earth Sci. Reviews, vol.12, pp. 1-33.

Streckeisen, A. (1976). To each plutonic rock its proper name, Earth-Science Reviews, vol.12, pp.1-33.

Taylor, S.R. and McLennan, S.M. (1985): The continental crust: Its Composition and Evolution, Blackwell, Oxford, UK. pp.312.

Taylor, S.R. and McLennan, S.M. (1985): The continental crust: Its composition and evolution. Blackwell, Oxford, 295 p.

Taylor, S.R., Emelens, C.H. and Exley, C.S., (1956): Some anomalons K/Rb ratio in igneous rocks and their petrological significance : Geochim. Cosmochim. Acta, V.10, pp. 224-229.

Taylor, S.R., Heier, K.S. and Sverdrup, P.L. (1960): Contribution to the mineralogy of Norway. No. 5. Trace element variations in three generations of feldspars from Landsverk I Pegmatite, Evje, Southern Norway, Norsk. Geol. Tidsskr. v. 40, pp.

Taylor, S-R. and Mc. Lennan (1985), Continental crust: In composition and Evolution Blackwell London.

Tuttle, O.F. and Bowen, N.L. (1958): Origin of granite in the light of experimental studies in the system $NaAlSi_3O_8$-SiO_2-H_2O. Geol. Soc. Am. Mem., v. 74, pp. 153.

Veevers. J.J., (2005). Edge Tectonics (Trench Rollback, Terrane, Export) of Gondwanaland – Pangea Synchronized by Supercontinental Heat, V. 8, pp-449-456.

Verma, R.K. and Banerjee P., (1992): Nature of the continental Crust along the Son-Narmada Lineament inferred from gravity and deep seismic sound data. Tectonophysics, V.202, pp. 375-397.

Whalen, J.B., Currie, K.L. and Chappel, B.W. (1987): A-type granites: Chemical characteristics, discrimination and petrogenesis. Contrib. Mineral. Petrol. 95, pp. 407-419.

White, W. M., (2001): Geochemistry, Published by John – Hopkins University Press.

Winchester, J.A. and Floyd, P.A., (1977): Geochemical discrimination of different magma series and their differentiation products using immobile elements, Chemical Geology, vol.20, pp.325-343.

Yedekar, D.B. Jain, S.C., Nair, K.K. and Dutta, K.K., (1990): The Central Indian Collision Suture. In: Precambrian of central India, Geol. Surv. Ind., Sp. Pub., 28, pp 1-43.

Zainuddin, S.M, Rahman, A. & Mondal, M.E.A. (1992). Geochemical fingerprints of Bundelkhand granites as an indicator of minor Indian plate collision during Precabrian. In. Ahmad, R. & Sheikh, A.M. Eds., Geology in South Asia-1, 161-168.